ROLE OF REDUCED SULFUR SPECIES IN PROMOTING THE TRANSFORMATION OF INSECTICIDES IN THE ENVIRONMENT

by

Tong Wu

A dissertation submitted to the Graduate Faculty in Chemistry in partial fulfillment of the requirements for the degree of Doctor of Philosophy, The City University of New York

2007

This manuscript has been read and accepted by the Graduate Faculty in Chemistry in satisfaction of the dissertation requirement for the degree of Doctor of Philosophy.

Prof. Urs Jans

January 20, 2007 — Date

Chair of Examining Committee

Prof. Gerald Koeppl

January 20, 2007 — Date

Executive Officer

Prof. David Locke

Prof. Teresa Bandosz

Supervisory Committee

THE CITY UNIVERSITY OF NEW YORK

Abstract

ROLE OF REDUCED SULFUR SPECIES IN PROMOTING THE TRANSFORMATION OF INSECTICIDES IN THE ENVIRONMENT

by

Tong Wu

Adviser: Professor Urs Jans

Organophosphate (OP) and carbamate compounds are wildly used in agriculture. The exposure to these chemicals may be a high risk for adverse health effects. Recent studies have shown that organophosphate chemicals are consistently present in the air, rain and surface waters, suggesting a long environmental half-life. Although transformation is the only ultimate sink for these compounds in the environment, some transformation reactions produce compounds that are even more toxic than the original compounds. One possible type of transformation of OPs and carbamates is nucleophilic substitution, the focus of this dissertation.

It is reported that high concentrations of reduced sulfur species can occur under anaerobic conditions. Reduced sulfur species are good nucleophiles and reductants that can possibly undergo reactions with OPs and carbamates. In this work, model systems consisting of homogeneous aqueous solutions with reduced sulfur species (hydrogensulfide/bisulfide (H_2S/HS^-), polysulfides (S_n^{2-}), thiophenolate (PhS^-) or thiosulfate ($S_2O_3^{2-}$)) were used to study the degradation of OPs and carbamates. The model systems, being simpler than environmental milieus, help to clarify the mechanisms. For carbamates, the reaction rates are independent of the concentration

of reduced sulfur species. For the OPs, the reaction rates are first-order in the concentration of the different reduced sulfur species. The activation parameters of the reaction of OPs with bisulfide were determined from the measured second-order rate constants over a temperature range of 5-60 ºC. The resulting data indicates that OPs undergo a S_N2 reaction with the reduced sulfur species. The transformation products indicate that the nucleophilic substitution of reduced sulfur species occurs at the carbon atom of an alkoxy group to form the desalkyl OP. The formation of corresponding phenol, a minor degradation product, could be attributed entirely to hydrolysis. The determined second-order rate constants show that the reaction of an OP with polysulfides is about 15 to 50 times faster than the reaction of the same OP with bisulfide. The reaction rate constants for chlorpyrifos and parathion with the bisulfide and polysulfide are about factor of 10 smaller than for chlorpyrifos-methyl and parathion-methyl, while the reaction rate constants for fenchlorphos with the bisulfide and polysulfide are similar as chlorpyrifos-methyl and parathion-methyl.

Dedicated to those who made this thesis possible:

My parents, my husband

Acknowledgments

I would like to express my gratitude to everybody who helped me through the process of working and completing this dissertation.

First of all I want deeply to thank my mentor Professor Urs Jans for giving me an opportunity to work on such an interesting topic. He not only helped me in project design and development in my research work, but also took much time and energy to review all of my reports and papers and made valuable comments as well as corrections.

I am very thankful to my colleagues and to all those people who offered me a great deal of help, especially Qiu Gan, who help me with the setup and trouble-shooting the GC and GC-MS.

Special thanks are also given to my parents and my husband for their consistent encouragement during my Ph.D. research work.

I thank Professor David Locke and Professor Teresa Bandosz for serving as my supervision committee members, for their constructive comments during committee meeting and the revision of this dissertation.

Finally, I acknowledge the financial support from by the National Science Foundation, the Herman Frasch Foundation and the Petroleum Research Fund.

Table of Contents

List of Schemes

List of Tables

List of Figures

Chapter 1. Introduction and Overview

More chemicals are being used today than ever before (Zoldoske et al. 1990). In the United States, novel chemicals are being evaluated for possible use at a rate of 1000 – 1600 per year. In Europe, a report by the European Inventory cited over 100,000 chemicals in use (Hart 1993). Since nearly all of the chemicals in use are likely to find their way into terrestrial and aquatic environments, regulating authorities such as the US Environmental Protection Agency (EPA) require that these compounds be assessed as to their possible harm to living organism. However, regulating authorities have been faced with two significant obstacles: 1) problems related to chemicals in the environment are highly complex, with many variables such as temperature, pH, and sunlight having an impact on a chemical's fate and effects (Zoldoske et al. 1990) and 2) there is a serious lack of biological data on chemicals in use (Hart 1993). Both of these problems involve the lack of adequate information concerning the fate and effects of chemicals in the environment. Since the number of compounds in use and the cost of evaluating the hazards of these compounds are ever increasing, researchers have turned to the development of predictive models to estimate the required information. The development of accurate predictive models, called quantitative structure activity relationships (QSAR), would allow industry and regulating authorities to quickly and cheaply determine the possible hazards of a chemical without exhaustive and costly laboratory research. However, to develop accurate predictive models a good understanding of the various factors that will affect a chemical in the environment is necessary.

With the environmental problems caused by the use of organochlorine insecticides, emphasis has shifted to the use of carbamate and organophosphorus (OP) compounds which tend to be less persistent in aquatic systems (Coats 1993). However, many researchers have reported incidents in which OP compounds have been found in surface and ground water samples, challenging the belief that they are ephemeral in the environment (Zaki et al. 1982; Liu et al. 2001). A contributing factor to the appearance of these insecticides in aquatic systems is their enhanced stability under certain conditions. Temperature and pH were reported to be the most important environmental factors in determining the aquatic fate of OPs (McEwen et al. 1979).

Any compound entering an aquatic system is subject to many different processes that could affect availability to aquatic organisms, convert it from one form to another or degrade the chemical. Which transport or transformation processes a chemical will likely undergo depend on how the chemical partitions between the different compartments (water, sediment, biota) in an aquatic system (Figure 1-1).

Biota

Unquestionably the most important compartment which a compound can partition into are the different organisms which make up an aquatic community. The degree of harm any compound will inflict on the inhabitants of our streams, rivers, lakes and oceans will depend on a chemical's ability to enter an organism, negotiate the various detoxification mechanisms possessed by the organism, reach the target site and successfully interact with the appropriate receptor.

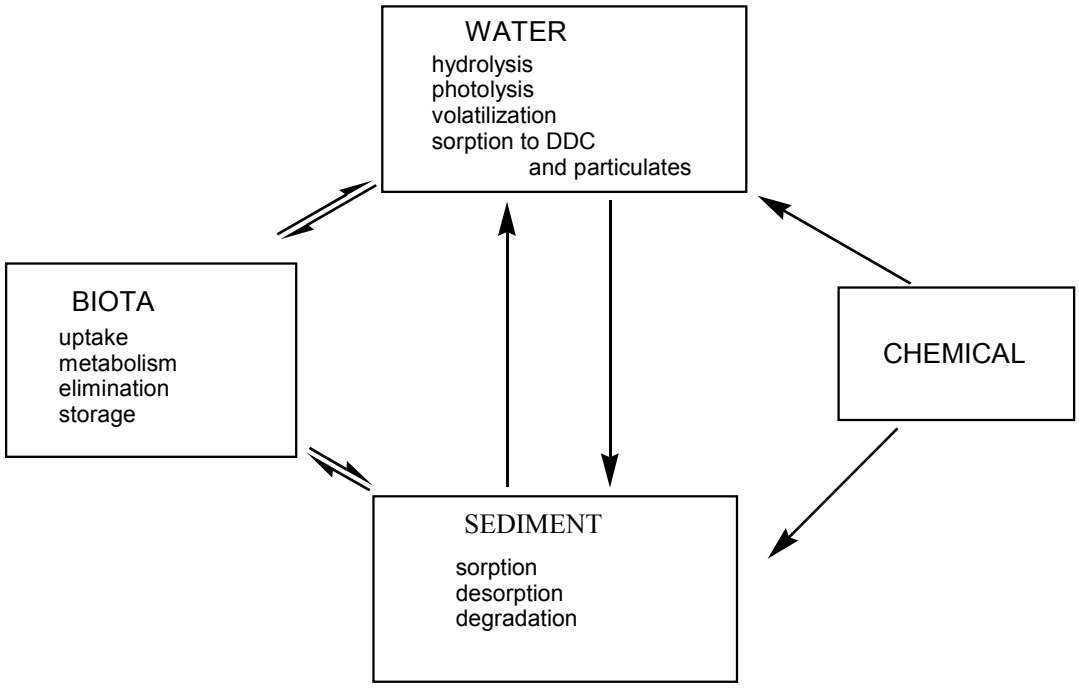

Figure 1-1: Chemical partitions in the aquatic system

For example, for a compound to reach the target site within the body of an aquatic invertebrate (such as the midge, *Chironomns. riparius*) the compound must pass through the insect's cuticle which is covered by a thin wax layer. Three factors have been cited as important for this: 1) lipid solubility of the compound, 2) affinity of the compound for other cuticular components such as protein and chitin, and 3) solubility of the compound in the insect's hemolymph (Yamashiro-Matsumura et al. 1985). According to O'Brien (O'Brien 1963), the lipophilicity of the compound is very important since this determines the rate and amount of compound that penetrates the wax layer covering the cuticle, there is the opportunity for it to be stored, limiting the amount entering the organism. Once the compound has dissolved into the hemolymph it would be transported throughout the insect's body. However, at this point the compound would be subject to attack by the insect's

mixed function oxidase system, which could detoxify or possibly activate the compound. Further, the insecticide may be stored in various organs or tissues (in vertebrates, adipose tissue has long been known to be a storage site) making the insecticide bio-unavailable. Intoxication will occur once the compound has reached the target site. Even so, a compound that has bound to the appropriate target site may be removed from the active site by hydrolases present in the insect, or simply fall off due to weak interactions between the compound and target site.

Overall it is clear that any model that would describe the effects of a compound on aquatic environment must account for many different chemical and physical processes that occur in the aquatic system.

Sediment

Sediment has long been known to change the bioavailablity of many chemicals which enter aquatic communities. Researchers have determined that numerous nonpolar organic compounds adsorb to the organic carbon in sediment, reducing their availability and therefore toxicity to aquatic organisms. Pittinger (Pittinger et al. 1989) found that the toxicity of four surfactants was lower to the midge, *C. riparius* if the route of exposure was through contaminated sediment. Nebeker (Nebeker et al. 1989) found that higher total organic carbon in sediment caused a reduction in the toxicity of DDT to the freshwater amphipod, *Hyalella azteca*. Although the carbon content of sediment will affect the availability of many compounds, other factors such as structural characteristics of the chemical, as well as the pH and temperature of the medium will also be important in determination of the availability of the chemical in an aquatic environment.

Water:

Hydrolysis is the splitting of an organic compound with water, hydroxide and/or hydrogen ions (Zoldoske et al. 1990). It has long been known to be an important factor in the degradation of many organic compounds. Mabey and Mill (Mabey et al. 1978) reported the abiotic half-lives of a number of organic chemicals which ranged from seconds to thousands of years. Eichelberger and Lichtenberg (Eichelberger et al. 1971) in a study conducted with 28 pesticides in river water, reported that all but one organophosphorus (OP) insecticide had undergone some transformation in eight weeks.

Chemicals in water can be transformed by hydrolysis, and can also be altered by sunlight. The photolysis of chemicals in water is reported to be affected by sunlight intensity, latitude, time of day and depth of water (Zepp et al. 1977).

Not only can pollutants be hydrolyzed in the water column, but also they are capable of sorbing to dissolved organic material (DOM) as well as suspended particulates. It was reported that sorption of xenobiotics to dissolved organic matter in the interstitial water of sediment can decrease the bioavailability of such compounds (Nebeker et al. 1989). Pape-Lindstrom (Pape-Lindstrom et al. 1997) reported that when several neutral lipophilic compounds were added to beakers containing water and sediment, up to 60% of the aqueous fractions of the chemicals were found to bind to DOC and suspended particulates. The reduction of availability due to sorption on DOM, particulates and sediment was cited as the cause of subsequent decrease in toxicity of these compounds to midges added to the beakers of water and sediment.

Water-borne xenobiotics leave aquatic environments by volatilization, thereby decreasing their concentration in water. The rate of volatilization is dependent on the vapor pressure and solubility of the compound in water. Dilling (Dilling et al. 1975) reported that five organochlorine compounds (methylene chloride, chloroform, 1,1,1-trichloroethane, trichloroethylene, and tetrachloroethylene) placed in water at 25 ºC and stirred continuously, evaporated to 10% of the original concentration in less than 90 minutes. Henry's law constant (HLC), which relates the concentration of a gas dissolved in a liquid to the partial pressure of the gas in solution, is often used to describe the volatility of a compound.

The main objective of this dissertation is the evaluation of transformation reactions of organophosphorus triesters (OPs) and carbamate under environmentally relevant sulfidic conditions. In such environment, the existence of reduced sulfur species can accelerate the degradation of organic contaminant (Lippa et al. 2002; Loch et al. 2002). It has also been reported the sulfur nucleophile has a higher ability to attack the saturated carbon than the hydroxide, while it is known that hydrolysis of the investigated OPs occurs through a nucleophilic attack either on the phosphorus atom or the carbon atom of the alkoxy group (Schwarzenbach et al. 2003), and the hydrolysis of carbamate occurs through a $E1_{cb}$ mechanism (Strathmann et al. 2001; Strathmann et al. 2002). Therefore, the focus of the dissertation was on the kinetics of the S_N2 reaction of OPs with reduced sulfur species.

In this dissertation, the studies on the toxicity and environmental fate of both OPs and carbamate were reviewed in Chapter 2, and Chapter 2 also introduces the availability of reduced sulfur species in the aqueous environment. Then, the

information regarding the hydrolysis and effect of reduced sulfur species on the degradation of carbamate is discussed in Chapter 3. Although the hydrolysis of OPs was the most thoroughly studied degradation pathway of OPs, the rate constants reported for the OP hydrolysis often differ by more than an order of magnitude between different authors, therefore, the kinetics of hydrolysis of the five OPs were investigated, and a detailed quantification of the products is provided in Chapter 4. The mechanism of reaction of OPs with reduced sulfur species is discussed in Chapter 5 and 6. Chapter 5 and 6 also provide the degradation products distribution that is essential to develop the reaction mechanism. Future studies involving the nucleophilic substitution with reduced sulfur species can apply the gained understanding of reaction mechanism and kinetics.

It was assumed that nucleophilic attack by reduced sulfur species at the carbon atom of the methoxy groups is the dominant mechanism for OPs, in this thesis, this hypothesis was proved by both the kinetic data and product detection, and also, the second-order rate constants for the OPs with common reduced sulfur species were also determined.

Finally, relationship between the OP structure and the measured rates of reaction is developed in Chapter 7. The quantitative structure-activity relationship (QSAR) developed in this work relates the reaction rate to the change in the electrostatic charge on the carbon atom of alkoxy group.

Chapter 2. Transformation of Organophosphorus and Carbamate Compounds in the Environments: A Review

2.1 Introduction

Large quantities of organic and inorganic agrochemicals are produced each year. It is reported that the total conventional pesticide use, including home, structural, and other applications, averages about 1 billion pounds in the United States (Gianessi et al. 1995). Agrochemicals are a possible series of microcontaminants that have potential adverse effects on the ecosystem. They are likely to be released into the aquatic environment through runoff, leaching, and improper application (Kolpin et al. 1998; Fernández-Pérez et al. 2000). Many pesticides show relatively high persistence in surface water. This allows their transport over long distances and migration into very sensitive aquatic environment such as ground water that is used for drinking water by about 50% of the population (Kolpin et al. 2002).

Numerous studies have demonstrated the occurrence of pesticides in the environment throughout the United States over the past three decades, including organophosphate, carbamate, organochlorine, and pyrethriod compounds, particularly in agricultural areas (urban areas have seldom been sampled). It is reported that people can be exposed to pesticides during their dermal contact with the floors and other surfaces, especially for children who are developmentally immature; they may also be at higher risk for adverse health effects (Eskenazi et al. 1999).

The occurrence study showed that abiotic processes could control the fate of organic contaminants under anaerobic conditions. It has been found that certain

agrochemicals undergo significant transformation under anoxic conditions by chemical rather than microbial processes (Barbash et al. 1989; Foster et al. 1996; Miller et al. 1998; Strathmann et al. 2001). The possible transformation mechanisms are compound-specific. They typically include reduction reactions and nonreduction reactions (e.g., hydrolysis, substitution). While some organic pollutants are transformed through surface-catalyzed reactions on particles, others are degraded by homogenous reactions. In this chapter, the toxicity and environmental fate of organophosphate and carbamate are carefully discussed. This chapter also reviews the literature on the types of the abiotic transformation reactions that can occur in dark, aqueous environments.

2.2. Toxicity of Pesticides

2.2.1 Organophosphorus insecticides

The organophosphorus insecticides (OPs) of major commercial and toxicological interest are esters or thiols derived from phosphoric, phosphonic, phosphinic or phosphoramidic acid. The basic chemical structure of OPs is displayed in Figure 2-1.

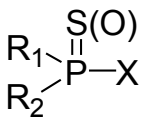

Figure 2-1. Chemical structure of insecticides of the organophosphate family.

Usually, R_1 and R_2 are aryl or alkyl groups that are bonded to the phosphorus atom either directly (forming phosphinates), or through an oxygen or sulphur atom (forming phosphates or phosphothioates). In other cases, R_1 is directly bonded to the phosphorus atom, and R_2 is bonded to an oxygen or sulphur atom (forming

phosphonates or thiophosphonates). In phosphoramidates, at least one of these groups is -NH_2. The amino group of the phosphoramidates may be un-, mono- or bi-substituted. The atom double-bonded with phosphorus is either oxygen or sulphur. Finally, the -X group may belong to a wide range of halogen, aliphatic, aromatic or heterocyclic groups. The -X group, also binding to the phosphorus atom through an oxygen or sulphur atom is called 'leaving group', because, it is released from the phosphorus atom when the OP is hydrolysed by phosphotriesterases (PTE), or upon interaction with protein targets. The OPs exert their main toxicological effects through non-reversible phosphorylation of acetylcholinesterase (AChE). AChE is a remarkably efficient serine hydrolase. It catalyzes the hydrolysis of the neurotransmitter acetylcholine (ACh) at cholinergic synapses. The hydrolysis reaction is initiated by the nucleophilic attack of Ser-200 on the carbonyl center of ACh to form an acetylated enzyme intermediate that is coupled with the release of the first product, choline. The free enzyme is regenerated by hydrolysis of the acetylated enzyme intermediate and release of the second product, acetate. In the presence of organophosphates, the active site Ser-200 is phosphorylated to form a phosphorylated enzyme intermediate (Scheme 2-1).

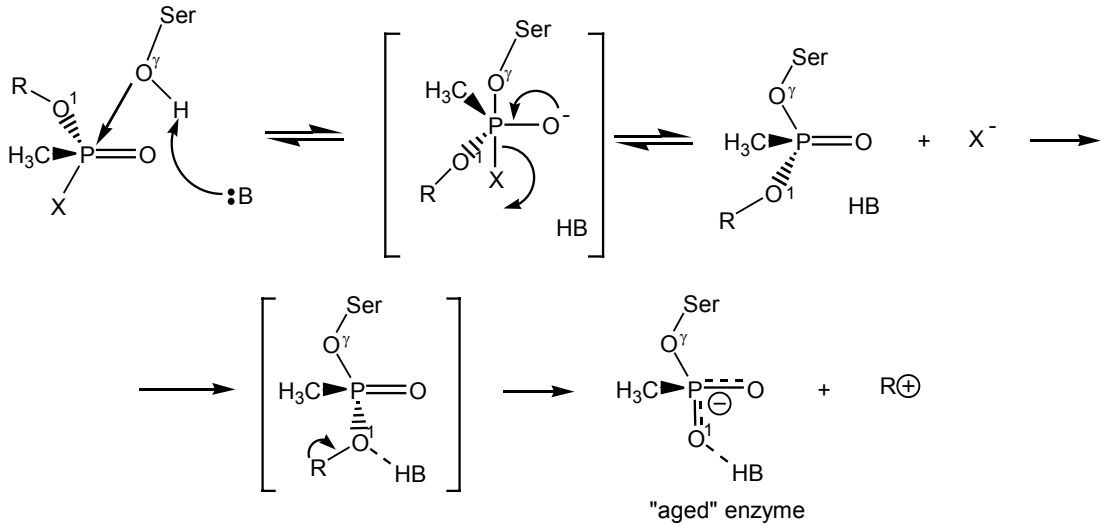

Scheme 2-1: Reaction of AChE with a phosphonate nerve agent (Millard et al. 1999). The scheme begins with the reversible enzyme-OP complex and ends with irreversibly inhibited aged enzyme. The phosphylation leaving group is depicted as X (fluoride ion in the case of soman, sarin, or DFP (diisopropylphosphorofluoridate)); The enzyme's catalytic general base, probably Nε2 of His440, is depicted as :B; R is a branched alkyl group; and R+ is a hypothetical carbonium ion which reacts in water to yield primarily the alcohol product, ROH . The top panel shows phosphylation, and the lower panel shows dealkylation (aging). Phosphonylation is expected to occur via a trigonal bipyramidal intermediate (depicted in brackets in the upper panel), or a transition state resembling such a structure, with inversion of stereochemistry at P. For reaction of AChE with DFP, an –OiPr group replaces the -CH_3 bonded to P.

In this case, the hydrolysis of the phosphorylated enzyme intermediate is very slow. If AChE is not reactivated by an oxime nucleophile such as 2-PAM, the phosphorylated enzyme intermediate can undergo a base-assisted dealkylation

reaction resulting in formation of ‘‘aged’’ AChE that is permanently inactivated (Millard et al. 1999). The half-time for aging is dependent on the nerve agent bound to the active site, pH, and ionic strength (Berman et al. 1986). The inhibition of this enzyme causes over-stimulation of nicotinic and muscarinic acetylcholine receptors. The typical symptoms of poisoning are agitation, muscle weakness, muscle fasciculations, miosis, hypersalivation, sweating (WHO 1986; WHO 1986). Severe poisonings may cause respiratory failure, unconsciousness, confusion, convulsions and/or death. This toxic effect is called ‘organophosphorus induced delayed neuropathy’ and the symptoms of this neuropathy (paralysis and ataxia) appear between 14 and 24 days after the poisoning (Lotti 1992). The OPs are mainly detoxified through oxidation and hydrolysis. The two main enzyme groups involved in the hydrolysis of these compounds are phosphotriesterases (PTEs) and carboxylesterases (CbEs).

2.2.2. Carbamate insecticides

The compounds derived from carbamic acid are probably the insecticides with the widest range of biocide activities. The structure of the biologically active carbamates is displayed in Figure 2-2.

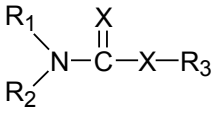

Figure 2-2. Chemical structure of pesticides of the carbamate family.

In these structures X can be oxygen or sulphur, R_1 and R_2 are usually organic radicals, but R_1 or R_2 may also be hydrogen. When R_2 is hydrogen and R_1 is methyl, the carbamate exhibits insecticide activity; if R_1 is an aromatic group the compounds are used as herbicides, while fungicide activity is present if R_1 is an

enzimidazole moiety. R_3 is mostly an organic radical, and sometimes a metal. The toxic acute effects of carbamates are very similar to the acute effects derived from the poisoning of OPs. Both groups of compounds are inhibitors of AChE and therefore, cause very similar symptoms. The reaction of AChE with carboxyl ester substrates, including ACh, proceeds through an unstable tetrahedral intermediate (TI) before collapsing to a short-lived ($t_{1/2}$ ~50 μs) acetyl-enzyme (Froede et al. 1984; Millard et al. 1999) (Scheme 2-2). The acetyl-enzyme subsequently undergoes nucleophilic attack by water, passing through a second TI, and the regenerated enzyme is expelled as the leaving group (deacylation). The two-step catalytic mechanism renders AChE susceptible to rapid, stoichiometric, and essentially irreversible inhibition by a class of organophosphorus acid anhydride (OP) inhibitors, typified by the phosphonate nerve agents, which can act as "hemisubstrates" to trap the enzyme in a structure that closely resembles the negatively charged deacylation TI (Scheme 2-2).

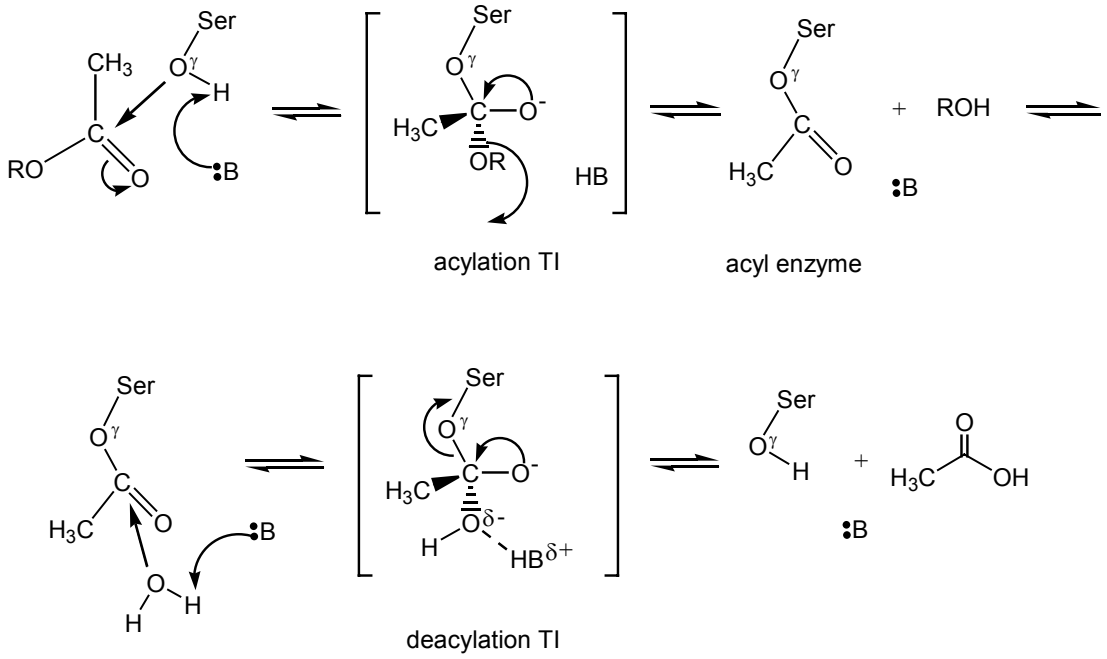

Scheme 2-2: Reaction of AChE with a natural carboxyl ester substrate, such as ACh (Millard et al. 1999). The scheme begins with the reversible enzyme-substrate complex and ends with free enzyme. The enzyme's catalytic general base, probably Nε2 of His440, is depicted as :B, and the first product is depicted as ROH (choline in the case of ACh). The top panel shows acylation and the lower panel shows deacylation. For both reactions, the carbonyl carbon is expected to proceed from its planar geometry to a tetrahedral intermediate with an asymmetric negative charge distribution (depicted in brackets) during nucleophilic attack. Note that the theoretical deacylation TI for AChE is expected to resemble the aged OP-AChE conjugate (depicted in Scheme 2-1).

Nevertheless, OPs and carbamates differ in the stability of the complex with AChE. Indeed, OPs are able to phosphorylate serine residues of AChE in a non-reversible way, whereas the carbamylation of the same serine residue is less stable,

the typical decarbamylation time being between 30 and 40 min (Kuhr et al. 1976). Carbamate insecticides are also able to reversibly inhibit neuropathy target esterase. However, carbamates are not able to 'age' the inhibited enzyme, and therefore, they are not inducers of neuropathy (Lotti 1992). When animals are dosed with carbamates before neuropathic OPs, carbamates are able to protect from organophosphorus-induced delayed neuropathy. This protective effect is related with the inhibition and no aging of neuropathy target esterase by carbamates. Indeed, the neuropathic OPs are not able to inhibit and 'age' neuropathy target esterase since it has been previously inhibited in a reversible way by the carbamate (Lotti 1992). However, when carbamates are dosed after neuropathic or subneuropathic doses of OPs they promote the delayed neuropathy or make it more severe. This toxic effect is called 'promotion' of delayed neuropathy (Lotti 1992; Lotti et al. 1999).

As was described for the OPs, the main detoxification routes of carbamate insecticides are hydrolysis and oxidation, and the hydrolysis by CbEs (carboxylesterases) is a most effective detoxification route. Although the role of esterases in the carbamate detoxification is well understood, there are no in-depth toxicological and biochemical studies in mammals on interactions between these enzymes and carbamate insecticides.

2.3. Fate of Pesticides in the Environment

Agrochemicals that are present in surface water may associate with the particles and become part of the sediment phase. It is also likely that some agrochemicals are transported into salt marshes and into the bottom layer of estuaries (Schwarzenbach

et al. 1985; Racke 1993; Augspurger et al. 1996; Noblet et al. 1996; Wall et al. 1998). In sediments, salt marshes and the bottom layer of estuaries, anoxic conditions are typically prevalent. Transformation processes occurring under anoxic conditions may represents an important sink for agrochemicals. The same transformation processes are likely to be of importance in constructed wetlands. One design criterion for constructed wetlands is to maximize retention times in order to remove pesticides from the surface runoff by sorption followed by sedimentation. Over time, contaminated sediments may eventually re-release agrochemicals into the environment. In order to utilize the potential attenuating capacity of engineered wetlands, a better understanding of the fate of agrochemicals under anoxic conditions is desirable. This understanding is critical in designing constructed wetlands for areas where natural wetlands have been put into crop production in order to increase farm yield. Moreover, if transformation products are of toxicological concern, information is also needed concerning their subsequent fate in wetland environment.

The degradation of OPs in water can occur via a variety of pathways. Oxidation of OPs to the corresponding oxons, sulfones, and sulfoxides has been reported widely (Lacorte et al. 1994; LaCorte et al. 1995). Oxidation can occur either biotically via specific enzymes or abiotically by radical mechanisms, ozone, dissolved oxygen, or aqueous chlorine. Photodegradation can occur either by a direct photolysis of OPs, which have an absorption spectrum overlap with the solar spectrum or by indirect photodegradation, whereby dissolved humic and fulvic acids can act as a sensitizer or when particles can lead to semiconductor-promoted photodegradation.

Hydrolysis of OPs is perhaps the most thoroughly studied process. It can occur by a homogeneous mechanism, where H_2O and OH^- (H^+ catalysis is less common) act as nucleophiles in an S_N2 mechanism. Alternatively, it can take place when dissolved metal ions enhance the rate of hydrolysis by catalysis (Mortland et al. 1967; Wan et al. 1994). Finally, heterogeneous surfaces such as Fe and Al oxides and different clays can enhance the rate of hydrolysis by providing surface sites at which the nucleophile and the OP can react (Racke et al. 1996; Smolen et al. 1997; Dannenberg et al. 1998). The mechanism of surface catalyzed hydrolysis of OPs remains largely uncertain at this time, although many mechanisms have been proposed (Smolen et al. 1997).

2.3.1. Adsorption

Adsorption by soil can be a key step in the degradation of an OP in many aquatic environments. The degree of adsorption and the rate and extent of ultimate degradation are influenced by a number of factors. These include solubility, volatility, charge, polarity, molecular structure, and the size of the pesticides. The adsorption of an OP by soil components may have several effects. Under some conditions it can retard degradation of OPs by separating the pesticide from the enzymes that degrade it, while at other conditions, an enhancement may occur. Abiotic hydrolytic degradation may also be enhanced by adsorption (Smolen et al. 1998). Furthermore, the loss of OPs by volatilization or leaching is diminished after adsorption.

The forces holding a pesticide to soil particles may be of several types. Physical adsorption via van der Waals forces arises from dipole-dipole interactions between the pesticide and soil particles. Ion exchange is especially effective for cationic

pesticides adsorbed to negatively charged soil particles. Protonation of neutral OPs can also result in the ion exchange mechanism of adsorption. Hydrogen bonding is another mechanism by which OPs can adsorb to soils. Finally, a metal-ligand chelate can form between soil mineral ions such as Fe^{3+} and Al^{3+} and oxygen, nitrogen, or sulfur atoms of OPs (Dannenberg et al. 1998; Smolen et al. 1998). Adsorption and the resulting reduced mobility of OPs in soils are important factors affecting their behavior in nature. From an environmental point of view, it is of great importance to assess the sorption of pesticides by soil, because these phenomena affect other processes that determine the compounds' final fate, such as chemical, photochemical, and microbiological decomposition, volatilization, uptake by plants and difftusion (Beltran et al. 1995). This, together with the increasingly frequent occurrence of OPs in the surface and groundwater worldwide, has drawn the attention of environmental researchers.

Adsorption of OPs in soils is best described by an adsorption isotherm, which may be obtained by measuring adsorption at a number of different concentrations. Frequently, such isotherms are nonlinear, and it is found that they may be described by the empirical Freundlich equation:

$$C_s = KC_w^n \qquad (2\text{-}1)$$

$$\ln C_s = \ln K + n\ln C_w \qquad (2\text{-}2)$$

where C_s, is the amount of adsorbed pesticide on 1 g of soil (g/g soil), C_w, is the concentration of the pesticide in the solution at equilibrium (g/mL of aqueous phase), K and n are constants. K is the amount adsorbed for an equilibrium concentration of 1 g/mL soil, and therefore it represents the adsorption at low levels

of adsorbate concentration and n is a measurement of the intensity of adsorption and reflects the degree to which adsorption is a function of concentration.

Major factors that affect the adsorption of a given pesticide in soil include the organic matter content in soils (OMC), the characteristics of soil (i.e., clay content, moisture content, porosity, permeability, pH of soil, etc.), the temperature of soil, the cation exchange capacity (CEC), and the structure of pesticides. Among these factors, OMC has been proven to be the most important one (Sanchez-Martin et al. 1991; Arienzo et al. 1994; Beltran et al. 1995). The capacity of OMC to retain the pesticide varies depending on where the soils are derived. The characteristics of soils are another significant factor determining the degree of adsorption. Baskaran (Baskaran et al. 1996) concluded that soils exhibiting greater adsorption contain short-range order clays (e.g., allophane). Domagalski and Dubrovsky (Domagalski et al. 1992) assessed the contamination of 13 pesticides in ground water in the San Joaquin valley, where about 10% of the total US pesticides are used. Their results showed that the areas that are most susceptible to contamination of ground water by pesticide residues (i.e., low adsorption) are the coarse-grained or sandy soils without hardpan layers, low clay content, high permeability and porosity, cracked or channeled soil structure and low soil moisture-holding capacity.

Adsorption is an exothermic process. Thus, the adsorption of pesticides in soil decreases as the temperature increases. Mandal and Adhikari varied the temperature from 10 to 33.0 °C; this change resulted in decreasing adsorption, although not significantly (Mandal et al. 1997). Previous studies obtained different results on the effects of soil pH on OP adsorption. Mandal and Adhikari (1997) concluded that pH

showed very little effect on the adsorption of methyl parathion and fenitrothion in soils (Mandal et al. 1997). The molecular structure of OPs has an important influence on adsorption, because it determines the physical and chemical properties. Few studies have investigated the kinetics of OP adsorption in soils. Sujatha and Chacko studied the adsorption of malathion and methyl parathion to three different estuarine sediment types (Sujatha et al. 1992). They observed that the kinetics of pesticide adsorption follows a first-order pattern. Data from Baskaran showed sorption to be a two-stage process with a short initial phase of rapid sorption, followed by an extended period of slower sorption (Baskaran et al. 1996). They concluded that the initial rapid sorption appears to be on the external surface of the sorbents and, as sorption proceeds, rates slow and sorption is by diffusion onto internal sites.

2.3.2. Photodegradation

The photodegradation of various OPs has been studied over the last few years. Photodegradation includes homogeneous photodegradation, heterogeneous photodegradation, and sensitized photodegradation. The rates of homogeneous degradation are usually relatively fast, and the products of degradation vary, ranging from the oxidized P=S bond, to products resulting from isomerization of the starting OP (Durand et al. 1994; Wan et al. 1994). Because many of the studies use a significant fraction of methanol to increase the solubility of the OP for analytical detection reasons(Durand et al. 1994; Sharrna et al. 1994), it is unclear what effect methanol may play as a sensitizer and how relevant the obtained rate constants are for natural water systems. Some of the photodegradation studies using ambient sunlight suggest very short half-lives of the order of hours or less. Therefore, one

can conclude that selected OPs have a significant absorption spectrum overlap with solar wavelengths. Photolysis may also be a very important degradation pathway in the aqueous environment.

Heterogeneous photodegradation of OPs can occur in natural waters due to the presence of semiconductor solids such as iron oxides and oxidants such as hydrogen peroxide. It is important to realize that H_2O_2, has also been detected in sunlit surface waters around the world (Zika et al. 1985; Moffett et al. 1990). Thus, processes that can produce H_2O_2 in sunlit waters may also affect the loss rates of OPs. It is reported that the OPs such as phorate, malathion and diazinon undergo photooxidation in UV/TiO_2, UV/H_2O_2 and UV/TiO_2/H_2O_2 systems (Doong et al. 1997). Although it is unlikely that these combinations are often available in ambient waters, they can provide a useful framework and a reference point for the importance of iron oxide catalyzed photodegradation in sunlit surface waters. And it also reported that the degradation of OPs in the UV/Fe/H_2O_2 system was more effective than that of OP in the UV/H_2O_2 system (Doong et al. 1998). The key question is how important is heterogeneous photodegoradation of OPs in the overall degradation scheme. First of all, the photodegradation is limited to the surface waters receiving sufficient sunlight and containing heterogeneous surfaces, secondly other substrates (present at higher concentrations when compared with OPs) may adsorb to the surfaces of semiconducting solids and thus be preferentially photodegraded. No studies in ambient waters have been carried out in order to pinpoint the importance of heterogeneous photodegradation pathways, although in controlled laboratory studies the degradation of OPs occurs quite rapidly.

Just like the heterogeneous photodegradation of OPs, the sensitized photodegradation has also been investigated. Acetone and humic substances were added as a photosensitizer in the photolysis of pesticides in laboratory studies (Barcelo et al. 1993; Kamiya et al. 1998). Factors that will determine its importance in natural waters include sunlight intensity, the sources and the concentrations of humic and fulvic acids, the concentration of nitrate (a common source of OH radicals) in natural waters, and the presence of other compounds in water (e.g., carbonate and bicarbonate ions), which can scavenge the photoactive species of DHM (dissolved humic material) or OH radicals. Finally, as mentioned before, certain OPs photolyze quite readily via a direct absorption of sunlight and would be less likely to undergo significant sensitized photodegradation.

During photodegradation of OPs, several types of products are typically formed. For instance, during photodegradation of Fenitrothion, the oxidation of P=S to P=O was observed, in addition to the formation of S-methyl isomer of Fenitrothion (Durand et al. 1994; Lacorte et al. 1994). A cleavage of the P-O bond (similar to what is expected during hydrolysis) was also observed with the concomitant production of 3-methyl-4-nitrophenol. Some short-lived intermediates were also observed at the beginning of the photodegradation. In the photodegradation of Diazinon under UV irradiation in a water/soil suspension, Diazinon's isomer, isodiazinon, was found as one of the products. This product is again formed by internal rearrangement, similar to the case of the S-methyl isomer of Fenitrothion (Mansour et al. 1997). In photodegradation studies of several other OPs, several simple ionic products including PO_4^{3-}, SO_4^{2-}, NH_3. NO_3^-, and Cl^- were formed. These products can be

considered to be the final, stable products formed via several short-lived intermediates. Finally, it is important to realize that depending on the hydrolytic half-life of the OP, it is entirely plausible that both photodegradation and hydrolysis occur simultaneously. Therefore. The product identities obtained in many "photodegradation studies" may not be due to photodegradation, but also due to hydrolysis.

2.3.3. Oxidation

The oxidation of OPs can occur by a direct absorption of light, by an attack of photoproduced radicals, or by aqueous oxidants such as dissolved oxygen, aqueous chlorine, or by enzymatic reagents such as oxygenases.

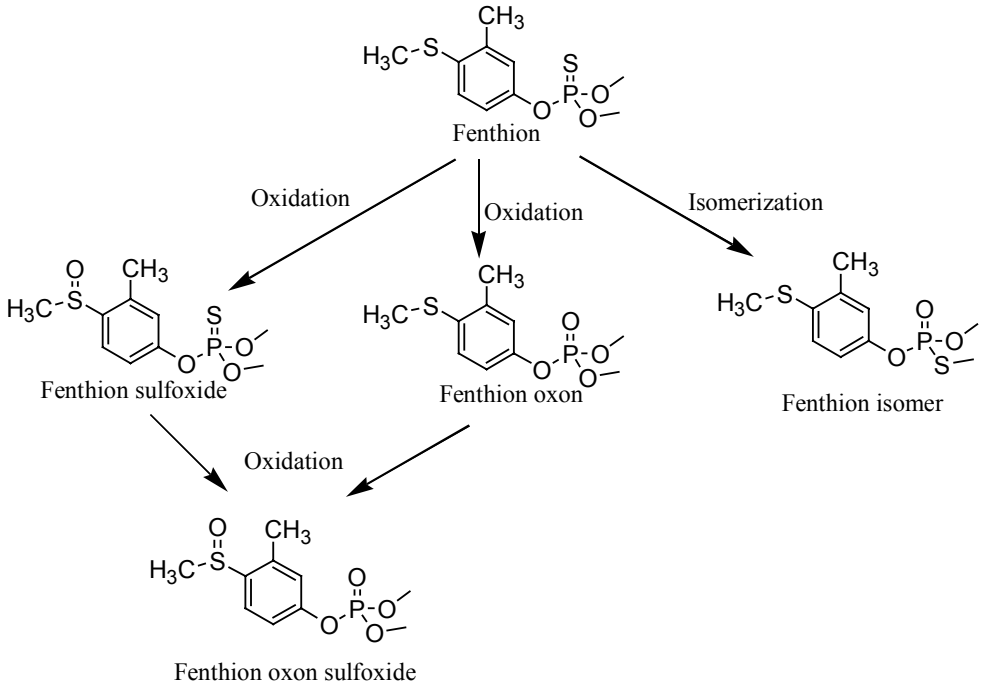

Scheme 2-3. Structural formula of fenthion and its degradation products and schema of the oxidative pathway after fenthion with N-bromosuccinimide (Lacorte et al. 1997)

In Scheme 2-3, Fenthion and its oxidation products are shown (Lacorte et al. 1997). The oxidation schemes shown Scheme 2-3 in are quite typical for other OPs as well, and thus can be used as an example of the types of products expected during OP oxidation. In the case of Fenthion (Scheme 2-3), the products were found after oxidation with N-bromosuccinimide. These products are Fenthion oxon (from the replacement of the doubly bonded S with O, Fenthion sulfoxide (from the oxidation of the S in one of the ester side chains), Fenthion oxon sulfoxide (from the combination of the above two), and finally the S-methyl isomer of Fenthion (by an internal rearrangement). An oxidation product that is not shown in Scheme 2-3, but whose formation is possible during the oxidation of OPs is sulfone. Sulfone is formed when sulfoxide in the ester side chain is further oxidized to yield two S=O bonds on a single sulfur atom. Demeton S and Phorate are two examples of OPs, whose oxidative degradation has yielded both sulfoxides and sulfones.

2.3.4 Hydrolysis

Hydrolysis is the most thoroughly studied degradation pathway of OPs. Hydrolysis in the environment includes biotic and abiotic pathways.

2.3.4.1 Biotic Hydrolysis

Enzymes that are able to hydrolyze many OPs are known from a large number of aquatic species (i.e.. from fish to bacteria) (Landis 1991). These enzymes are currently called the organophosphorus acid anhydrases (OPH), although they have also been referred to as an esterase, DFPase, phosphotriesterase, somanase, parathion hydrolase, and paraoxonase. The natural substrates for the OPH are not known. However, these enzymes are capable of hydrolyzing a wide variety of organophosphorus acetylcholinesterase inhibitors. In aquatic species, the enzymes

have been identified and partially characterized from squid, fish, invertebrates such as Rangia cuneata, the protist Tetrahymena thermophila, and various thermophilic and other bacteria. The enzymes have evolved in response to the metabolism of naturally occurring organophosphates and halogenated organic compounds (Landis 1991). Enzymatically mediated hydrolysis is an important and rapid degradation pathway for many OPs. It can be considered a catalytic process whereby the enzyme acts as a catalyst. The mechanism of enzymatic hydrolysis has not been thoroughly investigated, although it is likely that it is similar to hydroxide ion induced S_N2 abiotic hydrolysis. Enzymatic hydrolysis may also result in somewhat different products compared with abiotic hydrolysis. An example of this is the ease of P-S cleavage for many OPs as observed by Lai and Wild (Lai et al. 1995), while in the case of phorate, there is no cleavage of the P-S bond observed (Hong et al. 2000), although it should occur readily based on thermodynamic considerations. The importance of these pathways to the overall OP fate is unknown, although it was found that "biotransformation" was one of the most important processes for disulfoton and thiometon transformation in the Rhine River (Wanner et al. 1989). The main question is whether the "biotransformation" as described by Wanner and Schwarzenbach (Wanner et al. 1989) was enzymatic hydrolysis or biotic oxidation. Finally, it is not clear how ubiquitous OPH is in most natural waters and thus how important its role is in the overall OP fate.

2.3.4.2 Abiotic Hydrolysis

The abiotic hydrolysis of OPs was examined in different environmental related condition. Both homogeneous and heterogeneous studies were carried out at a variety of different condition. And the activation enthalpy and entropy were also

studied for the OPs in order to use the activation enthalpy and entropy approach to gain insight into the kinetics and mechanisms of OP hydrolysis. Some useful insight can be gained following this type of treatment, although there are still too many variables to pinpoint the mechanism.

As for other esters, hydrolysis of OPs occurs via acid-catalyzed, base-catalyzed, and neutral mechanisms. And the hydrolysis products of these compounds, that is, the di- and monoesters, are also of environmental concern inasmuch as thay usually react at a lower rates as compared to the triesters (Mabey et al. 1978; Wolfe 1980). When trying to understand the reactivity of OPs, it is important to realize that such compounds may react by nucleophilic displacement (S_N2) both at the phosphorus atom (with an alcohol moiety being the leaving group) and at the carbon bound to the oxygen of an alcohol moiety (with the diester being the leaving group)

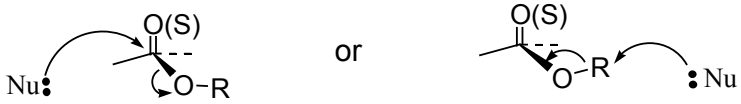

(2-3)

For attack at a saturated carbon atom, OH^- is a better nucleophile than H_2O by about a factor of 10^4. Toward phosphorus, which is a harder electrophilic center, the nucleophilicity increases dramatically. For example, OH^- is about 10^8 times stronger than H_2O as a nucleophile for triphenyl phosphate (Barnard et al. 1961). Consequently, the base-catalyzed reaction generally occurs at the phosphate atom leading to the dissociation of the alcohol moiety that is the best leaving group (P-O cleavage).

Depending on the alcohol moieties present, the neutral reaction as well as reactions with soft nucleophiles (e.g.. HS^-, CN^-) may also proceed by nucleophilic

substitution at a carbon atom (C-O cleavage). Therefore, if a good leaving group is present, the neutral reaction may proceed by both reaction mechanisms, that is C-O as well as P-O cleavage. For example, Weber (1976) found that at 70 °C and pH 5.9, parathion reacted 90% by C-O cleavage. At lower temperatures, a higher proportion of the neutral reaction occurred by P-O cleavage. This observation can be explained by the higher activation energy of the reaction involving C-O cleavage as compared to P-O cleavage (Weber 1976). This example shows us that when dealing with OPs, we have to be aware that under different conditions, different hydrolysis mechanism may prodominate.

In most cases, hydrolysis of OPs is quite insensitive to acid catalysis unless there is a base function present in one of the alcohol moieties. If such a base is protonated, the reactivity is enhanced. Examples are the two insecticides diazoxon and diazinon, where protonation of one of the nitrogens of a pyrimidine ring renders the alcohol moiety a much better leaving group (Faust et al. 1972; Mabey et al. 1978).

Metal ion-catalyzed hydrolysis of OPs is an important process focuses on the speciation of the metal ion and its concentration. Wan and co-workers (1994), investigated the catalyzed hydrolysis of some OPs by Hg(II) ion. The presence of $HgCl_2$, at 20 ppm increased the initial hydrolysis rates of malathion. fenitrothion, fenthion, and parathion-methyl in a pH 5.5 buffer by two to three orders of magnitude, while Hg(II) ion had little effect on dichlorvos hydrolysis. The hydrolysis was found to be first order with respect to both the Hg(II) ion and the OP (Wan et al. 1994). The main hydrolysis product was 3-methyl-4-nitrophenol for fenitrothion, and 4-nitrophenol for parathion-methyl.

Earlier studies on metal-promoted hydrolysis have reported overall rate constants as a function of the total metal concentration and the effect of metal ion speciation (Smolen et al. 1997; Zeinali et al. 1998). The divalent metal ion-catalyzed hydrolysis of thionate (P=S) and oxonate (P=O) OPs has been examined with three proposed mechanisms: (1) metal ion coordination of the thionate sulfur or oxonate oxygen to enhance the electrophilicity of P; (2) metal ion coordination and induced deprotonation of H_2O to create a reactive nucleophile; and (3) metal ion coordination of the leaving group to facilitate its leaving (Smolen et al. 1997). There are three advantages in reporting the relative importance of the different species: (1) results can be extrapolated from one situation to another, (2) rates can be predicted for specific conditions, and (3) a better understanding of the catalysis mechanism can be obtained.

In ambient waters, many chelating agents are present, and although some of the above studies probed the effect of metal ion speciation, it is still unknown how effective these metal ions are in the presence of strong chelating agents such as siderophores and components of humic and fulvic acids. No studies to date have really addressed this important issue. A second important consideration is whether some of the aforementioned metal ions are going to be present at high enough concentrations in natural waters to effect catalysis. For example, Hg(II) is not usually present even at submicromolar levels, and therefore its influence may be very limited. Some of the other ions are more abundant, yet the aforementioned speciation may reduce the overall catalytic ability.

The abiotic hydrolysis of the OPs was examined in different soils and minerals, which were chosen to represent a variety of physicochemical characteristics (Torrents et al. 1994; Racke et al. 1996) for investigating heterogeneous hydrolysis. Correlation analyses indicated that soil pH was the independent variable displaying the strongest association with the hydrolytic rate constants of OPs (Racke et al. 1996). The study of oxide surface-catalyzed hydrolysis of carboxylate and phosphorothioate esters proved the organic pollutant degradation might be affected via interaction with the surfaces of oxides and other soil minerals (Torrents et al. 1994). The heterogeneous hydrolysis may also involve the adsorption of the pesticide into the interlayer space of soils and minerals forming a complex with the interlayer cations, and enhancing the electrophilicity of phosphorus atom. The above facilitates an S_N2 attack by OH^- and the cleavage of the P-S bond (Sanchez-Martin et al. 1991).

Heterogeneous hydrolysis is another pathway difficult to assess carefully. Factors such as the presence of other chemicals that may preferentially adsorb to the surface of metal oxides or clay particles must be considered. Secondly, the hydrolysis products may also adsorb to the clay particles or metal oxides, slowing down the further hydrolysis of OPs themselves. Other factors that have been shown to play an important role in heterogeneous OP hydrolysis include the nature of the clay material, the identity of the exchangeable cations, soil moisture content, and soil pH. Although the ultimate degradation product of OPs is phosphate, it is seldom formed at a fast enough rate to be of consequence in most environmental systems. The di- and monoesters of OPs typically hydrolyze at much lower rates when compared

with the triesters. Moreover, it is very likely that the most environmentally relevant degradation products originate from the thioester side chain of OPs, because the thioester side chain is usually the leaving group after the initial hydrolysis step (i.e., the cleavage of the P-S bond in phosphorodithioates). Furthermore, it contains the most complicated and varied structural moieties. As the sulfur-containing ester group is usually a much better leaving group than the alkoxy groups (either methoxy or ethoxy in most cases), the initial phosphorus containing hydrolysis product is either $(RO)_2P(S)OH$ or $(RO)_2P(S)SH$. It needs to be noted that the formation of a P-O bond is very favorable from a thermodynamic point of view (i.e., P-O bond is ~40% stronger than P-S bond), particularly in H_2O. The hydrolysis products of OPs can be numerous and usually involve the cleavage of the P-S bond (in the case of phosphorodithioates and phosphorothiolates) or the P-O bond (in the case of phosphorothioates) that results in the best leaving group. A good example of the P-O bond cleavage can be found from the hydrolysis of diazinon (a phosphorothioate) where the oxygen attached to the pyrimidine ring can stabilize the negative charge most effectively. Similar behavior can be found for the other phosphorothioates. The same argument regarding the leaving groups can also be made for phosphates. Once the initial cleavage has occurred, the ester (or thioester) fragment can undergo additional reactions.

OPs may be degraded into compounds that also have pesticidal activity against target and/or non-target pests (Coats 1993). Relatively few studies have documented, the level of product pesticidal activity. However, the few studies indicate that the products may' be more, less, or similar in activity to the parent

pesticide (Coats 1993). The prolonged efficiency of many insecticides against foliar feeding insects depends on OP absorption, from soil by plants and their metabolism into water-soluble but equally toxic anticholinesterase agents (Sogorb et al. 2002). In the soil, the more water-soluble products of OPs are less toxic to insect larvae than the parent OPs, although when these compounds are topically applied toxicity is similar. For example, the hydrolysis of chlorpyrifos to 3.5,6-trichloro-2-pyridinol results in a total loss of insecticidal activity, but the product is bioactive against several fungal pathogens.

It is clear from the field studies that various OP pesticide degradation mechanisms are concurrently reducing their load in the aquatic environment. As hydrolysis, photodegradation, and microbial degradation all have large seasonal fluctuations, their relative importance in OP fate also varies from one season to the next (Wanner et al., 1989). Some of the field studies have identified OP degradation products, while others have not. Without the proper monitoring for OP degradation products, it is difficult to ascertain which degradation pathway is the most dominant one, more importantly it also makes it difficult to assess the overall ecological impact of OPs in ambient waters.

Furthermore, multiple pathways are simultaneously degrading the OPs, and therefore it is very desirable to characterize the stable final products of OP degradation. In order to isolate and assess the relative importance of various degradation pathways in field studies, it may be useful to manipulate the ambient water samples and carry out additional experiments in the laboratory (e.g., the addition of biocide followed by OP spiking can aid in the determination of abiotic

degradation rate). The addition of radiolabeled OPs to collected ambient water samples may be another way to assess their degradation in a simple, robust way. Finally, it should be noted that the molecular structure of the OP plays a very important role in determining the degradation rate; therefore, generalizations regarding degradation rates must be made with extreme caution.

2.4. Reduced sulfur species

Anoxic conditions can give rise to high concentrations of reduced sulfur species. These versatile environmental "reagents" are capable of reacting with a wide array of pollutants, including organic contaminants that undergo nucleophilic substitution reaction. This reaction may take place at rates which exceed those of hydrolysis under conditions that are common in reducing environments. In the discussion, a "sulfur nucleophile" is not only a nucleophile which contains sulfur, but one in which the atom that donates electrons to form a bond with the electrophile is a sulfur atom.

The most common sulfur nucleophiles encountered in natural waters are the following species: H_2S, HS^-, S^{2-}, thiolate anions (RS^-), polysulfides (S_n^{2-}, where n>1), $S_2O_3^{2-}$, $S_4O_6^{2-}$, and SO_3^{2-}. Unlike sulfate, all of these nucleophiles are thermodynamically unstable in the presence of O_2. Hence, they are most commonly found in hypoxic environments (i.e., natural waters containing very low or undetectable levels of dissolved O_2), usually in the presence of high concentrations of reduced organic matter. Environments of this type include marine, estuarine, and marsh porewaters, groundwaters containing high concentrations of leachate derived from domestic refuse (e.g., beneath landfills), and hydrogeologic zones located far down-gradient from their recharge areas (Barbash et al. 1989).

The speciation of sulfur among its various forms in a particular environment arises from a balance among several simultaneous chemical and biochemical processes, including oxidation and reduction (usually with microbiological mediation), hydrolysis, dissolution, and precipitation. Decomposition of organic matter by sulfate reducing bacteria leads to the formation of hydrogen sulfide and an increase of other metabolites.

Hydrogen sulfide occurs naturally in crude petroleum, natural gas (even up to 28%), volcanic gases, and some hot springs. Sulfate-reducing bacteria obtain their energy by using sulfates to oxidize organic matter or hydrogen, thereby reducing the sulfates to hydrogen sulfide. They are especially efficient in low-oxygen environments, such as in swamps and standing waters. Hydrogen sulfide-producing bacteria also operate in the human colon, and the odor of flatulence is largely due to trace amounts of the gas. They can also be found in the mouth and contribute to bad breath. Hydrogen sulfide can also result from industrial activities, such as food processing, sewage treatment, coke ovens, paper mills (using the sulphate method), tanneries, and petroleum refineries, in coal mines (as iron sulfides such as pyrite decompose) and anywhere where sulfur comes in contact with organic material at high temperatures. Hydrogen sulfide is a covalent hydride chemically similar to water (H_2O) since oxygen and sulfur occur in the same periodic table group. Hydrogen sulfide dissociates in solution into hydrogen cations H^+ and the bisulfide anion HS^-:

$$H_2S \rightarrow HS^- + H^+ \qquad (2\text{-}4)$$

$K_a = 1.3\times10^{-7}$ mol/L; $pK_a = 6.89$.

The sulfide ion, S^{2-}, is known in the solid state but not in aqueous solution (c.f. oxide). The second dissociation constant of hydrogen sulfide is often stated to be around 10^{-13}, but it is now clear that this is an error caused by oxidation of the sulfur in alkaline solution. The current best estimate for pK_{a2} is 19±2 (Giggenbach 1971; Meyer et al. 1983). The hydrogen sulfide could process biotic or abiotic oxidation with oxygen or other oxidants in water. HS^- oxidation can either result in complete regeneration of sulfate, or result in the formation of sulfur species of intermediate oxidation state including polysulfides (Giggenbach 1972; Giggenbach 1974; Licht et al. 1997; Gun et al. 2000), which are more highly reactive nucleophiles than HS^-.

$$HS^- + \frac{(n-1)}{8} S_8(s) \longleftrightarrow S_n^{2-} + H^+ \; ; \; K_{eq} = \frac{[S_n^{2-}][H^+]}{[HS^-]} \qquad (2\text{-}5)$$

Unlike the other reduced sulfur nucleophiles, polysulfides represent a group of compounds with varying number of sulfur atoms. Polysulfides are formed through the reaction between HS^- and S^0. According to Giggenbach (Giggenbach 1972), all ions S_n^{2-} with n = 2-5 are formed in significant amounts within the small pH range of 10-13, while the tetra- and pentasulfide ions predominated in solutions of intermediate alkalinity (pH 9-14).

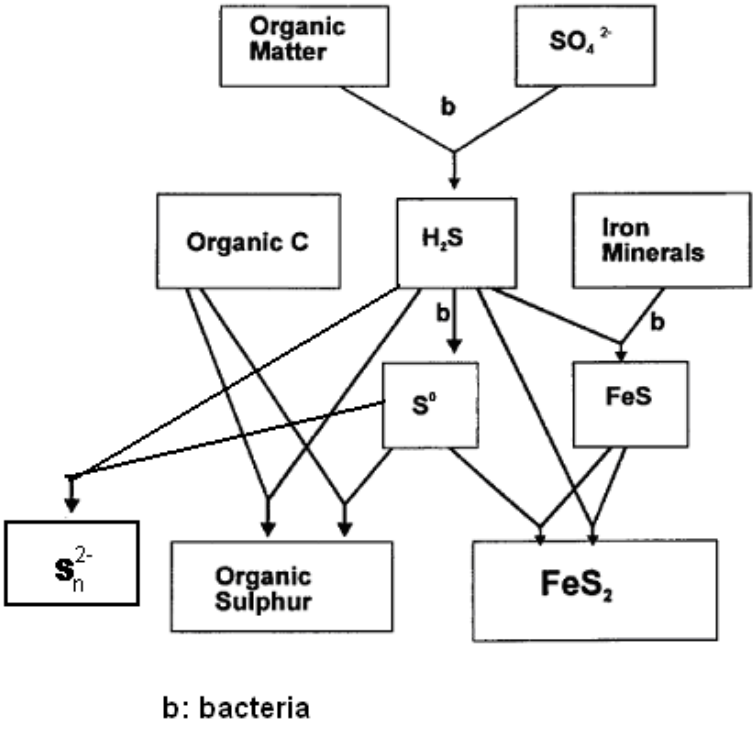

Figure 2-3: Sulfur diagenesis model in anoxic marine sediments.

Figure 2-3 shows an sulfur diagenesis model in anoxic marine sediments (Henneke et al. 1997). Species which are partially reduced (i.e., forms in which sulfur exhibits an oxidation state between those of SO_4^{2-} and $H_2S(aq)$), such as S_n^{2-}, $S_2O_3^{2-}$, $S_4O_6^{2-}$, and SO_3^{2-} may be produced by the oxidation of $H_2S(aq)$ and sulfide minerals, the reductive dissolution of goethite by HS^-, the hydrolysis of polysulfides, and microbial processes (Boulegue et al. 1982; MacCrehan et al. 1995). The concurrent operation of several of these processes in a particular environment may give rise to a complex assemblage of sulfur nucleophiles. For example, Boulegue and Church (Boulegue et al. 1982) detected $H_2S(aq)$, S_8, $S_2O_3^{2-}$, SO_3^{2-}, S_n^{2-}, SO_4^{2-}, thiols, and organic polysulfides in the porewaters of a salt marsh along the Delaware estuary.

Table 2-1: Reduced inorganic sulfur species in marine sediments

Species	Source/Role	Sediment Type	Concentration
Sulfide HS^-	Product dissimilatory SO_4^{2-} reduction; energy resource; pyrite deposition	Salt marsh [a] Coastal Estuary [b]	0 - 5.5 mM 0.4 - 2.3 mM 0.5 μM – 5.6 mM
Zero-valent sulfur S^0	Intermediate HS^- oxidation; product $S_2O_3^{2-}$ reduction; respiration	Salt marsh [a] Coastal Estuary [b]	Saturated 0.1 – 0.2 mM < 0.1 – 67 μM
Thiosulfate $S_2O_3^{2-}$	Intermediate HS^- oxidation; product S^0 + SO_3^{2-}	Salt marsh [a] Coastal Estuary [b]	0.1 – 0.6 mM 0.01 – 0.03 mM 0.1 – 7.1 μM
Sulfite SO_3^{2-}	Intermediate SO_4^{2-} reduction, intermediate HS^- oxidation via $S_2O_3^{2-}$	Salt marsh [a] Coastal [b]	< 10^{-4} – 0.2 mM 0.07 mM
Tetrathionate $S_4O_6^{2-}$	Oxidation of $S_2O_3^{2-}$; intermediate SO_4^{2-} reduction	Salt marsh	0.17 – 0.31 μM
Polysulfides S_n^{2-}(n = 2-5)	Reaction of HS^- and S^0; mobilization S^0 and transition metal ions	Salt marsh [a] Estuary [c]	10^{-3} – 0.43 mM 0.02 – 0.2 mM

a Data from Boulegue et al. (1982)

b Data from MacCrehan et al. (1995)

c Data from Shea et al. (1988)

They attributed the observed sulfur speciation to a steady state interaction between the various reduced sulfur species diffusing upward from hypoxic sediments (chiefly H_2S(aq), thiols, and organic polysulfides) and O_2 diffusing downward from the sediment-water interface.

Table 2-2: Hydrophilic organosulfur compounds in marine sediments[a]

Species	Source/Role	Sediment Type	Concentration
Dimethylsulfonio propanoate (DMSP)	Plant osmoslyte	Salt marsh	100 – 200 μM
3-mercapto propanoate	DMSP demethylation product; abiotic addition of HS^- to acrylate	Salt marsh Coastal Estuary	0.5 – 20 μM 20 – 230 nM < 0.04 – 11.8 μM
2-mercapto propanoate	Abiotic acrylate addition of HS^-	Salt marsh Estuary	< 0.5 μM < 0.04 – 3.8 μM
Cystein	Assimilatory SO_4^{2-} reduction, microbial protein degradation	Estuary	< 0.04 – 12.4 μM
Glutathione	Redox cofactor; cysteine repository; S^0 metabolism	Salt marsh Estuary	10 – 2400 μM < 0.04 – 5.4 μM
mercaptopyruvate	Cysteine metabolite; sulfur donor	Coastal Estuary	0.5 – 20 μM < 0.04 – 1.4 μM
mercaptoacetate	Mercaptopyruvate metabolite	Coastal Estuary	< 0.5 μM < 0.04 – 0.60 μM
monothioglycerol		Coastal Estuary	< 0.5 – 20 μM 1.6 – 4.3 μM
N-acetylcysteine		Coastal Estuary	< 0.5 μM < 0.03 – 0.3 μM
thiomalate	Mercaptopyruvate metabolite	Estuary	< 0.04 – 0.08 μM
Also detected: Coenzyme M, 2-mercaptoethanol.			

[a] Data from MacCrehan et al. (1995).

Table 2-1 and 2-2 summarize data from several studies on the distribution and abundance of reduced sulfur species in natural water. The concentrations of reduced sulfur species depend on the sediment depth and sampling time, therefore, the data shows here only give a range of the concentration for each species observed. Noted that the sediment thiols identified to date are generally found in nM to low μM concentrations, whereas the inorganic sulfur species in the same porewaters were generally measured to be in 10's of μM to low mM concentrations.

It has been reported that reduced sulfur species could react with organic compound through nucleophilic substitution (Roberts et al. 1992; Lippa et al. 2002; Loch et al. 2002), elimination (Gan et al. 2006), and NOM mediated reduction (Perlinger et al. 1996; Guo et al. 2006), while the nucleophilic substitution is a very important degradation pathway for many organic contaminant in anoxic and hypoxic conditions.

Hard-soft acid-base (HSAB) model was used to predict the relative reactivity on the nucleophiles and the substrates. HSAB model classified Lewis acids (electrophiles) and bases (nucleophiles) as either "hard" or "soft". Hard acids and bases are relatively small, and exhibit low polarizability and a comparatively low tendency to form covalent bonds. Soft acids and bases have the opposite characteristics. Stated simply, the model postulates that hard acids react most readily with hard bases, and soft acids react most readily with soft bases (Pearson 1963). When using this model to predict the relative reactivity of HS^- and OH^- (important in aqueous solution) towards an OP compound. Sulfur lies directly below oxygen in the periodic table,

indicating that HS^- is more polarizable and has a HOMO which is higher in energy than its oxygen counterpart. HS^- is thus a "softer" nucleophile than OH^-, and consequently would be expected to show a greater reactivity with respect to nucleophilc displacement at a saturated carbon. Conversely, OH^- would be expected to show a stronger affinity toward hard electrophiles and hence result the leaving of the phenyl group of OP compounds. These predictions are consistent with experimental data on the reactivities of HS^- and OH^- in Chapters 4, 5, and 6. Swain and Scott (Swain et al. 1953) developed a Linear Free Energy Relationship to quantify the relative nucleophilicity of various nucleophiles towards reaction with methyl bromide.

$$\log (k/k_{H2O}) = s * n \quad (a) \qquad (2\text{-}6)$$

where k and k_{H2O} are the second-order rate constants for the displacement by a given nucleophile and water, respectively, n quantifies the nucleophilicity of a given nucleophile, and s is a measure of the sensitivity of the methyl halide to nucleophilic attack. Thus when methyl halide is the substrate, equation (2-6) leads directly to the value of n for each nucleophile in aqueous solution at 25 °C (Duboc 1978). This relationship can used to predict the nucleophilicities of a number of nucleophiles is greater than water. However, although water is not a strong nucleophile, it is present in such a high concentrations (55.6 M) that it can effectively outcompete most of the nucleophiles in the natural aqueous environment.

The approximate order of reactivity of sulfur nucleophiles with respect to the displacement of halide from a primary n-alkyl bromide decreases in the following order (Barbash et al. 1989):

$S_5^{2-} \approx S_4^{2-} \approx$ n-HexS$^- >$ n-BnS$^- \approx C_6H_5S^- > HS^- \approx SO_3^{2-} \geq S_2O_3^{2-} >$ RSR' $>> H_2O$

Therefore, it appears that 1) the reactivity of an aliphalic thiolate increases with increasing length of the alkyl chain, which resulted from the increase in polarizability and the decrease in the degree of solvation with increasing alkyl chain length; 2) The protonation of a sulfur nucleophile causes substantial reduction in its nucleophilicity, which is in accordance with the general theory of nucleophilic substitution reactions; 3) The reactivity of an anionic sulfur nucleophile is also greatly diminished when a second alkyl (or arylalkyl) group is attached to the terminal sulfur atom, which probably is a result of both the neutralization of the negative charge (thereby reducing the electron density) and an increase in crowding at the sulfur atom. Beside the above listed tendency, there also other factors that change the nucleophilicity of reduced sulfur species, while the effect of these factors are different for different substrates.

2.5. Summary and Conclusions

Consider all the research, the transformation reactions of OPs in the environment allow general statements to be made regarding the transformation reactions that might be important for various OPs under various conditions. And although much literature reported that the reduced sulfur species greatly promoted the degradation of organochlorine compounds, research on the OPs is limited. So the main objective of this research is to determine whether the sulfur nucleophiles in natural

waters are sufficiently reactive and present in high enough concentrations to react with OP contaminants at rates which are environmentally significant.

Chapter 3. Influence of Reduced Sulfur Species on the Hydrolysis of Carbamate Pesticides

3.1. Introduction:

Chemical pesticides are widely used in agriculture because they contribute to pest control in a very effective way. The three main groups of chemical insecticides are (a) organophosphorus compounds, (b) pyrethroids, and (c) carbamates. Among all of these groups, carbamates probably own the widest range of pesticide activities because they are insecticides, fungicides, and herbicides. Carbamates are commonly used insecticides in agriculture and in urban gardens. They are also effective in controlling pests in buildings and on a wide range of indoor plants (Alvares 1993). The carbamates are a family of compounds whose general structure ($R_1OCONR_2R_3$) is derived from carbamic acid by the introduction of different substituents. Their great success in agricultural applications has led to a continued increase in the use of these pesticides, but their acute toxicity is of great concern and makes the determination of the carbamates at very low concentrations necessary (Delgado et al. 2001). *N*-Methyl-carbamates are among the most widely used insecticides in both agriculture and horticulture. Members of the *N*-methyl-carbamate family of insecticides include carbaryl, carbofuran, oxamyl, methomyl, aldicarb, and pirimicarb. Table 3-1 lists the structure of four investigated carbamates. They are carbaryl, carbofuran, oxamyl, and methomyl. Carbaryl is the most widely used *N*-methyl-carbamate insecticide in use today. In 1997 an estimated 4.9 million pounds of carbaryl were used to treat over 3 million acres in the United States alone. Carbaryl is a nonionic, moderately mobile compound in the environment, and

although it is degraded through both abiotic and microbially mediated processes, carbaryl is the second most widely detected insecticide in surface water (Martin et al. 2003). Carbofuran, which is most commonly sold under the trade name Furadan, is a systemic *N*-methylcarbamate pesticide with predominantly contact and stomach action. It is mainly used as a soil-applied chemical to control soil-dwelling and foliar-feeding insects and nematodes on a variety of agricultural crops, including maize, corn, rice, potatoes, alfalfa, and grapes (Tomlin 1994). Oxamyl and methomyl belong to a class of compounds known as oxime carbamates (or carbamoyloximes). They are widely used for the control of insect and nematode pests. Nearly three million pounds are applied annually to U.S. agricultural fields (Gianessi et al. 2000). They are systemic pesticides, taken up through root or leaf surfaces and distributed throughout the plant (Hassall 1990). Concern has risen due to their extremely high water solubility (280 g/L for oxamyl and 58 g/L for methomyl) (Hornsby et al. 1996) and low sorption affinity to soils (Cox et al. 1993); both properties suggest a high degree of mobility in soil and aquatic environments. In fact, oxamyl and methomyl have been detected by groundwater surveys conducted throughout the United States (Ritter 1990).

Table 3-1: Structure of Four Investigated Carbamate

Common name	Molecular Structure	IUPAC name	M.W.
carbofuran	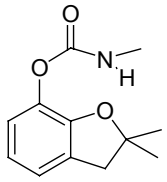	2,3-dihydro-2,2-dimethylbenzofuran -7-yl methylcarbamate	221.25
carbaryl	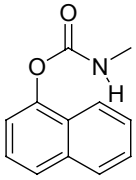	1-naphthyl methylcarbamate	201.22
oxamyl	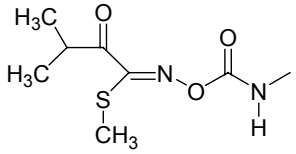	N,N-dimethyl-2-methyl carbamoyloxyimino-2-(methylthio)acetamide	218.07
methomyl	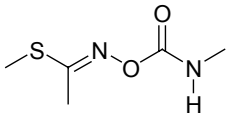	S-methyl-N-[(methylcarbamyl)oxy] thioacetamide	162.05

The acute toxic effects of carbamate pesticides are based on the inhibition of acetylcholinesterase. Indeed, they are able to carbamylate a serine residue of acetylcholinesterase, yielding an inhibited enzyme and originating the typical cholinergic acute effects (lacrimation, salivation, miosis, convulsions, and death) on the basis of acetylcholine accumulation on synaptic terminals (Alvares 1993). And also the carbamylated enzyme-inhibitor complex can be hydrolyzed by a water molecule, yielding a free active enzyme (Alvares 1993). In addition to the described cholinergic effects, the carbamates exhibit other important toxic effect called "promotion" (Lotti et al. 1999). When animals are treated with carbamates after subneuropathic insults (organophosphates, 2,5- hexanedione,

bromophenylacetylurea, or even traumatic axonopathy which is a disorder cause by the psychological injury and affecting primarily the axons of peripheral nerve fibres (*3*)), the subsequent neuropathy is promoted or becomes more severe.

Carbofuran is a potent cholinesterase inhibitor [IC_{50} in rats is (1.2-3.3) $\times 10^{-8}$ M], so it is highly toxic to humans and wildlife through the oral and inhalation routes of exposure (acute oral LD_{50} in rats is 8 mg kg^{-1}) (Gupta 1994). In fact, carbofuran has been involved in recent years in numerous cases of bird poisoning, which prompted the U.S. Environmental Protection Agency and Agriculture Canada to review all registered uses of granular carbofuran in their respective countries (James 1995; Augspurger et al. 1996). As a result of its widespread use worldwide, with ~300,000 pounds of active ingredient applied per year in the period 1992 - 1995 in only California (CDPR 1993; 1995). Carbaryl controls a wide spectrum of insect pests across a wide range of use sites, both agricultural and non-agricultural. EPA reviewed carbaryl's use patterns on many sites, and used that information in forming a regulatory position and determining the mitigation measures necessary to address risks of concern. In particular, EPA considered the benefits associated with the use of carbaryl on citrus, especially in Florida and California, and grapes to evaluate occupational and ecological risks (EPA).

Oxamyl and methomyl act by inhibiting the enzyme acetylcholinesterase. The fate of oxamyl and methomyl in the environment is of interest because their acute toxicity ranks among the highest of all pesticides in use today (oral LD_{50} rat 5 mg/kg for oxamyl and 21 mg/kg for methomyl) (Hassall 1990). Groundwater contamination by pesticides has been of increased concern in recent years (Kolpin et

al. 1998). Since a large number of pesticides, including carbamate pesticides, have been detected in groundwaters that serve as sources of drinking water. Reported carbamate pesticides concentrations have often been found to exceed recommended health guidelines (Zaki et al. 1982; Moye et al. 1988; Barbash et al. 2001). Concern about groundwater contamination by carbamate pesticides is especially high because their properties (high aqueous solubility and low sorption to most soils) suggest a high degree of mobility in soils and groundwater (Hornsby et al. 1996). Abiotic carbamates degradative processes that are important in soil include hydrolysis, oxidation, reduction, and photolysis (on the soil surface). Although investigations of the significance and mechanisms of hydrolysis have been conducted for several carbamates, hydrolysis has not been thoroughly examined as other important means of degradation (microbial degradation, photolysis). Due to the complex nature of the aqueous environment, in which it is often difficult to isolate simultaneously operating degradative processes, may have discouraged more extensive investigations. However, published reports indicate that for carbamate insecticides, the two main routes for the degradation are the oxidation and the hydrolysis of the carbamic ester bond (Alvares 1993). The chemical structure of carbamate insecticide renders these compounds susceptible to hydrolysis. In addition, the products resulting from the oxidation of parental carbamate still conserve the intact carbamic bond; therefore, they can also be hydrolyzed. Thus, hydrolysis seems to be a critical step in the degradation route of carbamates.

Inorganic sulfur species are known to be very strong nucleophiles and reductants, HS^- is the dominant reduced sulfur species in neutral or near neutral solution (Licht

et al. 1990; Licht et al. 1997). It is reported that concentrations of hydrogen sulfide species (HS^-/H_2S) can reach up to 5 mM (MacCrehan et al. 1995).

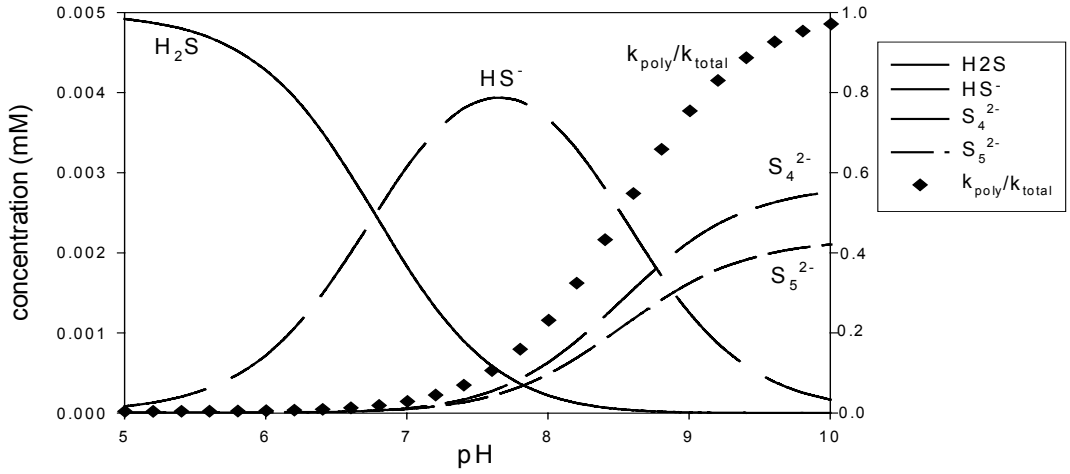

Figure 3-1: Calculated distribution of hydrogen sulfide/polysulfide species illustrating how the relative contribution of $k_{Sn^{2-}}[S_n^{2-}]$ to the overall pseudo first-order rate constant $k_{overall}$ would be expected to vary with pH. Assumptions: 5 mM $[H_2S]_T$ in equilibrium with elemental sulfur; based on equilibrium constants reported by Giggenbach; S^{2-}, HS_4^-, and HS_5^- have been included in the calculations, but their concentrations are very small and have been neglected in the Figure. The overall pseudo first-order rate constant was calculated as $k_{overall} = k_{H2S}[H_2S] + k_{HS^-}[HS^-] + k_{Sn^{2-}}([S_4^{2-}] + [S_5^{2-}])$, assuming: $k_{H2S}=0.001\ M^{-1}s^{-1}$, $k_{HS^-}=0.01\ M^{-1}s^{-1}$, $k_{Sn^{2-}}=1\ M^{-1}s^{-1}$. $k_{poly}/k_{overall}= k_{Sn^{2-}}[S_n^{2-}]/k_{overall}$. Polysulfides dominate the abiotic fate of a contaminant if $k_{poly}/k_{overall} > 0.5$.

According to Giggenbach (Giggenbach 1972; Giggenbach 1974), the tetra- and pentasulfide ion are the predominated ions in solutions of intermediate alkalinity when S_8 is in excess (Figure 3-1). It is reported that the concentration of polysulfide could be 0.5 mM in salt mash porewater (Gun et al. 2000). Studies have shown that

polysulfide can be the fate determining reagent for some organic contaminants (Barbash et al. 1989; Roberts et al. 1992; Miller et al. 1998).

It has been reported that the hydrolysis of primary carbamates (e.g., carbofuran, carbaryl) proceeds through an elimination mechanism involving the formation of an isocyanate (Hegarty et al. 1973; Strathmann et al. 2001) (Equation 3-1).

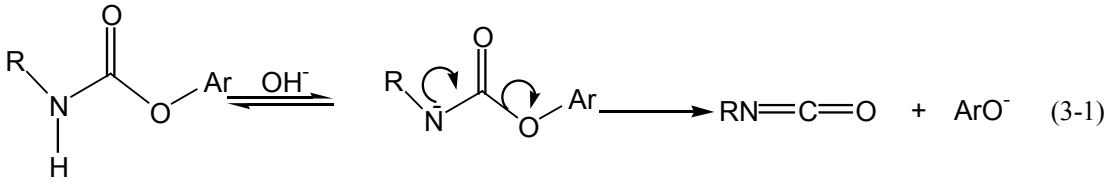

(3-1)

In the presence of reduced sulfur species, intermediates of the hydrolysis might react with reduced sulfur species resulting in the formation of degradation products. Even though the oxime carbamates (or carbamoyl oximes which form the oxime after hydrolysis) are likely to undergo a base-catalyzed elimination reaction (E1cb mechanism) in aqueous solution, which means the acyl-oxygen bond cleavage is considered in the transition state in accordance with the E1cb pathway (Equation 3-2).

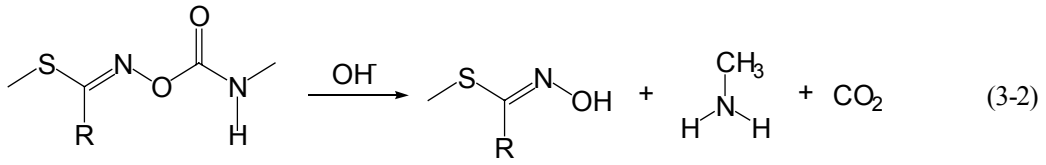

(3-2)

It is possible that strong nucleophiles such as polysulfides will react with carbamates. In the case of carbaryl, such a nucleophilic replacement with attack occurring at the carbonyl carbon would result in 1-naphthol being the leaving group (Equation 3-3).

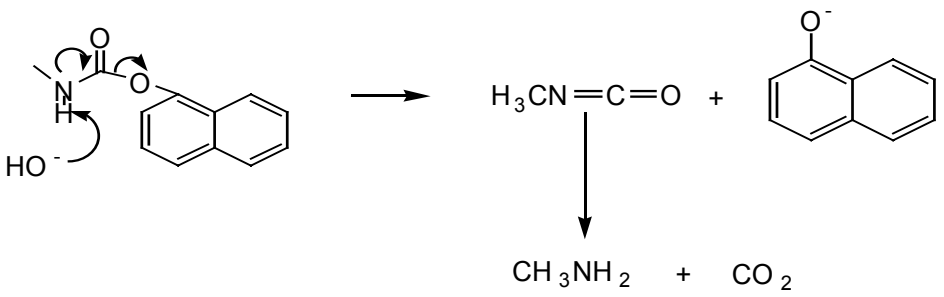

(3-3)

A nucleophilic attack at the methyl carbon bound to the nitrogen is also possible. Such a reaction would result in a dealkylation of the carbaryl.

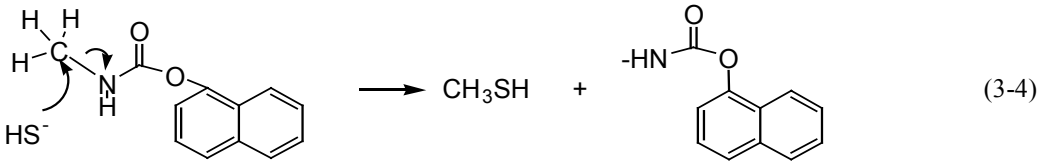

(3-4)

Dealkylation appears to be a common transformation pathway for agrochemicals with the requisite functionality, however the reaction mechanisms for this process have not been thoroughly investigated. The N-dealkylation of carbaryl in the environment has been reported, but it is proposed that this reaction requires the presence of microorganisms (Mora et al. 1996). A careful study of the reaction products should provide an answer to the question of whether the dealkylation of carbaryl could occur through reaction with strong sulfur nucleophiles. Most carbamates are thermally unstable. Hence it is necessary to analyze them by liquid chromatography rather than by gas chromatography (Cox et al. 1964; De Llasera et al. 2001).

3.2. Experimental Procedure and Analytical Methods:

3.2.1. Chemical reagents

Carbaryl (99%), 1-naphthol (99%), carbofuran (99%), carbofuran-3-keto (99%), 2,3-dihydro-2,2-dimethylbenzofuran-7-ol (99%), oxamyl (99%) and methomyl (99%) were obtained from Chem Service (West Chester, PA), and were used without further purification.

Sodium chloride, sodium phosphate (monobasic, H_2O), sodium phosphate (dibasic, $7H_2O$), starch soluble, and methanol were purchased from Fisher Chemicals (Fair Lawn, NJ). Potassium iodide was purchased from EM Science (Gibbstown, NJ). Potassium iodate was purchased from Mallinckrodt Inc (Paris, KY). Ethyl acetate, was purchased from Spectrum Chemical Mfg. Corp (Gardena, CA). All the chemicals were high purity reagent grade and were used without further purification.

3.2.2. Experiment System

All glassware was soaked in 1 M HNO_3 over night, rinsed several times with Milli-Q water, and dried at 200ºC overnight before use. Glassware used with H_2S was washed with methanol/NaOH to remove sulfur impurities prior to acid washing. Experiments were conducted at pH values from 6.5-8.5 with sodium phosphate buffer. Sodium tetraborate buffer was used for experiments at pH from 8.5-10.2. A Fisher Accumet pH meter with an Orion Ross electrode was used to measure pH. All solutions were prepared inside a controlled-atmosphere glovebox (97% N_2, 3% H_2) using a Milli-Q water with a resistivity of 18 MΩ*cm (Millipore Corp., Milford, MA). Prior to use, Milli-Q water was purged (>1 h/L) with ultrahigh purity argon, and then brought into the glovebox immediately.

The reaction solutions were prepared by initially mixing together pH buffer (50 mM sodium phosphate), electrolyte (100 mM sodium chloride), methanol (5%) and Na_2S or Na_2S_4 from aqueous stock solutions. After equilibrating overnight, the solution was transferred to a 20 mL syringe and an appropriate amount of carbaryl was added from a methanol stock (~5 mM) to initiate the reaction. The glassware including syringes for slow reaction experiments (longer than 2 weeks) was autoclaved 30 min at 120 °C to inhibit biological growth. In addition, the buffer solutions were filtered (0.2 μm, Anotop 25-sterile, Whatman Ltd., Maidstone, England) before spiking of pesticide stock solution. The initial pesticide concentration in carbaryl kinetic experiments was 100 μM. Syringes were maintained in a dark, temperature-controlled water bath (25 ºC, Polyscience) in order to prevent phototransformation by exposure to light. Rates were measured by monitoring parent compound concentrations. Reactions were followed at least for three half lives whenever it was possible. The hydrolysis of carbamates is very slow below pH 4. By adding 6 M HCl into the reaction solution, the hydrolysis of carbamates is stopped and the concentration monitored. The experiments were conducted by adding 1 mL reaction solution to a test tube with addition of 2 drops of 6 M HCl, shaken for 10 seconds and transferred to a vial for quantitative analysis.

3.2.3. Preparation of 50 mM hydrogen sulfide stock solution

HS^- solution was prepared by dissolving washed crystals of $Na_2S{\cdot}9H_2O$ in deoxygenated water and stored in the anaerobic glovebox. The concentration of HS^- was determined by iodometric titration. The value of pH was measured at the beginning and at the end of each reaction. The pH value measured at the end of reaction was used for calculation.

3.2.4. Preparation of 10 mM polysulfide solution

About 0.2 g of Na_2S_4 was weighed in anaerobic chamber, washed with deoxygenated toluene twice, and moved out of chamber and purged with ultrahigh purity argon till all the toluene evaporated, the bottle was moved back into the chamber and the crystal was dissolved with prepared deoxygenated borate buffer solution (50 mM sodium borate, 100 mM sodium chloride).

3.2.5. Iodometric Titration

The total hydrogen sulfide concentration was determined by iodometric titration. At the beginning of each measurement the thiosulfate solution (~2 mM) was standardized using 0.66 mM KIO_3 solution, which allowed calculating the exact concentration of thiosulfate solution.

To standardize a ~2 mM thiosulfate solution 10 mL of 0.66 mM KIO_3 was put in an Erlenmeyer flask, 0.08 g of potassium iodide and one pasteur pipet (0.5 mL) of ~6 M HCl was added, which leads to the formation of an exactly known amount of iodine. The iodine was then titrated with the thiosulfate solution. The amount thiosulfate needed allowed the calculation of the exact thiosulfate concentration. To determine the total hydrogen sulfide concentration, the above procedure was repeated with 1 mL of reaction solution, titrated with thiosulfate solution and the starch solution was used to find the end point.

3.2.6. Analytic methods

The samples were taken at specific time intervals and 2 drops of 6 M HCl was added, and the mixture was decanted into a autosample vial and stored in a refrigerator for analysis.

The samples of carbaryl and carbofuran were analyzed by high performance liquid chromatography (HPLC). HPLC enabled simultaneous determination of the parent compound and its degradation products. Separation was conducted using a Waters 2690 HPLC instrument under the following conditions: Lichrospher RP-18 column (60 Å, 5 μm, 3.0 mm×100 mm, EM Separations, Gibbstown, NJ) with insert Lichrocart precolumn containing 10 μm C_{18} packing material; 9.2% acetonitrile, 45.2% methanol and 45.2% Milli-Q water for 10 minutes; flow rate, 0.38 mL/min. For the sample with polysulfide, the mobile phase was 9.2% acetonitrile, 45.2% methanol and 45.2% 1 mM Milli-Q water to 100% methanol in 18 minutes; flow rate, 0.38 mL/min. 10 μL sample was injected. A photodiode array detector (Waters 996) was used to monitor the target substances and associated derivatives. The UV absorbance at 276 nm was used for integration.

The loss of oxamyl, methomyl and the formation of oxamyl oxime, methomyl oxime was monitored by reverse-phase HPLC under following conditions: Xterra MS C_{18} column (125 Å, 5 μm, 3.9 × 150 mm, Waters Corporation, Milford, MA) with 3.9 × 20 mm guard column containing 5 μm C_8 packing material. The flow rate was set at 0.7 mL/min and an isocratic eluent (5 mM acetic acid in 15% acetonitrile/85% H_2O v/v) was used. The injected volume was 20 μL. Chromatographic peaks for oxamyl, methomyl, oxamyl oxime, and methomyl oxime were identified by retention time comparison with authentic standards at three different eluent ratios (7, 15, and 25% acetonitrile).

3.3. Result and Discussion:

3.3.1. Kinetics of Hydrolysis:

The hydrolysis of individual pesticides in aqueous buffered solutions was studied at 25°C and with an ionic strength of 0.25 M. These values corresponded to the mean values recorded in the salt marshes and sediments. Plots of ln[carbamate] vs time are linear for all reactions monitored indicating that overall degradation follows pseudo-first-order kinetics (k_{obs}, h^{-1}):

$$-\frac{d[carbamate]}{dt} = k_{obs}[carbamate] \qquad (3-5)$$

Therefore, in a buffered solution of constant pH, the following equation applies:

$$\ln(C/C_0) = k_{obs}t \qquad (3-6)$$

where C_0 and C are the concentrations of the pesticide at time zero and at time t, respectively.

The pH of groundwaters and surface waters can vary significantly from one setting to another. Carbamate hydrolysis kinetics were evaluated for pH 2-10, a range representative of natural waters. Results are illustrated in Figure 3-2.

Due to the limitation of the experimental methods, only rate constants greater than $6.0 \times 10^{-5}\ h^{-1}$ could be reliably determined using the experimental approach and data analysis methods. Figure 3-2, shows the rate constants for carbamate hydrolysis, measured as a function of pH. Carbamate hydrolysis is exceedingly slow at subneutral pH. Below pH 6.8, the k_{obs} values for carbofuran data indicate that the

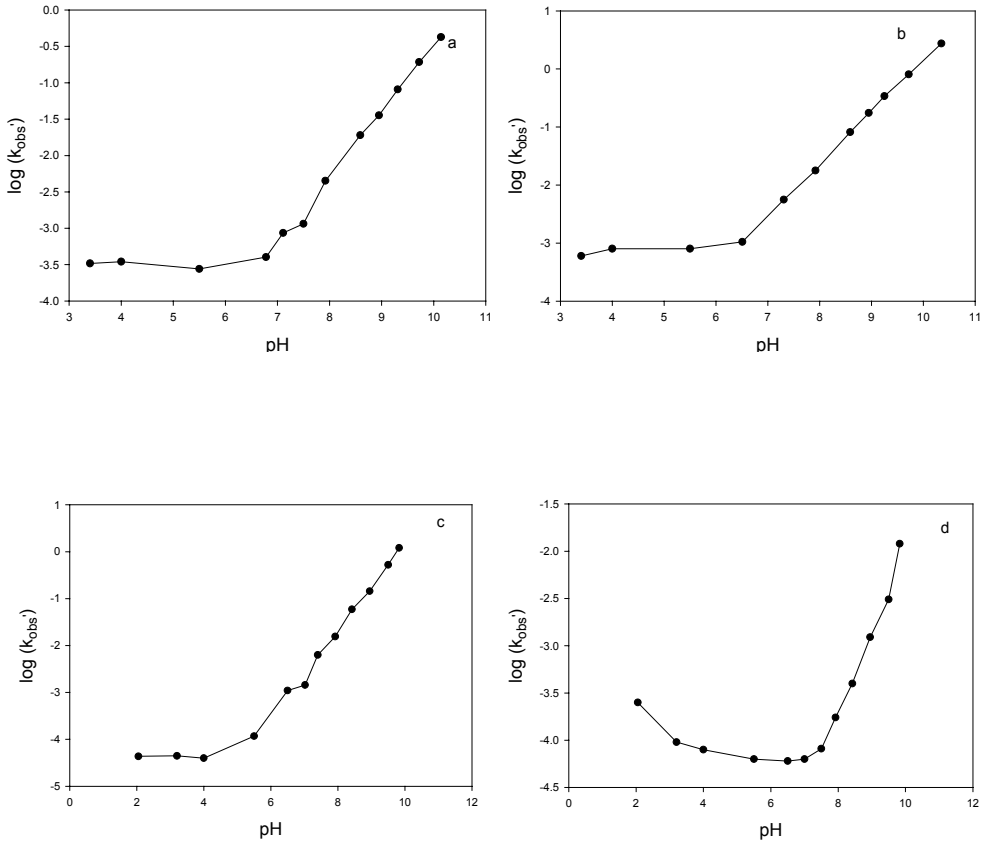

Figure 3-2. Hydrolysis of carbofuran (a), carbaryl (b), oxymyl (c), and methomyl (d) for different pH values. Ionic strength is 0.25 equiv/L (established with NaCl), 0.050 M sodium phosphate or sodium tetraborate buffer, 5% methanol and at 25.0 °C.

be accurately measured. For methomyl, hydrolysis is even slower; k_{obs} can only be measured accurately at pH > 7.4 and pH < 4.5. Hydrolysis of carbaryl is faster while compare to the other three carbamates, so the rate constants below pH 7 can be determined. In agreement with earlier reports, hydrolysis of carbamates are base-catalyzed reactions, with k_{obs} increasing approximately 10-fold for each unit increase in pH. This variation corresponds to the change in hydroxide ion

concentration [OH^-]. Second-order rate constant are calculated and listed in Table 3-2 (numbers in parentheses indicate 95% confidence intervals).

Table 3-2: Second-Order Rate Constants for Hydrolysis[a] of Carbamates at 25.0 °C

Carbamates	k_A ($M^{-1}h^{-1}$)	k_N(h^{-1})[c]	k_B($M^{-1}h^{-1}$)
Carbofuran	NA[b]	$(3.2 \pm 1.7) \times 10^{-4}$	$(3.5 \pm 0.4) \times 10^{2}$
Carbaryl	NA	$(7.2 \pm 4.5) \times 10^{-4}$	$(1.2 \pm 0.1) \times 10^{4}$
Oxymyl	NA	$(4.0 \pm 2.6) \times 10^{-5}$	$(1.8 \pm 0.1) \times 10^{4}$
Methomyl	$(2.2 \pm 0.7) \times 10^{-2}$	$(7.3 \pm 4.9) \times 10^{-5}$	$(1.6 \pm 0.1) \times 10^{2}$

[a] Second-order rate constant determined from hydrolysis at different pH (see Figure 3-2). [b] No acid catalysis detected in the hydrolysis. [c] According to the hydrolysis mechanism, k_N is negligiable. The data shows here was determined from Figure 3-2, which might result from the limitation of our experimental design.

From Table 3-2, k_B of oxymyl and carbaryl are more than 30 times faster than the other two carbamates. As discussed above, the hydrolysis of carbamates is an E1cb reaction; the rate determination step would be the formation of carbonanion of the oxime group, so the pK_a value of the conjugate base of the amide group is a very important parameter in predicting the rate constants. In this research, the computer program SPARC (online software package, available on the Internet at http://ibmlc2.chem.uga.edu/sparc) was used to estimate pK_a values for Lewis base groups present in the structure of the four carbamates (Karickhoff et al. 1991; Hilal et al. 1995). A complete list of SPARC results is provided in the Figure 3-3. The estimated pK_a values are all less than 1.0 (conjugate acids of the oxime nitrogen, amide nitrogen, and carbonyl oxygen moieties) or greater than 10.5 (amide

nitrogen). According to these results, the nonionic carbamate species predominates throughout the pH range investigated here.

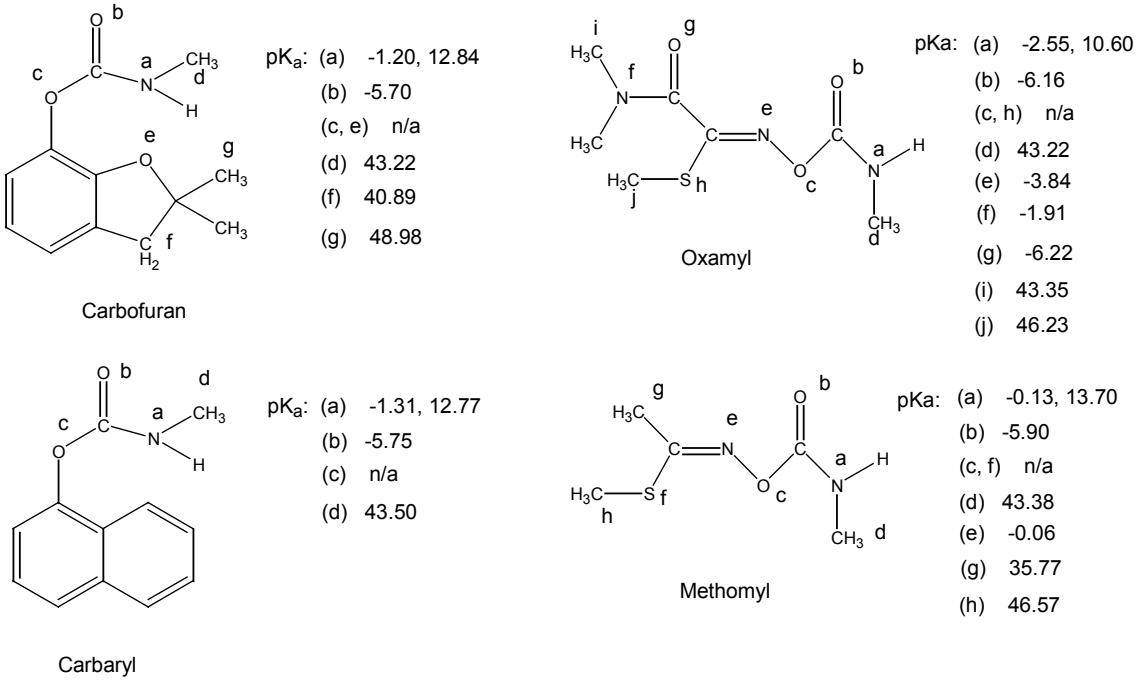

Figure 3-3: Estimated pK_a values for conjugated acids of Lewis base donor groups present in the structures of carbofuran, carbaryl, oxamyl and methomyl. Second number listed for (a) represents the pKa of the Lewis base group itself. Values estimated using the online software package SPARC, available on the Internet at (http://ibmlc2.chem.uga.edu/sparc).

The larger value of k_{OH^-} for oxamyl (relative to methomyl) is due, in part, to greater acidity at the *N*-methyl carbamate amide nitrogen; the conjugate base of the amide group is the reactive species for E1cb elimination (Hegarty et al. 1973; Hegarty et al. 1974). According to SPARC pK_a calculations, deprotonation of this group is much more favorable for oxamyl than for methomyl (estimated pK_a, 10.6 for oxamyl; 13.7 for methomyl). For carbofuran and carbaryl, estimated pK_a values on the amide group are similar (12.84 for carbofuran and 12.77 for carbaryl), although

the deprotonation of amide group is more favorable for carbaryl than for carbofuran, but the large difference on the reaction rate constants are not only corresponding to the acidity at the *N*-methyl carbamate amide nitrogen.

It is worth briefly noting that the increase loss of methomyl (but not other three carbamates) was also observed at the two lowest pH conditions examined (pH 2.05 and 3.20). The acid catalysis rate constant was calculated to be $(2.2 \pm 0.7) \times 10^{-2}$ $M^{-1}h^{-1}$, while more data will still be needed to better describe the kinetics of the reaction. Strathmann and Stone (Strathmann et al. 2002) also reported the acid catalyzed hydrolysis in their research, they reported acid catalyzed hydrolysis rates of 3.99 (±0.10) $\times 10^{-4}$ h^{-1} at pH 2.09 and 7.45 (±0.82) $\times 10^{-5}$ h^{-1} at pH 3.09, while the acid catalyzed hydrolysis rate in our research are 2.51 (±0.54) $\times 10^{-4}$ h^{-1} at pH 2.05 and 9.55 (±1.17) $\times 10^{-5}$ h^{-1} at pH 3.20.

3.3.2. Products of hydrolysis

Since carbamate hydrolysis occurs by E1cb reaction pathways, the corresponding oxime elimination product should be the only product. Pseudo-first-order rate expressions can also be written for the formation of the oxime elimination products that were also monitored using HPLC. Pseudo-first-order rate constants were calculated for each batch reaction using the software package Scientist for Windows (1986). Scientist calculates these parameters (along with the initial concentration of the parent compound) by fitting (method of least squares) numerically integrated solutions of the system of differential rate expressions to experimental data for parent compound loss and reaction product appearance. By fitting product formation

data simultaneously with parent compound loss data, it is better able to assess the importance of reaction pathway.

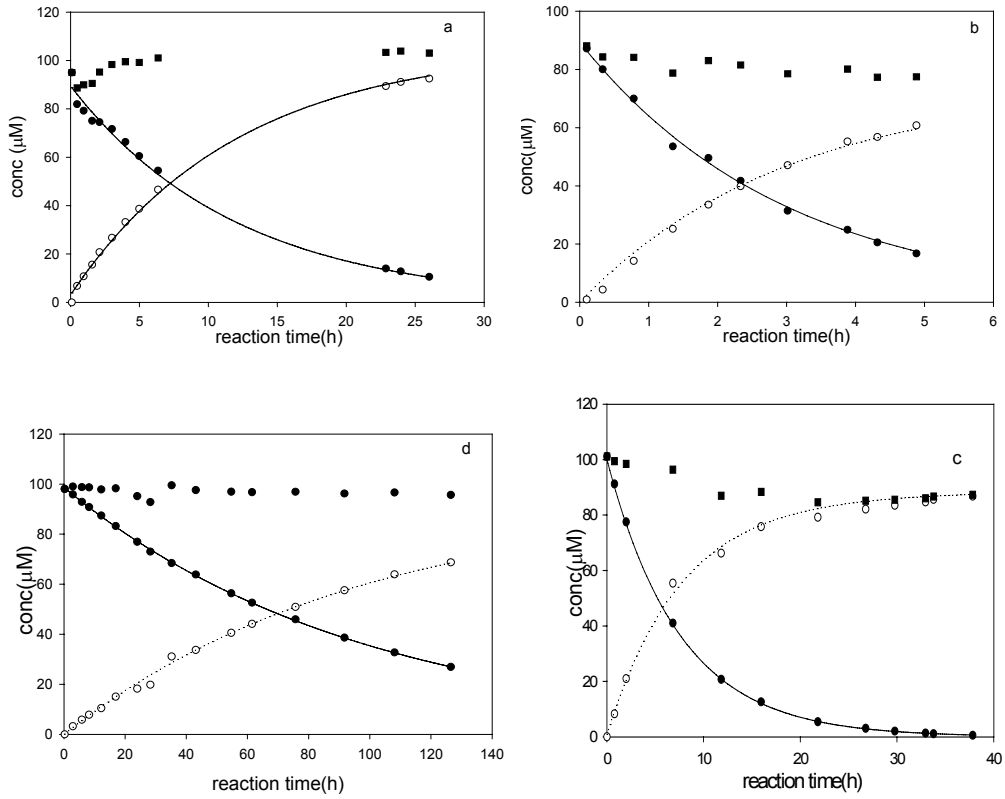

Figure 3-4: Hydrolysis (a) carbofuran at 9.31, (b) carbaryl at 9.25, (c) oxymyl at 8.95 (d) methomyl at 9.83, showing the degradation of carbamate (●), the formation of phenol or oxime (o) and the total mass of parent compounds and the elimination products (■), 0.050 M sodium tetraborate buffer, ionic strength is 0.25 equiv/L (established with NaCl) and at 25.0 °C.

For all batch reactions conducted in this study (except the reaction of methomyl at pH < 5), the carbamate will transform into phenol or oxime. Figure 3-4 shows the hydrolysis time-courses of these four carbamates at pH 9-10. From the figure, it is easy to recognize that the mass balance of the reaction was good. The percentage

mass recovery of phenol (oxime) + carbamates at the end of the experiment ranged from 90.3% to 103% indicating primarily a one step reaction and a stable product. Also only methomyl degrades at the two lowest pH conditions examined (pH 2.09 and 3.09) but without the detection of products. It has been reported that the methylthiolacetate was formed under these pH conditions by the GC-MS analysis of reactor headspace gases but not at higher pH (Strathmann et al. 2002). Therefore, the methomyl degradation at low pH values was ascribed to an acid-catalyzed hydrolysis reaction rather than to E1cb elimination. Therefore, further research would be needed for the elucidation of the mechanism of acid catalysis of methomyl.

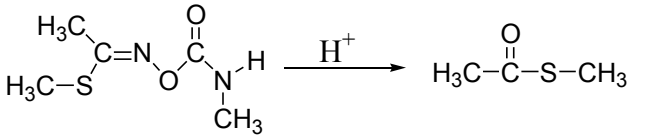

Methomyl S-methylthioacetate

3.3.3. Reaction of carbamates with reduced sulfur species

Natural groundwaters and surface waters contain a variety of reduced sulfur species, some present in abundant concentrations. A series of kinetic experiments were carried out to assess the effects of these reduced sulfur species on the rate of oxamyl degradation. Experimental results indicate that HS^- and polysulfides have no noticeable effect on the rate of carbamate degradation.

From Table 3-3, the degradation rate of carbamates is in good agreement with the formation of the phenol or oxime. The mass balance is 91.5% to 110%. According to the assumption, the elimination reaction results in the formation of the phenol or the corresponding oxime, and the nucleophlic reaction by the reduced sulfur species

Table 3-3: Pseudo-First-Order Rate Constants for Carbamates Degradation. [a]

		k_{obs} (h^{-1})[b]	k_{form} (h^{-1})[c]
carbofuran	pH 9.31	$(8.3 \pm 0.2) \times 10^{-2}$	$(9.5 \pm 0.2) \times 10^{-2}$
	4.5 mM HS^-, pH 9.25	$(9.2 \pm 0.2) \times 10^{-2}$	$(8.9 \pm 0.2) \times 10^{-2}$
	1.4 mM S_n^{2-}, pH 9.24	$(9.3 \pm 0.2) \times 10^{-2}$	$(9.0 \pm 0.2) \times 10^{-2}$
carbaryl	pH 9.25	$(3.3 \pm 0.4) \times 10^{-1}$	$(2.8 \pm 0.3) \times 10^{-1}$
	4.8 mM HS^-, pH 9.27	$(3.4 \pm 0.2) \times 10^{-1}$	$(3.3 \pm 0.2) \times 10^{-1}$
	2.2 mM S_n^{2-}, pH9.28	$(3.4 \pm 0.2) \times 10^{-1}$	$(3.4 \pm 0.2) \times 10^{-1}$
oxymyl	pH 8.95	$(1.3 \pm 0.1) \times 10^{-1}$	$(1.1 \pm 0.1) \times 10^{-1}$
	2.5 mM HS^-, pH 9.01	$(1.4 \pm 0.1) \times 10^{-1}$	$(1.2 \pm 0.1) \times 10^{-1}$
	3.1 mM S_n^{2-}, pH 8.90	$(1.3 \pm 0.2) \times 10^{-1}$	$(1.4 \pm 0.2) \times 10^{-1}$
methomyl	pH 9.83	$(1.0 \pm 0.1) \times 10^{-2}$	$(0.9 \pm 0.1) \times 10^{-2}$
	4.0 mM HS^-, pH 9.88	$(1.1 \pm 0.1) \times 10^{-2}$	$(1.1 \pm 0.2) \times 10^{-2}$
	4.2 mM S_n^{2-}, pH 9.79	$(1.0 \pm 0.2) \times 10^{-2}$	$(1.1 \pm 0.1) \times 10^{-2}$

[a]: all reaction solutions contain 0.050 M sodium tetraborate buffer, ionic strength is 0.25 equiv/L (established with NaCl) and at 25.0 °C. [b]: k_{obs} is the parent compounds losing rate, [c]: k_{form} is the formation rate of phenol or oxime, k_{obs} and k_{form} were calculated by simultaneous fitting with Scientist.

will result in the dealkylation of carbamate, and the products may undergo on further degradation to form the phenol or oxime. Therefore, the product distribution will not determine the reaction pathway. But if there is an additional degradation pathway other than elimination, the reaction rate constant should increase. Since no promotion in the rate constants was observed, the nucleophilc reaction is not important for the degradation of carbamate at aqueous solution; elimination is still the major degradation pathway, and the reaction of carbamate with reduced sulfur species can be ignored.

3.4. Environmental Significance.

Carbamates are used throughout the world for protection of a variety of crops. Not surprisingly, their persistence varies widely among these diverse settings and is controlled by a number of abiotic and biological processes. This study demonstrates that changing pH can exert a marked influence on the kinetics of carbamate elimination. Accurately predicting the fate and persistence of agrochemicals in aqueous environments requires an understanding of the important processes by which these chemicals degrade and the environmental factors that influence the rates of individual degradation pathways. This work establishes an improved kinetic model for carbamate degradation that accounts for the effect of pH on elimination kinetics. This study only examined a small set of environmental varieties; the other species in subsurface aqueous environments will also influence degradation of carbamates.

Therefore, further investigations into the link between the speciation and its reactivity with oxime carbamates is of great interest.

Chapter 4. Factors Affecting the Hydrolytic Degradation of Phosphorothionate Pesticides in Clean Batch Systems

4.1. Introduction of Phosphorothionate Pesticides:

A good understanding of the pesticide fate in agriculture is necessary to properly assess human exposure and the environmental impact of these compounds. Organophosphorus insecticides (OPs), most of which are esters and thioesters of phosphoric and thiophosphoric acid, are widely used throughout the world and have in many cases replaced organochlorine pesticides due to their high insecticidal activity and relatively low persistence. OPs have a common mode of action in vertebrates and invertebrates; thus, they often lack selectivity between nontarget organisms and insect pests. OPs can irreversibly inhibit the enzyme acetylcholinesterase, which is essential for central nervous system function in both humans and insects. An excess accumulation of the key neurotransmitter acetylcholine, which is normally released from nerve terminals and then rapidly hydrolyzed by acetylcholinesterase, results in a marked buildup of acetylcholine that leads to a marked dysfunction of many autonomic and behavioral systems, often causing respiratory paralysis and death (Khan 1980; Coats 1993). The amount of OPs used has declined since 1980, from an estimated 131 million pounds in 1980 to 73 million pounds in 1999 in the U.S. However, OPs usage in percent of total insecticide usage has increased, from 58% in 1980 to 70% in 2001 (Donaldson et al.).

Since the discovery in the early 1980s of trace residues of pesticides in well water in many agricultural areas of the United States, there have been numerous reports of water contamination by these compounds in most countries where intensive agriculture is practiced (Armstrong et al. 1995). As the movement of water through the soil is the main principal mechanism for the pesticides to reach the surface and groundwater, there has been increased research interest aimed at understanding the process that controls the penetration of pesticides into the soil and their subsequent contamination of groundwater and surface water, which can contaminate directly very sensitive ecosystems. Accumulation of these toxic pesticides in groundwater is influenced by the physical, chemical, and biological properties. Thermal decomposition, pH variations in water, and hydrolysis play a major role in the breakdown and degradation of pesticides (Lee et al. 1986; Ou et al. 1986; Singh et al. 1990**;** Cavalier et al. 1991). OPs are among the most prevalent pesticides encountered in groundwater and surface waters (Hallberg 1989; Kolpin et al. 1998; Kim et al. 1999); for example, chlorpyrifos and parathion-methyl, which are part of this study, were detected at 85 out of 139 streams across 30 states in the U.S. during 1999 and 2000, and the maximum concentration were 0.31 and 0.01 ppm respectively (Kolpin et al. 1998). A better understanding of how these OPs interact with dissolved and suspended species present in the water or in porewaters will improve the ability to predict the fate of these contaminants and related compounds in diverse environmental settings.

The degradation of OPs and their kinetics in aqueous solutions has been reported extensively (Faust et al. 1972; Meikle et al. 1978; Hong et al. 1998; Holden et al.

2001; Liu et al. 2001; Pehkonen et al. 2002). Oxidation of OPs can lead to the formation of the corresponding oxons, sulfones, and sulfoxides. Photodegradation can occur either by a direct photolysis or by indirect photolysis, in which dissolved humic and fulvic acids can act as a sensitizer (Noblet et al. 1996; Kamiya et al. 2001). Hydrolysis of OPs is perhaps the most thoroughly studied process. It can occur by a homogeneous or heterogeneous mechanism. Homogenous hydrolysis can take place when dissolved metal ions enhance the rate of hydrolysis by catalysis (e.g., Cu^{2+} and Pb^{2+} for chlorpyrifos-methyl, zinophos, diazinon, parathion-methyl, and fenchlorphos) (Smolen et al. 1997). Surfaces such as Fe and Al oxides and different clays can enhance the rate of heterogeneous hydrolysis by providing surface sites at which the nucleophiles and the OPs can react (Lee et al. 1986; Racke et al. 1996). Homogeneous hydrolysis of OPs can occur via two pathways: i) attack by OH^- and H_2O at the phosphorus atom, which is a relatively "harder" electrophilic site, and ii) attack by H_2O at the carbon atoms within the alcoholate ester linkages, which are relatively "softer" electrophilic sites.

The primary purpose of this study was to closely examine hydrolysis rates and products of five organophosphorothionate esters (Table 4-1). The effects of parent compounds concentration, buffer concentration, methanol content, and acid/base speciation on rates of organophosphorothionate esters reactions were systematically investigated in well-defined solutions at 25 °C in order to determine the relevant second-order rate constants. Products were characterized by HPLC-PDA.

Table 4-1: Chemical structures of the five pesticides studied.

Common name	Molecular Structure	IUPAC name	M.W.	CAS no.
Chlorpyrifos-Methyl	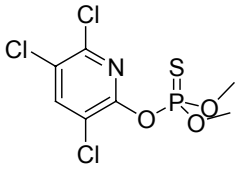	O,O-Dimethyl O-(3,5,6-trichloro-2-pyridyl) phosphorothionate	322.53	5598-13-0
Parathion-Methyl	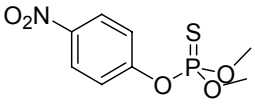	O,O-Dimethyl O-(4-nitrophenyl) phosphorothionate	263.21	298-00-0
Chlorpyrifos	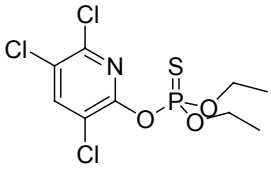	O,O-Diethyl O-(3,5,6-trichloro-2-pyridyl) phosphorothionate	348.93	2921-88-2
Parathion	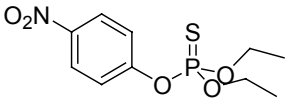	O,O-Diethyl O-(4-nitrophenyl) phosphorothionate	291.26	56-38-2
Fenchlorphos	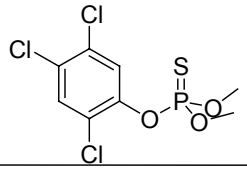	O,O-Dimethyl O-(2,4,5-trichlorophenyl) phosphorothionate	321.55	299-84-3

4.2. Materials and Methods

All chemical reagents were of the highest purity available. Unless otherwise stated, all solutions were prepared inside a controlled-atmosphere glovebox (96% N_2, 4% H_2, Pd catalyst; Coy Laboratory Products, Grass Lake, MI) using deionized water (Milli-Q water) with a resistivity of 18 MΩ•cm (Millipore Corp., Milford, MA). Prior to use, Milli-Q water was purged with high purity argon for one hour; and immediately brought into the glovebox. All glassware was soaked in 1 M HNO_3 overnight and was rinsed several times with Milli-Q water prior to use. Glassware

having prior contact with sulfur species was first soaked in 1 M NaOH/methanol solution and was rinsed several times with Milli-Q water prior to soaking in HNO_3.

4.2.1. Chemicals.

Chlorpyrifos (99.7%), chlorpyrifos-methyl (99.7%), desmethyl chlorpyrifos-methyl sodium salt (DmCPM) (70%-86%), and 3,5,6-trichloropyridinol (98%), were provided by Dow AgroSciences (Indianapolis, IN). Parathion-methyl (98.7%), parathion (99.5%) and fenchlorphos (98.3%) were purchased from Chem Service (West Chester, PA). 4-Nitrophenol (99+%) and 2,4,5-trichlorophenol (98%) were purchased from Aldrich (Milwaukee, WI).

All solvents and reagents that were used were analytical grade or equivalent. They were used without further purification, and were obtained from Fisher Scientific (Pittsburgh, PA) and EMD Chemicals (Gibbstown, NJ).

4.2.2. Experimental Systems.

The reaction solutions were prepared in volumetric flasks and then transferred to 20 mL glass syringes equipped with a polycarbonate stopcock and a PTFE needle tubing. The syringes contained three PTFE rings to facilitate mixing. NaCl was added to all solutions to yield an ionic strength of 0.25 equiv/L except the reactions for ionic effects and methanol effects. The glassware for slow hydrolysis experiments was autoclaved to inhibit biological growth. In addition, the buffer solutions were filtered (0.2 μm, Anotop 25-sterile, Whatman Ltd., Maidstone, England). Filtering of the buffer solution and assembly of autoclaved glassware were carried out in a biological safety cabinet to prevent any microbial contamination. The polycarbonate stopcocks used in the hydrolysis experiments were rinsed with 80% 2-propanol and air-dried in the biological safety cabinet prior

to their use in a hydrolysis experiment. The spike solutions of organophosphate were prepared by dissolving each parent compound in deoxygenated methanol. Experiments conducted at methanol concentrations from 0 to 20% indicated that these levels of methanol did not affect the reaction rates.

Reaction kinetics was generally determined under pseudo-first-order conditions, with added nucleophile concentrations ranging from 0.2 mM to 20.0 mM. Parent compound decay, and wherever possible, product formation, were monitored by HPLC-PDA and GC-FID. Reactions were initiated by spiking solutions (50-100 μL) containing the appropriate OP compound, yielding initial concentrations ranging from 10 to 50 μM. Reactors were vigorously mixed for 30 s and were incubated at the appropriate temperature (5.0-60.0 ± 0.1 °C). Aliquots (1 mL) were periodically extracted into ethyl acetate (1 mL), followed by HPLC or GC analysis.

4.2.3. HPLC Analysis.

The loss of parent organophosphates and the formation of selected reaction products were monitored by reversed-phase HPLC with photodiode array detector. An HPLC system (Waters 2690, Waters Corp., Milford, MA) was used. A Lichrospher RP-18 column (60 Å, 5 μm, 3.0 mm×100 mm, EM Separations, Gibbstown, NJ) was used for detection of chlorpyrifos-methyl and parathion-methyl. The flow rate was set at 0.7 mL/min. An Xterra MS C_{18} column (125 Å, 5 μm, 3.9 mm×150 mm, Waters, Milford, MA) was used for detection of chlorpyrifos, parathion and fenchlorphos. The flow rate was set at 1 mL/min. An isocratic eluent (1 mM phosphoric acid in 75% acetonitrile/25% H_2O v/v) was used to monitor the hydrolysis of chlorpyrifos-methyl, chlorpyrifos and fenchlorphos. For the hydrolysis of parathion-methyl and

parathion, a gradient method was used. The mobile phase was 42% methanol and 58% 1 mM phosphoric acid to 70% methanol and 30% phosphoric acid in 16 minutes. The injected volume was 10 μL. Chromatographic peaks for organophosphates and hydrolysis products were identified by retention time comparison with authentic standards.

For selected reactions, ion pair chromatography was used to monitor the formation of organophosphate diester. In this case the Xterra MS C_{18} column (125 Å, 5 μm, 3.9 mm×150 mm) was used for all five organophosphate compounds. The flow rate was set to 0.65 mL/min. A gradient method was used, which started from 10% of A (0.25 mM tetrabutyl ammonium sulfate in 85% acetonitrile, pH adjusted with phosphoric acid to 4) and 90% of C (0.25 mM tetrabutyl ammonium sulfate in milli-Q water, pH adjusted with phosphoric acid to 4) to 22% of A and 78% C in 14 minutes, hold for 4 minutes, then change to 25% of A and 75% of B (Milli-Q water), hold for 3 minutes and changed back to 10% of A and 90% of C. The injection volume was 10 μL.

4.2.4. Data Analysis.

Pseudo-first-order constants (k_{obs} values) were obtained by regressing the natural log of the parent compound concentration versus time. Except for very slow experiments, reactions were followed over 2 to 3 half-lives to verify first-order kinetics. In these experiments, the five organophosphates reacted via competing processes. Efforts were made in such situations to determine rate constants for the relevant reactions using the program *Scientist for Windows* (v. 2.01; MicroMath, Inc.). This software is capable of determining rate constants and associated

parameters by fitting experimental data to numerically integrated solutions of systems of differential rate expressions.

4.3. Result and Discussion

4.3.1. Hydrolysis of Organophosphate at 25°C.

Hydrolysis is the most thoroughly studied degradation pathway of OPs, but the rate constants reported for the OP hydrolysis often differ by more than an order of magitude between different authors. For this reason, the kinetics of hydrolysis of the five OPs was investigated. In addition of interest was a detailed quantification of the products, which is usually not available from the literature.

The hydrolysis of individual pesticides in aqueous buffered solutions was studied at 25°C and with an ionic strength of 0.25 M. These values corresponded to the typical values reported for salt marshes and sediments. Plots of ln[OP] vs time are linear for all reactions monitored indicating that overall degradation follows pseudo-first-order kinetics (k_{obs}, h^{-1}):

Pseudo-first-order disappearance rate constants measured for five OPs in pH-adjusted Milli-Q water are listed in Appendix along with other parameters associated with each determination. The initial concentrations given are predicted values based on initial volumes of added OPs stock solution. These values generally agree (± 5 %) with values calculated from the intercepts of the kinetic plots. Disagreement between predicted and calculated initial concentration occurred in several experiments where significant (>10%) sorption to container walls created an initial curvature in the kinetic plots while the initial concentration of OPs might be so high that it exceed the solubility.

For sorption of OPs to container walls, it is assumed that the sorption-desorption reactions are fast relative to hydrolysis. In order to minimize the effect of the sorption-desorption reactions, optimization of the initial reaction condition was performed; the initial concentration for each of the OP was chosen based on the experimental result. Catalysis by buffers was also considered, and the result of three experiments that verifies the absence of a measurable buffer catalysis is shown in Figure 4-1.

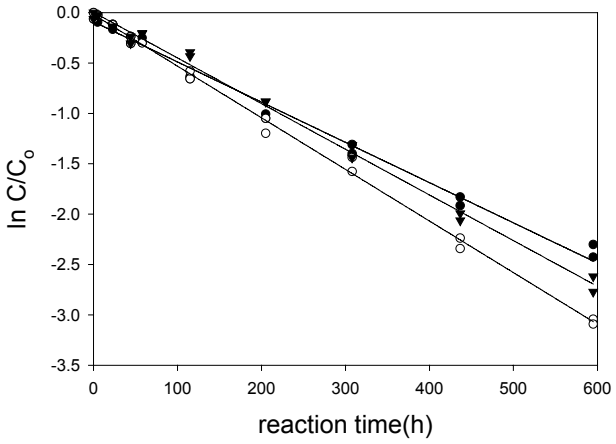

Figure 4-1. Plot of ln C/Co vs. time for the hydrolysis of chlorpyrifos-methyl in 5 mM phosphate buffer at pH 9.03 (●), 20 mM phosphate buffer at pH 9.05(▼), and 50 mM phosphate buffer at pH 9.02 (o), with 100 mM NaCl and at 25.0 °C.

The graph shows data from experiment of chlorpyrifos-methyl at a buffer concentration of 0.050 M (phosphate-phosphate monobasic), at a lower buffer concentration of 0.020 M and 0.005 M. The slopes from these three time-courses are identical within experimental uncertainty (data for individual runs shown in Table 4-2 and Appendix). Figure 4-1 also serves to illustrate a typical experimental plot. Those experiments at higher pH generally showed less scatter about the least-

Table 4-2. Observed Pseudo-First-Order Rate Constants for OPs in Buffered Milli-Q Water

	pH	Initial Conc (μM)	Temp (°C)	No.of kinetic points	Duration (h)	Conc of buffer (mM)	k_{obs} (h^{-1})
CPM	9.05	36	25.0 ± 0.1	9	595	50	$4.60 (\pm 0.12)\times10^{-3}$
	9.02	37	25.0 ± 0.1	9	595	20	$5.11 (\pm 0.46)\times10^{-3}$
	9.03	34	25.0 ± 0.1	9	595	5	$4.04 (\pm 0.35)\times10^{-3}$
MPT	9.20	105	50.0 ± 0.1	12	213	50	$2.17 (\pm 0.17)\times10^{-2}$
	9.22	106	50.0 ± 0.1	12	213	20	$2.12 (\pm 0.04) \times10^{-2}$
	9.20	87	50.0 ± 0.1	12	213	5	$2.36 (\pm 0.22) \times10^{-2}$
FEN	8.45	28	60.0 ± 0.1	10	31	50	$5.77 (\pm 0.21)\times10^{-2}$
	8.47	37	60.0 ± 0.1	10	31	20	$6.12 (\pm 0.17) \times10^{-2}$
	8.40	34	60.0 ± 0.1	10	31	5	$6.04 (\pm 0.22) \times10^{-2}$
CPE	8.47	8	50.0 ± 0.1	10	77	50	$1.02 (\pm0.13)\times10^{-2}$
	8.40	7	50.0 ± 0.1	15	165	20	$0.99 (\pm 0.06)\times10^{-2}$
	8.40	8	50.0 ± 0.1	15	165	5	$0.83 (\pm 0.014) \times10^{-2}$
EPT	9.34	35	25.0 ± 0.1	15	4107	50	$3.48 (\pm 0.22)\times10^{-4}$
	9.22	28	25.0 ± 0.1	15	4107	20	$3.35 (\pm 0.31)\times10^{-4}$
	9.29	27	25.0 ± 0.1	15	4107	5	$3.60 (\pm 0.11) \times10^{-4}$

squares line, those at lower pHs usually had larger estimates of standard error. Rate constants for the disappearance kinetics of all five investigated OPs at different

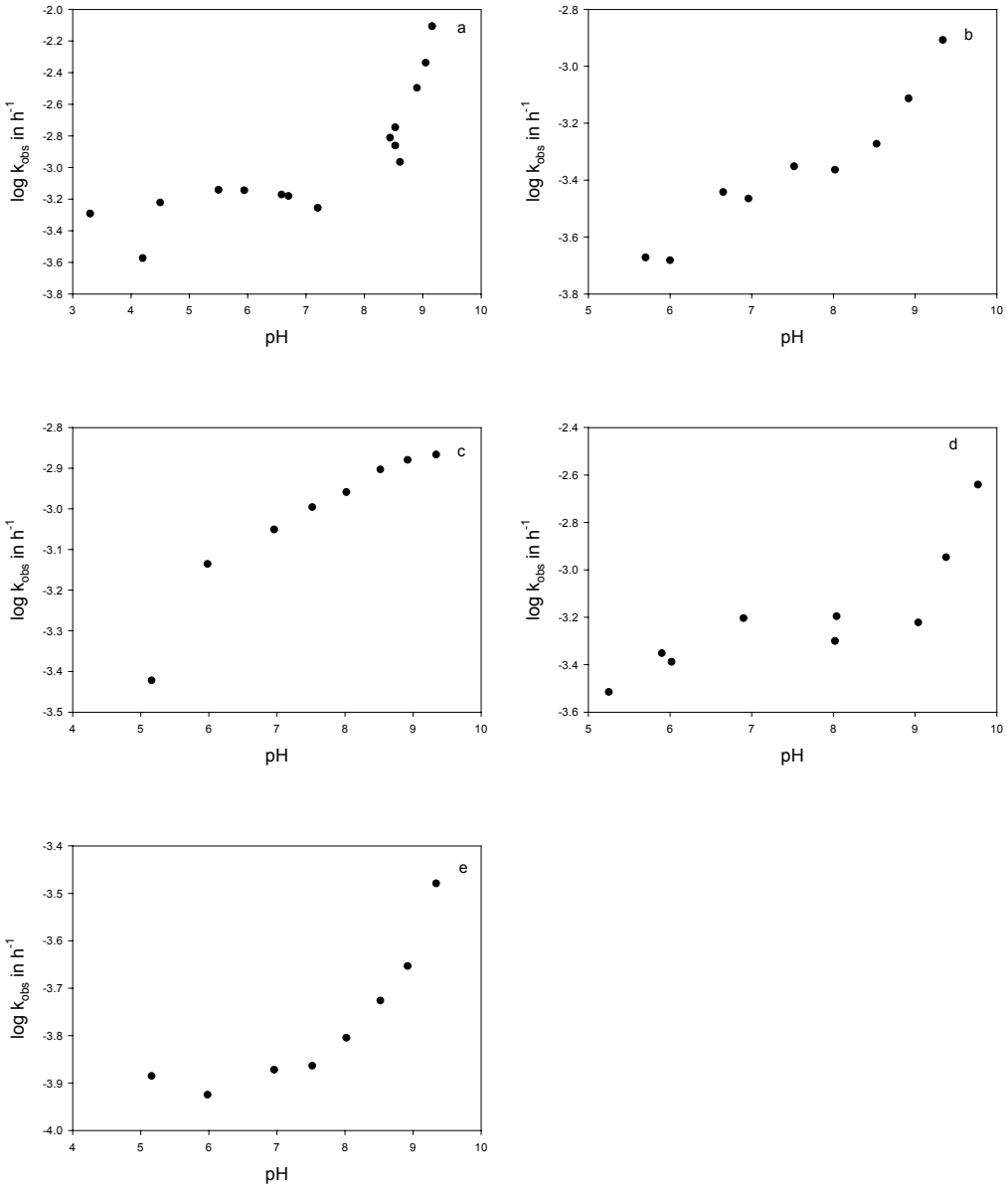

Figure 4-2. Hydrolysis of chlorpyrifos-methyl (a), parathion-methyl (b), fenchlorphos (c), chlorpyrifos (d) and parathion (e) for different pH values at 25 °C in buffered Milli-Q water. Ionic strength is 0.25 equiv/L (established with NaCl), 0.050 M sodium phosphate or sodium tetraborate buffer, 5% methanol and at 25.0 °C.

buffer concentration are all listed in Table 4-2, along with associated experimental conditions for each run.

The hydrolysis data for chlorpyrifos-methyl, parathion-methyl, fenchlorphos, chlorpyrifos and parathion are shown in Figures 4-2.

Rate constants measured at room temperature at pH below 8 show considerable variation, presumably due for the most part to the difficulties inherent in measuring rate constants for very slow reactions. However, the absence of pH dependence above pH 8 in the rate constant is obvious except for fenchlorphos.

On the basis of previous literature reports, it was anticipated that the OPs would react by a neutral hydrolysis reaction at pH's below 8 (Weber 1976; Meikle et al. 1978). The neutral hydrolysis rate constants, given in Table 4-3 along with the pH rate profile in Figure 4-2, support this pH-independent pathway over the pH range of 4.2-7.5.

Table 4-3: Second-Order Rate Constants for Hydrolysis[a] of OPs at 25.0 °C

OPs[b]	k_N (h^{-1})	k_B ($M^{-1}h^{-1}$)
Chlorpyrifos-methyl	$3.0\ (\pm 0.6) \times 10^{-4}$	$3.6\ (\pm 0.5) \times 10^{2}$
Parathion-methyl	$2.8\ (\pm 0.8) \times 10^{-4}$	43 (±8)
Fenchlorphos	$3.0\ (\pm 1.4) \times 10^{-4}$	9.8 (±5.2)
Chlorpyrifos	$4.0\ (\pm 1.0) \times 10^{-4}$	30.5 (±5.6)
Parathion	$1.2\ (\pm 0.3) \times 10^{-4}$	9.2 (±1.0)

[a] Second-order rate constant determined from hydrolysis at different pH (see Figure 4-2). [b] no acid catalysis detected in the hydrolysis.

The overall reaction for the pH-independent hydrolysis is shown in eq 4-1 (e.g., chlorpyrifos-methyl). The mechanism is believed to involve neocleophilic attack of water at the α-carbon of the alkoxy groups to give ethanol or methanol and desalkyl phosphorothioic acid as the products (Meikle et al. 1978).

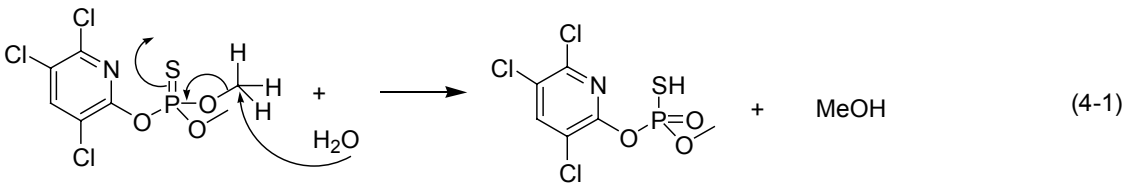

Chlorpyrifos-methyl DmCPM (4-1)

In environmental studies of the hydrolysis of organophosphate and organophosphorothionate esters, it is generally assumed that alkaline hydrolysis proceeds by second-order kinetics, i.e., first order in hydroxide and first order in OP concentration as shown in eq 4-2.

$$-\frac{d[OP]}{dt} = k_B[OP][OH^-] \qquad (4-2)$$

This assumption has the advantage that, if one determines the second-order disappearance rate constant *(k_B)* at one alkaline pH (generally somewhere between pH 8 and pH 12), it is possible to calculate the pseudo-first-order rate constant (k_{obs}) at any other alkaline pH (eq 4-3).

$$k_{obs} = k_N + k_B[OH^-] \qquad (4-3)$$

On the one hand, our data support the assumption that the disappearance rate constants of the five investigated OPs are first order in the OP concentration. On the other hand, our data do not support the assumption that the disappearance expression is first order in hydroxide activity for all five OPs. This is consistent with

a similar conclusion reached by Macalady and Wolfe (Macalady et al. 1983) based on studies in 0-50% methanol-water and acetonitrile-water solutions, where they conclude that there is a solvent effect when the content of methanol or acetonitrile is higher than 25 %. Furthermore, our result suggest that buffer catalysis would be negligible at the buffer concentrations used here, such finding are also supported by the conclusion reached by Macalady and Wolfe (Macalady et al. 1983). Neither are ionic strength (electrostatic) effects believed to be the cause of the deviation from first order since one of the reacting species is uncharged (Frost et al. 1961). A visual inspection of the alkaline region of the pH rate profile (Figure 4-2) suggests that the hydrolysis of parathion and fenchlorphos is not first order in hydroxide activity. Linear least-squares analysis of the data of parathion from pH 7.7 to pH 9.5 gives an r^2 of 0.92 and the data of fenchlorphos from pH 8.0 to pH 9.5 gives an r^2 of 0.64. This deviation from eq. 4-1 is not consistent with the mechanisms generally proposed for organophosphate triester hydrolysis. Therefore, this deviation could be caused by the pH-independent neutral hydrolysis.

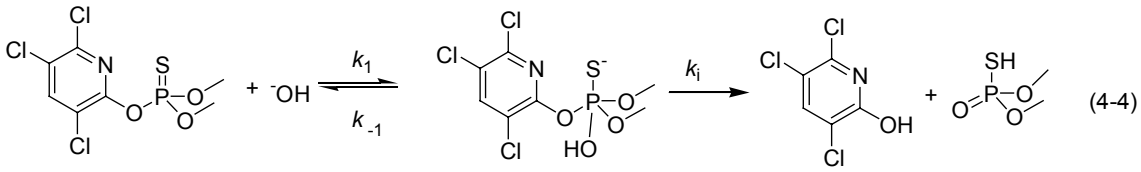

Chlorpyrifos-methyl

trichloropyridinol

Equation 4-4 represents a generalized reaction scheme that parallels the one proposed by Barnard (Barnard et al. 1961; Barnard et al. 1966; Macalady et al. 1983) for base catalyzed hydrolysis of organophosphates. In the case of organophosphate triesters, the observed second-order kinetics necessitates that $k_i >> k_1$; thus, k_l and the OH^- activity are rate determining (Cox et al. 1964). To account

for the OPs hydrolysis data, a less restrictive consideration was given to eq. 4-4. This mechanism is different from the generally proposed hydrolysis mechanism (S_N2), first-order reaction to both the OP and the hydroxide ion (Schwarzenbach et al. 2003). And it is also different from the assumption of Kirby and Warren, who proposed that substitution reactions at phosphorus atom are postulated to occur by an S_N2 mechanism with no intermediate formed (Kirby et al. 1967). A general expression for the value of k_{obs} as a function of hydroxide activity implied by this mechanism (eq. 4-5) is not practical because the concentration of the pentavalent charged intermediate is unknown. One can solve, however, for the value of k_{obs} vs. OH^- activity if equilibrium in the first reaction is assumed. Defining $K = k_l/k_{-l}$, the rate expression becomes (neglecting the neutral hydrolysis contribution) (equation conducting process in Appendix C)

$$-\frac{d[OP]}{dt} = \frac{k_i K[OH^-][OP]}{1+K[OH^-]} \qquad (4\text{-}5)$$

where [OP] represents the total organophosphate concentration, which includes the pentavalent intermediate. The observed first-order rate constant, consequently, is given by eq 6, where $[OH^-]$ here represents hydroxide activity.

$$\frac{1}{k_{obs}} = \frac{1}{k_i} + \frac{1}{k_i K[OH^-]} \qquad (4\text{-}6)$$

Equation 4-6 implies that, under conditions where equilibrium between OPs and the charged intermediate is maintained, a plot of $1/k_{obs}$ vs. $1/[OH^-]$ should be a straight line. Deviations from the equilibrium assumption would result if $k_i >> k_{-l}$, a condition that is independent of pH, or if $k_l[OH^-] << k_i$, a condition that is certain to result in departures from equilibrium when the pH is low. This assumption is good

for our result of fenchlorfos; a plot of k_{obs} vs. [OH^-] for fenchlorfos gives an linear least-squares analysis (r^2) of 0.64, while a plot of $1/k_{obs}$ vs. $1/[OH^-]$ for fenchlorfos gives an r^2 of 0.99 (Figure 4-3).

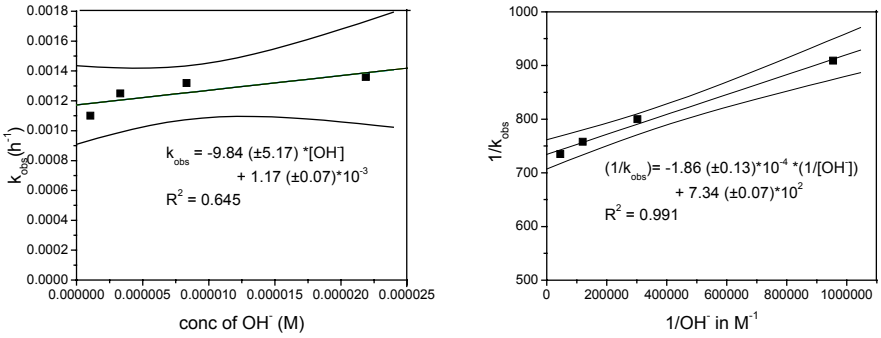

Figure 4-3. Plot of observed rate constant vs. concentration of OH^- (a) and $1/k_{obs}$ vs. $1/[OH^-]$ (b) for the base catalyzed hydrolysis of fenchlorphos at 25 °C in buffered Milli-Q water. Ionic strength is 0.25 equiv/L (established with NaCl), 0.050 M sodium phosphate or sodium tetraborate buffer, 5% methanol and at 25.0 °C.

Kirby and Warren's conclusion, that the pentavalent intermediate does not exist, is confirmed in the hydrolysis experiments for trimethyl phosphate (Kirby et al. 1967). However, in our case, since the sulfur atom connected to the phosphorus atom is bigger and less electronegative than the oxygen atom, and the big aryl leaving group could also possibly to stabilize the pentavalent intermediate. Therefore, the pentavalent intermediate might exist in the base catalyzed hydrolysis of some organophosphorothionate investigated here; these would explain the regression deviation of the base-catalyzed hydrolysis for parathion and fenchlorphos.

4.3.2. Product of hydrolysis

The hydrolysis of OPs may involve loss of either the phenolate-leaving group or one of the alcoholate leaving groups. Measurements of the product concentrations

during the hydrolysis reaction can provide information regarding the mechanism. Unfortunately, several of the earlier reported studies on the hydrolysis of these compounds did not clearly report the reaction conditions under which the products were found, making it difficult to compare the results (Faust et al. 1972; Lartiges et al. 1995; Hong et al. 1998; Hong et al. 2001). Identification of the reaction conditions (i.e., pH, buffer concentration, and temperature) is necessary to make inferences from laboratory results regarding behavior about in the natural environment. In our hydrolysis experiments, two products for each of the OP were detected by HPLC. Therefore both of the pathways (attack at the phosphorous and attack at alkoxy carbon (eq.4-1 vs. eq.4-4)) exist, and in addition, no further reaction of the two products was observed under our experimental conditions. And even though these products were reported in several earlier studies of chlorpyrifos

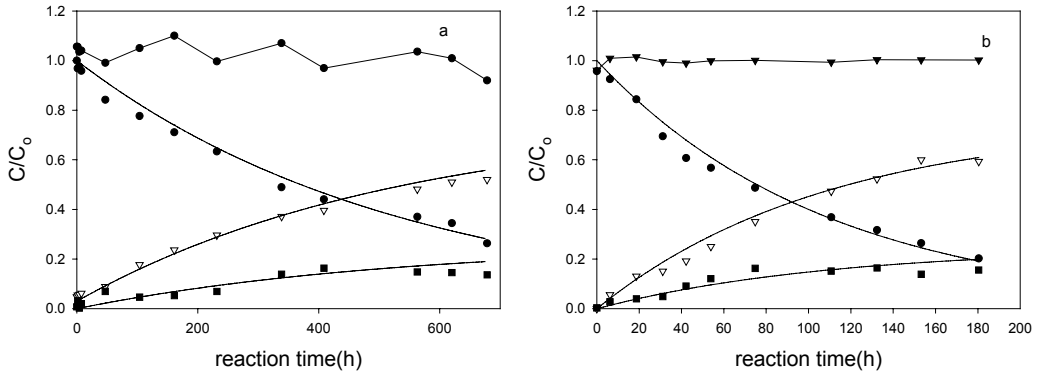

Figure 4-4. Reaction time-course of two chlorpyrifos-methyl hydrolysis at pH 8.53 (a) and pH 9.16 (b), unreacted chlorpyrifos-methyl (●), trichloropyridinol (▽), desmethyl chlorpyrifos-methyl (■), and the total concentration of the three compounds (▼), with 50 mM phosphate or borate buffer, 100 mM NaCl and at 25.0 °C.

hydrolysis (Macalady et al. 1983), the distribution of each product with varying pH were not reported. Therefore, in this study, the distribution of the products was carefully investigated on the basis of the mechanisms proposed in Equation 4-1 & 4-4.

Figure 4-4 shows the hydrolysis time-course of chlorpyrifos-methyl at pH 8.5 and pH 9.2. It is in agreement with our assumption. At a pH higher than 7.5, the base-catalyzed hydrolysis is more important and the product is the corresponding phenol. Similar results were also observed for parathion-methyl, fenchlorphos, chlorpyrifos and parathion. Table 4-4 listed the hydrolysis rate constants for selected pH. According to the previous discussion, the nucleophilic attack at the phosphorus atom by the hydroxide ion will result in the formation of the phenol. Table 4-4 shows the phenol will also form in a neutral solution. The formation rate accounts for about 15 to 40% of the total parent compound degradation rate. The result suggests that H_2O might also attack the phosphorus atom of the parent compounds to result in the formation of phenol group.

As we discussed in the first part, the formation of desalkyl OPs is independent of pH, the k'_{DaOP} for each of the OPs should be the same in the range of error. Our results for fenchlorphos, chlorpyrifos and parathion are in good agreement with this assumption. However, for chlorpyrifos-methyl and parathion-methyl, the formation of desmethyl compounds at pH 9.3 is about 2 times larger than the formation at pH 7 and pH 8.5.

Table 4-4: Hydrolysis rate constants of OPs at 25.0 °C in clean batch system [a]

	pH	time (h)	k'_{obs} (h^{-1})[b]	k'_{phenol} (h^{-1})[c]	k'_{DaOP} (h^{-1})[c]
CPM	pH 6.58	1788	$6.73 (\pm 0.64)\times10^{-4}$	$1.98 (\pm 0.13)\times10^{-4}$	$5.68 (\pm 0.41)\times10^{-4}$
	pH 8.53	679	$1.79 (\pm 0.14)\times10^{-3}$	$1.47 (\pm 0.11)\times10^{-3}$	$0.49 (\pm 0.06)\times10^{-3}$
	pH 9.16	181	$7.83 (\pm 0.33)\times10^{-3}$	$6.91 (\pm 0.71)\times10^{-3}$	$1.25 (\pm 0.12)\times10^{-3}$
MPT	pH 6.96	2403	$3.43 (\pm 0.29)\times10^{-4}$	$8.68 (\pm 2.20)\times10^{-5}$	$2.79 (\pm 0.17)\times10^{-4}$
	pH 8.53	2403	$5.34 (\pm 0.43)\times10^{-4}$	$2.45 (\pm 0.34)\times10^{-4}$	$2.44 (\pm 0.32)\times10^{-4}$
	pH 9.34	1427	$1.24 (\pm 0.13)\times10^{-3}$	$1.15 (\pm 0.09)\times10^{-3}$	$0.75 (\pm 0.09)\times10^{-3}$
FEN	pH 5.98	4108	$5.32 (\pm 0.73)\times10^{-4}$	$2.11 (\pm 0.31)\times10^{-4}$	$3.45 (\pm 0.30)\times10^{-4}$
	pH 8.02	4108	$1.10 (\pm 0.21) \times10^{-3}$	$1.05 (\pm 0.23)\times10^{-3}$	$3.29 (\pm 0.22)\times10^{-4}$
	pH 9.34	2974	$1.36 (\pm 0.13) \times10^{-3}$	$1.13 (\pm 0.16)\times10^{-3}$	$0.29 (\pm 0.08)\times10^{-3}$
CPE	pH 6.96	980	$6.25 (\pm 1.18)\times10^{-4}$	$0.94 (\pm 0.10)\times10^{-4}$	$5.07 (\pm 0.63)\times10^{-4}$
	pH 8.04	2426	$6.37 (\pm 0.88)\times10^{-4}$	$1.97 (\pm 0.35)\times10^{-4}$	$4.63 (\pm 0.45)\times10^{-4}$
	pH 9.38	1844	$1.13 (\pm 0.16)\times10^{-3}$	$6.67 (\pm 0.86)\times10^{-4}$	$5.34 (\pm 0.14)\times10^{-4}$
EPT	pH 6.96	2403	$1.34 (\pm 0.12)\times10^{-4}$	$0.21 (\pm 0.07)\times10^{-4}$	$1.22 (\pm 0.32)\times10^{-4}$
	pH 8.52	2403	$1.88 (\pm 0.07)\times10^{-4}$	$0.42 (\pm 0.10)\times10^{-4}$	$1.48 (\pm 0.23)\times10^{-4}$
	pH 9.34	1427	$3.32 (\pm 0.26)\times10^{-4}$	$2.08 (\pm 0.18)\times10^{-4}$	$1.44 (\pm 0.16)\times10^{-4}$

[a] Determined via simultaneous nonlinear regression techniques using Scientist for Windows, k'_{phenol} is the formation rate of phenol, k'_{DaOP} is the formation rate of desalkyl OPs, and k'_{obs} is the degradation rate of OPs, [b] Determined through linear regression techniques. [c] Standard deviation resulting from the nonlinear regression. All reactions were conducted at 0.050 M sodium phosphate or sodium tetraborate buffer with ionic strength adjusted with NaCl to 0.25 equiv/L, 5% or 10% methanol at 25.0 °C.

4.3.3. Determination of Arrhenius Parameters

A temperature dependence of many reactions can be described by the empirical Arrhenius equation (Schwarzenbach et al. 2003). The equation can be written in log-linear form

$$\ln k_{obs} = \ln A - \frac{E_a}{R}\left(\frac{1}{T}\right) \qquad (4\text{-}7)$$

where A is the pre-exponential or frequency factor, E_a is the activation energy, R is the gas constant, and T is the absolute temperature. For a reaction that exhibits Arrhenius temperature dependence, a plot of ln k_{obs} vs 1/T will give a straight line with a slope of E_a/R and the intercept equal to ln *A*. Arrhenius plots of the hydrolysis data for the five organophosphates are shown in Figure 4-5. The data do appear to exhibit an Arrhenius dependence on temperature, and therefore the parameters derived by linear regression can be used to predict hydrolysis rates at any temperature of interest.

The Arrhenius data obtained are summarized in Table 4-5. These Arrhenius parameters can in turn be used to estimate the hydrolysis rates at lower temperatures more characteristic of field conditions. These results show the importance of performing hydrolysis experiments at multiple temperatures. In the absence of Arrhenius data, there would be no accurate way to predict the approximately 2-5 fold decreases in hydrolysis rates for the 10 °C drop of the five OPs.

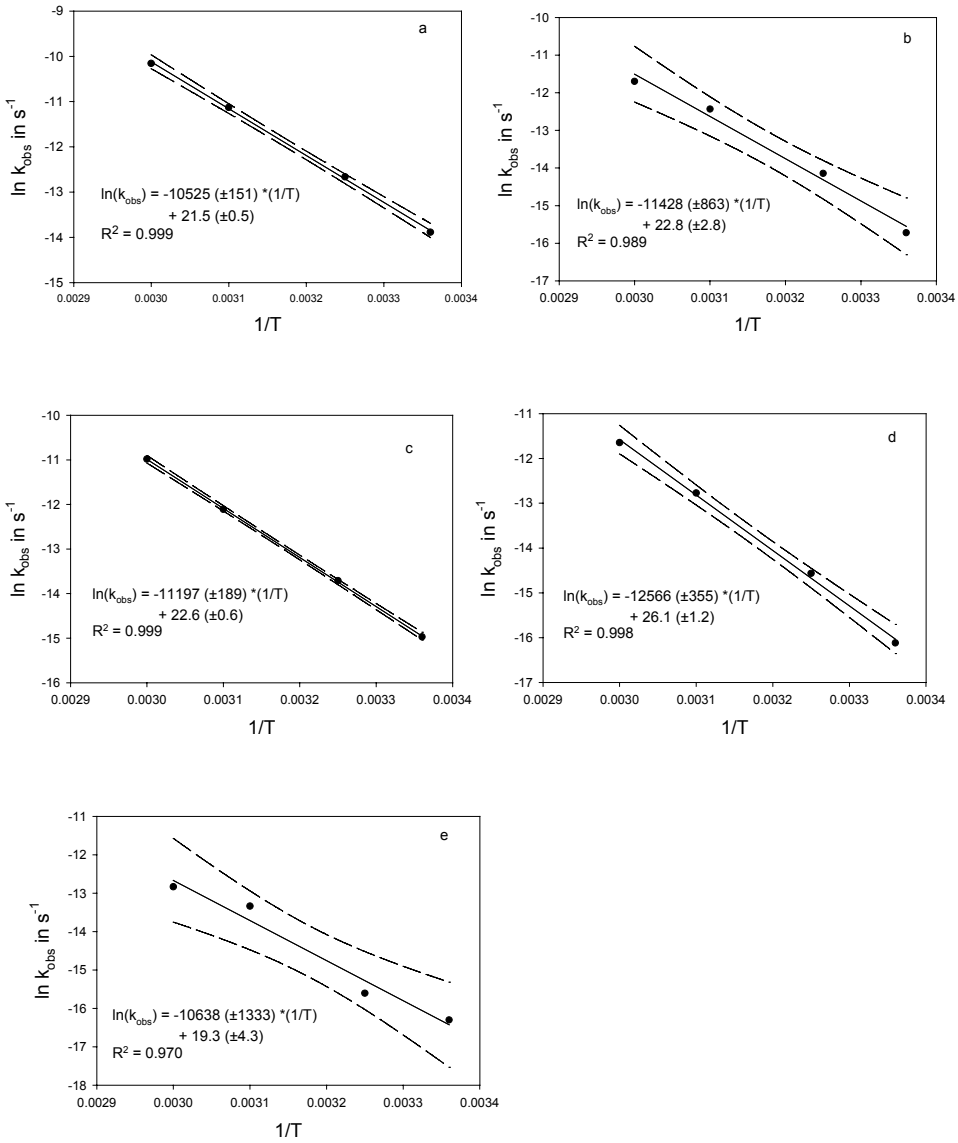

Figure 4-5. Arrhenius plot of the abiotic hydrolysis rate data for chlorpyrifos-methyl (a), parathion-methyl (b), fenchlorphos (c), chlorpyrifos (d), and parathion (e) at pH 8.5. Solid lines represent linear regressions of ln(k_{obs}) values determined; dashed lines represent 95% confidence intervals. All reactions were conducted at 0.050 M sodium phosphate buffer with ionic strength adjusted with NaCl to 0.25 equiv/L, 5% for chlorpyrifos-methyl and parathion-methyl, 10% methanol for fenchlorfos, chlorpyrifos, and parathion.

Table 4-5. Calculated Arrhenius Data for hydrolysis of OPs at pH 8.4[a]

OP [c]	E_a ($kJ*mol^{-1}$)	ln A	R^2 (adj.)
Chlorpyrifos-methyl	87.51 (±1.26)	21.46 (±0.46)	0.999
Parathion-methyl	95.01 (±7.18)	20.74 (±0.52)	0.989
Fenchlorphos	93.09 (±1.57)	22.61 (±0.60)	0.999
Chlorpyrifos	104.48 (±2.95)	26.13 (±1.13)	0.998
Parathion	88.44 (±11.08)	19.26 (±4.24)	0.970

[a] Stated uncertainties represent 95% confidence limits. [b] Calculated at 298.15 K. [c] Reaction rate constants for all five OPs were measured at 25, 35, 50 and 60 °C, All reactions were conducted at 0.050 M sodium phosphate buffer with ionic strength adjusted with NaCl to 0.25 equiv/L, 5% or 10% methanol at 25.0 °C.

The interpretation of the hydrolysis data is complicated by several factors. First, these compounds are known to undergo neutral and base catalyzed hydrolysis (Freed et al. 1979). At pH 8.5, it is reasonable to suspect a significant contribution from both hydrolytic mechanisms. Thus, the observed hydrolysis rates are most likely the result of two competing hydrolysis mechanisms, each with their own activation energies. Thus, it would be more appropriate to refer to the activation energies determined as "apparent activation energies" since the specific mechanisms are not known (Brezonik 1994).

4.3.4. Effect of chloride on the degradation

As discussed above, the hydrolysis of OPs is through the nucleophilic substitution both at the phosphorus atom (with the phenol moiety being the leaving group) and at the carbon bound to the oxygen of an alcohol moiety (with the diester being the leaving group). As a common nucleophile, the effect of chloride in the hydrolysis was investigated due to the relatively high concentration of sodium chloride used as

electrolyte in the reaction, and the nonnucleophilic ion ClO_4^- was used to adjust the ionic strength.

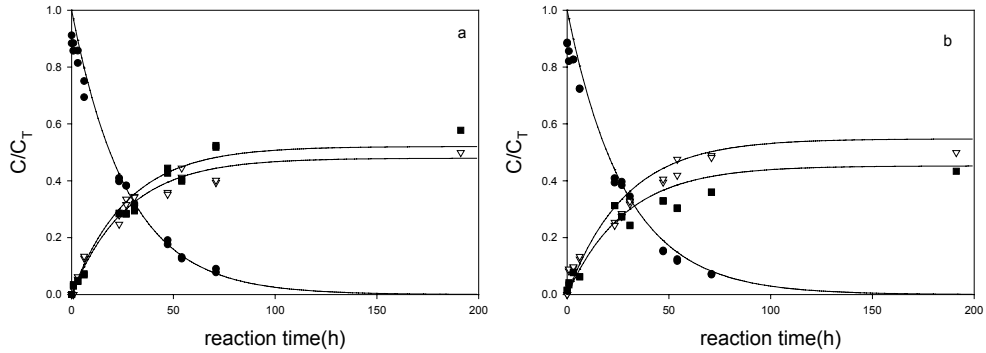

Figure 4-6. Reaction time-course of chlorpyrifos-methyl hydrolysis with 100 mM NaCl (a) and 100 mM $NaClO_4$ (b), unreacted chlorpyrifos-methyl (●), formed trichloropyridinol (▽), formed desmethyl chlorpyrifos-methyl (■), with 50 mM phosphate, at pH 7.10 and 50.0 °C. C_T is the total initial concentration of all three compounds (chlorpyrifos-methyl, trichloropyridinol and desmethyl chlorpyrifos-methyl).

Figure 4-6 shows the hydrolysis of chlorpyrifos-methyl in the presence of the nonnucleophilic ion ClO_4^- and nucleophilic ion Cl^-, respectively. The formation rates of trichloropyridinol and desmethyl chlorpyrifos-methyl are similar, which enable us to compare the rate. Figure 4-6a shows that the formation rate of trichloropyridinol is smaller than the formation rate of desmethyl chlorpyrifos-methyl, while at the same condition; the formation rate of trichloropyridinol is bigger than the formation rate of desmethyl chlorpyrifos-methyl. The hydrolysis rate constants for chlorpyrifos-methyl and parathion-methyl at pH 7.1 are also summarized in Table 4-6.

Table 4-6: Hydrolysis Rate Constants of OPs at 50.0 °C in clean batch system

	Reaction condition	k'_{obs} (h^{-1})[a]	k'_{phenol} (h^{-1})[b]	k'_{DaOP} (h^{-1})[b]
CPM	100 mM NaCl, pH 7.06	3.69 (± 0.06)×10^{-2}	1.76 (± 0.16)×10^{-2}	1.91 (± 0.12)×10^{-2}
	100 mM $NaClO_4$, pH 7.10	3.42 (± 0.07)×10^{-2}	1.87 (± 0.15)×10^{-2}	1.59 (± 0.17)×10^{-2}
MPT	100 mM NaCl, pH 7.07	1.40 (± 0.03)×10^{-2}	1.50 (± 0.11)×10^{-3}	1.33 (± 0.04)×10^{-2}
	100 mM $NaClO_4$, pH 7.12	1.27 (± 0.06)×10^{-2}	1.53 (± 0.07)×10^{-3}	1.15 (± 0.05)×10^{-2}

[a] Determined through linear regression techniques, k'_{phenol} is the formation rate of phenol, k'_{DaOP} is the formation rate of desalkyl OPs, and k'_{obs} is the degradation rate of OPs, [b] Determined via simultaneous nonlinear regression techniques using Scientist for Windows, standard deviation resulting from the nonlinear regression. All reactions were conducted in 0.050 M sodium phosphate; ionic strength equal to 0.25 equiv/L, 5% methanol at 50.0 °C.

Table 4-6 lists the hydrolysis rates of chlorpyrifos-methyl and parathion-methyl with and without chloride ion. For both compounds, chlorpyrifos-methyl and parathion-methyl, the phenol formation rates are unchanged within the 95% confidence interval. The formation of trichlorpyridinol, which is the product of nucleophilic attack on the phosphorus atom, the formation rate is 1.76 (± 0.16)×10^{-2} h^{-1} in chloride compare with 1.87 (± 0.15)×10^{-2} h^{-1} in perchlorate for chlorpyrifos-methyl; and the formation rate of 4-nitrophenol is 1.50 (± 0.11)×10^{-3} h^{-1} in chloride compare with 1.53 (± 0.07)×10^{-3} h^{-1} in perchlorate for parathion-methyl. For the chlorpyrifos-methyl, the formation rate of desmethyl compound is 1.91 (± 0.12)×10^{-2} h^{-1} in the presence of chloride ion, which is 20% higher than that with perchlorate (1.59 (± 0.17)×10^{-2} h^{-1}) as electrolyte. And for the parathion-methyl, the formation

rate of desmethyl compound is 1.33 (± 0.04)×10^{-2} h^{-1} which is 15% higher than that with perchlorate (1.15 (± 0.05)×10^{-2} h^{-1}). Therefore, it can be concluded that the chloride ion, as a relatively "softer" nucleophile, will only attack the carbon atom of the methoxy group on the chlorpyrifos-methyl and parathion-methyl to form the desmethyl compounds.

Table 4-7: Hydrolysis rate constants of chlorpyrifos-methyl at pH 7 in clean batch system

	Reaction condition	k'_{obs} (h^{-1})[a]	k'_{phenol} (h^{-1})[b]	k'_{DaOP} (h^{-1})[b]
60.0 °C	100 mM NaCl, pH 7.05	7.99 (± 0.03)×10^{-2}	3.71 (± 0.11)×10^{-2}	4.33 (± 0.12)×10^{-2}
	100 mM $NaClO_4$, pH 7.08	7.28 (± 0.04)×10^{-2}	3.82 (± 0.12)×10^{-2}	3.40 (± 0.11)×10^{-2}
50.0 °C	100 mM NaCl, pH 7.06	3.69 (± 0.06)×10^{-2}	1.76 (± 0.16)×10^{-2}	1.91 (± 0.12)×10^{-2}
	100 mM $NaClO_4$, pH 7.10	3.42 (± 0.07)×10^{-2}	1.87 (± 0.15)×10^{-2}	1.59 (± 0.17)×10^{-2}
40.0 °C	100 mM NaCl, pH 7.05	8.80 (± 0.16)×10^{-3}	4.27 (± 0.16)×10^{-3}	4.43 (± 0.13)×10^{-3}
	100 mM $NaClO_4$, pH 7.10	8.36 (± 0.19)×10^{-2}	4.32 (± 0.20)×10^{-3}	3.98 (± 0.20)×10^{-3}

[a] Determined through linear regression techniques, k'_{phenol} is the formation rate of phenol, k'_{DaOP} is the formation rate of desalkyl OPs, and k'_{obs} is the degradation rate of OPs, [b] Determined via simultaneous nonlinear regression techniques using Scientist for Windows, Standard deviation resulting from the nonlinear regression. All reactions were conducted at pH 7, 0.050 M sodium phosphate; ionic strength equal to 0.25 equiv/L, 5% methanol at 50.0 °C.

Further research was undertaken to investigate the effect of chloride at the room temperature. According to Table 4-6, the hydrolysis occurring on the phosphorus atom accounts for about 50% of the total hydrolysis reactions for either with Cl^- or

with ClO_4^- for chlorpyrifos-methyl, while only about 10-15% of degradation reaction occurs on the phosphorus atom for parathion-methyl. So chlorpyrifos-methyl was chosen for temperature-dependent reaction at 40, 50°C and 60 °C, and the chloride effect equals to the difference of the desmethyl chlorpyrifos-methyl formation rate for the Cl^- and ClO_4^- under the same conditions. After determining the Arrhenius parameters, the reaction rate contribution of chloride at 25 °C could be calculated.

Table 4-7 lists the hydrolysis rates of chlorpyrifos-methyl with and without chloride ion. For chlorpyrifos-methyl at the three different temperatures, the phenol formation rates are the same within the 95% confidence interval. The formation rate of trichlorpyridinol, is 3.71 ($\pm$ 0.11)$\times 10^{-2}$ h^{-1} in chloride compared with 3.82 ($\pm$ 0.12)$\times 10^{-2}$ h^{-1} in perchlorate at 60 °C; and at 40 °C the formation rate of trichlorpyridinol is 4.27 ($\pm$ 0.16)$\times 10^{-3}$ h^{-1} in chloride compare with 4.32 ($\pm$ 0.20)$\times 10^{-3}$ h^{-1} in perchlorate. For the reaction at 60 °C, the formation rate of desmethyl chlorpyrifos-methyl is 4.33 ($\pm$ 0.12)$\times 10^{-2}$ h^{-1} with addtion of chloride ion, which is 27% higher than that with perchlorate (3.40 ($\pm$ 0.11)$\times 10^{-2} h^{-1}$) as electrolyte. And the formation rate of desmethyl compound at 40 °C is 4.43 ($\pm$ 0.13)$\times 10^{-3}$ h^{-1} which is 12% higher than that with perchlorate (3.98 ($\pm$ 0.20)$\times 10^{-3}$ h^{-1}). Figure 4-7 shows the temperature dependence of calculated reaction rate constants with chloride. The determined E_a for chloride attacking the methoxy group is 117.9 ($\pm$ 18.1) kJ/mol. By extending the curve to 1/T = 0.003356 (corresponds to 25 °C), the k_{Cl^-} equals to 1.6.$\times 10^{-5}$ h^{-1}, which is only about 2% of total hydrolysis and 4% of the estimate desmethyl chlorpyrifos-methyl formation.

Therefore, our results suggested that the effect of chloride at the room temperature could be ignored.

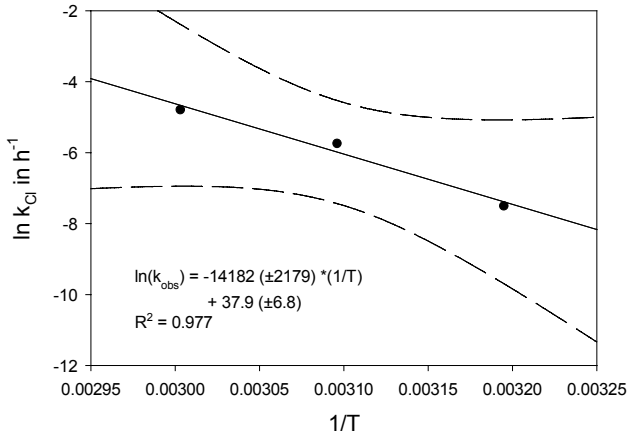

Figure 4-7. Fitted Arrhenius plot of the effect of chloride in the abiotic hydrolysis for chlorpyrifos-methyl at pH 7.1. Solid lines represent linear regressions of ln(k_{obs}(NaCl) - k_{obs}($NaClO_4$)) values determined; dashed lines represent 95% confidence intervals. All reactions were conducted at 0.050 M sodium phosphate buffer with ionic strength adjusted with electrolyte to 0.25 equiv/L, 5% methanol.

4.4. Possible Experimental Artifacts

It is evident that experimental errors such as losses due to volatilization, biodegradation, pH changes, etc., would cause results opposite in the sense to those observed. The erroneous lowering of observed hydrolysis rates could stem from several possible causes: (1) contamination of the glassware used for extraction, (2) changing of extraction efficiency as a function of analyte concentration, (3) degradation of pesticide standards and/or internal standard, (4) degradation products or other compounds coeluting with analytes, and/or (5) sorption-desorption onto container walls. After careful consideration and investigation of each of the above

factors, we conclude that the experimental controls were sufficient to preclude these processes from having a significant effect on the experimental observations. Thus, we firmly believe the data obtained in this study are valid and not the result of experimental artifacts.

4.5. Conclusions

The results of this study have important implications for pesticide fate modeling in aquatic systems. The Arrhenius data derived in this study emphasize the importance of understanding the temperature dependence of environmental fate processes. The effect of buffer concentration and methanol content on the observed hydrolysis rates of the organophosphates was found to be minimal, equivalent to only 5-10% of variation. These results suggest that in the absence of catalytic effects, abiotic hydrolysis is very slow for these pesticides under typical field conditions and may be insignificant relative to other processes. Moreover, the results underscore the need for developing a greater understanding of the relative impact of processes such as catalysis, biodegradation, and DOM association on the fate of organophosphate pesticides.

Chapter 5. Nucleophilic Substitution Reactions of Chlorpyrifos-methyl with Sulfur Species

5.1. Introduction

Organophosphorus insecticides (OPs), most of which are esters and thioesters of phosphoric and thiophosphoric acid, are widely used throughout the world and have in many cases replaced organochlorine pesticides. The amount of organophosphate insecticides used has declined since 1980, from an estimated 131 million pounds in 1980 to 73 million pounds in 1999 in U.S. agriculture. However, organophosphate usage as a fraction of total insecticide usage has increased from 58% in 1980 to 70% in 2001 (Donaldson et al.). OPs are also among the most prevalent pesticides encountered in ground and surface waters (Hallberg 1989; Kolpin et al. 1998). Organophosphorus compounds are used as insecticides for their inhibitory activity toward cholinesterase, a key enzyme involved in the metabolism of acetylcholine (one of the major neurotransmitters) (Khan 1980). Because cholinesterase is a rather common enzyme among animals that have a neural system, these pesticides can actually cause harm to many non-target species. In recent years, the U.S. EPA has begun to consider tougher regulations regarding the use of organophosphorus compounds (EPA 2000).

In general, OPs are less persistent in the environment than organochlorine compounds. The half-lives for OPs in natural water are in the range of days to months (Weber 1976; Mabey et al. 1978; Smolen et al. 1997; Pehkonen et al. 2002). The major pathways of degradation for OPs are hydrolysis, oxidation, photolysis, and biodegradation (Pehkonen et al. 2002). Oxidation of OPs to the corresponding oxons, sulfones, and sulfoxides has been reported widely (Wolfe et al. 1977).

Oxidation can occur either biotically via specific enzymes or abiotically by radical mechanisms, ozone, dissolved oxygen, or aqueous chlorine. Photodegradation can occur either by a direct photolysis of OPs, which have an absorption spectrum overlap with the solar spectrum, or by indirect photodegradation, whereby dissolved humic and fulvic acids can act as sensitizer or when particles can lead to semiconductor-promoted photodegradation. Hydrolysis of OPs is perhaps the most thoroughly studied process. It can occur by a homogeneous pathway, where H_2O and OH^- (H^+ catalysis is less common) act as nucleophiles in an S_N2 mechanism. In addition, the presence of dissolved metal ions can enhance the rate of hydrolysis. For example, the presence of Hg^{2+} can increase the initial hydrolysis rate of malathion, fenitrothion, fenthion, and parathion-methyl in a pH 5.5 buffer by two to three orders of magnitude, the hydrolysis was found to be first-order with respect to both the Hg^{2+} ion and the OPs (Wan et al. 1994). Cu^{2+} and Pb^{2+} show significant promotion at relatively low pH for zinophos, diazinon, chlorpyrifos-methyl, parathion-methyl, and fenchlorphos, but at high pH, a decrease in Cu^{2+} catalysis stems from decreased solubility of Cu^{2+} (Mortland et al. 1967; Smolen et al. 1997). Heterogeneous surfaces such as Fe and Al oxides and different clays can enhance the rate of hydrolysis by providing surface sites at which the nucleophiles and the OP can react (Racke et al. 1996; Dannenberg et al. 1998). Biotransformation of OPs is also reported to be an important and rapid degradation pathway (Bakke et al. 1976; Wanner et al. 1989; Landis 1991). However, the occurrence of the microorganisms and the enzymatic degradation mechanisms has not been

thoroughly investigated. Therefore, it is difficult to predict the contribution of biotransformation to the overall fate of OPs in the environment.

OPs that are present in surface water may associate with particles and can eventually become part of the sediment phase. It is also likely that some organophosphorus insecticides are transported into salt marshes and into the anoxic bottom layers of estuaries, which may also contain high concentrations of hydrogen sulfide species (H_2S and HS^-), polysulfides (S_n^{2-}, where n = 2-5), thiosulfate and organosulfur species. These reduced sulfur species are produced via different microbial sulfate reduction pathways under hypoxic conditions (Howarth et al. 1979; Trudinger et al. 1981), while polysulfides are also produced under oxic conditions (Gun et al. 2000). Concentrations of hydrogen sulfide, polysulfides and thiosulfate in coastal marine sediment porewaters have been reported to be as high as 5.6, 0.33 and 0.6 mM, respectively (MacCrehan et al. 1995). Several organosulfur species were reported to be found in the same sediment, for example, glutathione and cysteine can reach concentrations as high as 2.4 mM and 12.4 μM, respectively (Barbash et al. 1989).

Reduced sulfur species are capable of reacting with a wide array of pollutants, including organic contaminants that undergo nucleophilic substitution reactions (Roberts et al. 1992; Lippa et al. 2002; Loch et al. 2002; Lippa et al. 2004). It has been reported that reduced inorganic and organic sulfur species are the most potent nucleophiles present in the environment (Edwards et al. 1962; Barbash et al. 1989; Schwarzenbach et al. 2003). The potential therefore exists for such highly reactive reduced sulfur nucleophiles to serve as environmental “reagents” affecting the

abiotic degradation of OPs. Because of its abundance in the subsurface environment, bisulfide (HS^-) has been shown to play an important role in the degradation of organochlorine compounds (Roberts et al. 1992). It also has been reported that the lesser abundant polysulfides relative to HS^- can outweigh bisulfide due to their considerably greater reactivity toward relatively simple alkyl halides (Loch et al. 2002; Lippa et al. 2004).

Chlorpyrifos-methyl (CPM) (Scheme 5-1) is a widely used organophosphorus insecticide. It is registered for use in the control of insects on certain stored grain, including wheat, barley, oats, rice, and sorghum as well as for empty grain bins. An average of about 80,000 pounds of active ingredient is used on 5% to 10% of all the stored grain (Hartley et al. 1987). Its ethyl analog, chlorpyrifos, was reported to be used in amounts in excess of 10 million lb/year in U.S. agriculture in 2001 (Donaldson et al.). Chlorpyrifos-methyl and chlorpyrifos are quite persistent under neutral and acidic conditions typical of surface waters, soils and aquifer sediments. The use of these two compounds has been restricted due to their high adverse effects (Eskenazi et al. 1999) and high-end residue value in food (Pico et al. 2003). Chlorpyrifos-methyl was chosen for this study because of its increased solubility in water.

In aqueous solution without any other nucleophiles present, phosphate triesters degrade via a S_N2 reactions with attack of OH^- occurring at the phosphorus atom resulting in cleavage of a P-O bond (Cox et al. 1964; Faust et al. 1972). It has also been reported that some phosphate triesters display cleavage of an O-C bond in water, indicating that organophosphate compounds can also undergo a nucleophilic

substitution reaction at the carbon atom of an alkoxy group (Weber 1976; Wanner et al. 1989; Schwarzenbach et al. 2003).

In a previous study (Jans et al. 2003), it was proposed that in bisulfide solution chlorpyrifos-methyl is likely to undergo a nucleophilic substitution with the attack of bisulfide (HS^-) occurring at the carbon of the methoxy group (Scheme 5-1). The reaction rate constant of the reaction of chlorpyrifos-methyl with HS^- was reported, however the major products of the reaction were not characterized.

SCHEME 5-1:

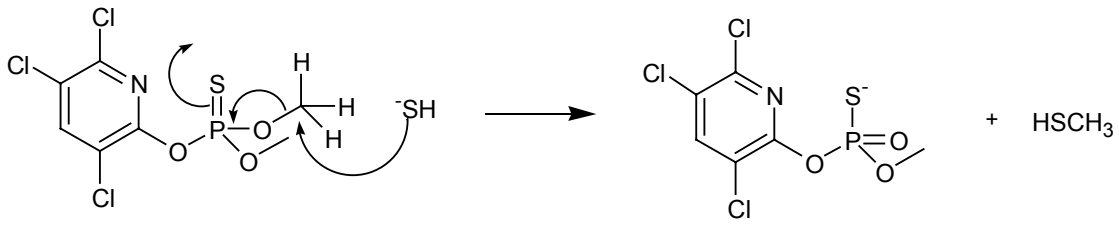

Chlorpyrifos-methyl Desmethyl chlorpyrifos-methyl

Several studies indicate that polysulfides (S_n^{2-}), thiosulfate ($S_2O_3^{2-}$) and thiophenolate (PhS^-) are stronger nucleophiles than bisulfide. Polysulfides and thiosulfate are abundant in anoxic and suboxic aqueous environments (Barbash et al. 1989; MacCrehan et al. 1995). Thiophenol was chosen as an organosulfur nucleophile, although the concentration of thiophenol in natural water is not reported, thiophenol containing compounds are likely to result from the reaction of natural organic matter with bisulfide (Perlinger et al. 2002). Therefore, in this study, these four nucleophiles were chosen and the reactions with chlorpyrifos-

methyl were monitored at varying pH and nucleophile concentration in order to obtain second-order rate constants.

The reaction of chlorpyrifos-methyl with the four reduced sulfur species are examined in detail; a reaction mechanism is proposed to account for the observed products, intermediates, kinetics, and stoichiometry. Detailed understanding of the pathways and rate constants whereby chlorpyrifos-methyl reacts with HS^-, S_n^{2-}, thiophenolate and thiosulfate will improve our ability to predict the fate of chlorpyrifos-methyl and related compounds in diverse environmental settings.

5.2. Materials and Methods

5.2.1. Chemicals

All chemical reagents were used as received. O,O-Dimethyl O-(3,5,6-trichloro-2-pyridyl)phosphorothionate (chlorpyrifos-methyl) (99.7%, CAS registry no. 5598-13-0), desmethyl chlorpyrifos-methyl sodium salt (DmCPM) (70%-86%), and the hydrolysis product, 3,5,6-trichloropyridinol (98%, CAS registry no. 6515-38-4), were provided by Dow AgroSciences (Indianapolis, IN).

All solvents and reagents that were used were analytical grade or equivalent. They were used without further purification, and were obtained from Fisher Scientific (Pittsburgh, PA) and EMD Chemicals (Gibbstown, NJ). All solutions were prepared inside a controlled-atmosphere glovebox (96% N_2, 4% H_2, Pd catalyst; Coy Laboratory Products, Grass Lake, MI) using argon-purged deionized water (Milli-Q water) with a resistivity of 18 MΩ·cm (Millipore, Bedford, MA).

5.2.2. Reduced Sulfur Solution Preparation and Analysis.

Na_2S stock solutions were prepared with $Na_2S•9H_2O$ (98%; EM Science) and deoxygenated Milli-Q water. Crystals were rinsed with Ar-purged water to remove surface oxidation products, blotted with a cellulose wipe, and then transferred to an Ar-purged three-necked flask. The flask was then connected to an Ar-purged closed glassware system consisting of a reservoir bottle (containing Milli-Q water), glass tubing, stopcocks, and an argon tank. Before rerouting the argon flow and forcing the reservoir content into the flask containing the washed sodium sulfide crystals, the Milli-Q water was purged with argon for 1 h. Then the sodium sulfide stock solution was transferred into the glovebox.

Polysulfide stock solutions were prepared via dissolution of purified sodium tetrasulfide crystals (Na_2S_4, 90+% technical grade; Alfa Aesar). Na_2S_4 crystals were purified by grinding the crystal in a mortar, rinsing with deoxygenated toluene in the glovebox to remove excess elemental sulfur contamination and were then dried under argon. The crystals were moved back into the glovebox and dissolved in deoxygenated Milli-Q water.

Thiophenol stock solutions were prepared via dissolution of thiophenol (99%, Lancaster Synthesis, Pelham, NH) in deoxygenated methanol. Thiophenol was placed inside the glovebox immediately at arrival in the lab. The concentration of thiophenol stock solution was monitored by iodometric titration and HPLC. In order to determine the extinction coefficient of thiophenol on the HPLC, the external standards were prepared in the glovebox and analyzed with HPLC as soon as possible. The results of the two methods were in good agreement (the difference of measured concentrations of thiophenol using these two methods was always smaller

than 5 %). Reaction solution containing thiosulfate was prepared by dissolving the sodium thiosulfate crystals directly. The concentration of thiosulfate was determined by iodometric titration.

All four nucleophile concentrations were determined by iodometric titration, and the sodium thiosulfate solution for the titration was standardized against potassium iodate daily (Skoog et al. 1999).

5.2.4. Experimental System.

All glassware was soaked in 1 M HNO_3 overnight and was rinsed several times with Milli-Q water prior to use. Unless otherwise stated, reaction solutions were prepared in an anaerobic glovebox and equilibrated overnight. The reaction solutions were prepared in volumetric flasks and then transferred to 20 mL glass syringes equipped with a polycarbonate stopcock and PTFE needle tubing. The syringes contained three PTFE rings to facilitate mixing. All reaction solutions contained 5% methanol and 50 mM buffer (sodium phosphate or sodium tetraborate). NaCl was added to all solutions to yield an ionic strength of 0.25 equiv/L except the reactions for ionic strength effects. The glassware for slow hydrolysis experiments was autoclaved to inhibit biological growth. In addition, the buffer solutions were filtered (0.2 μm, Anotop 25-sterile, Whatman Ltd., Maidstone, England). Filtering of the buffer solution and assembly of autoclaved glassware were carried out in a biological safety cabinet to prevent any microbial contamination. The polycarbonate stopcocks used in the hydrolysis experiments were rinsed with 80% 2-propanol and air-dried in the biological safety cabinet prior to their use in a hydrolysis experiment. The spike solutions of organophosphate were prepared by dissolving parent compounds in deoxygenated methanol. Experiments conducted at methanol concentrations from

0 to 20% indicated that these levels of methanol did not affect the reaction rates in either the presence or the absence of reduced sulfur species in the range of error. An Accumet pH meter (Fisher Scientific) with a Ross combination pH electrode (ThermoOrion, Beverly, MA) was used to measure the pH in the reaction solutions. The total hydrogen sulfide content ($[H_2S]_T$) of bisulfide solutions, representing the sum of all hydrogen sulfide species ($[H_2S] + [HS^-] + [S^{2-}]$), was measured by iodometric titration. Bisulfide ion concentrations were computed from ($[H_2S]_T$) and pH values, using acidity constants (Millero 1986) that were corrected for ionic strength through activity coefficients determined from the Davies approximation. The total reduced sulfur content $[S(-II)]_T$ of polysulfide solutions represents the sum of $[H_2S]_T$ and $[H_2S_n]_T$, where the latter represents the total concentration of polysulfides, hydropolysulfides, and sulfanes numerically equal to $\sum([S_n^{2-}] + [HS_n^-] + [H_2S_n])$ for n = 2-5. For these solutions, $[S(-II)]_T$ was measured by iodometric titration. Methods appropriate for determining concentrations of individual polysulfide species in complex matrices have not been developed. The polysulfide concentrations were calculated based on the measurement of $S(-II)_T$ and the equilibrium constants reported by Giggenbach (Giggenbach 1972) with excess S(0) as described in detail by Lippa and Roberts (Lippa et al. 2002).

5.2.5. Kinetic Experiments

Reaction kinetics were measured under pseudo-first-order conditions, with an initial chlorpyrifos-methyl concentration of 25 μM, which was typically less than 0.5-1% of the total reduced sulfur species concentration. The reaction solutions were spiked with aliquots (100 μL) of chlorpyrifos-methyl stock solution in deoxygenated methanol. Reactors were vigorously mixed for 30 s in the glovebox and were

incubated in a water bath at 25.0 ± 0.1 °C. Aliquots (1 mL) were periodically taken, 2 drops of 6 M HCl were added, and the mixture was extracted with ethyl acetate, followed by analysis via HPLC. The acidification ensures the extraction of products (calculated pK_a value of desmethyl chlorpyrifos-methyl is reported to be 1.7 in 7% alcohol) (Kabachnik et al. 1960). Pseudo-first-order rate constants were obtained by performing a linear regression of the natural logarithm of the parent compound concentration versus time. Reactions were monitored over sufficient time (two to three half-lives) to verify pseudo-first-order kinetics. For selected experiments, the pseudo-first-order rate constants for the degradation of parent compounds and for the formation of degradation products were concurrently determined via nonlinear regression techniques using Scientist for Windows, version 2.01 (MicroMath Scientific Software, Salt Lake City, UT).

5.2.6. Product Derivatization

The chlorpyrifos-methyl transformation products were alkylated using CH_3I (Alfa Aesar, 99%). A 2-mL aliquot of reaction mixture (containing in most cases 25 μM organophosphate product and up to 10 mM sulfur nucleophile) was added to 1 mL of a 0.1 M CH_3I/0.02 M $Na_2B_4O_7$ buffer solution (pH 9) and then heated at 60°C in a water bath for 1 h. After cooling to room temperature, the solution was extracted with ethyl acetate, and the extract was analyzed via GC/MS. Additional analyses of the reaction mixtures were conducted without derivatization, after acidifying samples to below pH 1 using hydrochloric acid, followed by extraction into ethyl acetate. This allowed the determination of the chlorpyrifos-methyl fraction that had converted to desmethyl chlorpyrifos-methyl. However, the derivatization condition

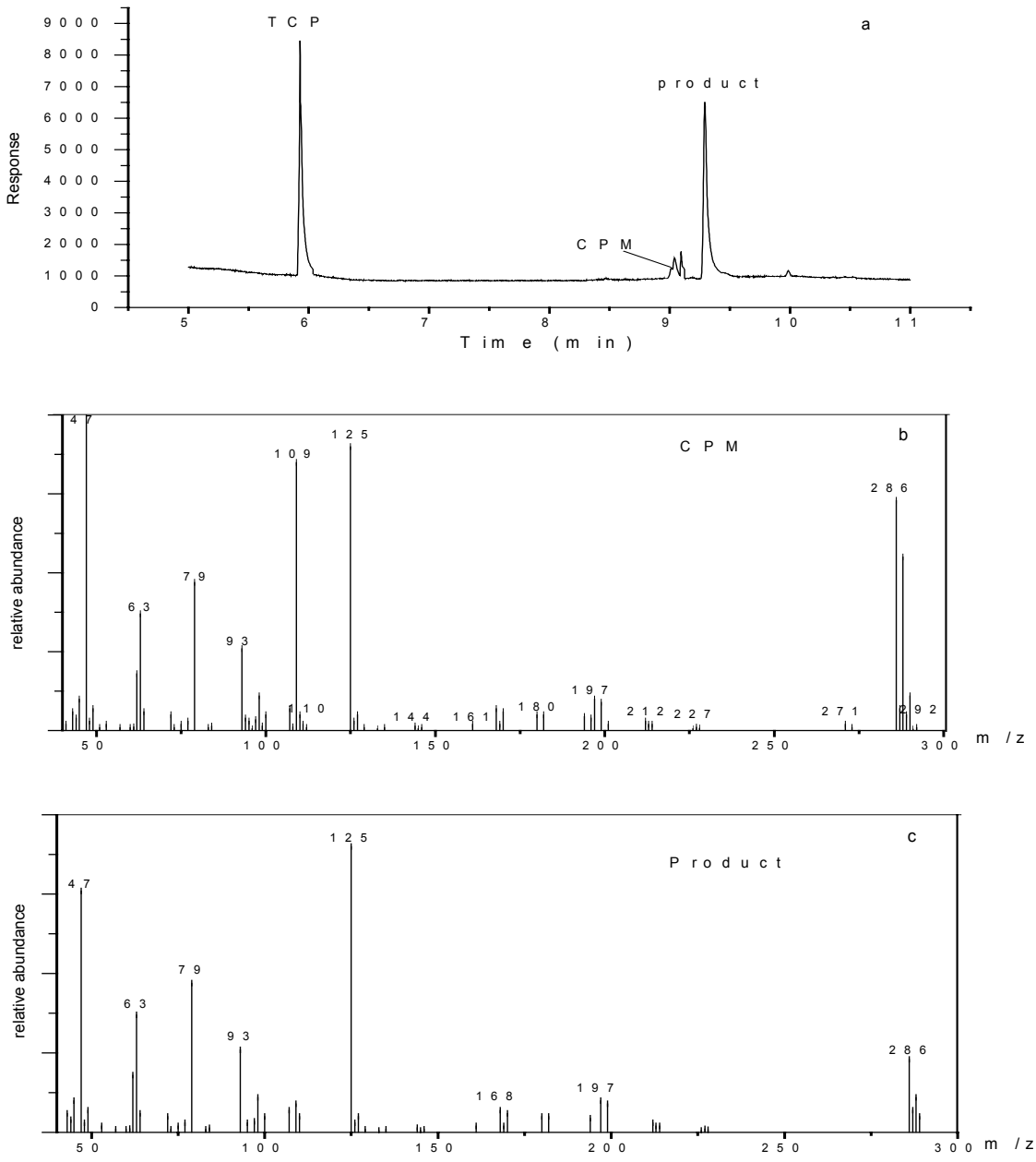

Figure 5-1. (a) Gas chromatogram of derivatized reaction solution, (b) the MS spectrum of chlorpyrifos-methyl, and (c) the MS spectrum of derivatized product (chlorpyrifos-methyl with HS^- at pH 8 for 5 days, and derivatized with CH_3I at 60℃ for 45 min).

led to some hydrolysis of the formed product, therefore the quantification was not possible (Figure 5-1a).

5.2.7. GC and GC/MS Analysis.

Ethyl acetate extracts were analyzed using a Series 8000 GC (Fisons Instruments) equipped with a split/splitless injector, a FID (EL980, Fisons Instruments), and an EC-5 fused-silica capillary column (30 m × 0.25 mm × 0.25 μm film thickness; Alltech, Deerfield, IL). Chlorpyrifos-methyl transformation products were analyzed using a Trio1000 quadrupole GC/MS (Fisons Instruments) equipped with a split/splitless injector and an AT-1 fused-silica capillary column (30 m × 0.25 mm × 0.25 μm film thickness; Alltech). Ionization mode for MS analyses of products was electron impact (EI). The EI mass spectra were generated using an electron energy of 70 eV and were monitored for ions m/z 50-400 in full scan mode.

5.2.8. HPLC Analysis.

The reactions of chlorpyrifos-methyl were followed by Waters 2690 liquid chromatograph equipped with a Waters 996 photodiode array detector. For samples with bisulfide, separation was conducted using the following conditions: Lichrospher RP-18 column (60 Å, 5 μm, 3.0 mm×119 mm, EM Separations, Gibbstown, NJ); 70% methanol and 30% 1 mM phosphoric acid for 12 minutes; flow rate: 0.7 mL/min. For the sample with polysulfide and thiosulfate, the mobile phase was 70% methanol and 30% 1 mM phosphoric acid to 100% methanol in 22 minutes; flow rate: 0.7 mL/min. For the samples with thiophenolate, the mobile phase was 70% methanol and 30% 1 mM phosphoric acid to 90% methanol and 10% 1 mM phosphoric acid in 22 minutes; flow rate, 0.45 mL/min. For selected

reactions, an ion pair chromatography method was used to monitor the formation of desmethyl chlorpyrifos-methyl. In this case a gradient method was used, which started from 10% of A (0.25 mM tetrabutyl ammonium sulfate in 85% acetonitrile, pH adjusted with phosphoric acid to 4) and 90% of C (0.25 mM tetrabutyl ammonium sulfate in Milli-Q water, pH adjusted with phosphoric acid to 4) to 22% of A and 78% C in 10 minutes, held for 2 minutes, then changed to 25% of A and 75% of B (Milli-Q water), held for 3 minutes and changed back to 10% of A and 90% of C. The injection volume was 10 μL. To determine the concentration of chlorpyrifos-methyl and its products, wavelength of 289 nm was chosen, and wavelength of 254 nm was chosen to analyze thiophenol and thioanisole.

5.2.9. Product Quantitation.

Trichloropyridinol could be quantified using reference material that was commercially available. Due to a lack of pure desmethyl chlorpyrifos-methyl (DmCPM), the quantification was based on the following assumptions. An impure standard of DmCPM (70-86%) from Dow AgroSciences allowed us to develop analytical methods and determine the retention time of DmCPM. The extraction efficiency of DmCPM into ethyl acetate (after acidifying the aliquots of the reaction mixture to below pH 1) was obtained by analyzing both the organic and aqueous phase immediately after extraction. Since no DmCPM could be detected in the acidified aqueous phase after extraction, the extraction efficiency was assumed to be 100%. The UV spectrum of DmCPM obtained with the PDA detector was identical to chlorpyrifos-methyl (Figure 5-2), so it is assumed that the extinction coefficients (wavelength equal to 289 nm) of DmCPM and chlorpyrifos-methyl are the same.

These assumptions were supported by the results of the reaction of chlorpyrifos-methyl with thiophenol (see Scheme 5-3).

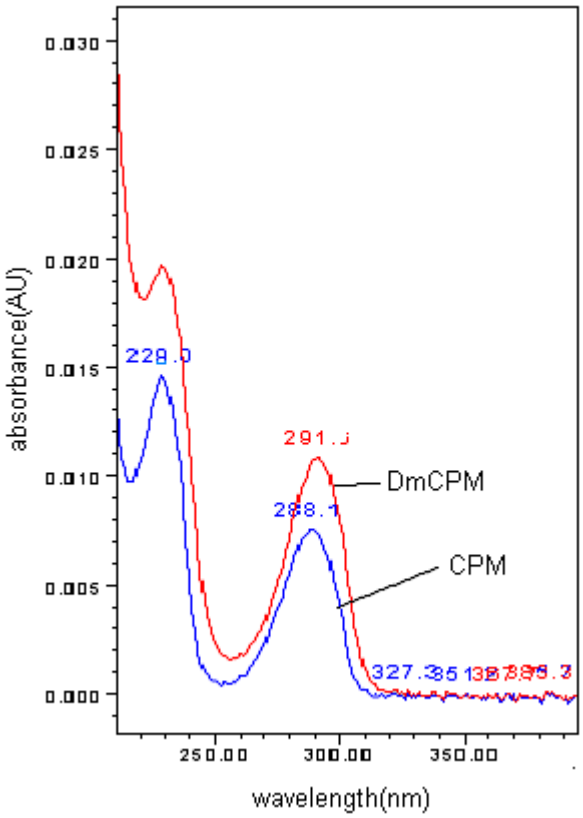

Figure 5-2. UV-Vis spectrum of chlorpyrifos-methyl and desmethyl chlorpyrifos-methyl.

5.3. Results and Discussion

5.3.1. Kinetics of Reactions with Sulfur Nucleophiles at 25°C.

The reaction of chlorpyrifos-methyl with hydrogen sulfide was assessed at different pH values. The plots of ln [parent compound] versus time are linear, indicating that the reactions of chlorpyrifos-methyl in these bisulfide solutions are first-order with respect to chlorpyrifos-methyl. The slope in such a semilogarithmic plot yields a pseudo-first-order rate constant, k_{obs}. Figure 5-3 shows representative time course

profiles for reactions of chlorpyrifos-methyl with HS^-. Linear regression analysis of log k_{obs} versus log $[H_2S]_T$ yielded a slope equal to 0.98 ± 0.05 (where the stated uncertainties reflect the 95% confidence limits) at pH 8.6. This result indicates that the reaction of chlorpyrifos-methyl with HS^- is an overall second-order process, first-order both in HS^- and in chlorpyrifos-methyl concentrations.

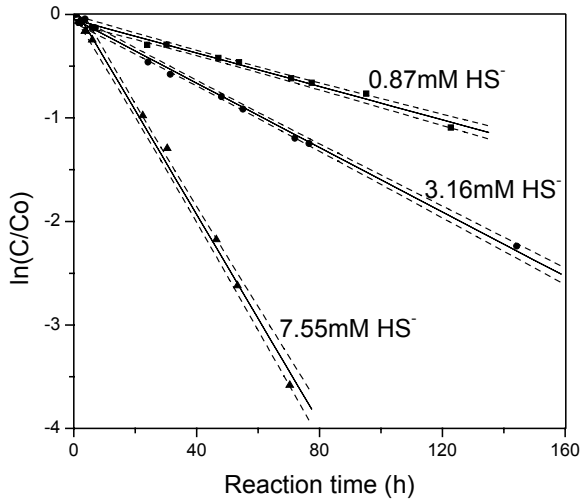

Figure 5-3. Example time courses for reactions of chlorpyrifos-methyl with HS^- at 25 °C and pH 8.6. All experiments were conducted at 0.050 M sodium phosphate and sodium tetraborate buffer, ionic strength 0.25 equiv/L (established with NaCl), 5% methanol and 25.0 °C.

All measured first-order rate constants, k_{obs} were corrected by subtracting $k_{control}$ values obtained in buffer control experiments conducted at the same temperature and pH to account for competing reactions by other nucleophiles (e.g., HO^-, HPO_4^{2-}, Cl^-). Because of differences in reactivity of the different hydrogen sulfide species (e.g., H_2S vs HS^-), a pH-dependent pseudo-first order rate constant is expected. This

corrected rate constant can be divided by the total concentration of hydrogen sulfide species, which results in the apparent second-order rate constant, k''_{app}. The apparent second-order rate constant can be given as the sum of second-order rate constant of hydrogensulfide times the mole fraction of hydrogensulfide plus the second-order

$$k''_{app} = \frac{k_{obs} - k_{control}}{[H_2S]_T} = k''_{H_2S} \times \frac{[H_2S]}{[H_2S]_T} + k''_{HS^-} \times \frac{[HS^-]}{[H_2S]_T}$$
$$= k''_{H_2S} + \frac{[HS^-]}{[H_2S]_T}(k''_{HS^-} - k''_{H_2S}) \qquad (5\text{-}1)$$

rate constant of bisulfide times the mole fraction of bisulfide (eq.5-1).

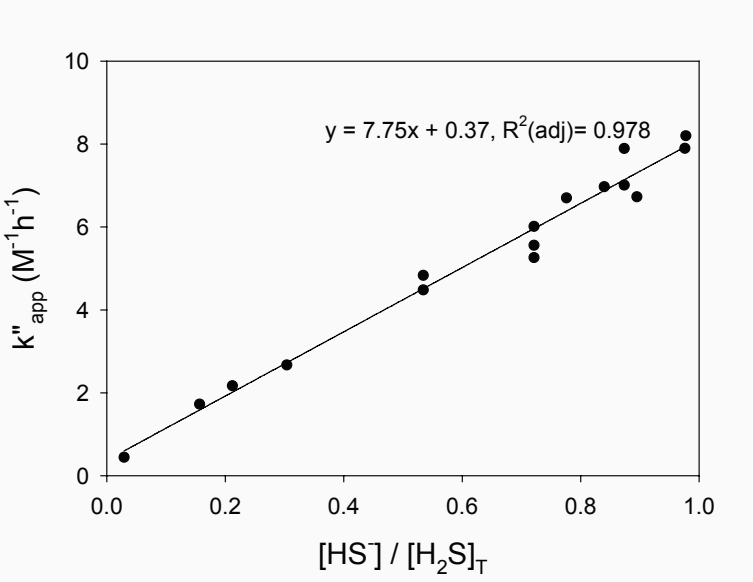

Figure 5-4. Plot of apparent second-order reaction rate constants, k''_{app} ($M^{-1}h^{-1}$), versus HS^- for reactions of chlorpyrifos-methyl with hydrogen sulfide/bisulfide for different pH values. Ionic strength is 0.25 equiv/L (established with NaCl), 0.050 M sodium phosphate and sodium tetraborate buffer, 5% methanol and at 25.0 °C.

From a plot of k''_{app} vs. ($[HS^-]/[H_2S]_T$) (Figure 5-4), k''_{H2S} and k''_{HS-} can be determined. The second-order rate constant for the reaction of bisulfide with chlorpyrifos-methyl is 2.2 (± 0.1) × 10^{-3} $M^{-1}h^{-1}$, the second-order rate constant for

the reaction of hydrogen sulfide with chlorpyrifos-methyl is 1.0 (± 2.1) × 10^{-4} $M^{-1}h^{-1}$, which is small and not significantly different from zero at the 95% confidence level (Table 5-1).

Table 5-1: Second-Order Rate Constants Determined for the S_N2 Reactions of Chlorpyrifos-methyl at 25.0 °C

Nucleophile	k" ($M^{-1}s^{-1}$)*	log k"	R^2(adj)
H_2S	1.0 (± 2.1) × 10^{-4}		
PhSH	0.3 (± 9.4) × 10^{-4}		
$S_2O_3^{2-}$	1.0 (± 0.1) × 10^{-3}	-3.0	0.964
HS^-	2.2 (± 0.2) × 10^{-3}	-2.7	0.978
PhS^-	2.1 (± 0.2) × 10^{-2}	-1.7	0.985
S_n^{2-}	3.1 (± 0.3) × 10^{-2}	-1.5	0.989

*: *Second-order rate constant of chlorpyrifos-methyl at 0.050 M sodium phosphate and sodium tetraborate buffer, ionic strength adjusted with NaCl to 0.25 eqiv/L, 5% or 10% MeOH at 25ºC.*

Similar results to the reaction with HS^- were obtained for reactions of chlorpyrifos-methyl with all other nucleophiles investigated. Linear regression analysis of log (k_{obs} - $k_{control}$) versus log [S_n^{2-}] yielded a slope equal to 1.08 ± 0.13. Linear regression analysis of log (k_{obs} - $k_{control}$) versus log [$S_2O_3^{2-}$] yielded a slope equal to 0.98 ± 0.11 and log k_{obs} versus log [PhS^-] yielded a slope equal to 1.10 ± 0.17. Therefore, the reactions of chlorpyrifos-methyl with these three nucleophiles also exhibited first-order dependence and the overall second order rate constants are listed in Table 5-1.

The dependence of the pseudo-first-order rate constant (k_{obs} - $k_{control}$) on polysulfide concentration was determined by conducting experiments at pH 8.0-9.5. Experimental solutions contained substantial concentrations of HS^- in addition to S_n^{2-} species. Second-order rate constants (k_{Sn2-}) were estimated by dividing pseudo-first-order rate constants by $\Sigma[S_n^{2-}]$, after first correcting k_{obs} to account for the contribution from hydrolysis and reaction with HS^-. Confidence limits on the second-order rate constants were calculated by propagating the errors associated with analysis of the reduced sulfur nucleophile and the pseudo-first-order rate constants. The resulting k_{Sn2-} value is 3.1 (± 0.3) × 10^{-2} $M^{-1}s^{-1}$.

The dependence of the corrected pseudo-first-order rate constant on PhS^- and $S_2O_3^{2-}$ concentration was determined by conducting experiments at constant pH and temperature. The pseudo-first-order rate constants were corrected for the contribution from hydrolysis, and the resulting second-order rate constants for the reaction of chlorpyrifos-methyl with PhS^- and $S_2O_3^{2-}$ are 2.1 (± 0.2) × 10^{-2} $M^{-1}s^{-1}$ and 1.0 (± 0.1) × 10^{-3} $M^{-1}s^{-1}$, respectively. The dependence of the pseudo-first-order rate constant (k_{obs} - $k_{control}$) on thiophenol concentration was determined by conducting experiments at pH 6.5-9.3, and the resulting second-order rate constant for the reaction of chlorpyrifos-methyl with PhSH is 0.3 (± 9.4) × 10^{-4} $M^{-1}h^{-1}$, which is close to zero.

5.3.2. Products of Chlorpyrifos-methyl Reactions with Sulfur Nucleophiles at 25°C

Prior to discussing the products of chlorpyrifos-methyl reactions with reduced sulfur species, the hydrolysis should be briefly discussed. Chlorpyrifos-methyl, like most of the other organophosphorus insecticides can undergo hydrolysis. Hydrolysis for

most of organophophorus triesters includes neutral reactions and base catalyzed reactions. In the hydrolysis of chlorpyrifos-methyl, the cleavage of the P-O bond will lead to the formation of trichloropyridinol (TCP), and the cleavage of the C-O bond will lead to the formation of desmethyl chlorpyrifos-methyl (DmCPM). In hydrolysis of organophophorus triesters, the OH^- (a "hard" nucleophile) will attack the relatively "harder" electrophilic center, the phosphorus atom to form trichloropyridinol; the "soft" nucleophile H_2O will attack both the "soft" carbon atom and the "harder" center phosphorus atom to form DmCPM and trichloropyridinol. Therefore, the reaction rates for attacking to both the carbon and phosphorus atom can be obtained by calculating the formation rate of TCP and DmCPM. Hydrolysis rate constants from pH 5.4 to 9.7 are shown in the Chapter 4. The observed hydrolysis rate is independent of pH over a wide pH range (5.4-8.6) indicating that H_2O is the dominant nucleophile under those conditions.

Figure 5-5 shows the degradation of chlorpyrifos-methyl and formation of the products for a hydrolysis experiment, for the reaction with HS^-, for the reaction with polysulfides, and for the reaction with thiophenolate. In Figure 5-5, trichloropyridinol is one of the products. In the hydrolysis experiment at pH 9.0, trichloropyridinol accounts for 76% of the chlorpyrifos-methyl that reacted. In the solution with 3.53 mM HS^-, more than 80% of chlorpyrifos-methyl reacted to form desmethyl chlorpyrifos-methyl, and in the reaction with polysulfides, the formation of desmethyl chlorpyrifos-methyl in percentage of chlorpyrifos-methyl consumed was even higher.

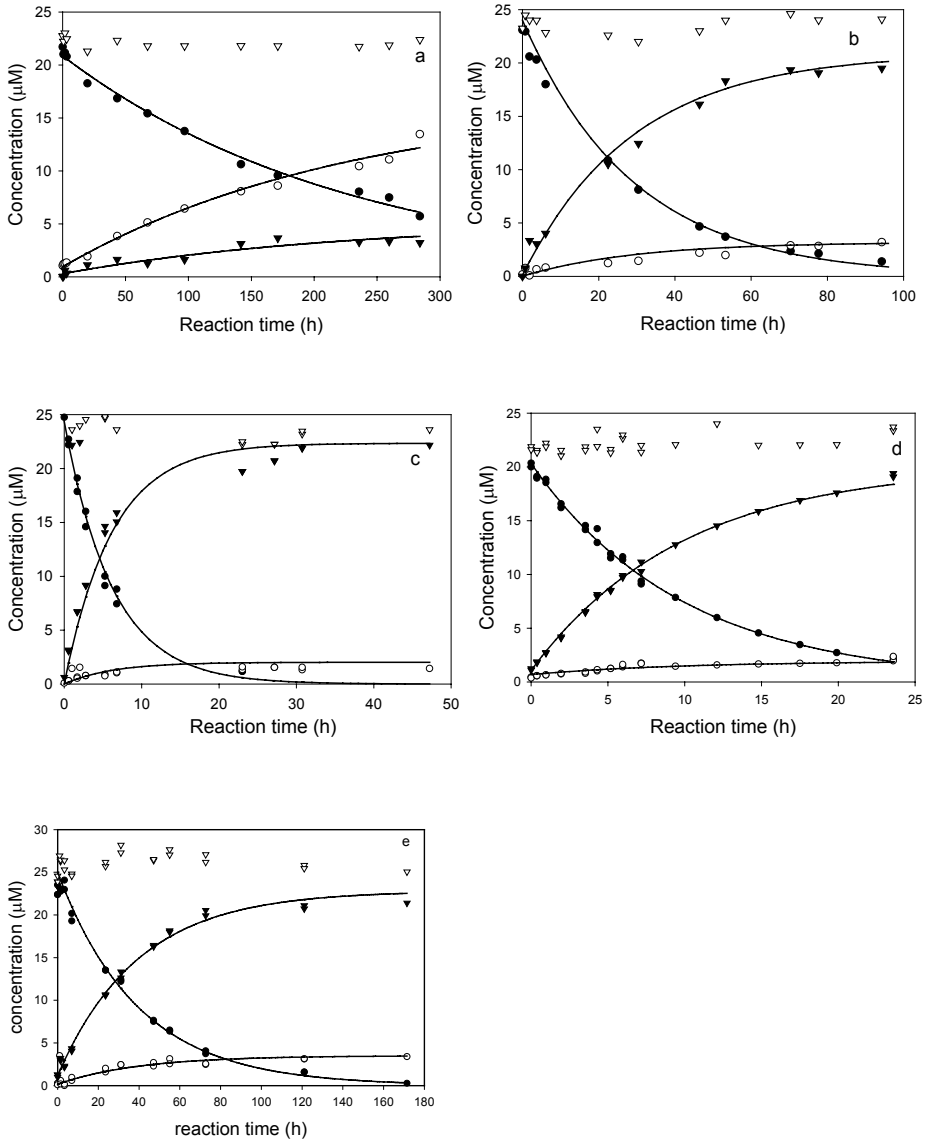

*Figure 5-5: Reaction of chlorpyrifos-methyl at (a) hydrolysis at 9.0, (b) with 3.53 mM HS^- at pH 8.6, (c) with 2.16 mM $\Sigma[S_n^{2-}]$ at pH 9.2, (d) with 1.2 mM PhS^- at pH 8.0, (e) with with 5.2 mM thiosulfate at pH 7.1, showing the degradation of chlorpyrifos-methyl (●), the formation of 3,5,6-trichloropyridinol (**o**) the assumed concentration of desmethyl chlorpyrifos-methyl (▼) and the mass balance (▽), 0.050 M sodium phosphate and sodium tetraborate buffer, ionic strength is 0.25 equiv/L (established with NaCl) and at 25.0 °C.*

The reactions of chlorpyrifos-methyl with thiophenolate and thiosulfate, which are shown in Figure 5-5d and 5-5e respectively, show similar tendencies as the reactions with bisulfide and polysulfides in terms of products distribution. From the data above, it is concluded that the deprotonated form of desmethyl chlorpyrifos-methyl, which is expected to be the dominant species at pH >3, is stable under the experimental conditions over the time period of the experiment. Only the nonionic form of desmethyl chlorpyrifos-methyl, which is present at low pH values, might undergo further hydrolysis or attack by negatively charged nucleophiles. The reactivity of trichloropyridinol toward HS^- was tested in separate experiments, showing that there is no reaction between trichloropyridinol and HS^- over the time interval relevant for the experiments presented here. Based on these observations, the following reaction scheme was used to model the experiments.

SCHEME 5-2:

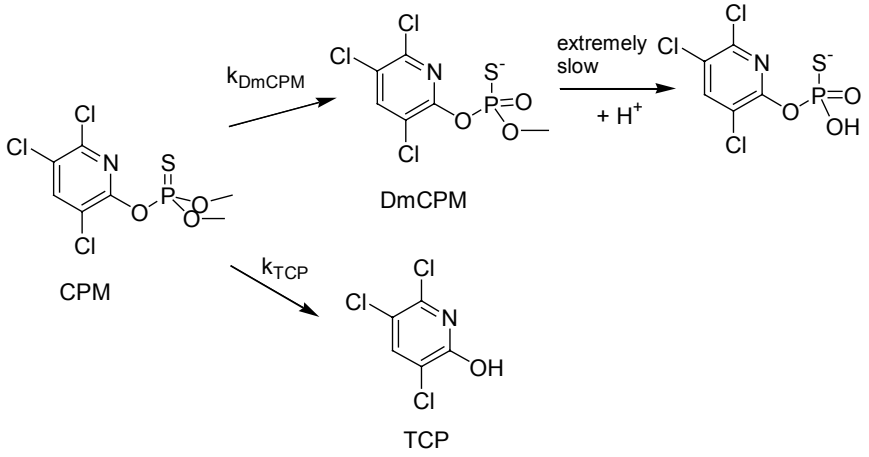

Since in our experiments, the reaction conditions did not lead to a significant degradation of trichloropyridinol or desmethyl chlorpyrifos-methyl, only two major products were considered. The data analysis of these experiments was performed

using nonlinear regression allowing the determination of k_{DmCPM} and k_{TCP} by fitting the degrading chlorpyrifos-methyl concentration and the forming trichloropyridinol and desmethyl chlorpyrifos-methyl concentration simultaneously (Table 5-2).

Table 5-2: Reaction Rate Constants of Chlorpyrifos-methyl [a]

Reaction condition	k'_{obs} $(s^{-1})^b$	k'_{TCP} $(s^{-1})^b$	k'_{DmCPM} $(s^{-1})^b$
pH 7.2, control buffer	$8.3 (\pm 0.9)\times10^{-7}$	$5.7 (\pm 0.7)\times10^{-7}$	NA[c]
pH 9.0, control buffer	$2.4 (\pm 0.1)\times10^{-6}$	$1.8 (\pm 0.1)\times10^{-6}$	$0.56 (\pm 0.02)\times10^{-6}$
pH 7.4, 3.8mM HS^-	$7.1 (\pm 0.4)\times10^{-6}$	$0.55 (\pm 0.03)\times10^{-6}$	$6.5 (\pm 0.3)\times10^{-6}$
pH 8.3, 3.0mM HS^-	$9.6 (\pm 0.4)\times10^{-6}$	$1.31 (\pm 0.01)\times10^{-6}$	$8.3 (\pm 0.03)\times10^{-6}$
pH 9.2, 1.8mM ΣS_n^{2-}	$4.5 (\pm 0.1)\times10^{-5}$	$0.17 (\pm 0.01)\times10^{-6}$	$4.3 (\pm 0.2)\times10^{-5}$
pH 9.2, 3.6mM ΣS_n^{2-}	$1.2 (\pm 0.01)\times10^{-4}$	$1.5 (\pm 0.03)\times10^{-6}$	$1.2 (\pm 0.01)\times10^{-4}$
pH 8.1, 2.1mM PhS^-	$3.2 (\pm 0.05)\times10^{-5}$	$9.4 (\pm 0.95)\times10^{-7}$	$3.2(\pm 0.04)\times10^{-5}$
pH 8.0, 1.2mM PhS^-	$2.6 (\pm 0.2)\times10^{-5}$	$0.11 (\pm 0.01)\times10^{-6}$	$2.6 (\pm 0.2)\times10^{-5}$
pH 7.0, 7.9mM $S_2O_3^{2-}$	$6.6 (\pm 0.4)\times10^{-6}$	$0.44 (\pm 0.07)\times10^{-6}$	$6.1 (\pm 0.4)\times10^{-6}$
pH 7.0, 5.2mM $S_2O_3^{2-}$	$4.9 (\pm 0.2)\times10^{-6}$	$0.42 (\pm 0.03)\times10^{-6}$	$4.5 (\pm 0.1)\times10^{-6}$

[a] Determined via simultaneous nonlinear regression techniques using Scientist for Windows based on the model shown in Scheme 5-2. [b] Standard deviation resulting from the nonlinear regression. [c] not measured. All reactions were conducted at 0.050 M sodium phosphate and sodium tetraborate buffer with ionic strength adjusted with NaCl to 0.25 equiv/L, 5% methanol and 25.0 °C.

Therefore, the experiments were modeled by assuming parallel reactions given by the expression:

$$\frac{-d[CPM]}{dt} = (k'_{TCP} + k'_{DmCPM}) * [CPM] = k'_{CPM} * [CPM] \quad (5\text{-}2)$$

$$\frac{d[TCP]}{dt} = k'_{TCP} * [CPM] \quad (5\text{-}3)$$

$$\frac{d[DmCPM]}{dt} = k'_{DmCPM} * [CPM] \quad (5\text{-}4)$$

The fitted rate constants in Table 5-2 show that all of the observed trichloropyridinol formation in experiments with reduced sulfur species can be explained by the trichloropyridinol formation due to hydrolysis (see k'_{TCP} values in Table 5-2). Based on these findings, it can be concluded that the observed results can be explained by the reduced sulfur species reacting with chlorpyrifos-methyl via an attack at the carbon of a methoxy group (Scheme 5-3).

SCHEME 5-3:

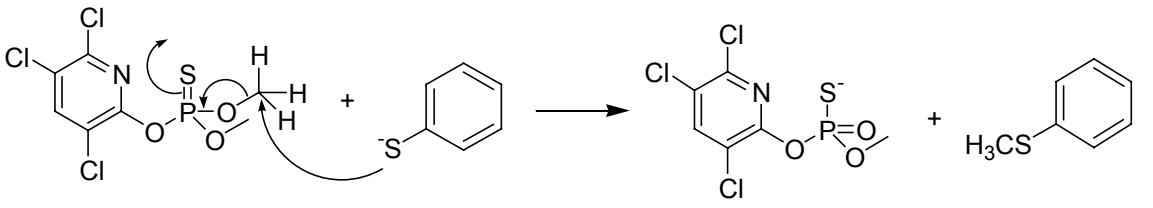

Chlorpyrifos-methyl DmCPM Thioanisole

This reaction of chlorpyrifos-methyl with thiophenolate leads to the formation of methylated sulfur species (thioanisole) that can also be used to determine the formation rate constant of desmethyl chlorpyrifos-methyl (Figure 5-5d and 5-6). The concentrations of the formed thioanisole are not signicantly different from the concentrations of desmethyl chlorpyrifos-methyl at any point in the time-course (the slope of [DmCPM] vs. [thioanisole] equal to 1). This observation supports the proposed mechanism that chlorpyrifos-methyl reacts with sulfur nucleophiles by a

nucleophilic substitution at the carbon of a methoxy group via the leaving of DmCPM.

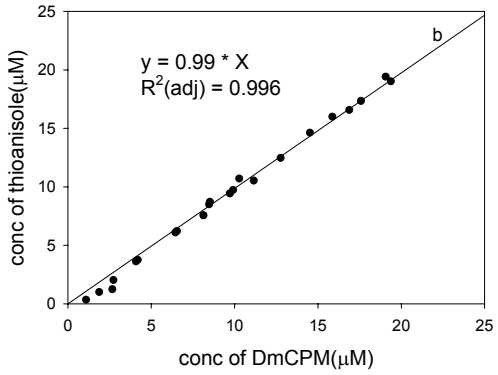

Figure 5-6: Correlation of the formation of DmCPM and thioanisole in the reaction of chlorpyrifos-methyl with 1.2 mM PhS^- at pH 8.0. Ionic strength is 0.25 equiv/L (established with NaCl) with 0.050 M sodium phosphate and sodium tetraborate buffer, 5% methanol and at 25.0 °C.

Additional studies on the identity of the products were conducted by methylating reaction solution that contained less than 10% of the initial parent compounds concentration with excess CH_3I, followed by extraction into *n*-hexane and analysis via GC/MS (EI). The formation of the desalkyl products from the reaction of chlorpyrifos-methyl with HS^- was supported by the analyses of methylated reaction mixtures. The total ion chromatogram (TIC) and related mass spectra for derivatized reaction mixtures are shown in Figure 5-1. Figure 5-1 shows that the major derivatization product is O-methyl S-methyl O-3,5,6-trichloropyridylphosphate (product at r_t = 9.385 min), and 3,5,6-trichloropyridinol (r_t = 5.987 min) and chlorpyrifos-methyl (r_t = 9.054 min) were detected. The derivatized product and chlorpyrifos-methyl have similar mass spectra, while the major difference is

fragment 109, which is the oxidation of fragment ($S=P(OCH_3)OCH_3$). This fragment is more likely to form in the product where S is bonded only to P than in the product where S is bonded to P and CH_3.

Our data indicates that the reduced sulfur species react with chlorpyrifos-methyl very likely via S_N2 mechanism. This will also allow us to evaluate the nucleophilicities of these environmentally relevant sulfur nucleophiles. Table 5-1 lists the measured second-order rate constants for the S_N2 reactions of chlorpyrifos-methyl with the nucleophiles. The Swain-Scott equation was used to evaluate the relative nucleophilicity of the measured reduced sulfur nucleophiles (Swain et al. 1953). The Swain-Scott equation is given as $\log k/k_o = sn$, where s is a constant characteristic of the substrate (s = 1 for MeBr), k_o the rate constant for the reaction of water, and n the nucleophilicity of the nucleophile reacting with MeBr. The relative order of k_{Nuc} values for the reactions of chlorpyrifos-methyl with three sulfur nucleophiles (HS^-, PhS^-, S_n^{2-}) tends to parallel that previously reported for S_N2 reactions of methyl bromide (Figure. 5-7).

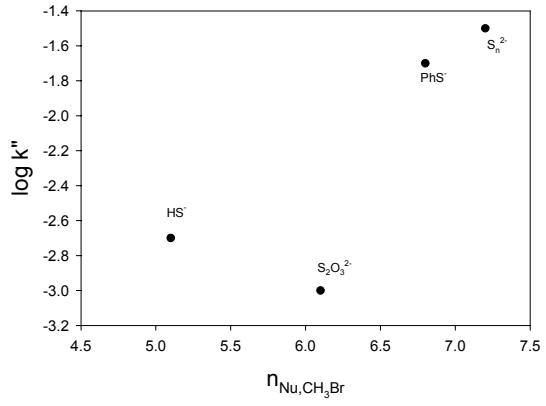

Figure 5-7: Logarithm of rate constants for reactions of chlorpyrifos-methyl with various reduced sulfur nucleophiles versus $n_{Nu,\ CH3Br}$.

Thiosulfate reacts 10 times faster than bisulfide with CH_3Br; whereas chlorpyrifos-methyl reacts about two times faster with bisulfide than with thiosulfate. It is quite likely that steric hindrance is responsible for the lower reactivity of the larger thiosulfate nucleophile towards chlorpyrifos-methyl. Similar observations of a relatively reduced nucleophilicity of thiosulfate are reported by Lippa and Roberts for the nucleophilic substitution reaction of chloroacetanilides with reduced sulfur species (Lippa et al. 2004).

5.4. Environmental Significance

The environmental fate of chlorpyrifos-methyl is controlled by a number of abiotic and biotic processes. Our results suggest that HS^-, S_n^{2-}, PhS^- and $S_2O_3^{2-}$ are sufficiently reactive as to control the fate of chlorpyrifos-methyl in anoxic and suboxic environments where the reduced sulfur species are abundant. Under these conditions, the organophosphorus diester is the major degradation product resulting from a nucleophilic attack by reduced sulfur species (e.g., HS^-, S_n^{2-}, PhS^-, $S_2O_3^{2-}$) at the carbon atom of the methoxy groups of the phosphorothionate ester. The calculated half-life of chlorpyrifos-methyl with just hydrolysis at pH 8 is 206 hours; this is 10 times greater than the calculated half-life in the presence of 5 mM of bisulfide that is 19 hours. The calculated half-life of chlorpyrifos-methyl with 0.33 mM polysulfides is 7 hours, and the calculated half-life with 0.5 mM thiosulfate is 170 hours. These values of reduced sulfur species represent the maximum concentrations reported for Great Marsh, DE sediment porewater (Boulegue et al. 1982). Therefore, reduced sulfur species present at environmentally relevant

concentrations represent an important sink for chlorpyrifos-methyl in anoxic coastal marine environments.

Our results also show that the reduced sulfur species have to be deprotonated in order to be good nucleophiles. Hydrogen sulfide and thiophenol in their protonated form are not environmentally relevant for chlorpyrifos-methyl degradation. For the same reason, some of the organosulfur species present in sediments, such as cysteine and glutathione are quite likely not relevant as nucleophiles due to their high pK_a values.

It is also worth mentioning that polysulfides are actually employed as a 30% aqueous solution in commercial preparations used for agricultural soil conditioning to take advantage of fungicidal qualities as well its use as an essential nutrient (Kohn et al. 1992). Therefore, a possible application of polysulfides and phosphorothionate pesticides to the same agriculture soils may result in significant sulfur species-involved reactions and significantly reduce the lifetime of the pesticide in the soil.

Chapter 6. Kinetic and Mechanism in the Reaction of Phosphorothionate Ester Pesticides with Reduced Sulfur Species

Charpter 5 describes the S_N2 reaction of chloropyrifos-methyl with different sulfur species in detail. It is demonstrated that the reduced sulfur species attacking the carbon atom of the methoxy group instead of the central phosphorus atom. In order to elucidate the distinctive features of the phosphorothioate group, extended research about similar compounds is needed. Therefore, in chapter 6, four more phosphorothionate ester pesticides were investigated. This also allows us to compare the relative reactivity of the OPs.

6.1. Introduction

Organophosphorus insecticides (OPs), most of which are esters and thioesters of phosphoric and thiophosphoric acid, are widely used throughout the world and have in many cases replaced organochlorine pesticides. The amount of organophosphate insecticides used has declined since 1980, from an estimated 131 million pounds in 1980 to 73 million pounds in 1999 in U.S. agriculture. However, organophosphate usage as a fraction of total insecticide usage has increased from 58% in 1980 to 70% in 2001 (Donaldson et al.). OPs are also among the most prevalent pesticides encountered in ground and surface waters (Hallberg 1989; Kolpin et al. 1998). OPs that are present in surface water may associate with particles and can eventually become part of the sediment phase. It is also likely that some organophosphorus insecticides are transported into salt marshes and into the anoxic bottom layers of estuaries, which may also contain high concentrations of hydrogen sulfide species (H_2S and HS^-), polysulfides (S_n^{2-}, where n = 2-5), thiosulfate and

organosulfur species. These reduced sulfur species are produced via different microbial sulfate reduction pathways under hypoxic conditions (Howarth et al. 1979; Trudinger et al. 1981), while polysulfides are also produced under oxic conditions (Gun et al. 2000). Concentrations of hydrogen sulfide, polysulfides and thiosulfate in coastal marine sediment porewaters have been reported to be as high as 5.6, 0.33 and 0.6 mM, respectively (MacCrehan et al. 1995). Several organosulfur species were reported to be found in the same sediment, for example, glutathione and cysteine can reach concentrations as high as 2.4 mM and 12.4 μM, respectively (Barbash et al. 1989).

Reduced sulfur species, which are the most potent "environmental" nucleophiles affecting the abiotic degradation, have been investigated for being a principal reactive reagent for chemical degradation of organic pollutant (Miller et al. 1998; Lippa et al. 2002; Lippa et al. 2004). They are responsible for considerable breakdown of pesticide molecules which can vary extensively with pH values (Barbash et al. 1989). In many coastal environments, increased biological activity during warmer months leads to depletion of dissolved oxygen. Under such conditions, microbial sulfate reduction can give rise to locally high concentrations of hydrogen sulfide species (H_2S and HS^-) and polysulfide ions (S_n^{2-}). Concentrations of hydrogen sulfide and polysulfides in coastal marine sediment porewaters have been reported as high as 5.6 and 0.33 mM, respectively (MacCrehan et al. 1995). Because of their abundance in the subsurface environments, bisulfide (HS^-) has been shown to play an important role in the degradation of the organochlorine compounds (Roberts et al. 1992; Miller et al.

1998). It also has been reported that the lesser abundant polysulfides relative to HS^- can outweigh bisulfide due to their considerably greater reactivity toward relatively simple alkyl halides (Edwards 1954; Edwards et al. 1962; Roberts et al. 1992; Miller et al. 1998).

In aqueous solution without any other nucleophiles present, phosphate triesters degrade via a S_N2 reactions with attack of OH^- occurring at the phosphorus atom resulting in cleavage of a P-O bond (Cox et al. 1964; Faust et al. 1972). It has also been reported that some phosphate triesters display cleavage of an O-C bond in water, indicating that organophosphate compounds can also undergo a nucleophilic substitution reaction at the carbon atom of an alkoxy group (Weber 1976; Wanner et al. 1989; Schwarzenbach et al. 2003).

Several studies indicate that polysulfides (S_n^{2-}), thiosulfate ($S_2O_3^{2-}$) and thiophenolate (PhS^-) are stronger nucleophiles than bisulfide. Polysulfides and thiosulfate are abundant in anoxic and suboxic aqueous environments (Barbash et al. 1989; MacCrehan et al. 1995). Thiophenol was chosen as an organosulfur nucleophile, although the concentration of thiophenol in natural water is not reported, thiophenol containing compounds are likely to result from the reaction of natural organic matter with bisulfide (Perlinger et al. 2002). Therefore, in this study, these four nucleophiles were chosen and the reactions with chlorpyrifos-methyl were monitored at varying pH and nucleophile concentrations in order to obtain second-order rate constants.

The primary purpose of this study was to more closely examine rates and products of reactions of five structurally related organophosphorothionate esters (Table 4-1 in

Chapter 4) with reduced sulfur nucleophiles. The effects of nucleophile concentration, nucleophile identity, and acid/base speciation on rates of organophosphorothionate esters reaction were systematically investigated in well-defined solutions at 25 °C in order to determine the relevant second-order rate constants. A reaction mechanism is proposed to account for the observed products, intermediates, kinetics, and stoichiometry. Products were characterized by gas chromatography/mass spectrometry (GC/MS) following methylation. In addition, the activation energies were determined. The influence of organophosphorothionate esters structure on reactivity was explored by measuring the rates and products of reactions of HS^- and S_n^{2-}. Detailed understanding of the pathways and rate constants whereby the investigated OPs reacts with HS^-, S_n^{2-}, thiophenolate and thiosulfate will improve our ability to predict the fate of other OPs and related compounds in diverse environmental settings. This information provides a consistent database of rate constants that can be used to test structure-activity relationships. Hence, this study serves as a bridge between purely theoretical studies and measurements in the environment.

6.2. Materials and Methods

All chemical reagents were of the highest purity available. Unless otherwise stated, all solutions were prepared inside a controlled-atmosphere glovebox (96% N_2, 4% H_2, Pd catalyst; Coy Laboratory Products, Grass Lake, MI) using deionized water (Milli-Q water) with a resistivity of 18 MΩ·cm (Millipore Corp., Milford, MA). Prior to use, Milli-Q water was purged with high purity argon; and immediately brought into the glovebox. All glassware was soaked in 1 M HNO_3 overnight and was rinsed several times with Milli-Q water prior to use. Glassware having prior

contact with sulfur species was first soaked in 1 M NaOH/methanol solution and was rinsed several times with Milli-Q water prior to soaking in HNO_3.

6.2.1. Chemicals.

Chlorpyrifos (99.7%), chlorpyrifos-methyl (99.7%), desmethyl chlorpyrifos-methyl sodium salt (DmCPM) (70%-86%), and 3,5,6-trichloropyridinol (98%) were provided by Dow AgroSciences (Indianapolis, IN). Parathion-methyl (98.7%), parathion (99.5%) and fenchlorphos (98.3%) were purchased from Chem Service (West Chester, PA). 4-Nitrophenol (99+%) and 2,4,5-trichlorophenol (98%) were purchased from Aldrich (Milwaukee, WI).

All solvents and reagents that were used were analytical grade or equivalent. They were used without further purification, and were obtained from Fisher Scientific (Pittsburgh, PA) and EMD Chemicals (Gibbstown, NJ).

Reduced sulfur solution preparation and analysis methods are listed in Chapter 4, which include the preparation of Na_2S stock solution, polysulfide stock solution, and thiophenol stock solutions.

The total hydrogen sulfide content ($[H_2S]_T$) of bisulfide solutions, representing the sum of all hydrogen sulfide species ($[H_2S] + [HS^-] + [S^{2-}]$), was measured by iodometric titration. Bisulfide ion concentrations were computed from ($[H_2S]_T$) and pH values, using ionization constants (Millero 1986) that were corrected for ionic strength through activity coefficients determined from the Davies approximation.

The total reduced sulfur content $[S(-II)]_T$ of polysulfide solutions represents the sum of $[H_2S]_T$ and $[H_2S_n]_T$, where the latter represents the total concentration of polysulfides, hydropolysulfides, and sulfanes numerically equal to $\sum([S_n2-] + [HS_n^-] + [H_2S_n])$ for n = 2-5. For these solutions, $[S(-II)]_T$ was measured by iodometric

titration. Methods appropriate for determining concentrations of individual polysulfide species in complex matrixes have not been developed. The total polysulfide content was used to determine total concentration of the reactive polysulfide dianion $\sum S_n^{2-}$ (numerically equal to $[S_4^{2-}] + [S_5^{2-}] + [S_6^{2-}]$) by assuming that the ratio of individual monoprotonated to fully deprotonated species was again dictated by equilibrium constraints. The polysulfide concentrations were calculated based on the measurement of $S(-II)_T$ and the equilibrium constants reported by Giggenbach (Giggenbach 1972)with excess S(0) as described in detail by Lippa and Roberts (Lippa et al. 2002).

6.2.2. Experimental Systems.

Unless otherwise stated, reaction solutions were prepared in an anaerobic glovebox and equilibrated overnight. The reaction solutions were prepared in volumetric flasks and then transferred to 20 mL glass syringes equipped with a polycarbonate stopcock and a PTFE needle. The syringes contained three PTFE rings to facilitate mixing. All reaction solutions contained 5% methanol and 50 mM buffer (sodium phosphate or borate). NaCl was added to all solutions to yield an ionic strength of 0.25 equiv/L except the reactions for ionic effects and methanol effects. The glassware for slow hydrolysis experiments was autoclaved to inhibit biological growth. In addition, the buffer solutions were filtered (0.2 μm, Anotop 25-sterile, Whatman Ltd., Maidstone, England). Filtering of the buffer solution and assembly of autoclaved glassware were carried out in a biological safety cabinet to prevent any microbial contamination. The polycarbonate stopcocks used in the hydrolysis experiments were rinsed with 80% 2-propanol and air-dried in the biological safety cabinet prior to their use in a hydrolysis experiment. The spike solutions of

organophosphate were prepared by dissolving parent compounds in deoxygenated methanol. Experiments conducted at methanol concentrations from 0 to 20% indicated that these levels of methanol did not affect the reaction rates in either presence or the absence of reduced sulfur species. An Accumet pH meter (Fisher Scientific) with a Ross combination pH electrode (ThermoOrion, Beverly, MA) was used to measure the pH in the reaction solutions.

Table 6-1: The effect of methanol in the reaction of chlorpyrifos-methyl with bisulfide[a]:

	pH	MeOH%	$[HS^-]_{tot}$(mM)	$k_{obs}(h^{-1})$	α_{HS-}	α_{H2S}	$k''(h^{-1}M^{-1})$
1	7.89	0	3.90	0.0286	0.890	0.110	7.31
2	7.82	5	3.84	0.0257	0.874	0.126	6.70
3	7.82	5	3.84	0.0246	0.874	0.126	6.41
4	7.97	10	3.95	0.0256	0.907	0.093	6.49
5	7.72	10	3.10	0.022	0.846	0.154	7.10
6	7.85	15	2.91	0.0201	0.881	0.119	6.91
7	7.92	20	3.16	0.0214	0.897	0.103	6.77
8	8.00	30	3.46	0.0198	0.913	0.087	5.72
9	7.91	25	2.49	0.0183	0.895	0.105	7.36
10	7.91	25	2.49	0.0172	0.895	0.105	6.91
11	8.67	50	3.15	0.0155	0.980	0.020	4.92
12	8.67	50	3.15	0.0166	0.980	0.020	5.26

[a]: 50mM Sodium phosphate was used as buffer and 100mM sodium chloride was used as electrolyte.

Table 6-1 lists the effect of methanol composition in the reaction of chlorpyrifos-methyl with bisulfide, the effect of methanol in the reaction of chlorpyrifos and

parathion with the other nucleophile was also investigated, and similar results were found in these experiments. *k*" was calculated by divide observed first-order rate constant (k_{obs}) with the concentration of total reduced sulfur species ($[HS^-]_{tot}$).

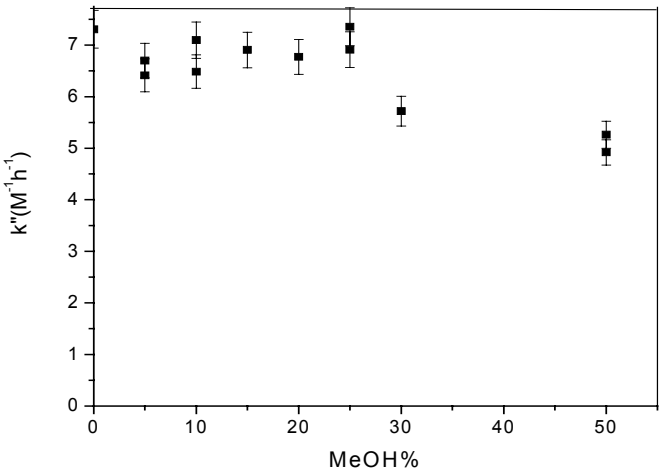

Figure 6-1: the change of second-order rate constant with methanol concentration.

Figure 6-1 showed the apparent second-order rate constant change with the [MeOH] in the buffer. From this figure, it can be concluded that the concentration of methanol has almost no effect between 0-20%. The investigated methanol level in our experiment was varied from 0-20%, therefore, in this range of methanol concentration, the solubility and solvation effect of both polysulfides and bisulfide was assumed not to change significantly enough to lead to a distinguishable difference in rate constants. In these experiments investigating the effect of methanol, the error bars were used to elucidate the statistical significance of the observed differences. And it is found that the differences of the entire observed rate constants (0-20% MeOH) are in the range of 10%. No trend was observed in the rate constants with increasing methanol concentration. Therefore, it was concluded that

the reaction rate constant does not change with increasing methanol concentration up to a concentration of 20% MeOH.

Reaction kinetics was generally determined under pseudo-first-order conditions, with nucleophile concentrations ranging from 0.2 mM to 20.0 mM. Parent compound decay and wherever possible product formation was monitored by HPLC-PDA and GC-FID. Reactions were initiated by spiking solutions (50-100 μL) containing the appropriate OP compounds, yielding initial concentrations ranging from 10 to 50 μM (25 μM for chlorpyrifos-methyl and parathion, 15 μM for fenchlorfos, 10 μM for chlorpyrifos, and 50 μM for parathion-methyl). Reactors were vigorously mixed for 30 s and were incubated at temperature controlled water bath temperature (5.0-60.0 ± 0.1 °C) in the dark to avoid possible photolysis. Aliquots (1 mL) were periodically extracted into ethyl acetate (1 mL), followed by HPLC or GC analysis.

6.2.3. Product Derivatization

The OPs transformation products were alkylated using CH_3I (Alfa Aesar, 99%). A 2-mL aliquot of reaction mixture (containing in most cases 25 μM organophosphate product and up to 10 mM sulfur nucleophile) was added to 1 mL of a 0.1 M CH_3I/0.02 M $Na_2B_4O_7$ buffer solution (pH 9) and then heated at 60°C in a water bath for 1 h. After cooling to room temperature, the solution was extracted with ethyl acetate, and the extract was analyzed via GC/MS. Additional analyses of the reaction mixtures were conducted without derivatization, after acidifying samples to below pH 1 using hydrochloric acid, followed by extraction into ethyl acetate. This allowed the determination of OPs concentration that had reacted to desalkyl OPs.

However, the derivatization condition led to some hydrolysis of the formed product, therefore the quantification was not possible.

6.2.4. GC and GC/MS Analysis

Ethyl acetate extracts were analyzed using a Series 8000 GC (Fisons Instruments) equipped with a split/splitless injector, a FID (EL980, Fisons Instruments), and an EC-5 fused-silica capillary column (30 m × 0.25 mm × 0.25 μm film thickness; Alltech, Deerfield, IL). OPs transformation products were analyzed using a Trio 1000 quadrupole GC/MS (Fisons Instruments) equipped with a split/splitless injector and an AT-1 fused-silica capillary column (30 m × 0.25 mm × 0.25 μm film thickness; Alltech). Ionization mode for MS analyses of products was electron impact (EI). The EI mass spectra were generated using an electron energy of 70 eV and were monitored for ions m/z 50-400 in full scan mode.

6.2.5. HPLC Analysis.

The loss of parent organophosphates and the formation of selected reaction products were monitored by reverse-phase HPLC with photodiode array detector. An HPLC system (Waters 2690, Waters Corp., Milford, MA) was used. A Lichrospher RP-18 column (60 Å, 5 μm, 3.0 mm×100 mm, EM Separations, Gibbstown, NJ) was used for detection of chlorpyrifos-methyl and parathion-methyl. The flow rate was set at 0.7 mL/min. An Xterra MS C_{18} column (125 Å, 5 μm, 3.9 mm×150 mm, Waters, Milford, MA) was used for detection of chlorpyrifos, parathion and fenchlorphos, the flow rate was set at 1 mL/min. An isocratic eluent (1 mM phosphoric acid in 75% acetonitrile/25% H_2O v/v) was used to monitor the reaction of chlorpyrifos-methyl, chlorpyrifos and fenchlorphos with hydrogensulfide and the hydrolysis. A gradient method was used to monitor the reaction of chlorpyrifos-methyl,

chlorpyrifos and fenchlorphos with polysulfides and thiosulfate. The mobile phase was 70% methanol and 30% 1 mM phosphoric acid to 100% methanol in 22 minutes. For the samples with thiophenolate, the mobile phase was 70% methanol and 30% 1 mM phosphoric acid to 90% methanol and 10% 1 mM phosphoric acid in 22 minutes; flow rate, 0.45 mL/min. The injected volume was 10 μL

For the reaction of parathion-methyl and parathion with hydrogensulfide and hydrolysis, a gradient method was used. The mobile phase was 42% methanol and 58% 1 mM phosphoric acid to 70% methanol and 30% phosphoric acid in 16 minutes. To monitor the reaction of parathion-methyl and parathion with polysulfides and thiosulfate, the mobile phase was 42% methanol and 58% 1 mM phosphoric acid to 100% methanol in 21 minutes. For the samples with thiophenolate, the mobile phase was 42% methanol and 58% 1 mM phosphoric acid to 90% methanol and 10% 1 mM phosphoric acid in 18 minutes, and changed to 100% for another 6 minutes; flow rate, 0.70 mL/min. The injected volume was 10 μL. Chromatographic peaks for organophosphates and hydrolysis products were identified by retention time comparison with authentic standards.

For selected reactions, an ion pair chromatography was used to monitor the formation of organophosphate diester. In this case the Xterra MS C_{18} column was used for all five organophosphorus compounds. The flow rate was set to 0.65 mL/min. A gradient method was used, which started from 10% of A (0.25 mM tetrabutyl ammonium sulfate in 85% acetonitrile, pH adjusted with phosphoric acid to 4) and 90% of C (0.25 mM tetrabutyl ammonium sulfate in milli-Q water, pH adjusted with phosphoric acid to 4) to 22% of A and 78% C in 14 minutes, held for

4 minutes, then changed to 25% of A and 75% of B (Milli-Q water), held for 3 minutes and changed back to 10% of A and 90% of C. The injection volume was 10 μL.

The integration wavelength for chlorpyrifos-methyl, chlorpyrifos and their products was 289 nm; the integration wavelength for parathion-methyl, parathion and their products was 273 nm, the integration wavelength for fenchlorfos and its products was 235 nm, and the integration wavelength for thiophenol and thioanisole was 254 nm.

6.2.6. Data Analysis

Pseudo-first-order or first-order rate constants (k_{obs}) were obtained by regressing the natural log of the parent compound concentration versus time. Except for very slow experiments, reactions were followed over 2 to 3 half-lives to verify first-order kinetics. In our experiments, OPs reacted via competing processes. Efforts were made in such situations to determine rate constants for the relevant reactions using the program *Scientist for Windows* (v. 2.01; MicroMath, Inc.). This software is capable of determining rate constants and associated parameters by fitting experimental data to numerically integrated solutions of systems of differential rate expressions

6.3. Result and Discussion

6.3.1. Kinetics of OPs Reactions with HS^- at 25 °C

Example time courses for reactions of chlorpyrifos-methyl, parathion-methyl, fenchlorphos, chlorpyrifos, and parathion with hydrogen sulfide at 3 different pHs are shown in semilogarithmic form in Figure 6-2.

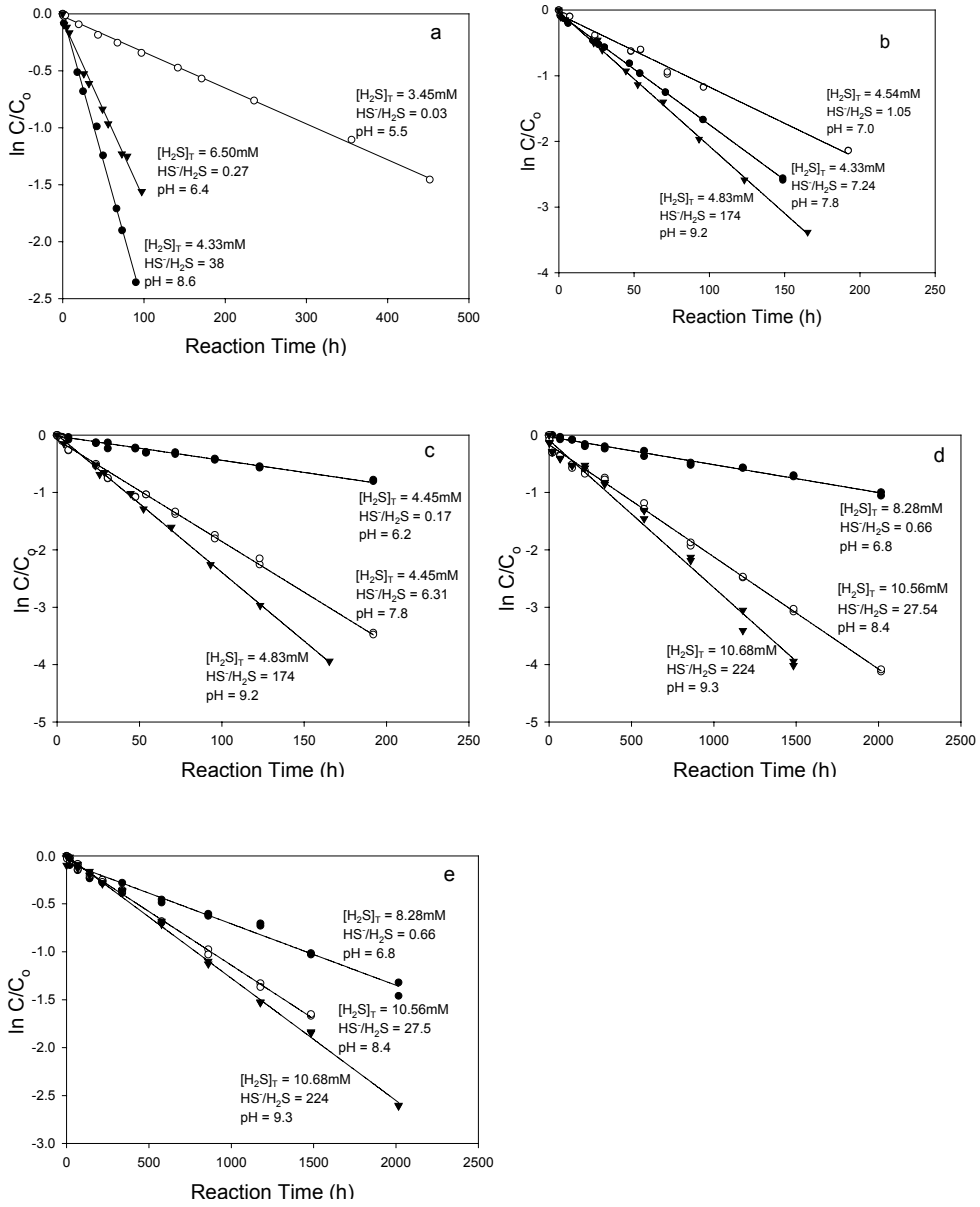

Figure 6-2. Example time courses for reactions of OPs with HS$^-$ at 25 °C and three different pHs. (a) chlorpyrifos-methyl; (b) parathion-methyl; (c) fenchlorphos; (d) chlorpyrifos; and (e) parathion. All experiments were conducted at 0.050 M sodium phosphate or 0.050 M sodium tetraborate buffer, ionic strength 0.25 equiv/L (established with NaCl), 5% methanol and 25.0 °C.

The high degree of linearity of the semilogarithmic plots shown in Figure 6-2 over several half-lives is indicative of a first-order dependence on the concentration of the organophophorus insecticides. All measured first-order rate constants, k_{obs} were corrected by subtracting $k_{control}$ values obtained in buffer control experiments conducted at the same temperature and pH to account for competing reactions by other nucleophiles (e.g., OH^-, HPO_4^{2-}, Cl^-).

The reaction order in HS^- was determined by regressing log ($k_{obs} - k_{control}$) versus log [HS^-] at constant pH.

$$\log (k_{obs} - k_{control}) = \log k_{HS^-} + a\log[HS^-] \qquad (6\text{-}1)$$

Linear regression analysis of log k_{obs} versus log [HS^-] yielded a slope (a) equal to 0.98 ± 0.05 (where the stated uncertainties reflect the 95% confidence limits) for chlorpyrifos-methyl at pH 8.6, 1.07 ± 0.08 for parathion-methyl at pH 8.8, 0.94 ± 0.14 for fenchlorphos at pH 8.3, 1.10 ± 0.12 for chlorpyrifos at pH 7.8, and 0.99 ± 0.04 for parathion at pH 9.3. This result indicates that the reaction of OPs with bisulfide is an overall second-order process, first-order both in [HS^-] and in OPs concentrations. The intercepts of the regressions are not significantly different from zero (at the 95% confident interval), which indicates that it is reasonable to subtract the rate measured for buffer control experiments from k_{obs} to account for competing reactions of other nucleophiles. A value for the second-order rate constants (k''_{app}, slope of k_{obs} versus [HS^-] plot) can be calculated by forcing the intercept through zero; this value is in good agreement with computing k''_{app} for each bisulfide concentration and then averaging the results for each OP. However, in a hydrogen sulfide solution, even with the correction of buffer control experiment, there are still

three different nucleophiles that have to be considered. The three nucleophiles are hydrogen sulfide (H_2S), bisulfide (HS^-), and sulfide (S^{2-}). The second dissociation constant (K_{a2}) of hydrogen sulfide is often stated to be around 10^{-13}, however these measurements might be incorrect due to oxidation of the sulfur in alkaline solution. The current best estimate for pK_{a2} is 19±2 (Giggenbach 1971; Meyer et al. 1983). Therefore, the degradation of OPs with sulfide can be neglected because the concentration of sulfide is too small to contribute significantly to k_{obs} (i.e., the mole fraction of S^{2-} is only 10^{-9} even around pH 10).

First-order rate constants were obtained from pH 6-10. These rate constants can be corrected for hydrolysis and divided by the total concentration of hydrogen sulfide species, which results in the apparent second-order rate constant, k''_{app}. This apparent second-order rate constant, k''_{app}, can be given by the expression

$$k''_{app} = \frac{k_{obs} - k_{control}}{[H_2S]_T} = k''_{H_2S} \times \frac{[H_2S]}{[H_2S]_T} + k''_{HS^-} \times \frac{[HS^-]}{[H_2S]_T} \qquad (6-2)$$

where $[H_2S]_T = [H_2S] + [HS^-]$.

Mole fraction of H_2S and HS^- as a function of $[H_2S]_T$:

$$\alpha_{HS^-} = \frac{[HS^-]}{[H_2S]_T} = \left(1 + \frac{H^+}{K_a}\right)^{-1} \qquad \alpha_{H_2S} = \frac{[H_2S]}{[H_2S]_T} = \left(1 + \frac{K_a}{H^+}\right)^{-1} \qquad (6-3)$$

The acid dissociation constant, K_a of H_2S is $10^{-6.98}$ (Millero 1986). After rearranging of equation 6-2 and equation 6-3, the apparent reaction constant k''_{app} can be given as a function of α_{HS^-} in terms

$$k''_{app} = k''_{H_2S} + \alpha_{HS^-}(k''_{HS^-} - k''_{H_2S}) \qquad (6-4)$$

Therefore, a plot of k''_{app} versus α_{HS^-} shows a linear correlation (Figure 6-3), and it allows the extraction of second-order rate constants k''_{H2S} and k''_{HS^-}.

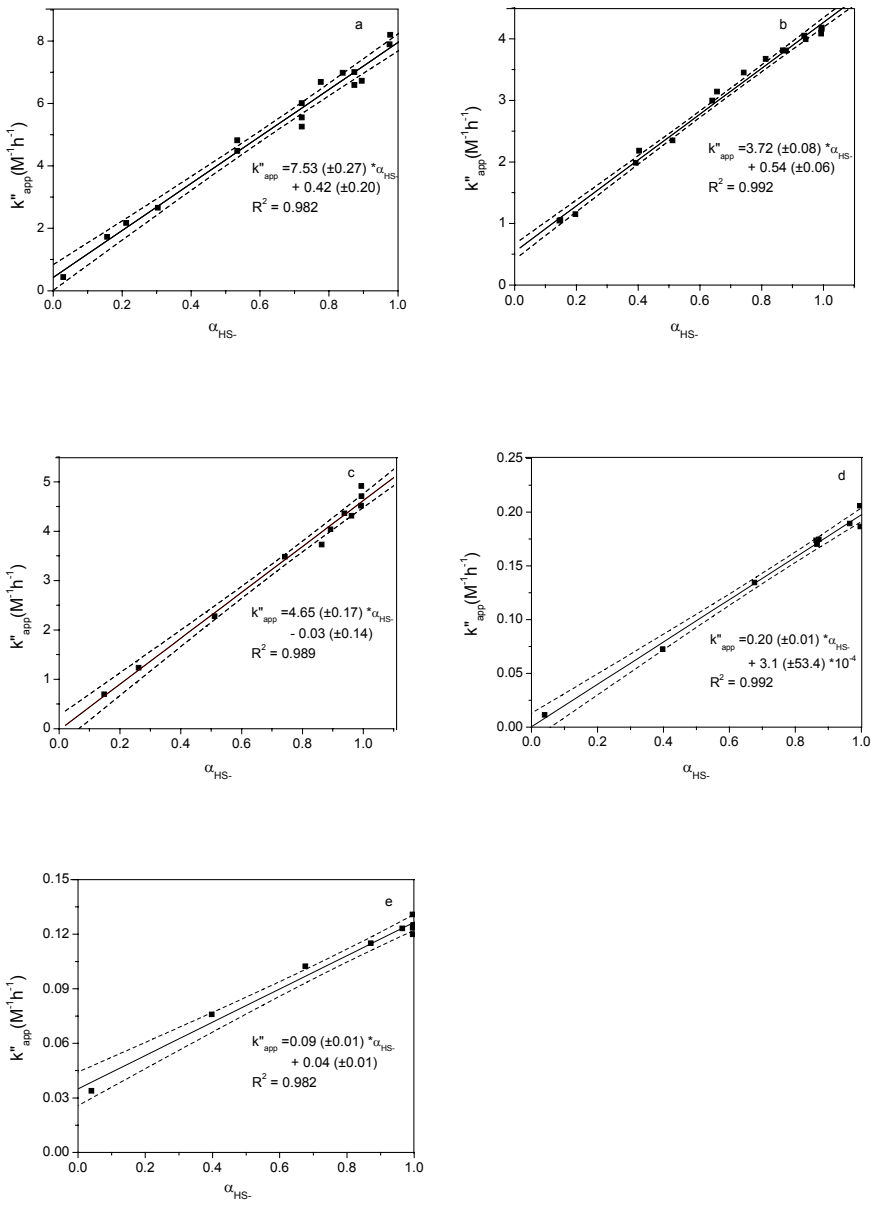

Figure 6-3: Plot of apparent second-order reaction rate constants, k''_{app} ($M^{-1}h^{-1}$), versus α_{HS^-} for reactions of hydrogen sulfide/bisulfide with (a) chlorpyrifos-methyl; (b) parathion-methyl; (c) fenchlorphos; (d) chlorpyrifos; and (e) parathion. Solid lines represent linear regressions of k''_{app} values determined at different pHs, dashed lines represent 95% confidence intervals. Ionic strength of reaction solution is 0.25 equiv/L (established with NaCl) with 0.050 M sodium phosphate and sodium tetraborate buffer, 5 or 10% methanol and at 25.0 °C.

Second-order rate constants (k''_{Nu} values) determined for reaction of OPs with HS^- and H_2S are summarized in Table 6-2. The results show that HS^- is the principal reactive species in the pH range investigated.

Table 6-2: Second-Order Rate Constants for Reactions of OPs with H_2S, HS^- and S_n^{2-} at 25.0 °C

OPs	k''_{H2S} $(M^{-1}h^{-1})^a$	k''_{HS-} $(M^{-1}h^{-1})^a$	k''_{Sn2-} $(M^{-1}h^{-1})^b$	k''_{Sn2-}/k''_{HS-}
Chlorpyrifos-methyl	0.42 (±0.20)	7.95 (±0.47)	112 (±7)	14
Parathion-methyl	0.54 (±0.06)	4.26 (±0.14)	88.9 (±3.7)	21
Fenchlorphos	0[c]	4.61 (±0.06)	108 (±8)	23
Chlorpyrifos	3.1 (±53.4) $\times 10^{-4}$	0.20 (±0.01)	3.9 (±0.2)	20
Parathion	0.04 (±0.01)	0.13 (±0.02)	6.6 (±0.4)	51

[a] Second-order rate constant determined from hydrogen sulfide solution at different pH (see Figure 6-3). [b] Second-order rate constant determined from k_{obs} values of polysulfide solutions containing known $\Sigma[S_n^{2-}]$ which were corrected for hydrolysis and reaction with HS^-. [c] This value was set to zero, the actual value resulting from Figure 6-3c is -0.03 (±0.14) $\times 10^{-4}$ $M^{-1}h^{-1}$.

6.3.2. Activation Barriers ($\Delta H^{\neq}$ and $\Delta S^{\neq}$) for Reaction with HS^-.

Statistically significant differences in k_{HS-} were observed for the five organophophorus insecticides investigated. The reactivity of the insecticides increases in the following order: parathion < chlorpyrifos << parathion-methyl ≅ fenchlorphos < chlorpyrifos-methyl. The most reactive OP, chlorpyrifos-methyl, was 70-fold more reactive than the least reactive compound, parathion. Subtle variations in structure of the OP influence their reactivity.

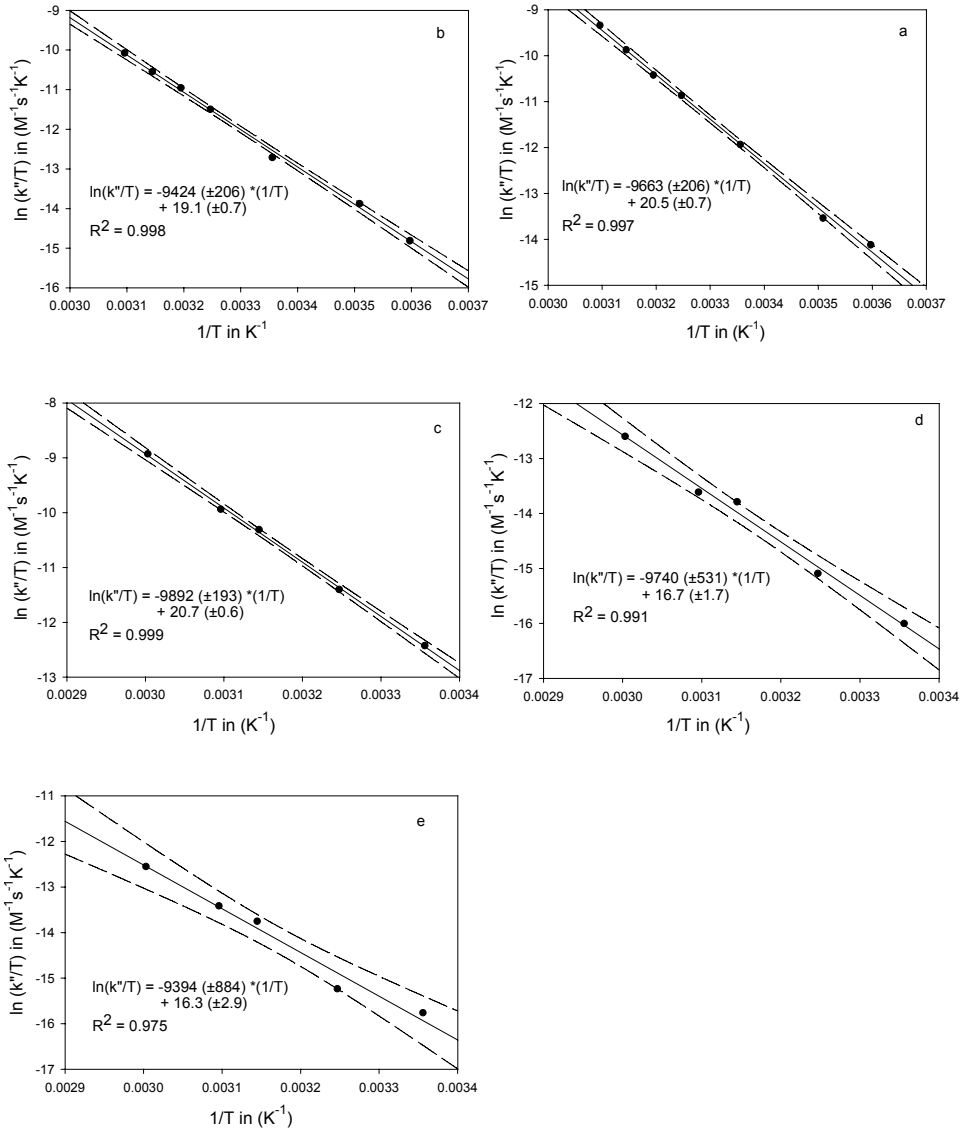

Figure 6-4. Temperature dependence of reactions of OPs with HS^-. Rate constants were determined in 0.050 M sodium phosphate buffer at pH 8.4 with (a) chlorpyrifos-methyl; (b) parathion-methyl; (c) fenchlorphos; (d) chlorpyrifos; and (e) parathion. Solid lines represent linear regressions of ln (k''_{app}/T) values versus 1/T (K^{-1}), dashed lines represent 95% confidence intervals. Ionic strength of reaction solution is 0.25 equiv/L (established with NaCl), 5 or 10% methanol and at 25.0 °C.

To explore whether these differences result from enthalpic or entropic effects, k''_{app} was measured in buffered solution (pH 8.4) over the temperature range of 5.0 to 60.0 °C, and activation parameters were determined. The temperature dependence of reactions in control experiments was also measured over comparable time period. A few experiments were also conducted at pH 6.0 for chlorpyrifos-methyl and parathion-methyl at 35.0 ± 0.1 °C to test whether H_2S could be contributing to the observed rate of reaction at higher temperatures. However, under these conditions k''_{H2S} proved to be too small to be experimentally accessible, and the effect of pH on k''_{app} was entirely consistent with HS^- as the sole reactive species. Data for each OP were plotted as shown in Figure 6-4 according to a linearized version of the Eyring expression (eq.6-5) where k is Boltzmann's constant, h is Planck's constant, R is the gas constant, T is temperature in Kelvin, and $\Delta H^{\neq}$ and $\Delta S^{\neq}$ are the enthalpic and entropic contributions, respectively, to the overall activation barrier $\Delta G^{\neq}$. Linear regression analyses of the data yielded $\Delta H^{\neq}$ and $\Delta S^{\neq}$ values summarized in Table 6-3.

$$\ln\left(\frac{k''_{app}}{T}\right) = \ln(k/h) - \Delta H^{\neq}/RT + \Delta S^{\neq}/T \qquad (6\text{-}5)$$

Figure 6-4 shows strikingly parallel nature to the plots. Indeed, differences in slopes (and thus $\Delta H^{\neq}$ values) are not significant for the five insecticides at the 95% confidence level. This would tend to suggest that reactivity contrasts stem primarily from entropic factors (e.g., steric hindrance), our results indicate $\Delta S^{\neq}$ for chlorpyifos is statistically larger than for chlorpyrifos-methyl. In this context, however, it should be mentioned, that precise experimental measures of $\Delta S^{\neq}$ are notoriously difficult to

determine. However, differences in steric hindrance (methoxy versus ethoxy) are quite likely the most important cause for the observed 70-fold difference in reactivity between the five insecticides.

Table 6-3. Calculated Arrhenius Data and Activation Barriers for Reactions of OPs with HS^- at pH 8.4[a]

OP [b]	E_a (kJ*mol^{-1})	$\Delta H^{\neq}$ (kJ*mol^{-1})	$\Delta S^{\neq}$ (J*mol^{-1}*K^{-1})	$\Delta G^{\neq}$ [c] (kJ*mol^{-1})
Chlorpyrifos-methyl	85.2 (±1.7)	82.7 (±1.7)	-27.1 (±5.7)	83.6 (±3.4)
Parathion-methyl	80.8 (±1.7)	78.3 (±1.7)	-38.9 (±5.7)	82.8 (±3.4)
Fenchlorphos	84.8 (±1.6)	82.2 (±1.6)	-25.1 (±5.1)	82.6 (±3.2)
Chlorpyrifos	83.6 (±4.5)	81.0 (±4.5)	-59.1 (±14.0)	91.5 (±8.6)
Parathion	82.4 (±7.4)	79.8 (±7.4)	-62.4 (±23.3)	91.3 (±14.3)

[a] Stated uncertainties represent 95% confidence limits. [b] Reaction rate constants for chlorpyrifos-methyl and parathion-methyl were measured at 5, 12, 25, 35, 45, 50 and 60 °C, reaction rate constants for chlorpyrifos, parathion and fenchlorphos were measured at 25, 35, 45, 50 and 60 °C. [c] Calculated at 298.15 K

6.3.3. Kinetics of OPs Reactions with S_n^{2-} at 25°C.

The dependence of the pseudo-first-order rate constant k_{obs} on polysulfide concentration was determined by conducting experiments at constant pH and temperature but at varying $\Sigma[S_n^{2-}]$. Experimental solutions contained substantial concentrations of HS^- in addition to S_n^{2-} species. Second order rate constants (k''_{Sn2-}) for the five investigated insecticides were estimated by dividing pseudo-first-order rate constants by $\Sigma[S_n^{2-}]$ after first correcting k_{obs} to account for the contribution from reaction with HS^-. Confidence limits on the second order rate constants were

calculated by propagating the errors associated with analysis of the reduced sulfur nucleophile and the pseudo-first-order rate constants. Resulting k''_{Sn2-} values are given in Table 6-2.

The validity of computing k''_{Sn2-} through subtracting $k''_{HS-}[HS^-]$ from k_{obs} was tested by conducting experiments for parathion-methyl in four solutions with different pH. For all the experiment with polysulfides, the S^0 was assumed to be saturated in the buffer solution; therefore, the ratios of $[HS^-]$ to $\Sigma[S_n^{2-}]$ were different and could be calculated through the equilibrium constants reported by Giggenbach (Giggenbach 1972). The second-order rate constants (k''_{Sn2-} and k''_{HS-}) were simultaneously determined through nonlinear regression analysis of the combined data, fitting experimental data to numerically integrated solutions to the following system of differential rate expressions.

$$\frac{d[MPT]}{dt} = -k_{obs}[MPT] = -(k''_{HS^-}[HS^-] + k''_{S_n^{2-}}\Sigma[S_n^{2-}]) \times [MPT] \qquad n = 2 \sim 5 \qquad (6-6)$$

The time-courses for parathion-methyl with polysulfides were in the range of 7-24 hours. During this period, hydrolysis is very small and can be neglected. Therefore, only the reactions of parathion-methyl with HS^- and S_n^{2-} were considered. In computing k''_{Sn2-} and k''_{HS-}, experimentally determined reduced sulfur nucleophile concentrations were used to calculate $[HS^-]$ and $\Sigma[S_n^{2-}]$. The resulting k''_{HS-} value (3.99 (±0.69) $M^{-1}h^{-1}$), is not significantly different from that determined in solutions containing bisulfide only (4.26 (±0.14) $M^{-1}h^{-1}$).

For all five OPs, a greater reactivity toward S_n^{2-} than toward HS^- was observed. The ratio of k''_{Sn2-}/k''_{HS-} varied from 14 to 51. Our data indicates that HS^- and S_n^{2-} react with the five OPs via S_N2 mechanism; therefore, the high reactivity of S_n^{2-} relative

to HS^- reflects the higher nucleophilicity of S_n^{2-} compare to HS^-. Among the factors that affect the nucleophilicity, basicity, polarizability, and solvation effects should be considered. HS^- is a slightly stronger base (pK_a of H_2S is 6.98, while pK_{a2} values of HS_4^- and HS_5^- are 6.1 and 6.7) (Meyer et al. 1977), which might appear counterintuitive to the high reactivity of S_n^{2-}. Therefore, it would be expected that the polarizability and solvation effects are responsible for the high reactivity of S_n^{2-}. Since the valence electrons of larger atoms are more polarizable and larger species have lower solvation energies, the differences in charge and size between the HS- and S_n^{2-} may also contribute to differences in reactivity. Polysulfides have an overall charge of -2, which can be distributed over several sulfur atoms via delocalization (Meyer et al. 1977) into d-orbitals (Pickerling et al. 1972). In contrast, HS^- has a localized charge of -1 and may, hence, be more strongly solvated despite its lower overall charge than a bulkier, more diffusely charged polysulfide dianion. If, in fact, repulsion between adjacent electron pairs contributes to increased nucleophilicity, one would predict S_2^{2-}, S_3^{2-}, S_4^{2-}, and S_5^{2-}, to have markedly different ground-state energies and, hence, different reactivities. Previously calculated energies of the highest occupied molecular orbital (E_{HOMO}) of S_3^{2-} (-4.66 eV) and S_4^{2-}, (+1.36 eV) (Luther 1990) confirm a large difference in ground-state energies of these two nucleophiles; other factors being equal, more negative E_{HOMO} indicates an increase in stability and hence a decrease in nucleophilic reactivity. This has been discussed by Lippa and Roberts for the nucleophilic substitution reaction of chloroazines with reduced sulfur species (Lippa et al. 2002). Differences in reactivity between

polysulfide dianions would be difficult to demonstrate in our experimental systems, since polysulfides ions rapidly disproportionate to an equilibrium mixture in water.

6.3.4. Kinetics of OPs Reactions with $S_2O_3^{2-}$ at 25 °C.

Similar results to the reaction with HS^- were obtained for reactions of the five OPs with $S_2O_3^{2-}$ investigated. The structure of $H_2S_2O_3$ is shown below:

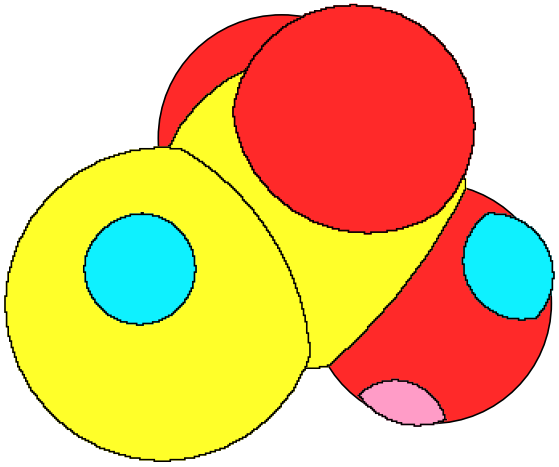

The light gray part represents the sulfur atom, the dark gray ball represents oxygen, the gray part shows the hydrogen atom, and the small ball at the bottom represent lone pair electron. This nucleophile is a spherical in structure; therefore, its steric hindrance would be much higher than the sulfur atom in bisulfide or polysulfides nucleophile that is more linear in structure.

The dependence of the corrected pseudo-first-order rate constant on $S_2O_3^{2-}$ concentration was determined by conducting experiments at constant pH and temperature. The pseudo-first-order rate constants were corrected for the contribution from hydrolysis. Linear regression analysis of log (k_{obs} - $k_{control}$) versus log [$S_2O_3^{2-}$] yielded a slope equal to 1.05 ± 0.11 for parathion-methyl, linear regression analysis of log (k_{obs} - $k_{control}$) versus log[$S_2O_3^{2-}$] yielded a slope equal to

0.94 ± 0.13 for fenchlorfos, linear regression analysis of log (k_{obs} - $k_{control}$) versus log [$S_2O_3^{2-}$] yielded a slope equal to 1.15 ± 0.23 for chlorpyrifos, and linear regression analysis of log (k_{obs} - $k_{control}$) versus log [$S_2O_3^{2-}$] yielded a slope equal to 1.07 ± 0.17 for parathion. Therefore, the reactions of these four OPs with $S_2O_3^{2-}$ exhibited first-order dependence and the overall second order rate constants are listed in Table 6-4.

Table 6-4: Second-Order Rate Constants for Reactions of OPs with PhSH, PhS^- and $S_2O_3^{2-}$ at 25.0 °C

OPs	k''_{PhSH} [a] ($M^{-1}h^{-1}$)	k''_{PhS-} ($M^{-1}h^{-1}$)	$k''_{S2O3^{2-}}$ [b] ($M^{-1}h^{-1}$)
Chlorpyrifos-Methyl	0.11 ± 3.38	73 ± 8	3.3 ± 0.4
Parathion-Methyl	0.29 ± 2.07	23 ± 3	2.4 ± 0.2
Fenchlorphos	0.54 ± 3.13	24 ± 2	1.7 ± 0.2
Chlorpyrifos	0 [c]	3.1 ± 0.3	0.01 ± 0.001
Parathion	0 [c]	1.7 ± 0.1	0.014 ± 0.001

[a] Second-order rate constant determined from thiophenol solution at different pH. [b] Second-order rate constant determined from k_{obs} values of thiosulfate solutions containing known [$S_2O_3^{2-}$] which were corrected for hydrolysis. [c] These values were set to zero, the actual value resulting from linear regression were -0.77 (±3.42) $M^{-1}h^{-1}$ for chlorpyrifos and –0.33 (±2.22) ×10^{-4} $M^{-1}h^{-1}$ for parathion.

The resulting second-order rate constant for the reaction of parathion-methyl with $S_2O_3^{2-}$ is 2.4 ± 0.2 $M^{-1}h^{-1}$. The resulting second-order rate constants for the reaction of fenchlorfos, chlorpyrifos, and parathion with $S_2O_3^{2-}$ are 1.7 ± 0.2, 0.01 ± 0.001, and 0.014 ± 0.001 $M^{-1}h^{-1}$, respectively. This shows, that the reaction of chlorpyrifos-methyl with $S_2O_3^{2-}$ is about 330 times faster than the reaction of chlorpyrifos with $S_2O_3^{2-}$, and the reaction of parathion-methyl with $S_2O_3^{2-}$ is about 150 times faster than the reaction of parathion with $S_2O_3^{2-}$. The comparision of the relative reactivity

of thiosulfate to the five OPs with the relative reactivity of bisulfide show that the reaction rate of methylated OP is only about 40 times faster than ethylated OP. The steric demand of both $S_2O_3^{2-}$ and ethyl group of the OPs side chain is responsible for the relatively low reactivity.

6.3.5. Kinetics of OPs Reactions with PhS^- at 25 °C

Similar results to the reaction with $\Sigma[Sn^{2-}]$ were obtained for reactions of the five OPs with PhS^- investigated. The structure of PhSH is shown below:

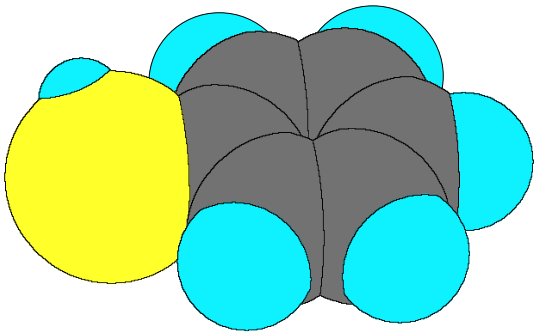

The light-gray part represents the sulfur atom, the dark-gray ball represents carbon of the benzene ring, and the gray part shows hydrogen atoms. This nucleophile has a planar structure; therefore, the steric hindrance of the sulfur atom in thiophenol would relative be smaller than of the sulfur atom in thiosulfate, but higher than of the sulfur atom in bisulfide or polysulfide nucleophile.

The dependence of the corrected pseudo-first-order rate constant on PhS^- concentration was determined by conducting experiments at constant pH (pH 9) and temperature (25 ºC). The pseudo-first-order rate constants were corrected for the contribution from hydrolysis. Linear regression analysis of log (k_{obs} - $k_{control}$) versus log [PhS^-] yielded a slope equal to 0.96 ± 0.07 for parathion-methyl, 1.02 ± 0.09 for fenchlorfos, 0.87 ± 0.18 for chlorpyrifos, and 1.05 ± 0.10 for parathion. Therefore,

the reactions of these four OPs with PhS^- exhibited first-order dependence and the overall second order rate constants are listed in Table 6-4.

The reaction of the five investigated OPs with thiophenol was assessed the same way as the reaction with hydrogen sulfide. The observed rate constant does include hydrolysis and the degradation promoted by thiophenol and thiophenolate. Hence, the reaction rate of OPs in a thiophenol solution containing PhSH and PhS^- can be expressed as the following equation

$$k_{obs} = k_{control} + k_s = k_{control} + k''_{PhSH}[PhSH] + k''_{PhS^-}[PhS^-] \qquad (6\text{-}7)$$

The different reactivity of PhS^- versus PhSH would result in a pH dependence of k_s. The control experiments were conducted in the absence of thiophenol to investigate hydrolysis rate constants in control buffer solution, ($k_{control}$), which were listed in Chapter 4. The corrected rate constant, k_s, obtained from k_{obs} after correction for hydrolysis, is divided by the total concentration of thiophenol species, which results in the apparent second-order rate constant, k''_{app}. k''_{app} is assumed to be the sum of contributions of PhS^- and PhSH and can be given by the expression

$$k''_{app} = (k_{obs} - k_h)/[PhSH]_T = k_s/[PhSH]_T = k''_{PhSH} + \alpha_{PhS^-} \cdot \left(k''_{PhS^-} - k''_{PhSH}\right) \qquad (6\text{-}8)$$

in which,

$$\alpha_{PhS^-} = \frac{[PhS^-]}{[PhSH]_T} = \left(1 + \frac{[H^+]}{K_a}\right)^{-1} \qquad (6\text{-}9)$$

and the acid dissociation constant of PhSH, pK_a is 6.50 at 25 °C (Dean 1985). The plot of k''_{app} versus α_{PhS^-} shows a linear correlation, which supports our assumption.

Linear regression analysis of k''_{app} versus α_{PhS^-} yielded a slope and intercept, which allow the extraction of rate constant for both PhSH and PhS^-.

The resulting second-order rate constants for the reaction of parathion-methyl, fenchlorfos, chlorpyrifos, and parathion with PhS^- are 23 ± 3, 24 ± 2, 3.1 ± 0.3, and 1.7 ± 0.1 $M^{-1}h^{-1}$ respectively. The resulting second-order rate constants for the reaction of parathion-methyl, fenchlorfos, chlorpyrifos, and parathion with PhSH are 0.29 ± 2.07, 0.54 ± 3.13, -0.77 (±3.42), –0.33 (±2.22) $\times 10^{-4}$ $M^{-1}h^{-1}$ respectively, which are all close to zero and not significantly different from zero. Therefore, as for H_2S vs. HS^-, only PhS^- was the sole reactive species in the reaction with the investigated OPs. PhSH does not contribute to the degradation of OPs.

6.3.6. Products of Organophosphorus Reactions with Reduced Sulfur Species

Our findings supports that chlorpyrifos-methyl, parathion-methyl, fenchlorphos, chlorpyrifos and parathion all react with reduced sulfur species via nucleophilic substitution at the α-carbon of the alkoxy group resulting in the formation of desalkyl organophosphate (Scheme 6-1). The reaction of the five OPs with thiophenol confirmed this mechanism through the simultaneous formation of desalkyl compounds and the alkylated thiophenolate. When comparing the reactions of OPs with thiophenol and with HS^-, the major products for both reactions have the same retention times and UV spectra in the HPLC, and the alkylated thiophenolate also formed in the reaction of thiophenol with all five OPs. The HPLC chromatogram and related UV spectra for a reaction mixture are shown in Figure 6-5 (for the reaction of parathion with thiophenol).

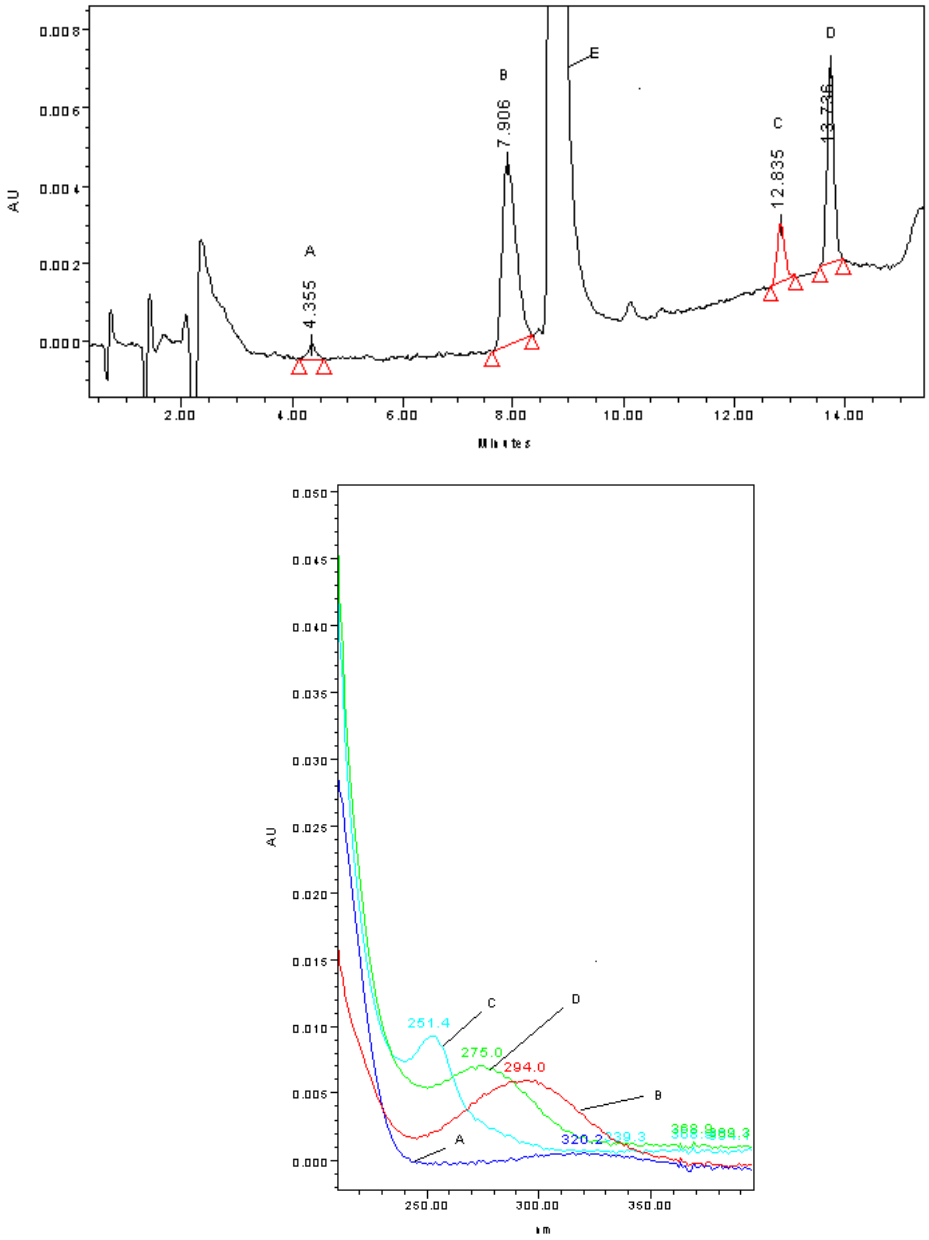

Figure 6-5. HPLC chromatogram and UV spectra of a sample in the reaction of parathion with 2.28 mM of thiophenol at pH 9.1. Compounds eluted in the order of 4-nitrophenol (A), desethyl parathion (B), excess thiophenol (E), ethyl thiophenolate (C), and parathion (D). The small peaks between peak E and peak C are impurities in the thiophenol.

Several experiments were performed to identify the desalkyl products that are anticipated from reactions with bisulfide, polysulfides, thiosulfate, and thiophenolate. Spent reaction solutions were acidified to pH 1, extracted with ethyl acetate, and analyzed (both the organic and aqueous phase; for calculation of the extraction efficiency) with HPLC-PDA. Three products (3,5,6-trichloropyridinol, 4-nitrophenol, and 2,4,5-trichlorophenol) could be quantified using reference materials that are commercially available. Due to a lack of pure desalkyl OPs standards, the quantification of desalkyl organophosphates was based on the assumptions for chlorpyrifos-methyl reported in Charper 5. The extinction coefficients of the other four desalkyl products were calculated by assuming the same formation rate of alkylated thiophenolate and desalkyl OPs in the reaction of the OPs with thiophenolate. These extinction coefficients were then used to quantify the desalkyl products in the corresponding reaction of OPs with HS^-, S_n^{2-}, $S_2O_3^{2-}$ and PhS^-.

Table 6-5 lists the fitted pseudo-first-order rate constants of the five OPs with HS^-, S_n^{2-}, $S_2O_3^{2-}$ and PhS^-, the pseudo-first-order rate constants were calculated for each batch reaction using Scientist for Windows according to the following model:

$$\frac{-d[OP]}{dt} = -(k'_{phenol} + k'_{DaOP}) * [OP] = k'_{OP}[OP] \qquad (6\text{-}10)$$

$$\frac{-d[Phenol]}{dt} = k'_{phenol} * [OP] \qquad (6\text{-}11)$$

$$\frac{-d[DaOP]}{dt} = k'_{DaOP} * [OP] \qquad (6\text{-}12)$$

Scientist calculates these parameters (along with the initial concentration of the parent compound) by fitting (method of least squares) numerically integrated

Table 6-5: Reaction Rate Constants of OPs with HS^- and S_n^{2-} at 25.0 °C [a]

	Reaction condition	k'_{obs} (h^{-1})[b]	k'_{phenol} (h^{-1})[b]	k'_{DaOP} (h^{-1})[b]
CPM	pH 9.16[c]	7.83 (± 0.33)×10^{-3}	6.91 (± 0.71)×10^{-3}	1.25 (± 0.12)×10^{-3}
	pH 7.4, 3.8 mM HS^-	2.54 (± 0.14)×10^{-2}	1.98 (± 0.13)×10^{-3}	2.27 (± 0.12)×10^{-2}
	pH 9.2, 3.6 mM ΣS_n^{2-}	0.42 (± 0.004)	5.55 (± 0.11)×10^{-3}	0.41 (± 0.006)
	pH 7.0, 7.9 mM $S_2O_3^{2-}$	2.39 (± 0.12)×10^{-2}	1.66 (± 0.20)×10^{-3}	2.12 (± 0.17)×10^{-2}
	pH 8.1, 2.1 mM PhS^-	0.12 (± 0.01)	3.29 (± 0.34)×10^{-3}	1.15 (±0.10)×10^{-1}
MPT	pH 9.34[c]	1.24 (± 0.13)×10^{-3}	1.15 (± 0.09)×10^{-3}	0.75 (± 0.09)×10^{-3}
	pH 7.4, 4.3 mM HS^-	1.52 (± 0.09)×10^{-2}	0.88 (± 0.22)×10^{-3}	1.59 (± 0.17)×10^{-2}
	pH 9.2, 3.2 mM ΣS_n^{2-}	0.19 (± 0.003)	1.05 (± 0.34)×10^{-3}	0.18 (± 0.007)
	pH 7.1, 5.8 mM $S_2O_3^{2-}$	1.15 (± 0.09)×10^{-2}	0.64 (± 0.14)×10^{-3}	1.06 (± 0.05)×10^{-2}
	pH 8.1, 2.1 mM PhS^-	5.37 (± 0.21)×10^{-2}	1.04 (± 0.25)×10^{-3}	5.19 (± 0.20)×10^{-2}
FEN	pH 9.34[c]	1.36 (± 0.13)×10^{-3}	1.27 (± 0.16)×10^{-3}	0.59 (± 0.08)×10^{-3}
	pH 7.4, 4.3 mM HS^-	1.60 (± 0.13)×10^{-2}	0.17 (± 0.01)×10^{-3}	1.45 (± 0.11)×10^{-2}
	pH 9.3, 3.6 mM ΣS_n^{2-}	0.30 (± 0.01)	1.5 (± 0.03)×10^{-3}	0.29 (± 0.02)
	pH 7.6, 5.2 mM $S_2O_3^{2-}$	9.72 (± 0.13)×10^{-3}	0.88 (± 0.19)×10^{-3}	8.92 (± 0.10)×10^{-3}
	pH 8.6, 1.2 mM PhS^-	2.81 (± 0.23)×10^{-2}	0.45 (± 0.08)×10^{-3}	2.79 (± 0.10)×10^{-3}
CPE	pH 9.38[c]	1.13 (± 0.16)×10^{-3}	6.67 (± 0.86)×10^{-4}	5.34 (± 0.14)×10^{-4}
	pH 7.3, 8.9 mM HS^-	1.22 (± 0.15)×10^{-3}	9.44 (± 0.95)×10^{-5}	1.07 (±0.13)×10^{-3}
	pH 9.4, 3.2 mM ΣS_n^{2-}	7.54 (± 0.86)×10^{-3}	6.39 (± 1.35)×10^{-4}	7.06 (± 0.45)×10^{-3}
	pH 7.6, 12 mM $S_2O_3^{2-}$	1.76 (± 0.24)×10^{-4}	4.53 (± 0.63)×10^{-5}	1.30 (± 0.27)×10^{-4}
	pH 7.0, 1.8 mM PhS^-	4.72 (± 0.66)×10^{-3}	5.24 (± 0.79)×10^{-4}	4.30 (± 0.60)×10^{-3}
EPT	pH 9.34[c]	3.32 (± 0.26)×10^{-4}	2.08 (± 0.18)×10^{-4}	1.44 (± 0.16)×10^{-4}
	pH 7.3, 8.9 mM HS^-	9.14 (± 0.11)×10^{-4}	0.44 (± 0.07)×10^{-6}	9.03 (± 0.82)×10^{-4}
	pH 9.4, 3.1mM ΣS_n^{2-}	2.03 (± 0.07)×10^{-2}	0.12 (± 0.05)×10^{-4}	1.98 (± 0.11)×10^{-2}
	pH 7.0, 12 mM $S_2O_3^{2-}$	6.14 (± 0.04)×10^{-4}	3.72 (± 0.43)×10^{-5}	5.86 (± 0.35)×10^{-4}
	pH 9.2, 1.5 mM PhS^-	2.84 (± 0.12)×10^{-3}	1.25 (± 0.25)×10^{-4}	2.77 (± 0.17)×10^{-3}

[a] Determined via simultaneous nonlinear regression techniques using Scientist for Windows. k'_{phenol} is the formation rate of phenol, k'_{DaOP} is the formation rate of desalkyl OPs, and k'_{obs} is the degradation rate of OPs, [b] Standard deviation resulting from the nonlinear regression. [c] Complete detail are reported in Chapter 3. All reactions were conducted at 0.050 M sodium phosphate and sodium tetraborate buffer with ionic strength adjusted with NaCl to 0.25 equiv/L, 5% or 10% methanol at 25.0 °C.

solutions of the system of differential rate expressions to experimental data for parent compound loss and reaction products appearance. By fitting products formation data simultaneously with parent compound loss data; it was possible to assess the importance of reaction pathways.

All the loss of the parent compounds can be explained by the formation of the two products for each OP. The phenols are minor products that can be mostly attributed to hydrolysis. The formation rates for the phenol in a typical experiment are more than 10 times smaller than the formation rate of the desalkyl OPs. These findings are in good agreement with the results in Chapter 5, and support the proposed mechanism of the reduced sulfur species reacting with the five investigated OPs via an attack at the α-carbon of the alkoxy groups.

Additional studies on the identity of the products were conducted by methylating the reaction solution that contained less than 10% of the initial parent compounds concentration with excess CH_3I, followed by extraction into *n*-hexane and analysis via GC/MS (EI). The formation of the desalkyl products from the reaction of OPs with HS^- and S_n^{2-} was supported by the analyses of those methylated reaction mixtures. The total ion chromatogram (TIC) and related mass spectra for derivatized reaction mixtures are shown in Figure 6-6 and 6-7 (for reaction of parathion). Figure 6-6 shows that the major derivatization product is O-ethyl S-methyl O-*p*-nitrophenylphosphate (B at r_t 10.10 min), and O-ethyl O-methyl O-*p*-nitrophenylthiophosphate (C at r_t 9.40 min) was detected as a minor derivatization product.

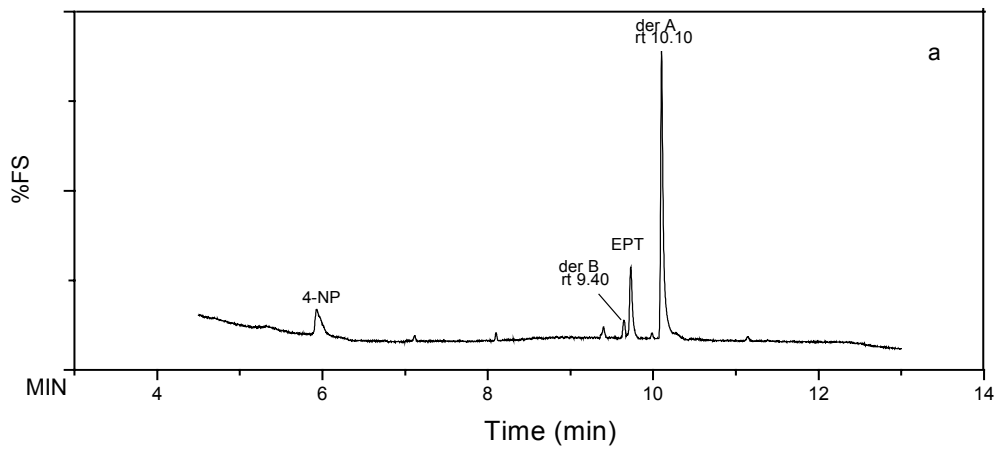

Figure 6-6: EI total ion chromatogram (TICs) for derivatized products obtained in reaction of polysulfides with parathion (parathion with 5 mM $\Sigma[S_n^{2-}]$ at pH 9 after 120 hours, and derivatized with MeI at 60℃ for 2 hours). The compounds eluted in the order of 4-nitrophenol (4-NP), minor methylated product with CH_3I (der B), parathion (EPT) and major methylated product with CH_3I (der A).

The identified products support that the postulated mechanism results in the formation of desalkyl OPs. As indicated in Figure S5a, the peak area for the S-methylated derivatization product of the reactions of HS^- and S_n^{2-} with parathion (O-ethyl, S-methyl, O-*p*-nitrophenylphosphate) was found to be more than 20 times larger than that of the peak for the O-methylated derivitization product (O-ethyl, O-methyl, O-*p*-nitrophenylphosphate). This is consistent with the Hard and Soft Acids and Bases model of reactivity (Pearson 1963), which posits that a soft (i.e., relatively polarizable) electrophile such as a methyl group will react more readily with a softer nucleophile (in this case, the sulfur bound to phosphorus) than a harder

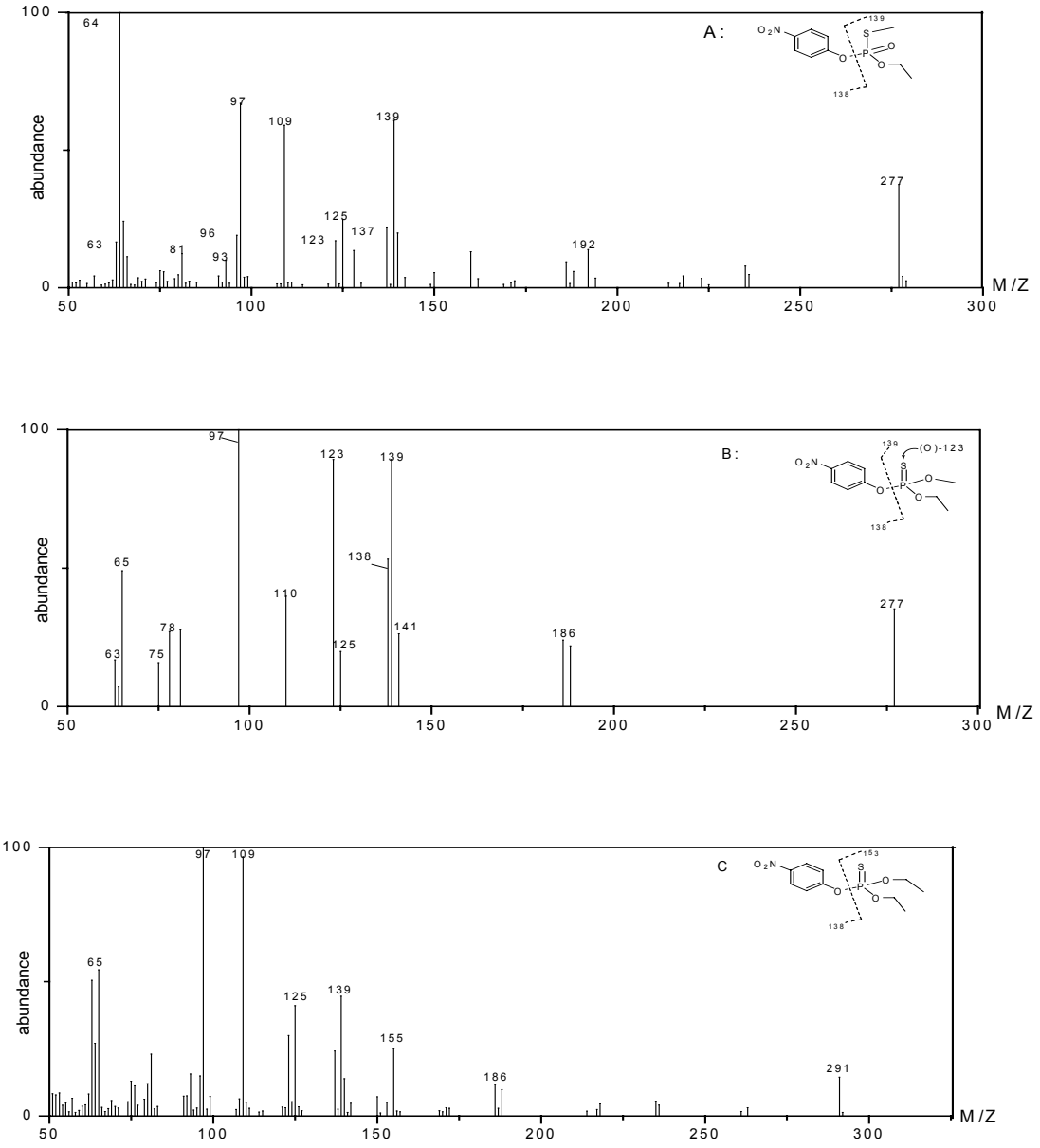

Figure 6-7. Mass spectra (EI) for major methylated product with CH_3I, retention time is 10.096 min (A), minor methylated product with CH_3I, retention time is 9.403 min (B), and unreacted parathion, retention time is 9.498 min (C). The major difference of (A) and (B) is the relative abundance of fragment 123.

one (the oxygen). For the other three insecticides, the corresponding products detected are consistent with the mechanism we proposed.

SCHEME 6-1:

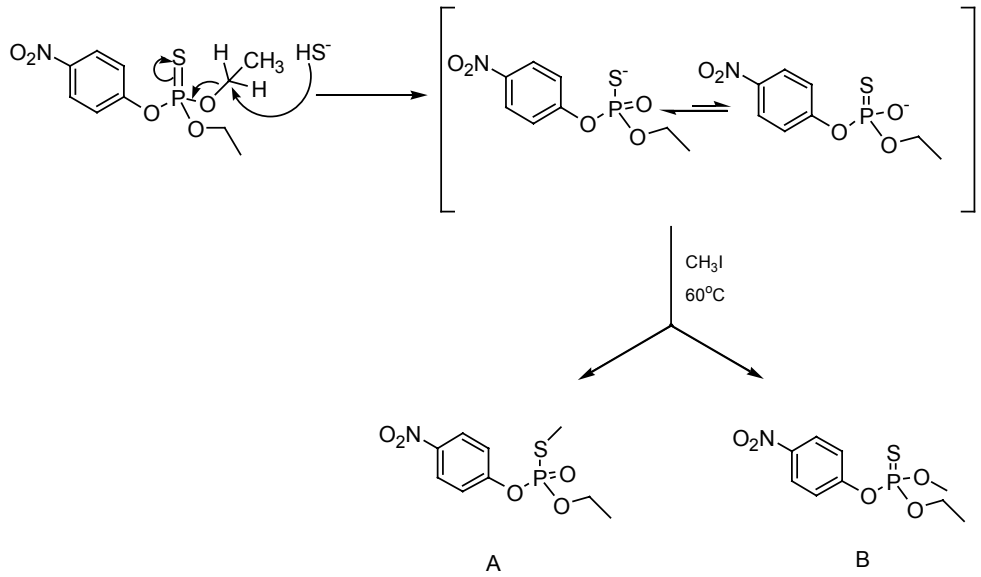

SCHEME 6-1: Proposed mechanism for the observed displacement of alkyl groups from alkoxy moieties on OPs by the reduced sulfur nucleophiles examined for this study, and the subsequent formation of products from derivitization with methyl iodide.

6.4. Conclusion

The environmental fate of OPs is controlled by a number of abiotic and biotic processes. Our results suggest that HS^- and S_n^{2-} are sufficiently reactive as to control the fate of OPs in anoxic and suboxic environments where the reduced sulfur species are abundant. Under these conditions, the organophosphorus diester is the major degradation product resulting from a nucleophilic attack by reduced sulfur

species (e.g., HS^-, S_n^{2-}) at the α-carbon atom of the alkoxy groups of the phosphorothionate ester. Since in a sensitive coastal environment such as sediment, estuaries, and salt marshes, anoxic conditions are prevalent and high concentrations of reduced sulfur species such as 5.6 mM bisulfide and 0.33 mM polysulfides (pH 7.2) were reported (MacCrehan et al. 1995), the half-lives of the five OPs in sulfidic environment can be predicted by multiplying measured second-order rate constants giving in Table 6-2 by the maximum reported concentrations of $[HS^-]$ and $[S_n^{2-}]$. The half-lives of OPs in the presence of 5.6 mM bisulfide and 0.33 mM polysulfides at pH 7.2 were calculated to be 7.6 h (chlorpyrifos-methyl), 5.9 h (parathion-methyl), 6.4 h (fenchlorphos), 229 h (chlorpyrifos) and 158 h (parathion), while the half-live of the OPs with only hydrolysis at pH 7.2 were calculated to be 387 h (chlorpyrifos-methyl), 1470 h (parathion-methyl), 1020 h (fenchlorphos), 1471 h (chlorpyrifos) and 1374 h (parathion). Therefore, our results suggest that HS^- and S_n^{2-} present at environmentally relevant concentrations are sufficiently reactive to control the fate of OPs

Chapter 7. Quantitative Structure Activity Relationships to Predict the Fate and Effect of Selected Organophosphorus Insecticides in Sulfidic Systems

7.1. Introduction

Organophosphates have been utilized in various applications since their initial discovery in the early 19th century (WHO 1986). Their most noted employment is usage as agricultural insecticides and chemical warfare agents. Organophosphates were introduced as pesticides after World War II and subsequently incorporated into common agricultural practices ever since (WHO 1986). It is estimated that at least 100 different organophosphate insecticides are currently used commercially worldwide (WHO 1986). The accumulation of these pollutants has raised environmental concerns due to the inherent toxicity of these compounds (USEPA Dec. 3, 2001). The most commonly detected insecticides in US within this class are illustrated in Figure 7-1 (Kolpin et al. 1998).

In general, the mechanism of toxicity involves the inhibition of enzyme activities and the release of neurotransmitters (WHO 1986). Acute toxicity results primarily from the inactivation of the enzyme AChE. However, other direct targets of organophosphate intoxication include the muscarinic and nicotinic acetylcholine receptors. Symptomatic manifestations of organophosphate intoxication leading to death include pinpoint pupils, breathing difficulties, coma, and convulsions. While the mechanism of toxicity is believed to be similar in all species, the chemical dosage directs the intensity of the response (WHO 1986).

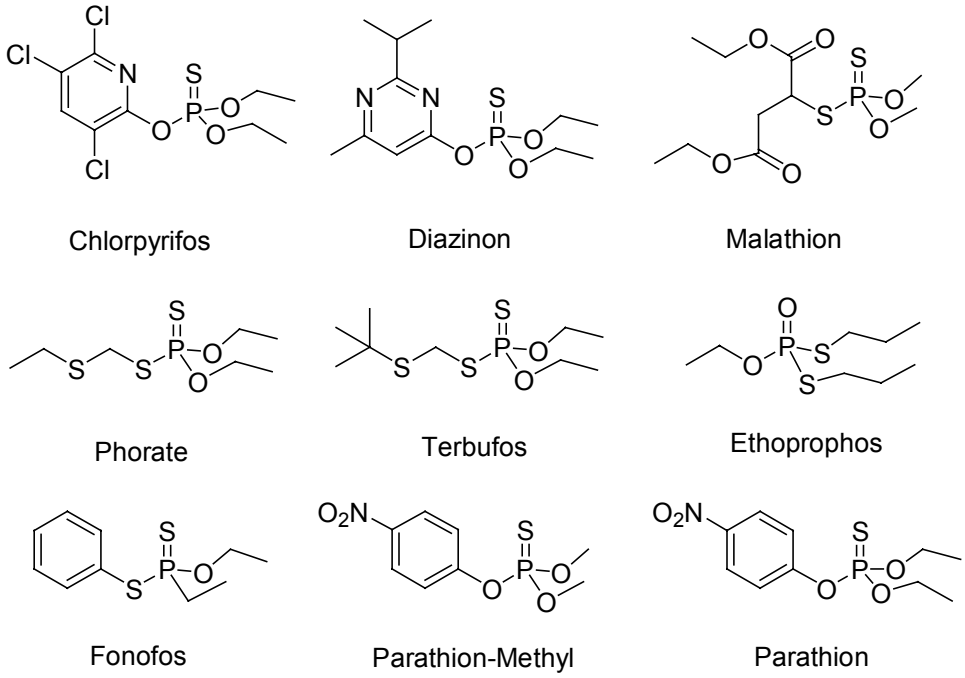

Figure 7-1: the most commonly detected organophosphate insecticides in US (Kolpin et al. 1998).

Although there are extensive production and resultant widespread exposure of environmental compartments to various amounts of these compounds, surprisingly few quantitative data on their reactivity are reported in the open literature. Because of the diversity of structures that result from different combinations of O, O, O-alkyl and aryl substituents, however, one would anticipate a wide variation in reactivity under environmental relevant conditions in the water column.

To assess the fate and transport of these chemicals in aquatic environments, a systems approach that incorporates rate expressions describing the individual process is logical and useful. Such an approach requires values of the physical and chemical constants used in the rate expressions. Although measured values of these constants are not always available, estimates may be obtained by use of quantitative structure-activity relationship (QSAR). Such correlations are receiving increased

attention in efforts to better describe environmental phenomena such as toxicity, bioconcentration, and sediment sorption. By providing data of reaction rate constants with environmental relevant reagents, the LFERs or QSAR are particularly applicable to the assessment of hydrolytic reactivity of organic compounds. Therefore, degradation rate in this system for classes of compounds can be readily evaluated (Wolfe et al. 1978; Wolfe 1980; Lippa et al. 2002). Organophosphate and organophosphorothionate triesters, depending on the substituents, react with reduced sulfur species through an S_N2 reaction where the sulfur nucleophile attacking the carbon atom of the alkoxy group (Chapter 5 and 6). The resulted desalkyl organophosphate would also be of environmental concern.

It has been reported the inhibition of erythrocyte cholinesterase by diethyl p-nitrophenyl phosphate (paraoxon) and some of its analogs proceeded with pseudo first-order kinetics (Fukuto et al. 1956; Fukuto et al. 1959). The rate constants for this inhibition were determined for the various paraoxon analogs, and these values paralleled the rates of hydrolysis of these phosphates in water. And it is also reported that once the drug reaches the receptor site, the inherent activity of the molecule takes over and caused the critical reaction which results in the biological response. In the present study, those OPs that are most susceptible to nucleophilic attack are assumed to be the best insecticides (Neely et al. 1970). Consequently, the rate of S_N2 reaction could be used as a measure of toxicity.

Therefore, the question of how the substituents of OPs influence their mode of action and detoxification through bimolecular reaction in plant prompted the parallel question of how these substituents influence reactivity with inorganic reduced sulfur

nucleophiles, such as HS^- and S_n^{2-}. Studies of OPs transformation in sulfidic natural water samples (Chapter 5 and 6) demonstrate that abiotic reactions with such nucleophiles can result in very rapid insecticide removal under such conditions. It is suggested that the features that are closely related to desired insecticidal properties may be similarly linked to reactivity in nucleophilic substitution reactions that can dominate insecticides fate in anoxic environments.

7.2. Overview of Computational OPs Study

The parameter describing the hydrophobicity of a compound, log K_{ow}, has been used more often in QSAR studies than any other descriptor (Nirmalakhandan et al. 1988). It has been used to describe both the effects on biota and fate of xenobiotics in aquatic systems. Researchers have shown that a linear relationship exists between the sorption of neutral organic compounds to sediment and log K_{ow}. Karickhoff (Karickhoff et al. 1979) demonstrated that sorption of several hydrophobic pollutants was linearly related to log $K_{ow.}$ It also demonstrated that sorption to sediment will increase with increasing log K_{ow} for nonionic compounds. Other researchers have demonstrated a linear relationship between such important parameters as the bioconcentration factor and log $K_{ow.}$ Neely (Neely et al. 1974) demonstrated a linear relationship between log K_{ow} and the log of bioconcentration factor of seven neutral organic compounds in trout muscle. Kenega and Goring (Kenega et al. 1980) found a strong relationship between K_{ow} and bioaccumulation of hydrophobic compounds in *Daphnia magna*. Not only has the fate of many chemicals been found to be predicted by K_{ow}, but K_{ow} has been shown to correlated with the toxicity of many compounds under site specific conditions. It also reported

that a good correlation existed between log K_{ow} values and toxicity of various industrial chemicals to fish (Veith et al. 1979). And also, the log K_{ow} for several lipophilic compounds correlated fairly well with toxicity, although correlations with pesticides did not result in significant relationships.

The steric parameter molecular volume (MV), has been used in a number of studies to describe the toxicity of neutral organic compounds which exert their toxicity through narcosis. It was found that the toxicities of nonpolar organic compounds to juvenile sheepshead minnows (*Cyprinodon variecatus*) as well as fathead minnows (*Primephales promelis*) could be predicted to within an order of magnitude by MV (McGowan et al. 1986). And although toxicity has been described by such parameters as log K_{ow}, water solubility, vapor pressure, and chemical potential, all these properties are related in that they are dependent on characteristic volume and temperature, and therefore claimed MV should be able to describe toxicity for a wide variety of compounds.

The molecular connectivity (MC) has also been used often in studies to describe such properties as toxicity, molar refraction, polarizability, water solubility, molar volume, and heat of vaporization (Kier et al. 1986). MC is a procedure for quantifying molecular structure based on fragments or subgraphs weighed by the degree of bonding between atoms (Kier et al. 1986). Quantifying molecular structure is done simply by counting structural features weighted by adjacent atoms where delta values are assigned to all atoms in a molecule except hydrogen (Hall et al. 1989). The summation of all delta values in a molecule results in a first order index. Higher order indexes, based on more complex substructures, are possible and

are used for multiple regression analyses with physical and biological processes (Hall et al. 1989). MC was also used to predict acute toxicity of a variety of pollutants including benzene and toluene to the guppy (Leegwater et al. 1994). Result showed that MC indices were equivalent to and sometimes superior to prediction from log K_{ow} values.

Correlations between rate constants for specific chemical reactions and values for a selected physical or chemical property of the organic compounds are also well established. Such correlations can be used to predict rate constants required to assess the behavior of organics in aquatic environments. Similar correlations of enzyme catalyzed reactions, although often more complex, have also been demonstrated (Wolfe et al. 1977; Wolfe et al. 1978; Wolfe 1980; Wolfe et al. 1980; Wolfe et al. 1986). Several studies have addressed the effect of chemical structure on susceptibility to microbial breakdown using bacteria isolated from soils and natural waters, but, unfortunately, the correlations have not been successful. The major difficulty with these studies has been the choice of a measurement of biological reactivity to use in the correlation. After the kinetics of microbial degradation of organics in natural water samples has been studied, the database of rate constants was used to examine the relationship of chemical structure to microbial degradation. In these studies, Wolfe and co-workers (Wolfe et al. 1978; Wolfe 1980) applied a second-order rate expression to describe the rate of disappearance of certain organics mediated by microorganisms in natural water samples. Linear regression analysis using the second-order rate constants, k_b (biological degradation rate, $L \cdot org^{-1}h^{-l}$), determined in these investigations and the

corresponding second-order alkaline hydrolysis rate constants, k_{OH^-} ($M^{-1}s^{-1}$), reported by Wolfe and co-workers (Zepp et al. 1975; Wolfe et al. 1977; Wolfe et al. 1977; Wolfe et al. 1986) gives the correlation described by the linear equation (log k_b = mlog k_{OH^-} + c). Values of *m* and c along with standard errors of the estimates and the correlation coefficient, r^2 could be given as 0.97, with adding the a second parameter, the octanol-water partition coefficient, log K_{ow}, the correlation (r^2) would be improved because the K_{ow} has been postulated to be proportional to the binding strength of a compound at the reaction site or proportional to biosorption by organisms (Kenega et al. 1980). The resulting equation is (log k_b = mlog k_{OH^-} + nlog K_{ow} +c). With the inclusion of log K_{ow} as a dependent variable, the multiple linear regression coefficient, r^2 was improved to 0.988.

Although there is a need for determining the persistence of xenobiotics in the environment, most of the QSAR researches for OPs were about the relationship between molecular structure and biological activity, and few attempts have been made to predict degradation rates in aquatic systems through the use of QSAR. Drossman and Mill (Drossman et al. 1988) found that the base-promoted hydrolysis of carbamates could be modeled using Hammett and Taft parameters σ, σ^*, and E_s, they reported that the correlation with carbamate hydrolysis rates and the Hammett and Taft parameters gave adjusted r^2 values as high as 0.97. Models based on linear free energy relationships have been developed to predict the hydrolysis rate constants for OP insecticides in water. Correlations between the linear free energy relationships parameters and OP hydrolysis rate constants gave adjusted r^2 values as high as 0.99.

The present chapter emphasizes the development of QSARs that will lead to physico–chemical properties that subsequently can be used as descriptors in a partial order ranking of OPs. The main objective is to find experimentally well–characterized compounds that can be used as substitutes in experimental studies of the environmental behavior of the untested compounds. Obviously, unique structural elements of the OP insecticides may well cause significant differences in the environmental fate of the OP insecticides. Nevertheless, some insecticides may mimic the investigated OPs by, *e.g*., exhibiting identical volatilization behavior, while others may display similar rates of degradation. Based on a partial order ranking, taking several parameters into account simultaneously, it appears possible to give the single compound an identity by comparing to structurally related OP insecticides. These substitutes will, based on an overall viewpoint exhibit analogous environmental characteristics and be models. Thus, such substitutes may well be used for preliminary experimental studies on the environmental fate of other OPs, and subsequently constitute the basis of selection of a limited number of necessary experimental studies applied the actual compounds in order to perform risk assessment.

7.3. Computational Methods

Calculations were also carried out on Dell PCs utilizing Pentium (R)M processors employing the Spartan 04 quantum mechanical program (J. Kong 2000). All geometries for gas-phase reactants, intermediates and transition state structures were fully optimized at the B3LYP/6-31G(d) level. Frequency calculations were performed using the optimized geometry structures with a 6-31G+(d,p) basis set.

(For each structure, the level of energy calculations and geometry optimizations employed is represented as B3LYP/6-31G+(d,p)//B3LYP/6-31G(d)). Transition state structures obtained from the frequency calculations were verified as first-order saddle points (with only one imaginary frequency). Mulliken atomic charge distributions and molecular orbital energies of each optimized structure were calculated via population analysis using tight self-consistent field (SCF) convergence criteria.

Attempts to apply a range of solvation models (PCM, IPCM, SCIPCM (Alexander et al. 1968)) all failed. Calculations of the OPs reactant and transition state structures including these solvation models yielded non-rectifiable errors. These errors may be attributable to program code limitations associated with the incorporation of a solvent reaction field into larger size calculations employing density functional theory. An attempt was made to incorporate explicit aqueous solvation (through addition of individual water molecules surrounding the molecule) but this proved infeasible in terms of computational effort.

7.4. Results and Discussion

The kinetics of the reaction of five OPs with HS^- in aqueous solution was determined over a range of temperatures (as described in Chapter 5 and 6). These results are summarized in Tables 7-1. Significant differences in reactivity were observed between ethylated and methylated OPs. Significant differences in entropy were also observed between ethylated and methylated OPs. From both the kinetic data and themodynamic results, the reaction of the OPs with bisulfide is proved to be an S_N2 reaction. Theoretical models of transition state structures for these

reactions were examined in hopes of clarifying the factors responsible for these observed differences. There is only limited research on the S_N2 reaction happens on the alkoxy group based on molecular level. Therefore, theoretical S_N2 reaction models of conventional S_N2 reactions ($CH_3Cl + HS^-$) were examined for purposes of comparison.

Table 7-1: Second-Order Rate Constants for Reactions of OPs with H_2S and HS^- at 25.0 °C

OPs	$k''_{H2S}(M^{-1}h^{-1})^a$	$k''_{HS-}(M^{-1}h^{-1})^a$
Chlorpyrifos-methyl	0.42 (±0.20)	7.95 (±0.47)
Parathion-methyl	0.54 (±0.06)	4.26 (±0.14)
Fenchlorphos	0[b]	4.61 (±0.06)
Chlorpyrifos	3.1 (±53.4) $\times 10^{-4}$	0.20 (±0.01)
Parathion	0.04 (±0.01)	0.13 (±0.02)

[a] Second-order rate constant determined from hydrogen sulfide solution at different pH, ionic strength of 0.25 equiv/L. Uncertainty represents 95% confidence limit. [b] This value was set to zero, the actual value resulting from Figure 6-3 is -0.03 (±0.14) $\times 10^{-4}$ $M^{-1}h^{-1}$.

7.4.1. Computational Models of Transition State Structures

S_N2 reactions are a fundamental process of chemistry. In the gas phase, both experiment (Olmstead et al. 1977; Laerdahl et al. 2002) and theory (Dedieu et al. 1972) indicate that the reactions involve double well potentials shown in Figure 7-2. Ion molecule complexes are deep minima, and the energy of the transition structure is often lower than that of the separate reactants.

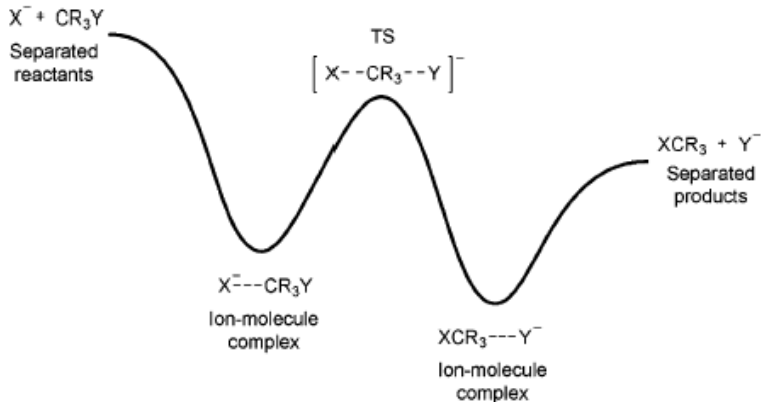

Figure 7-2. Generalized potential energy surface for S_N2 reactions in the gas phase

As illustrative examples, the transition states for the reactions of chlorpyrifos and chlorpyrifos-methyl with HS^- are shown in Figure 7-3. Similar transition state structures, displaying clear S_N2 axes of inversion and displacement vectors along the axes of inversion, were isolated for all the S_N2 reactions investigated. The geometries of the transition state structures closely resemble the anticipated geometries of the proposed intermediates, as shown in Figure 7-3.

The geometries obtained for these gas-phase transition state structures may not represent the true structures in aqueous solution. Previous researchers have determined (Jorgensen et al. 1986) that there are relatively small differences in the bond lengths (0.05 Å) for the polar S_N2 reaction ($Cl^- + CH_3Cl$) in the gas phase versus aqueous solution. And the influence of solvation on the reaction profile is profound (Figure 7-4); in solution, the relatively localized charges of reactants and products are solvated more strongly than the ion-molecule complexes or transition

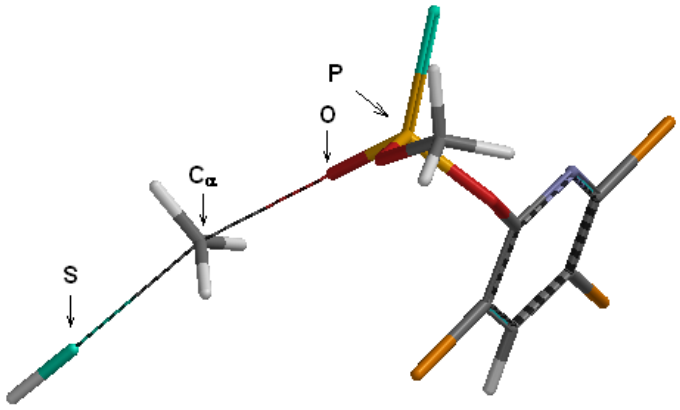

a) chlorpyrifos-methyl

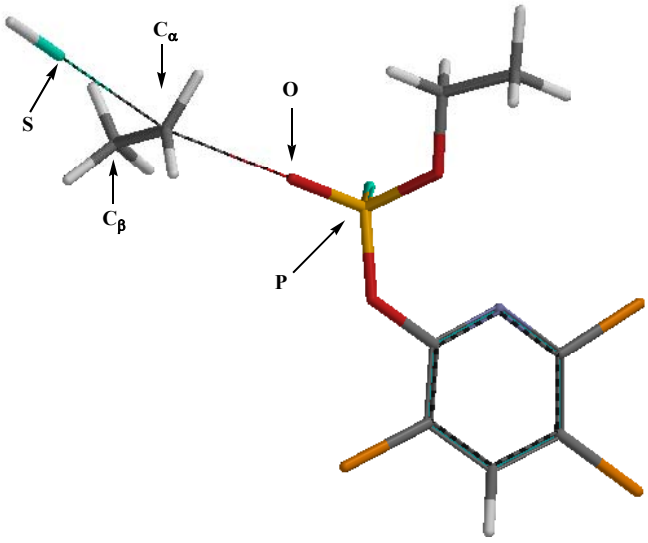

b) chlorpyrifos

Figure 7-3. Optimized transition state structures for reaction of HS- with (a) chlorpyrifos-methyl and (b) chlorpyrifos. Structures were located using a density functional theory method of electron correlation (B3LYP/6-31G(d)) and were used to calculate frequencies and energies at B3LYP/6-31G+(d,p)) level of theory. Transition states (a) and (b) were verified as first-order saddle points with one imaginary frequency at -292.2 cm^{-1}.

states. For example, the energy of activation for chloride attack on methyl chloride changes from 3 kcal/mol in the gas phase to above 20 kcal/mol in water.

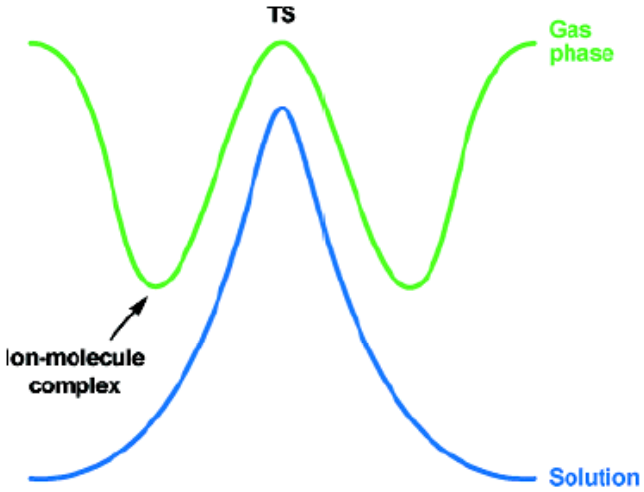

Figure 7-4. Contrast between gas (green) and solution (blue) phase potential energy surfaces for S_N2 reaction (Dedieu et al. 1972; Olmstead et al. 1977; Laerdahl et al. 2002).

The greatest effect on the geometries of the transition state structures for the reactions of HS^- with OPs may only be captured by explicitly including solvent molecules in the calculation (versus application of a simplified solvation model, such as PCM). Unfortunately this approach proved infeasible within the constraints of available computing facilities.

The structural characteristics (i.e., bond lengths and angles, and atomic charges) of the transition state structures for the reactions of five OPs were compared with those of the starting reactants to seek evidence of the effect of the side chain in the reaction. A summary of the geometric and charge changes for reactant and transition state structures for these investigated OPs is provided in Tables 7-2 and 7-3.

Table 7-2. Structural characteristics of reactants and transition states (t.s.) for reactions with HS^- [a]

Structure	Bond length (Å)						Bond angles (°)	
	P=S	P-O	O-C_α	C_α-C_β	C_α-S	C_α-H	∠ S-C_α-O	∠ S-C_α-H
Chlorpyrifos-methyl	1.945	1.617	1.414	__	∞	1.093	__	__
Chlorpyrifos-methyl(t.s)	1.953	1.524	2.461	__	2.940	1.092	166.43	85.89[b]
difference	*-0.008*	*0.093*	*-1.047*	__	__	*0.001*	__	__
Parathion-methyl	1.939	1.620	1.414	__	∞	1.091	__	__
Parathion-methyl (t.s.)	1.953	1.523	2.463	__	2.939	1.091	172.31	88.57
difference	*-0.014*	*0.097*	*-1.049*	__	__	*0*	__	__
Fenchlorfos	1.937	1.622	1.415	__	∞	1.093	__	__
Fenchlorfos (t.s)	1.951	1.522	2.462		2.941	1.091	168.21	85.24
difference	*-0.014*	*0.100*	*-1.047*	__	__	*0.002*	__	__
Chlorpyrifos	1.944	1.625	1.418	1.515	∞	1.094	__	__
Chlorpyrifos (t.s)	1.959	1.526	2.499	1.448	2.986	1.093	155.21	84.63
difference	*-0.015*	*0.099*	*-1.081*	*0.067*	__	*0.001*	__	__
Parathion	1.939	1.620	1.418	1.515	∞	1.095	__	__
Parathion (t.s.)	1.954	1.522	2.500	1.448	2.982	1.093	153.33	87.48
difference	*-0.015*	*0.098*	*-1.082*	*0.067*	__	*0.002*	__	__

[a] *Optimized and calculated at B3LYP/6-31+G(d,p)//B3LYP/6-31G(d) level of theory*

[b] *the 3 angle of ∠S-C_α-H are not the same, here shows the smallest angle.*

The dihedral angle of chlorpyrifos-methyl between the S_N2 axis of inversion and the leaving group is 166.43º, while the angles (∠S-C_α-O) of parathion-methyl and fenchlorfos are 172.31º and 168.21º, respectively. Compared to 180º (∠Cl-C-Cl for CH_3Cl with Cl^-), the difference is mainly attributed to the size of the phenyl group in the OPs, the chloride trichlorpyridinyl group and 2,3,5-trichlorophenol group show a bigger repulsion than the 4-nitrophenyl group. Unlike the reaction of CH_3Cl

with Cl^-, the reactant in our study is unsymmetric, therefore, the three angles of ∠S-C_α-H are not the same, and the data listed in Table 7-2 are the smallest.

Table 7-3. Calculated total atomic charges[a] on key atoms for all optimized[b] reactant and transition state (t.s.) structures

Structure	P	S(=P)	C_α	C_β	O	S
Chlorpyrifos-methyl	1.404	-0.671	0.141		-0.485	-2.0[c]
Chlorpyrifos-methyl (t.s.)	1.579	-0.945	0.533		-0.867	-1.087
difference	*-0.175*	*0.274*	*-0.392*		*0.382*	*-0.913*
Parathion-methyl	1.523	-0.703	0.246		-0.524	-2.0
Parathion-methyl (t.s.)	1.490	-0.900	0.530		-0.833	-1.096
difference	*0.033*	*0.197*	*-0.284*		*0.309*	*-0.904*
Fenchlorfos	1.474	-0.706	0.204		-0.501	-2.0
Fenchlorfos (t.s)	1.599	-0.938	0.506		-0.856	-1.084
difference	*-0.125*	*0.232*	*-0.302*		*0.355*	*-0.916*
Chlorpyrifos	1.404	-0.740	0.184	-0.120	-0.475	-2.0
Chlorpyrifos (t.s)	1.531	-0.965	0.562	-0.114	-0.832	-1.126
difference	*-0.127*	*0.225*	*-0.378*	*-0.006*	*0.357*	*-0.874*
Parathion	1.320	-0.664	0.143	-0.136	-0.472	-2.0
Parathion (t.s.)	1.623	-0.945	0.568	-0.096	-0.865	-1.112
difference	*-0.303*	*0.301*	*-0.425*	*-0.040*	*0.393*	*-0.888*

[a] *Mulliken charges obtained from population analysis*

[b] *Optimized and calculated at B3LYP/6-31+G(d,p)//B3LYP/6-31G(d) level of theory*

[c] *Charge of sulfur in HS^- nucleophile (included for the difference calculations)*

A considerable shortening of the bond (around 0.1 Å) linking the alkoxy oxygen and the phosphorus atom is manifested in the OPs transition state structure, consistent with the formation of a partial double bond between these atoms. Significant increases of the phosphorothionate bond (around 0.01 Å) for all five OPs demonstrate the partial breakage of the double bond. The increase in net charge on

the atoms comprising the S_N2 reaction center (~ Δ+0.4) demonstrates that significant electron density is transferred to the rest of the molecule. Another alkoxy group accepts substantial negative charge, which is principally transferred to the α-carbon.

Calculated structural characteristics for both the reactants and transition state structure agree with our observation in the degradation experiment. The S_N2 reaction occurred at the α-carbon will result in the leaving of the phosphorothionate diester, and the S=P-O bond of the diester will finally convert into S-P=O bond. For better understanding the structural characteristics, correlations of the second-order rate constants with HS^- vs. the Mulliken charges on the α-carbon (Table 7-3) are shown in Figure 7-5 for the five investigated OPs.

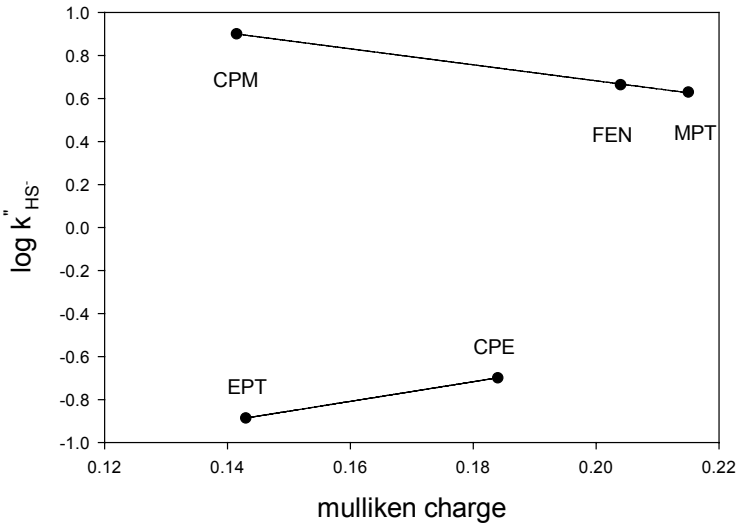

Figure 7-5. Linear free energy relationships for the reaction of five OPs with HS^- at 25°.

For the O,O-dimethyl substituted OPs, the three corresponding points enable us to generate a slope which is –3.72 ± 0.08 (r^2 = 0.999), but for the O,O-diethyl series,

the correlation can't be generated with only two points. These correlations show that the dimethyl substituted OPs are more reactive than the diethyl substituted OPs. And S_N2 reaction rate of O,O-dimethyl substituted OPs with HS^- might be slower with the increase of Mulliken charge on the α-carbon, but since the O,O-diethyl substituted OPs don't show the same correlation as the O,O-dimethyl substituted OPs, more experimental data are needed.

7.4.2. Relationship between K_{ow}, log *VP*, log *HLC*, log *Sol* and rate constant.

Since the relationship between Mulliken charge on the α-carbon of alkoxy group and the reaction rate constants of OPs with bisulfide is not clear, I also investigated the correlation with some other physico–chemical properties. Correlative-type QSARs for electro(nucleo)philic mechanisms for the biodegradation tend to include log K_{ow} to model uptake and a variety of quantum chemical descriptors to account for reactivity. So in this study the water solubility (log *Sol*), octanol–water partitioning (log K_{ow}), vapor pressure (log *VP*) and Henry's Law constants (log *HLC*) are used to model the reactivity of OPs with HS^-.

In the study of Carlsen (Carlsen 2005), the experimental data for 65 OPs were compared with EPI (estimation programs interface, available at http://www.epa.gov/pbt/framwork.htm) generated (logarithmic) values for the water solubility (log *Sol*), octanol–water partitioning (log K_{ow}), vapor pressure (log *VP*) and Henry's Law constants (log *HLC*), and a "Noise deficient" QSARs were obtained to show that to a certain extent selected insecticides may act as substitutes for OP compounds in preliminary experimental studies. And here I investigate the

dependence rate constants of OPs with bisulfide using the experiment values which are listed in Table 7-4.

Table 7-4: Physico–chemical data (solubilities, octanol–water partitioning, vapor pressures, Henry's Law constants)

OPs	Water *Solubility* *(mg/L)*	log K_{ow}	*VP, (mmHg at 25C)*	HLC atm m^3/mol
Chlorpyrifos-methyl	4.0	4.24	4.20×10^{-5}	3.75×10^{-6}
Parathion-methyl	57	2.86	1.80×10^{-5}	1.00×10^{-7}
Fenchlorphos	1.2	4.88	8.20×10^{-4}	3.20×10^{-5}
Chlorpyrifos	2.0	4.96	1.87×10^{-5}	2.93×10^{-6}
Parathion	6.54	3.83	9.65×10^{-6}	2.98×10^{-7}

Figure 7-6 contains the plots of the log of the second-order rate constants for the reaction of OPs with HS^- versus the water solubility (log *Sol*), octanol–water partitioning (log K_{ow}), vapor pressure (log *VP*) and Henry's Law constants (log *HLC*) for the five OPs selected. It is clear that the O,O-diethyl and O,O-dimethyl OPs should be discussed individually. For the HLC and vapor pressure, the reactivity for both series tends to increase with the increase of HLC and vapor pressure, while for log Sol, the reactivity for both series tends to decrease with increasing log Sol. For the log $K_{ow,}$ the reactivity of O,O-dimethyl OPs increase with increasing log $K_{ow,}$ but reactivity of O,O-diethyl OPs decrease with increasing log $K_{ow.}$

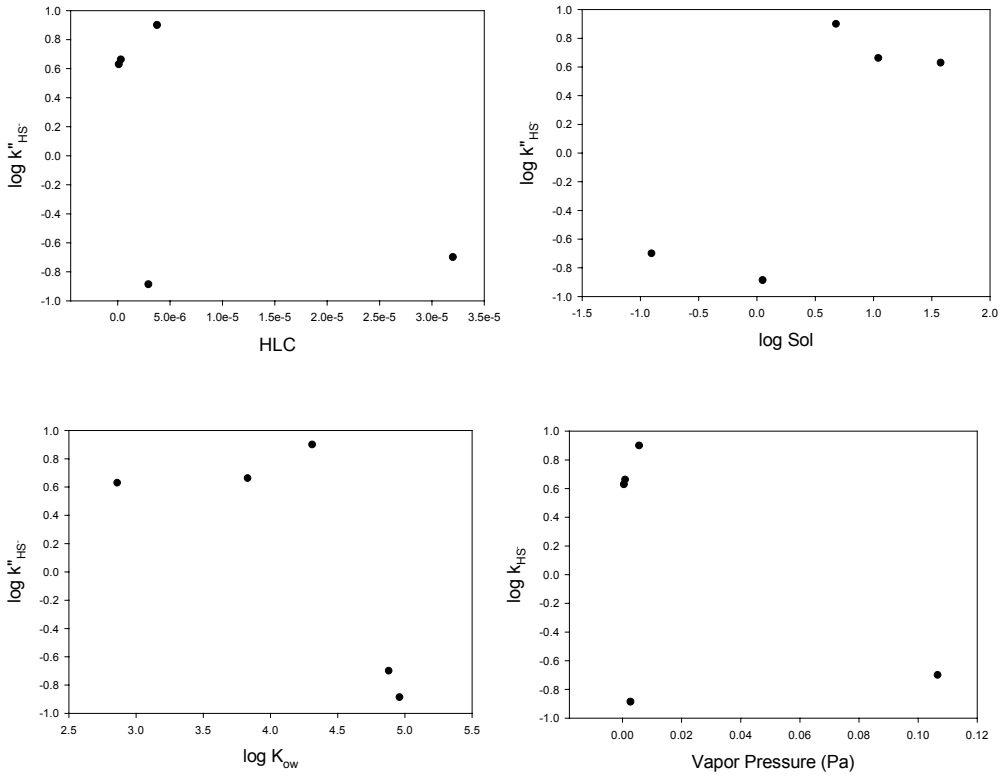

Figure 7-6. Linear free energy relationships for the reaction of five OPs with HS^-.

7.5. Conclusion

Unlike the organochlorine pesticides, the relatively complicated structure of OPs limited the QSAR research to the abiotic reaction, and most of the QSAR focused on the toxicology and biodegradation of the OPs. And since the abiotic degradation of OPs in aqueous environment is very important, the development of QSAR for the abiotic degradation would be necessary. Our result proved that the Mulliken charge on the α-carbon can be used as descriptors in a partial order ranking to establish a QSAR model. And water solubility (log *Sol*), octanol–water partitioning (log K_{ow}), vapor pressure (log *VP*) and Henry's Law constants (log *HLC*) might be used for QSAR. But still, more research on the structurally similar OPs is needed.

Appendix A.

Extraction efficiencies

Extraction efficiencies were determined by spiking a methanol solution containing the solute into buffer identically to the procedure for spiking samples. The buffer was then extracted within two hours of spiking with ethyl acetate or hexane for 30 seconds by votex mixing. The concentration of solute in the sample was determined relative to the working curve of the external standard. The initial concentration in the water was ~25 μM which was also determined relative to the working curve of the external standard by directly analyzing the buffer solution. The volume of the organic phase and aqueous phase was determined by using the acquiring mass divided by the density. The extraction efficiency is then calculated from the molarity of solute in the buffer solution divided by the molarity of solute in the initial water solution.

Table A-1 Extraction efficiencies of OPs and phenol

OPs	solvent	Aqueous conc(μM)	Conc. of extracts	Efficiency (%)
Chlorpyrifos-methyl	ethyl acetate	18.9	20.4	104
	hexane	18.9	19.3	97
Parathion-methyl	ethyl acetate	40.5	43.2	95
	hexane	40.5	38.4	94
Fenchlorfos	ethyl acetate	14.6	14.5	102
	hexane	14.6	16.7	99
Chlorpyrifos	ethyl acetate	10.5	12.1	108
	hexane	10.5	11.8	101
Parathion	ethyl acetate	30.0	33.7	99
	hexane	30.0	35.4	102
3,5,6-	ethyl acetate	24.6	22.7	92
trichloropyridinol	hexane	24.6	23.0	89
4-nitrophenol	ethyl acetate	25.2	24.0	81
	hexane	25.2	23.7	80
2,4,5-trichlorophenol	ethyl acetate	26.0	26.4	92
	hexane	26.0	24.5	93

Appendix B

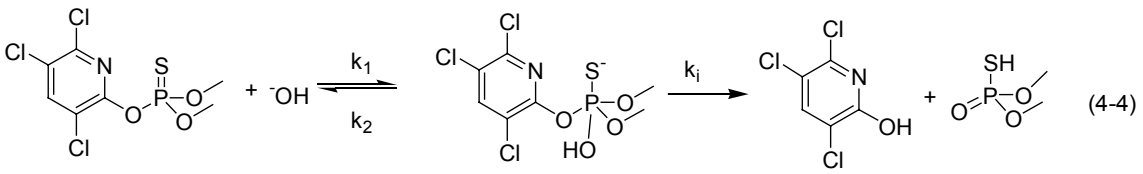

(4-4)

Chlorpyrifos-methyl

trichloropyridinol

A general expression for the value of k_{obs} as a function of hydroxide activity implied by this mechanism is not practical because the concentration of the pentavalent charged intermediate is unknown. One can solve, however, for the value of k_{obs} vs. OH^- activity if equilibrium in the first reaction is assumed.

$$\frac{-d[OP-OH]}{dt} = k_1[OP][OH^-] - k_{-1}[OP-OH] = 0 \qquad \text{(A - 1)}$$

Defining $[P_T]$ represents the total OP concentration, which equal to the total of OP and the pentavalent intermediate.

$$k_1([P_T]-[OP-OH])[OH^-] - k_{-1}[OP-OH] = 0 \qquad \text{(A - 2)}$$

Therefore:

$$[OP-OH] = \frac{k_1[P_T][OH^-]}{k_1[OH^-]+k_{-1}} \qquad \text{(A - 3)}$$

Defining $K = k_1/k_{-1}$, the expression becomes

$$[OP-OH] = \frac{K[P_T][OH^-]}{K[OH^-]+1} \qquad \text{(A - 4)}$$

then the pseudo-first order reaction equation could be represent by the following equation:

$$\frac{d[P_T]}{dt} = -k_{obs}[P_T] = -k_i[OP-OH] = -k_i\frac{K[P_T][OH^-]}{K[OH^-]+1} \qquad \text{(A - 5)}$$

The observed first-order rate constant, consequently, is given by where [OH^-] here represents hydroxide activity.

$$k_{obs} = k_i \frac{K[OH^-]}{K[OH^-]+1} \qquad \text{(A - 6)}$$

After rearrange the equation, the k_{obs} could be represent as:

$$\frac{1}{k_{obs}} = \frac{1}{k_i} + \frac{1}{k_i K[OH^-]} \qquad \text{(4-6)}$$

Equation 4-6 implies that, under conditions where equilibrium between OPs and the charged intermediate is maintained, a plot of l/kobsd vs. l/[OH-] should be a straight line. Deviations from the equilibrium assumption would result if $k_i >> k_{-l}$, a condition that is independent of pH, or if $k_l[OH^-] << k_i$, a condition that is certain to result in departures from equilibrium when the pH is low.

Appendix C

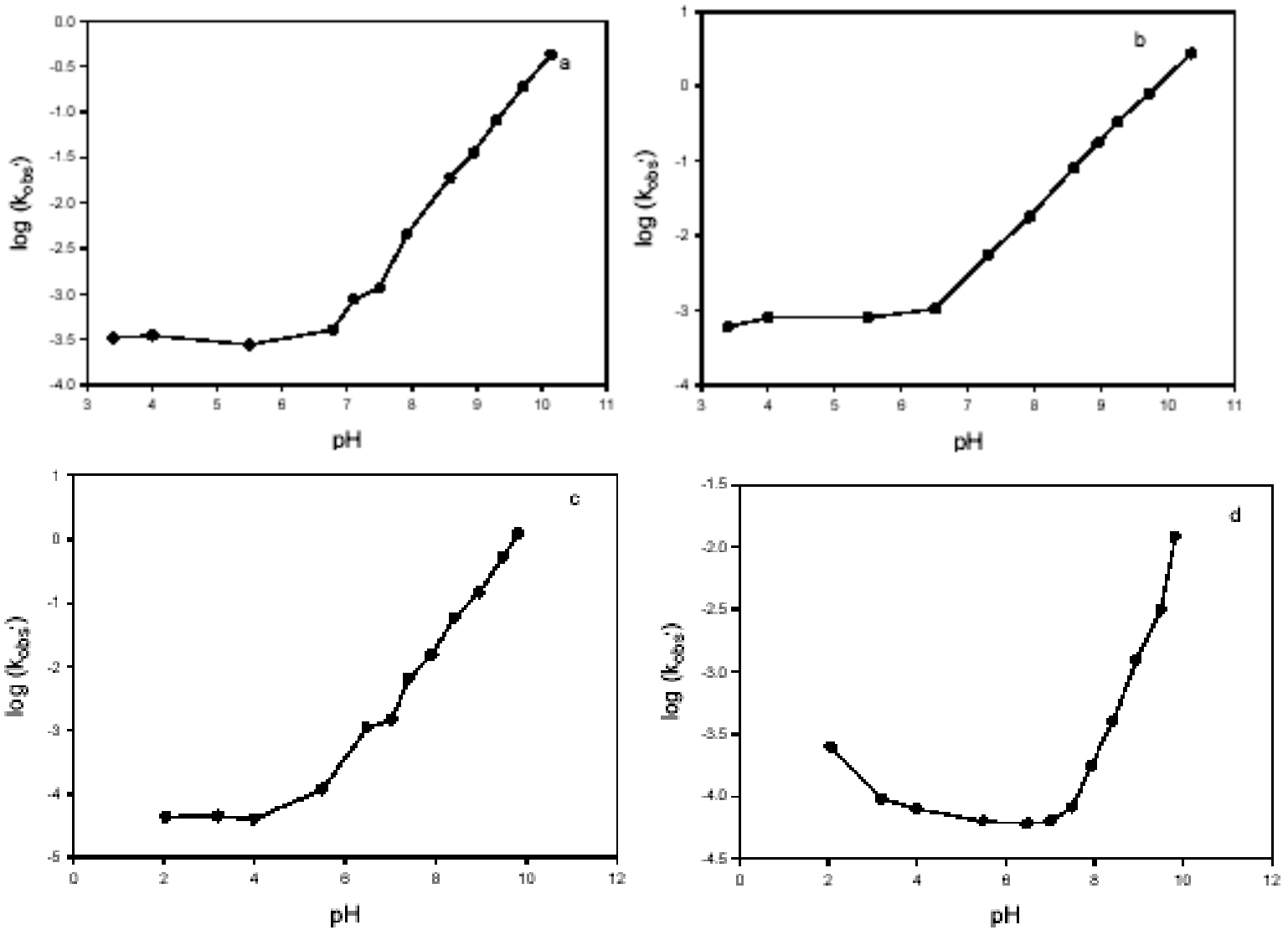

Figure 3-2. Hydrolysis of carbofuran, carbaryl, oxymyl, and methomyl for different pH values

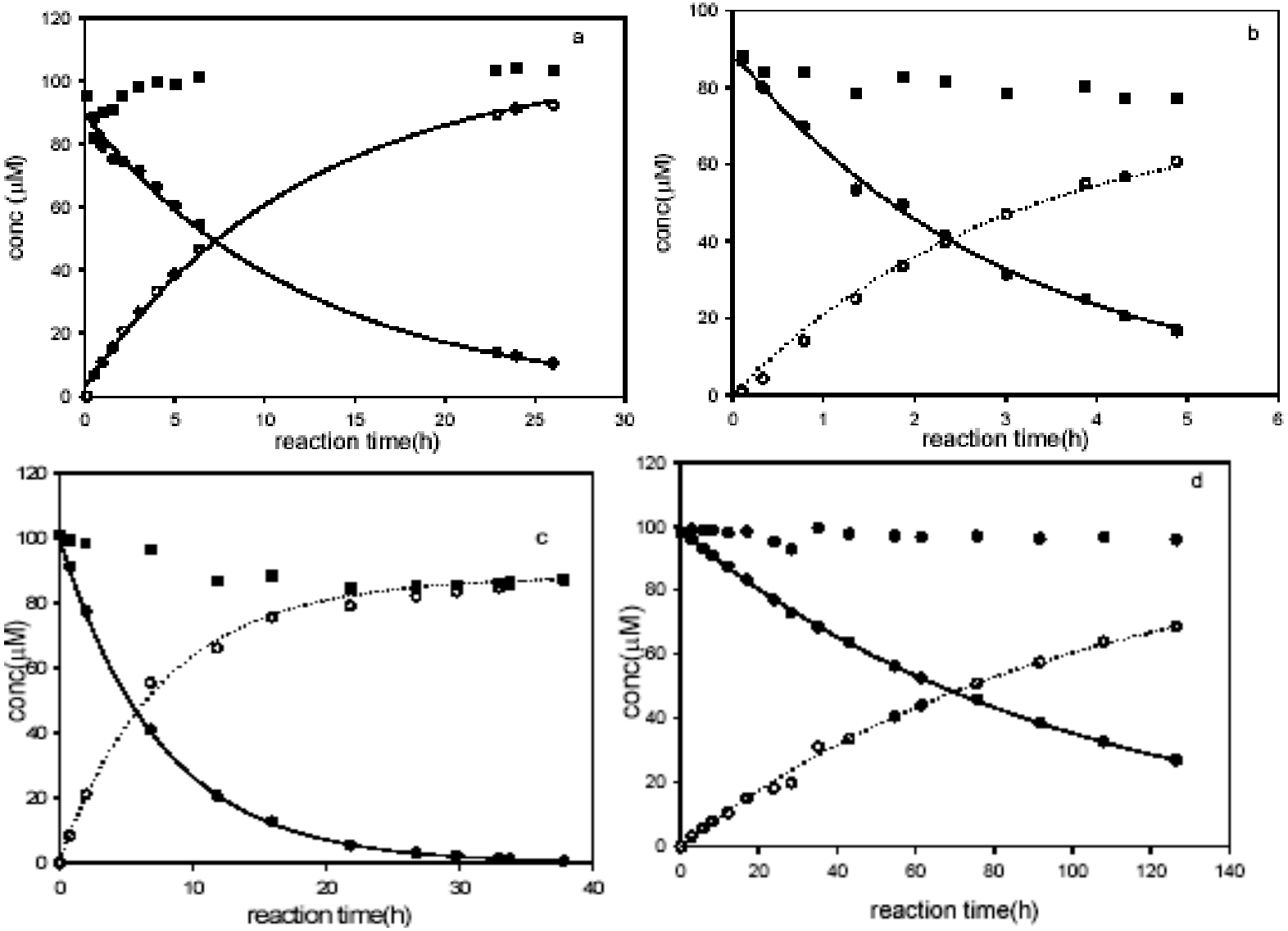

Figure 3-4: Hydrolysis of carbofuran at 9.31, carbaryl at 9.25, oxymyl at 8.95 methomyl at 9.83

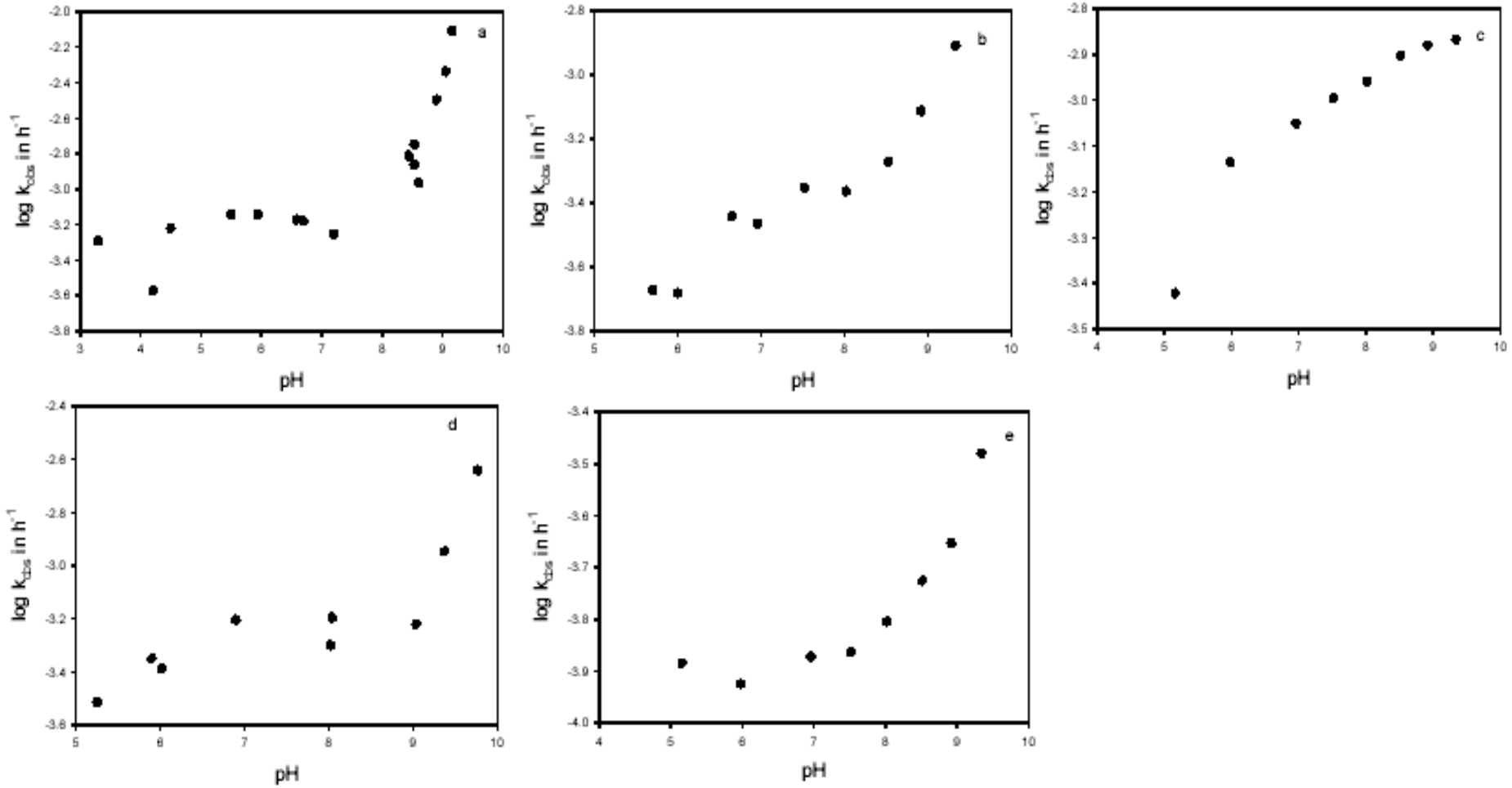

Figure 4-2. Observed rate constant vs. pH for the hydrolysis of five OPs

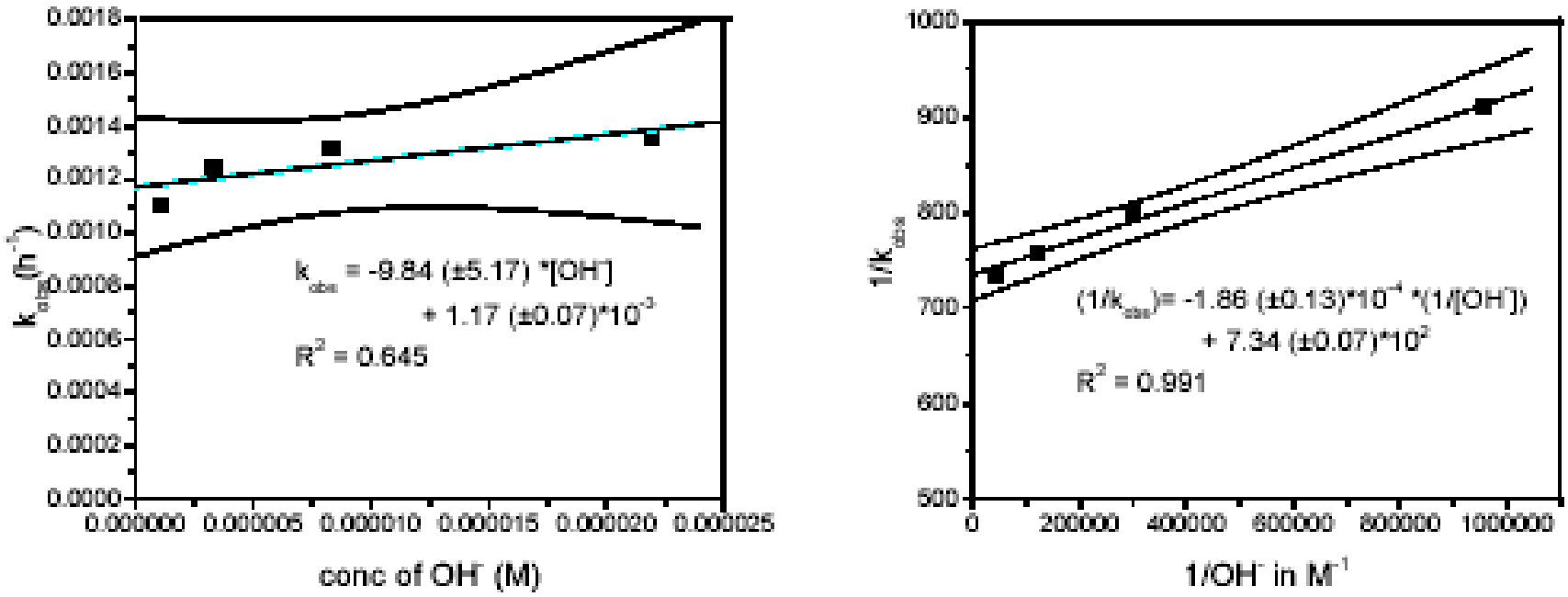

Figure 4-3. Plot of observed rate constant vs. concentration of OH^- (a) and $1/k_{obs}$ vs. $1/[OH^-]$(b) for the base catalyzed hydrolysis of fenchlorphos

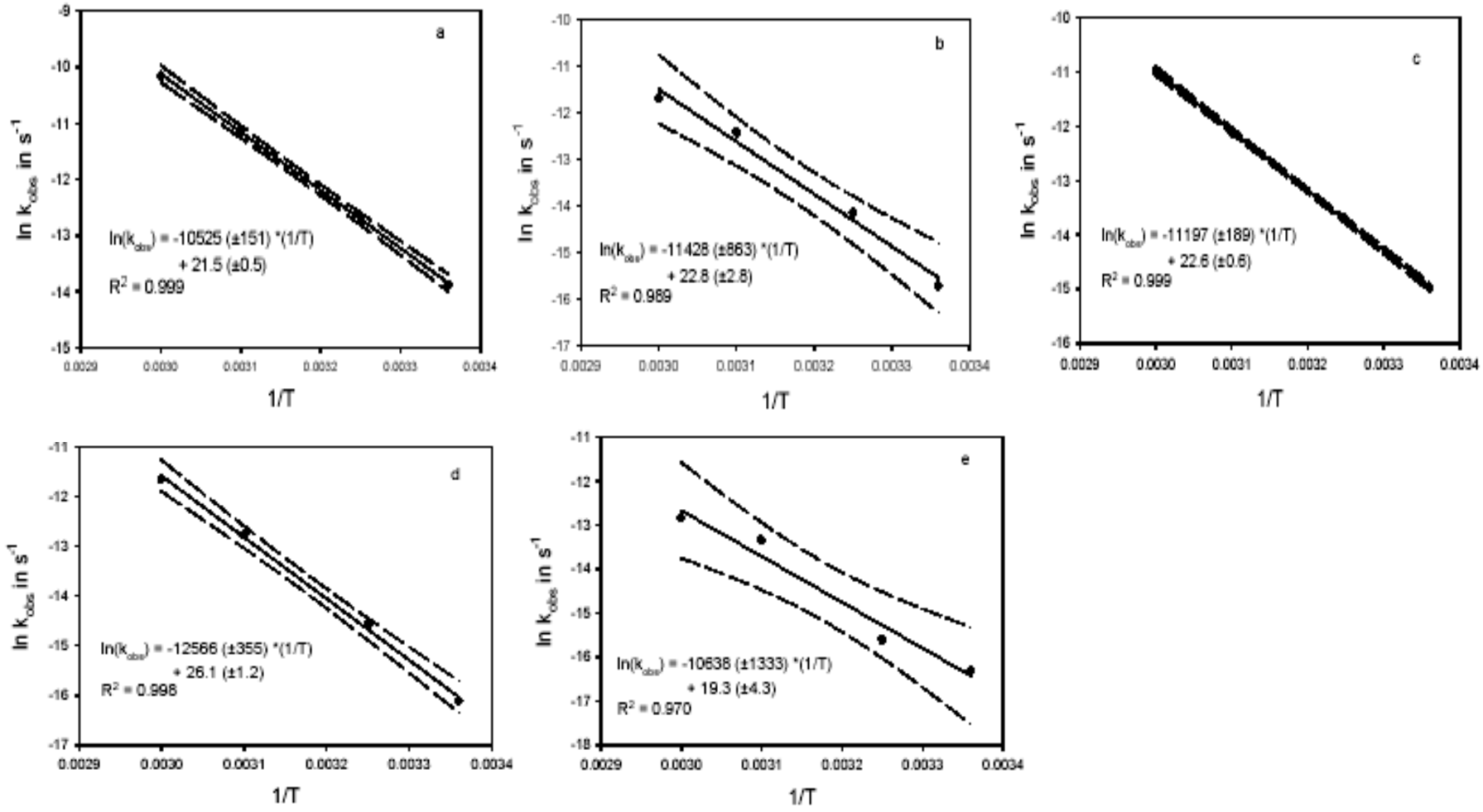

Figure 4-5. Arrhenius plot of the abiotic hydrolysis rate data for the five OPs at pH 8.5.

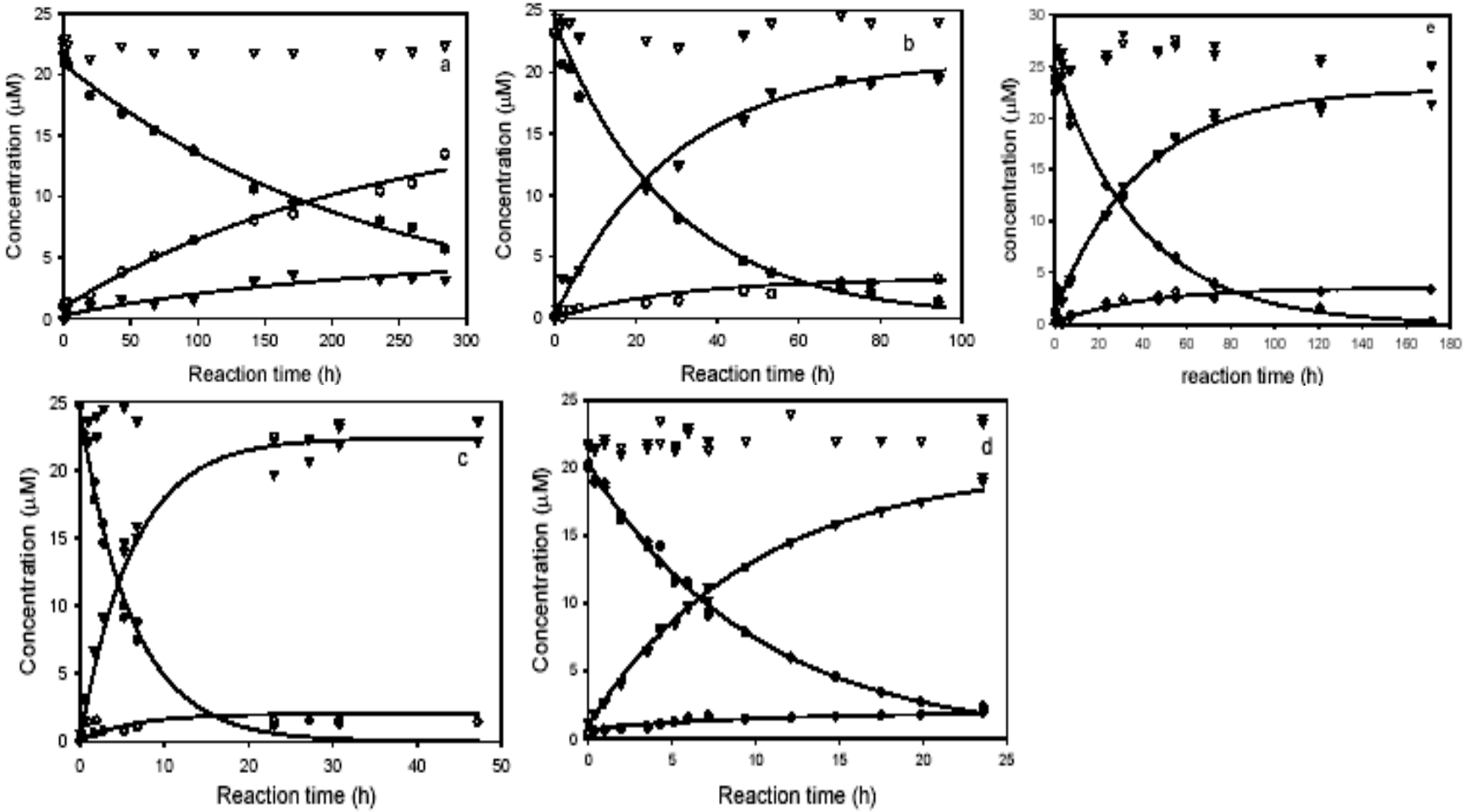

Figure 5-5. Hydrolysis of chlorpyrifos-methyl for different pH values

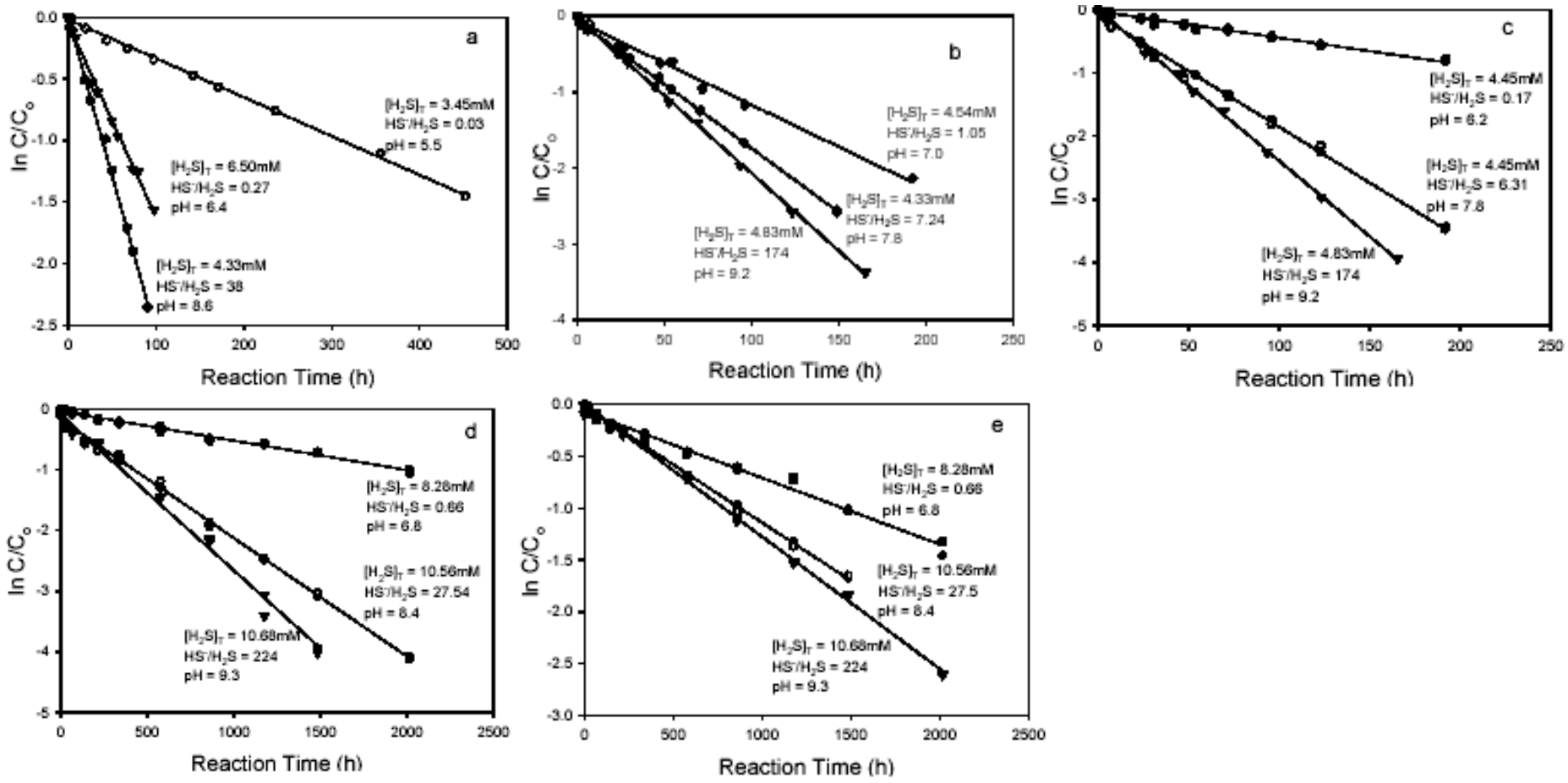

Figure 6-2. Example time courses for reactions of five OPs with HS^- at 25 °C and three different pHs

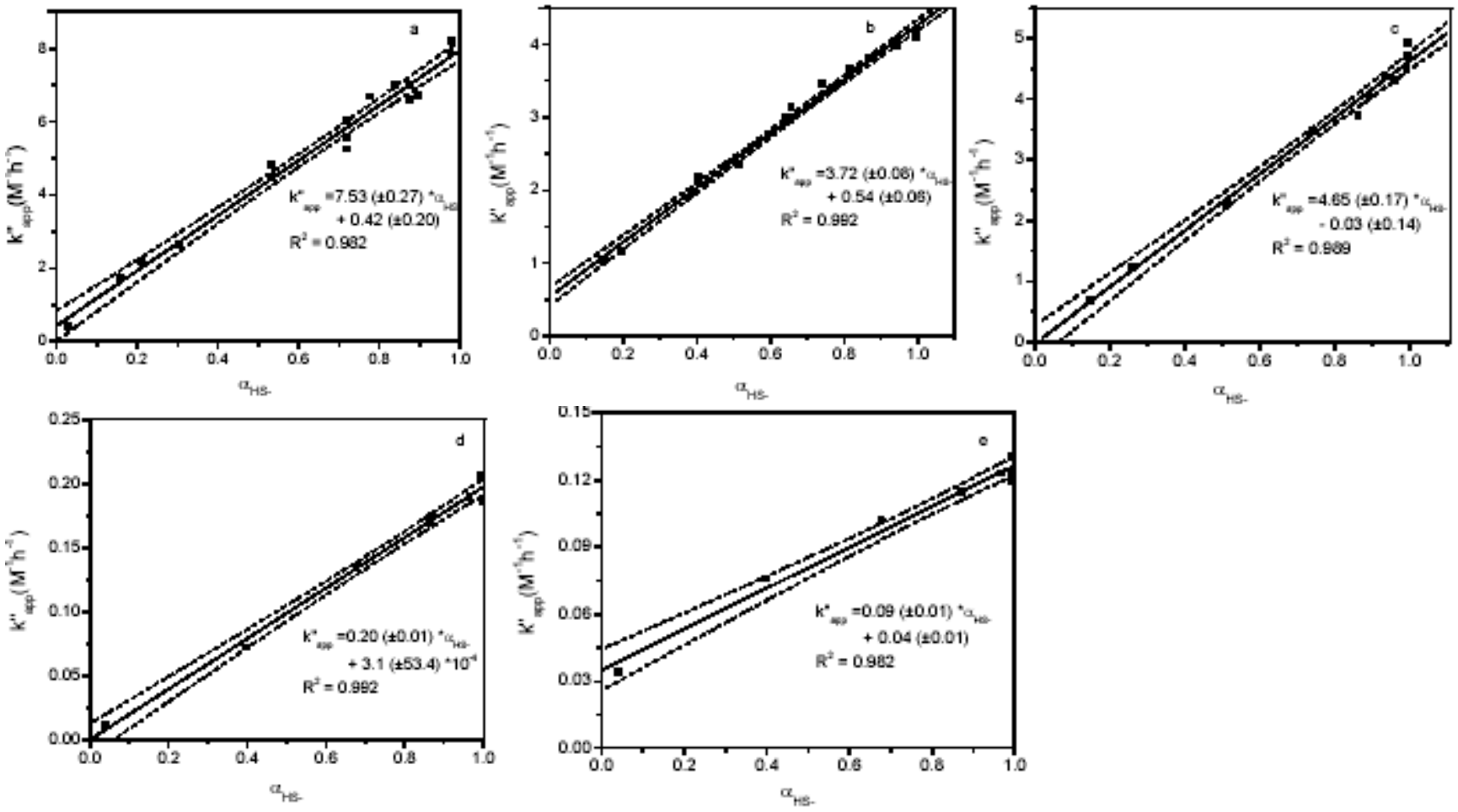

Figure 6-3: Plot of k''_{app} ($M^{-1}h^{-1}$), versus HS- for reactions of hydrogen sulfide/bisulfide with five OPs

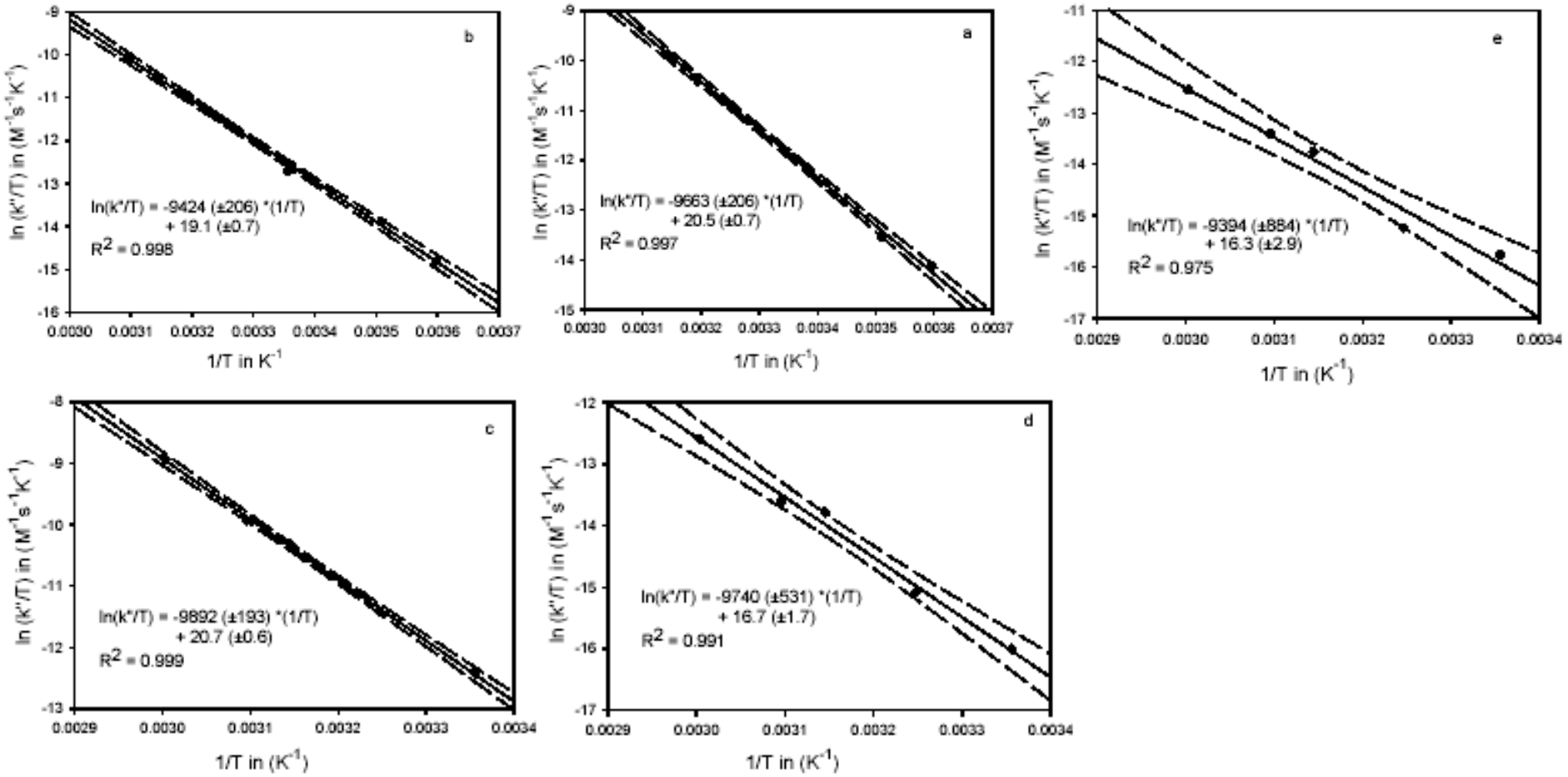

Figure 6-4. Temperature dependence of reactions of five OPs with HS^-

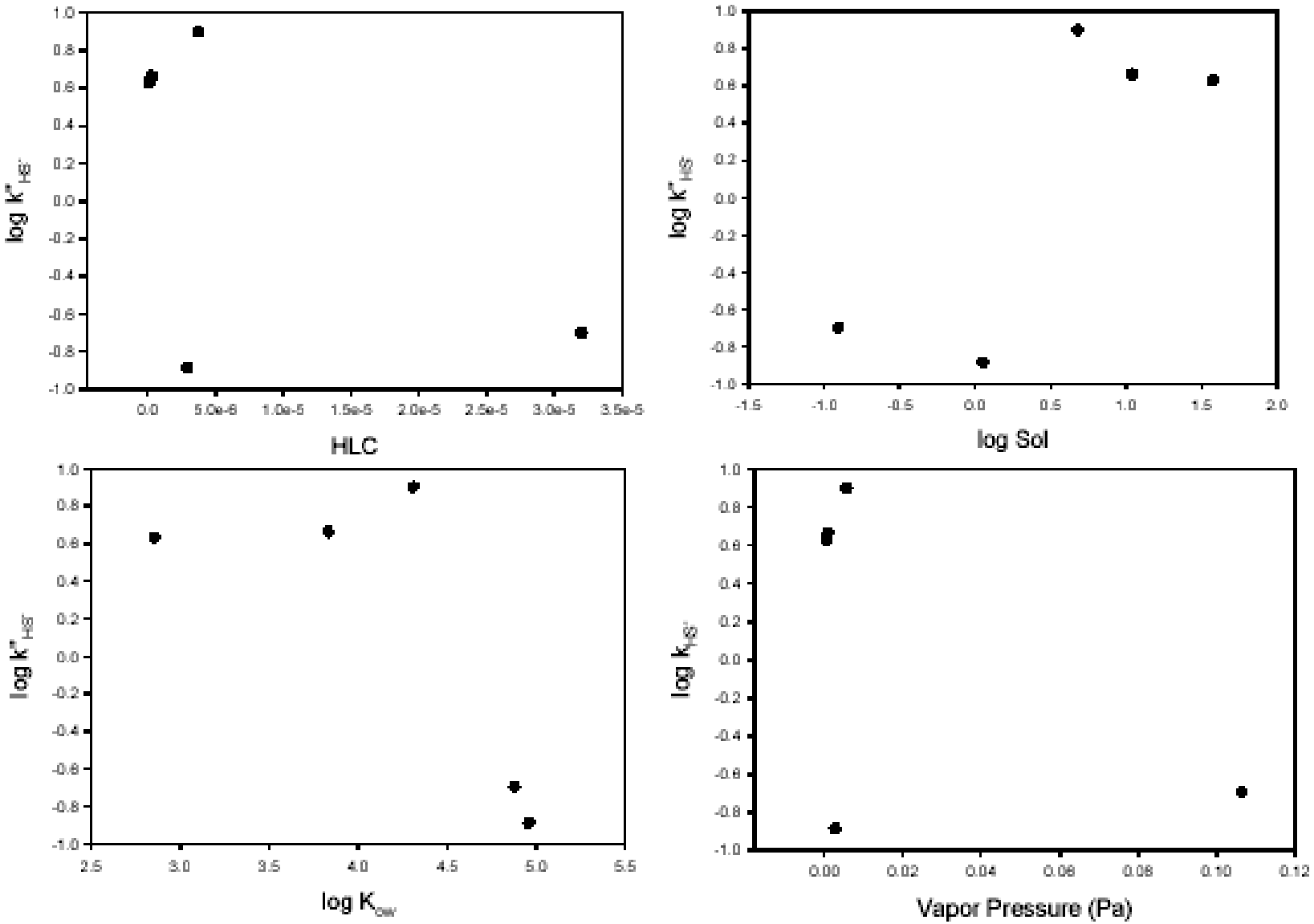

Figure 7-6. Linear free energy relationships for the reaction of five OPs with HS^-

Reference:

Scientist for Windows, Version 2.01, Micromath Scientific Software, Salt Lake City, UT, 1986

Farm Chemicals Handbook; ed.; Meister Publishing: Willoughby, OH, 1995.

Alexander, R., E. C. F. Ko, J. Parker and T. J. Broxton, Solvation of ions. XIV. protic-dipolar aprotic solvent effects on rates of bimolecular reactions. solvent activity coefficients of reactants and transition states at 25°. *J. Am. Chem. Soc.* **1968**, *20*, 5049-5069.

Alvares, A. P. Pharmacology and toxicology of carbamates. In *Clinical & Experimental Toxicology of Organophosphates and Carbamates*; ed.; B. Ballantyne and T. C. Marrs; Butterworth-Heinemann: Oxford, U.K., 1993; Vol. 40-46.

Arienzo, M., T. Crisanto, M. J. Sanchez-Martin and M. Sanchez-Camazano, Effect of soil characteristics on adsorption and mobility of ^{14}C-Diazinon. *J. Agric. Food Chem.* **1994**, *42*, 1803-1808.

Armstrong, A. C., A. M. Portwood and G. L. Harris Mechanistic modelling of pesticide leaching from cracking clay soils. In *Proceedings of Pesticide Movement to Water*; ed.; A. Walker, R. Allen, S. W. Baileyet al; British Crop Protection Council (BCPC) Monograph No.62. April 3-5: Coventry, UK, 1995; Vol.

Augspurger, T., M. R. Smith, C. U. Meteyer and K. A. Converse, Mortality of passerines adjacent to a North Caroline corn field treated with granular carbofuran. *J. Wildlife Dis* **1996**, *32*, 113-116.

Bakke, J. E. and C. E. Price, Metabolism of O,O-dimethyl-O-(3,5,6-trichloro-2-pyridyl)phosphorothionate in sheep and rats. *J. Environ. Sci. Health* **1976**, *B11*, 9-22.

Barbash, J. E. and M. Reinhard, Abiotic dehalogenation of 1,2-dichloroethane and 1,2-dibromoethane in aqueous solution containing hydrogen sulfide. *Environ. Sci. Technol.* **1989**, *23*, 1349-1358.

Barbash, J. E. and M. Reinhard Reactivity of sulfur nucleophiles toward halogenated organic compounds in natural waters. In *Biogenic Sulfur in the Environment*; ed.; E. S. Saltzman and W. J. Cooper; ACS: Washington, DC, 1989; Vol. 101-138.

Barbash, J. E., G. P. Thelin, D. W. Kolpin and R. J. Gilliom, Major herbicides in ground water: results from the National Water-Quality Assessment. *J. Environ. Qual.* **2001**, *30*, 831-845.

Barcelo, D., G. Durand and N. Debertrand, Photodegradation of the organophosphorus pesticides Chlorpyrifos, Fenamiphos and Vamidothion in water. *Toxicol. Environ. Chem.* **1993**, *38*, 183-199.

Barnard, P. W. C., C. A. Bunton, D. Kellerman, M. M. Mhala, B. Silver, C. A. Vernon and V. A. Welch, Reactions of organic phosphates. VI. The hydrolysis of aryl phosphates. *Journal of the Chemical Society [Section] B: Physical Organic* **1966**, *3*, 227-235.

Barnard, P. W. C., C. A. Bunton, D. R. Llewellyn, C. A. Vernon and V. A. Welch, Reactions of organic phosphates. V. Hydrolysis of triphenyl and trimethyl phosphates. *Journal of the Chemical Society* **1961**, 2670-2676.

Baskaran, S., N. S. Bolan, A. Rahbran and R. W. Tillman, Non-equilibrium, sorption during the movement of pesticides in soils. *Pestic. Sci.* **1996**, *46*, 333-343.

Beltran, J., F. Hemandez, F. J. Lopez and l. Morell, Study of sorption processes of selected pesticides on soils and ceramic porous cups used for soil solution sampling. *Intern. J. Environ. Anal. Chem.* **1995**, *58*, 287-303.

Berman, H. A. and M. M. Decker, Kinetic, equilibrium, and spectroscopic studies on dealkylation ("Aging") of alkyl organophosphonyl acetylcholinesterase. *J. Biol. Chem.* **1986**, *261*, 10646-10652.

Boulegue, J., C. J. Lord III and T. M. Church, Sulfur speciation and associated trace metals (Fe, Cu) in the pore waters of Great Marsh, Delaware. *Geochim. Cosmochimi. Acta* **1982**, *46*, 453-464.

Brezonik, P. L. *Chemical kinetics and process dynamics in aquatic systems*; ed.; Lewis Publishers: Boca Raton, FL, 1994.

Carlsen, L., A QSAR approach to physico-chemical data for organophosphates with special focus on known and potential nerve agents. *Internet Electronic Journal of Molecular Design* **2005**, *4*, 355-366.

Cavalier, T. C., T. L. Lavy and J. D. Mattice, Persistence of selected pesticides in groundwater samples. *Groundwater* **1991**, *29*, 225-231.

CDPR, (California Department of Pesticide Regulation), *Pesticide Use Reporting*; 1993; Sacramento, CA, http://www.cdpr.ca.gov/docs/pur/purmenu.htm

Coats, J. R., What happens to degradable pesticides? *Chemtech* **1993**, *23*, 25-29.

Cox, J. R. and O. B. Ramsay, Mechanisms of nucleophilic substitution in phosphate esters. *Chem. Rev.* **1964**, *64*, 317-352.

Cox, L., M. C. Hermosín and J. Cornejo, Adsorption of methomyl by soils of Southern Spain and soil components. *Chemosphere* **1993**, *27*, 837-849.

Dannenberg, A. and S. O. Pehkonen, Investigation of the heterogeneously catalyzed hydrolysis of organophosphorus pesticides. *J. Agric. Food Chem.* **1998**, *46*, 325-334.

De Llasera, M. P. G. and M. B. Gonzalez, Presence of carbamate pesticides in environmental waters from the northwest of Mexico: determination by liquid chromatography. *Water Res.* **2001**, *35*, 1933-1940.

Dean, J. A. *Lange's Handbook of Chemistry*; ed.; McGraw-Hill: New York, 1985.

Dedieu, A. and A. Veillard, Comparative study of some S_N2 reactions through ab initio calculations. *J. Am. Chem. Soc.* **1972**, *94*, 6730 - 6738.

Delgado, M. J. S., B. S.R., G. Toledano Fernandez-Tostado and P.-D. L. M., Stability Studies of Carbamate Pesticides and Analysis by Gas Chromatography with Flame Ionization and Nitrogen-Phosphorus Detection. *J. Chromatography A* **2001**, 287-296.

Dilling, W. L., N. B. Tefertiller and G. J. Kollos, Evaporation rates and reactivities of methylene chloride, chloroform, 1,1,1-trichloroethane, trichloroethylene, tetrachloroethylene and other chlorinated compounds in dilute aqueous solutions. *Environ. Sci. Technol.* **1975**, *9*, 833-838.

Domagalski, J. L. and N. M. Dubrovsky, Pesticide residues in ground water of the San loaquin valley, California. *J. Hydrol* **1992**, *130*, 299-338.

Donaldson, D., T. Kiely and A. Grube *Pesticides Industry Sales and Usage, 2000 and 2001 Market Estimates*, EPA 733-R-04-001; EPA Office of Pesticide Programs: http://www.epa.gov/oppbead1/pestsales/01pestsales/market_estimates2001.pdf; (accessed Jan.14, 2005)

Doong, R. A. and W. H. Chang, Photoassisted titanium dioxide mediated degradation of organophosphorus pesticides by hydrogen peroxide. *J. Photochem. Photobiol. A-Chem.* **1997**, *107*, 239-244.

Doong, R. A. and W. H. Chang, Photoassisted iron compound catalytic degradation of organophosphorous pesticides with hydrogen peroxide. *Chemosphere* **1998**, *37*, 2563-2572.

Drossman, H., H. Johnson and T. Mill, Structure activity relationships for environmental processes 1: Hydrolysis of esters and carbamates. *Chemosphere* **1988**, *17*, 1509-1530.

Duboc, C. The correlation analysis of nucleophilicity. In *Correlation Analytical Chemistry: Recent Advance*; ed.; N. B. Chapman and J. Shorter; Plenum: New York, NY, 1978; Vol. 313-355.

Durand, G., J. L. Abad, F. Sanchezbaeza, A. Mlesseguer and B. D., Unequivocal identification of compounds formed in the photodegradation of Fenitrothion in water-methanol and proposal of selected transformation pathways. *J. Agric. Food Chem.* **1994**, *42*, 814-821.

Edwards, J. and R. G. Pearson, The factors determining nucleophilic reactivity. *J. Am. Chem. Soc.* **1962**, *84*, 16-24.

Edwards, J. O., Correlation of relative rates and equilibria with a double basicity scale. *J. Am. Chem. Soc.* **1954**, *76*, 1540-1547.

Eichelberger, J. W. and J. J. Lichtenberg, Persistence of pesticides in river water. *Environ. Sci. Technol.* **1971**, *5*, 541-544.

EPA *Carbaryl IRED facts*: http://www.epa.gov/oppsrrd1/REDs/carbaryl_ired.pdf; (accessed Dec. 10, 2005)

EPA *Office of pesticide programs, overview on the chlorpyrifos-methyl revised risk assessment*: <http://www.epa.gov/oppsrrd1/op/chlorpyrifos-methyl.htm>, <http://www.epa.gov/pesticide/op/chlorpyrifos-methyl/overview>. (accessed April 19, 2004)

Eskenazi, B., A. Bradman and R. Castorina, Exposures of children to organophosphate pesticides and their potential adverse health effects. *Environ. Health. Persp.* **1999**, *107*, 409-419.

Faust, S. D. and H. M. Gomaa, Chemical hydrolysis of some organic phosphorus and carbamate pesticides in aquatic environments. *Environ. Lett.* **1972**, *3*, 171-201.

Fernández-Pérez, M., M. Villafranca-Sánchez, E. González-Pradas, F. Martinez-López and F. Flores-Céspedesl., Controlled release of carbofuran from an Alginate-Bentonite formulation: water release kinetics and soil mobility. *J. Agric. Food Chem.* **2000**, *48*, 938-943.

Foster, G. D. and K. A. Lippa, Fluvial loadings of selected organonitrogen and organophosphrus pesticides to chesapeake bay. *J. Agric. Food Chem.* **1996**, *44*, 2447-2454.

Freed, V. H., C. T. Chiou and D. W. Schmedding, Degradation of selected organophosphate pesticides in water and soil. *J. Agric. Food Chem.* **1979**, *27*, 706-708.

Froede, H. C. and I. B. Wilson, Direct determination of acetyl-enzyme intermediate in the acetylcholinesterase-catalyzed hydrolysis of acetylcholine and acetylthiocholine. *J. Biol. Chem.* **1984**, *259*, 11010-11013.

Frost, A. A. and R. G. Pearson *Kinetics and mechanism*; 2nd ed ed.; Wiley: New York, 1961.

Fukuto, T. R. and R. L. Metcalf, Pesticidal activity and structure, structure and insecticidal activity of some diethyl substituted phenyl phosphates. *J. Agric. Food Chem.* **1956**, *4*, 930-935.

Fukuto, T. R. and R. L. Metcalf, The effect of structure on the reactivity of alkylphosphonate esters. *J. Am. Chem. Soc.* **1959**, *81*, 372-377.

Gan, Q., R. M. Singh and U. Jans, Degradation of naled and dichlorvos promoted by reduced sulfur species in well-defined anoxic aqueous solutions. *Environ. Sci. Technol.* **2006**, *40*, 778 - 783.

Gianessi, L. P. and J. E. Anderson "Pesticide use in US crop production: national summary report," National Center for Food and Agriculture Policy, 1995, Washington, DC.

Gianessi, L. P. and M. B. Marcelli "Pesticide use in U.S. crop production: 1997. National Data Report," National Center for Food and Agricultural Policy, 2000, Washington, DC.

Giggenbach, W., Optical spectra of highly alkaline sulfide solutions and the second dissociation constant of hydrogen sulfide. *Inorg. Chem.* **1971**, *10*, 1333-1338.

Giggenbach, W., Optical spectra and equilibrium distribution of polysulfide ions in aqueous solution at 20^{o}C. *Inorg. Chem.* **1972**, *11*, 1201-1207.

Giggenbach, W. F., Equilibria involving polysulfide ions in aqueous sulfide solutions up to 240º. *Inorg. Chem.* **1974**, *13*, 1724-1733.

Gun, J., A. Goifman, I. Shkrob, A. Kamyshny, B. Ginzburg, O. Hadas, I. Dor, A. D. Modestov and O. Lev, Formation of polysulfides in an oxygen rich freshwater lake and their role in the production of volatile sulfur compounds in aquatic systems. *Environ. Sci. Technol.* **2000**, *34*, 4741-4746.

Guo, X. and U. Jans, Kinetics and mechanism of the degradation of methyl parathion in aqueous hydrogen sulfide solution: investigation of natural organic matter effects. *Environ. Sci. Technol.* **2006**, *40*, 900-906.

Gupta, R. C., Carbofuran toxicity. *J. Toxicol. Environ. Health* **1994**, *43*, 383-418.

Hall, J., F. P. Healey and G. G. C. Robinson, The interaction of chronic copper toxicity with nutrient limitation in two chlorophytes in batch culture. *Aquatic Toxicology* **1989**, *14*, 1-14.

Hallberg, G. R., Pesticides pollution of groundwater in the humid United States. *Agric. Ecosyst. Environ.* **1989**, *26*, 299-367.

Hart, J. F. *Land That Feeds Us*; ed.; The Commonwealth Fund Book Program: New York, W.W. Norton, 1993.

Hartley, D. and H. Kidd *The Agrochemicals Handbook*; 2nd ed.; The Royal Society of Chemistry: Nottingham, England, 1987.

Hassall, K. A. *The Biochemistry and Uses of Pesticides*; 2nd ed.; VCH: New York, 1990.

Hegarty, A. F. and L. N. Frost, Elimination-addition mechanism for the hydrolysis of carbamates. Trapping of an isocyanate intermediate by an o-amino-group. *J. Chem. Soc., Perkin Trans.* **1973**, *2*, 1719-1728.

Hegarty, A. F., L. N. Frost and J. H. Coy, Question of amide group participation in carbamate hydrolysis. *Journal of Organic Chemistry* **1974**, *39*, 1089-1093.

Henneke, E., I. George W. Luther, G. J. D. Lange and J. Hoefs, Sulphur speciation in anoxic hypersaline sediments from the eastern Mediterranean Sea. *Geochim. Cosmochim. Acta.* **1997**, *61*, 307-321.

Hilal, S., S. W. Karickhoff and L. A. Carreira, A rigorous test for SPARC's chemical reactivity models: estimation of more than 4300 ionization pKa's. *Quant. Struc. Act. Rel.* **1995**, *14*, 348-355.

Holden, A. J., L. Chen and I. C. Shaw, Thermal stability of organophosphorus pesticide triazophos and its relevance in the assessment of risk to the consumer of triazophos residues in food. *J. Agric. Food Chem.* **2001**, *49*, 103-106.

Hong, F. and S. Pehkonen, Hydrolysis of phorate using simulated environmental conditions: rates, mechanisms and product analysis. *J. Agric. Food Chem.* **1998**, *46*, 1192-1199.

Hong, F., S. O. Pehkonen and E. Brooks, Pathways for the hydrolysis of phorate: product studies by ^{31}P NMR and GC-MS. *J. Agric. Food Chem.* **2000**, *48*, 3013-1017.

Hong, F., K. Y. Win and S. O. Pehkonen, Hydrolysis of terbufos using simulated environmental conditions: rates, mechanisms, and product analysis. *J. Agric. Food Chem.* **2001**, *49*, 5866-5873.

Hornsby, A. G., R. D. Wauchope and A. E. Herner *Pesticide Properties in the Environment*; ed.; Springer: New York, 1996.

Howarth, R. W. and J. M. Teal, Sulfate reduction in a New England salt marsh. *Limn. Oceanogr.* **1979**, *24*, 999-1013.

Spartan'04, Wavefunction, Inc, Irvine, CA; Except for molecular mechanics and semi-empirical models, the calculation methods used in Spartan'04 have been documented in; J. Kong, C. A. W., A.I. Krylov. C.D. Sherrill, R.D. Adamson, T.R. Furlani, M.S. Lee, A.M. Lee, S.R. Gwaltney, T.R. Adams, C. Ochsenfeld, A.T.B. Gilbert, G.S. Kedziora, V.A. Rassolov, D.R. Maurice, N. Nair, Y.J. Kong, C.A. White, A.I. Krylov. C.D. Sherrill, R.D. Adamson, T.R. Furlani, M.S. Lee, A.M. Lee, S.R. Gwaltney, T.R. Adams, C. Ochsenfeld, A.T.B. Gilbert, G.S. Kedziora, V.A. Rassolov, D.R. Maurice, N. Nair, Y. Shao, N.A. Besley, P.E. Maslen, J.P. Dombroski, H. Daschel, W. Zhang, P.P. Korambath, J. Baker, E.F.C. Byrd, T. Van Voorhis, M. Oumi, S. Hirata, C.-P. Hsu, N. Ishikawa, J. Florian, A. Warshel, B.G. Johnson, P.M.W. Gill, M. Head-Gordon, J.A. Pople. Journal of Computational Chemistry, 1532, 2000

James, P. C., Internalizing externalities: granular carbofuran used on rapeseed in Canada. *Ecol. Econ.* **1995**, *13*, 181-184.

Jans, U. and M. H. Miah, Reaction of chlorpyrifos-methyl in aqueous hydrogen sulfide/bisulfide solutions. *J. Agric. Food Chem.* **2003**, *51*, 1956-1960.

Jorgensen, W. L. and J. K. Buckner, Effect of hydration on the structure of an S_N2 transition state. *J. Phys. Chem. B* **1986**, *90*, 4651-4654.

Kabachnik, M. I., T. A. Mastrukova, A. E. Shipov and T. A. Melentyeva, The application of the Hammett equation to the theory of tautomeric equilibrium: Thione-thiol equilibrium, acidity, and structure of phosphorus thio-acids. *Tetrahedron* **1960**, *9*, 10-28.

Kamiya, M. and K. Kamevama, Photochemical effects of humic substances on the degradation of organophosphoras pesticides. *Chemosphere* **1998**, *36*, 2337-2344.

Kamiya, M. and K. Kameyama, Effects of selected metal ions on photodegradation of organophosphorus pesticides sensitized by humic acids. *Chemosphere* **2001**, *45*, 231-235.

Karickhoff, S. W., D. S. Brown and T. A. Scott., Sorption of hydrophobic pollutants on natural sediments. *Water Res.* **1979**, *13*, 241-248.

Karickhoff, S. W., V. K. McDaniel, C. V. Melton, A.N., D. E. Nute and L. A. Carreira, Predicting chemical reactivity by computer. *Environ. Toxicol. Chem.* **1991**, *10*, 1405-1416.

Kenega, E. and C. Goring Relationship between water solubility, soil sorption, octanol-water partitioning and concentration chemicals in biota. In *Aquatic Toxicology. STP 707, (Third Symposium)*; ed.; J. C. Eaton, P. R. Parrish and A. C. Hendricks; American Society for Testing and Materials: Philadelphia (PA), 1980; Vol. 78-115.

Khan, S. U. *Pesticides in the Soil Environment*; ed.; Elsevier: Amsterdam, The Netherlands, 1980.

Kier, L. B. and L. H. Hall *Molecular Connectivity in Structure-Activity Analysis*; ed.; J. Wiley & Sons: New York, 1986.

Kim, D., J. Walters and R. Sava *Preliminary background results of organophosphate analysis and acute toxicity testing of surface water monitored for the red imported fire ant project in Orange County, March and April, 1999*; California Department of Pesticides Regulation [online]: http://www.cdpr.ca.gov/docs/rifa/rep1129.pdf; (accessed Jan.30, 2005)

Kirby, A. J. and S. G. Warren *The Organic Chemistry of Phosphorus*; ed.; Elsevier: New York, 1967.

Kohn, G. K. and D. R. Baker, Eds. *The agrochemical industry, In: Riegel's Handbook of Industrial Chemistry*; ed.; Van Nostrand Reinhold: New York, 1992.

Kolpin, D. W., J. E. Barbash and R. J. Gilliom, Occurrence of pesticides in shallow groundwater of the United States: initial results from the national water-quality assessment program. *Environ. Sci. Technol.* **1998**, *32*, 558-566.

Kolpin, D. W., E. T. Furlong, M. T. Meyer, E. M. Thurman, S. D. Zaugg, L. B. Barber and H. T. Buxton, Pharmaceuticals, hormones, and other organic wastewater contaminants in U.S. streams, 1999-2000: a national reconnaissance. *Environ. Sci. Technol.* **2002**, *36*, 1202-1211.

Kuhr, R. J. and H. W. Dorough Mode of action. In *Carbamate Insecticides: Chemistry, Biochemistry and Toxicology*; ed.; R. J. Kuhr and H. W. Dorough; CRC Press: Cleveland, OH., 1976; Vol. 41-70.

Lacorte, S. and D. Barcelo, Rapid degradation of Fenitrothion in estuarine waters. *Environ. Sci. Technol.* **1994**, *28*, 1159-1163.

Lacorte, S., G. Jeanty, J. L. Marty and D. Barcelo, Identification of Fenthion and Temephos and their transformation products in water by high-performance liquid chromatography with diode array detection and atmospheric pressure chemical ionization mass spectrometric detection. *J. Chromatography A* **1997**, *777*, 99-114.

LaCorte, S., S. B. Lartiges, P. Garrigues and D. Barcelo, Degradation of organophosphorus pesticides and their transformation products in estuarine waters. *Environ. Sci. Technol.* **1995**, *29*, 431-438.

Laerdahl, J. K. and E. Uggerud, Gas phase nucleophilic substitution. *International Journal of Mass Spectrometry* **2002**, *214*, 277-314.

Lai, K., N. J. Stolowich and J. R. Wild, Characterization of P-S bond hydrolysis in organophosphorothioate pesticides by organophosphorus hydrolase. *Arch. Biochem. Biophys.* **1995**, *318*, 59-64.

Landis, W. G., Distribution and nature of the aquatic organophosphorus acid anhydrases-enzymes for organophosphate detoxification. *Rev. Aquat. Sci.* **1991**, *5*, 267-285.

Lartiges, S. B. and P. P. Garrigues, Degradation kinetics of organophosphorus and organonitrogen pesticides in different waters under various environmental conditions. *Environ. Sci. Technol.* **1995**, *29*, 1246-1254.

Lee, C. C., R. E. Green and W. J. Apt, Transformation and adsorption of fenamiphos, fenamiphos sulfoxide and fenamiphos sulfone in molokai soil and simulated movement with irrigation. *J. Contam. Hydrol.* **1986**, *1*, 211-225.

Leegwater, J. A. and S. Mukamel, Semiclassical Green function calculation of four wave mixing in polarizable clusters and liquids. *Journal of Chemical Physics* **1994**, *101*, 7388-7398.

Licht, S. and J. Davis, Disproportionation of aqueous sulfur and sulfide: kinetics of polysulfide decomposition. *J. Phys. Chem. B* **1997**, *101*, 2540-2545.

Licht, S., F. Forouzan and K. Longe, Differential densometric analysis of equilibria in highly concentrated media: determination of the aqueous second acid dissociation constant of H2S. *Analytic Chemistry* **1990**, *62*, 1356-1360.

Lippa, K. A., S. Demel, I. H. Lau and A. L. Roberts, Kinetics and mechanism of the nucleophilic displacement reactions of chloroacetanilide herbicides: investigation of α-substituent effects. *J. Agric. Food Chem.* **2004**, *52*, 3010-3021.

Lippa, K. A. and A. L. Roberts, Nucleophilic aromatic substitution reactions of chloroazines with bisulfide (HS^-) and polysulfides (S_n^{2-}). *Environ. Sci. Technol.* **2002**, *36*, 2008-2018.

Liu, B., L. L. McConnell and A. Torrents, Hydrolysis of chlorpyrifos in natural waters of the Chesapeake Bay. *Chemosphere* **2001**, *44*, 1315-1323.

Loch, A. R., K. A. Lippa, D. L. Carlson, Y. P. Chin, S. J. Traina and A. L. Roberts, Nucleophilic aliphatic substitution reactions of propachlor, alachlor, and metolachlor with bisulfide (HS^-) and polysulfides (S_n^{2-}). *Environ. Sci. Technol.* **2002**, *36*, 4065-4073.

Lotti, M., The pathogenesis of organophosphate polyneuropathy. *Crit. Rev. Toxicol.* **1992**, *21*, 465-487.

Lotti, M. and A. Moretto, Promotion of organophosphate induced delayed polyneurophathy by certain esterase inhibitors. *Chem. Biol. Interact.* **1999**, *119/120*, 519-524.

Luther, G. W., III. The frontier-molecular orbital theory approach in geochemical processes. In *Aquatic Chemical Kinetics: Reaction Rates of Processes in Natural Waters*; ed.; W. Stumm; John Wiley: New York, 1990; Vol. 173-198.

Mabey, W. and T. Mill, Critical review of hydrolysis of organic compounds in water under environmental conditions. *J. Phys. Chem. Ref. Data* **1978**, *7*, 383-415.

Macalady, D. L. and N. L. Wolfe, New perspectives on the hydrolytic degradation of the organophosphorothioate insecticide chlorpyrifos. *J. Agric. Food Chem.* **1983**, *31*, 1139-1147.

MacCrehan, W. and D. Shea Temporal relationship of thiols to inorganic sulfur compounds in anoxic Chesapeake Bay sediment porewater. In *Geochemical Transformations of Sedimentary Sulfur*; ed.; M. A. Vairavamurthy and M. A. A. Schoonen; ACS Symposium Series 612; American Chemical Society: Washington, DC, 1995; Vol. 294-310.

Mandal, A. K. and M. Adhikari, Influence of soil properties on interactions of pesticides with soils. *J. Indian Chem. Soc.* **1997**, *74*, 114- l111 S.

Mansour, M., F. E. A., B. A and I. Scheunert, Experimental approaches to studying the photostability of selected pesticides in water and soil. *Chemosphere* **1997**, *35*, 39-50.

Martin, J. D., C. G. Crawford and S. J. Larson Pesticides in streams-Preliminary results from cycle I of the National Water Quality Assessment Program (NAWQA), 1992-2001, National Water Quality Assessment Program (NAWQA); 2003

McEwen, F. L. and G. R. Stephenson *The use and significance of pesticides in the environment*; ed.; John Wiley and Sons, Inc: New York, 1979.

McGowan, J. C. and A. Mellors *Molecular volumes in chemistry and biology: Applications including partitioning and toxicity*; ed.; Ellis Horwood Ltd: Chichester, 1986.

Meikle, R. W. and C. R. Youngson, The hydrolysis rate of chlorpyrifos, *O,O*-diethyl *O*-(3,5,6-trichloro-2-pyridyl) phosphorothioate, and its dimethyl analog, chlorpyrifos-methyl, in dilute aqueous solution. *Arch. Environ. Contam. Toxicol.* **1978**, *7*, 13-22.

Meyer, B., L. Peter and K. Spitzer, Trends in the charge distribution in sulfanes, sulfanesulfonic acids, sulfanedisulfonic acids, and sulfurous acid. *Inorg. Chem.* **1977**, *16*, 27-33.

Meyer, B., K. Ward, K. Koshlap and L. Peter, Second dissociation constant of hydrogen sulfide. *Inorg. Chem.* **1983**, *22*, 2345-2346.

Millard, C. B., G. Kryger, A. Ordentlich, H. M. Greenblatt, M. Harel, M. L. Raves, Y. Segall, D. Barak, A. Shafferman, I. Silman and J. L. Sussman, Crystal structures of aged phosphorylated acetylcholinesterase: nerve agent reaction product at the atomic level. *Biochemistry* **1999**, *38*, 7032-7039.

Miller, P. L., D. Vasudevan, P. M. Gschwend and A. L. Roberts, Transformation of hexachloroethane in a sulfidic natural water. *Environ. Sci. Technol.* **1998**, *32*, 1269-1275.

Millero, F. J., The thermodynamics and kinetics of the hydrogen sulfide system in natural waters. *Mar. Chem.* **1986**, *18*, 121-147.

Moffett, J. W. and O. C. Zafiriou, An investigation of hydrogen peroxide chemistry in seawater by isotope ratio mass spectrometry using $^{18}O_2$ and $H_2{}^{18}O_2$. *Limn. Oceanog* **1990**, *35*, 1221-1229.

Mora, A., J. Comejo, E. Revilla and M. C. Hermosin, Persistence and degradation of carbofuran in Spanish soil suspensions. *Chemosphere* **1996**, *32*, 1585-1598.

Mortland, M. M. and K. V. Raman, Catalytic hydrolysis of some organic phosphate pesticides by copper(II). *J. Agric. Food Chem.* **1967**, *15*, 163-167.

Moye, H. A. and C. J. Miles, Aldicarb contamination of groundwater. *Reviews of Environmental Contamination and Toxicology* **1988**, *105*, 99-146.

Nebeker, A. V., W. L. Griffis, C. M. Wise, E.Hopkins and J. A. Barbitta, Survival, reproduction and bioconcentration in invertebrates and fish exposed to hexachlorobenzene. *Environmental Toxicology and Chemistry* **1989**, *8*, 601-611.

Neely, W. B., W. E. Allison, W. B. Crummett, K. Kauer and W. Reifschneider, Structure activity analysis of some O,O-dialkyl (p-methylthio, p-methylsulfonyl) phenyl phosphates and phosphorothioates prepared for their insecticidal activity. *J. Agric. Food Chem.* **1970**, *18*, 45-49.

Neely, W. B., D. R. Branson and G. E. Blau, Partition coefficient to measure bioconcentration potential of organic chemicals in fish. *Environ. Sci. Technol.* **1974**, *8*, 1113-1115.

Nirmalakhandan, N. and R. E. Speece, Structure-activity relationships, quantitative techniques for predicting the behavior of chemicals in the ecosystem. *Journal of Environmental Science Technology* **1988**, *22*, 606-615.

Noblet, J. A., L. A. Smith and I. H. M. Suffet, Influence of natural dissolved organic matter, temperature, and mixing on the abiotic hydrolysis of triazine and organophosphate pesticides. *J. Agric. Food Chem.* **1996**, *44*, 3685-3693.

O'Brien, R. D., Mode of action of insecticides, binding of organophosphates to cholinesterases. *J. Agric. Food Chem.* **1963**, *11*, 163 - 166.

Olmstead, W. N. and J. I. Brauman, Gas-phase nucleophilic displacement reactions. *J. Am. Chem. Soc.* **1977**, *99*, 4219 - 4228.

Ou, L. T. and P. S. C. Rao, Degradation and metabolism of oxamyl and phenamiphos in soils. *J. Environ. Sci. Health* **1986**, *B21*, 25-33.

Pape-Lindstrom, P. A. and M. J. Lydy., Synergistic toxicity of atrazine and organophosphate insecticides contravenes the response addition mixture model. *Environmental Toxicology & Chemistry* **1997**, *16*, 2415-2420.

Pearson, R. G., Hard and soft acids and bases. *J. Am. Chem. Soc.* **1963**, *85*, 3533 - 3539.

Pehkonen, S. O. and Q. Zhang, The degradation of organophophorus pesticides in natural waters: a critical review. *Crit. Rev. Environ. Sci. Technol.* **2002**, *32*, 17-72.

Perlinger, J. A., W. Angst and R. P. Schwarzenbach, Kinetics of the reduction of hexachloroethane by juglone in solutions containing hydrogen sulfide. *Environ. Sci. Technol.* **1996**, *30*, 3408-3417.

Perlinger, J. A., V. M. Kalluri, R. Venkatathy and W. Angst, Addition of hydrogen sulfide to juglone. *Environ. Sci. Technol.* **2002**, *36*, 2663-2669.

Pickerling, T. L. and A. V. Tobolsky Inorganic and organic polysulfides. In *Sulfur in Organic and Inorganic Chemistry*; ed.; A. Senning; Marcel Dekker: New York, 1972; Vol. 19-38.

Pico, Y., R. Rodriguez and J. Manes, Capillary electrophoresis for the determination of pesticide residues. *Tren. Anal. Chem.* **2003**, *22*, 133-151.

Pittinger, C. A., D. M. Woltering and J. A. Masters, Bioavailability of sediment-sorbed and aqueous surfactants to Chironomus riparius (midge). *Environmental Toxicology & Chemistry* **1989**, *8*, 1023-1033.

Racke, K. D., Environmental fate of chloropyrifos. *Rev. Environ. Contam. Toxicol.* **1993**, *131*, 1-154.

Racke, K. D., K. P. Steele, R. N. Yoder, W. A. Dick and E. Avidov, Factors affecting the hydrolytic degradation of chlorpyrifos in soil. *J. Agric. Food Chem.* **1996**, *44*, 1582-1592.

Ritter, W. F., Pesticide contamination of ground water in the United States: A review. *J. Environ. Sci. Health* **1990**, *B25*, 1-29.

Roberts, A. L., P. N. Sanborn and P. M. Gschwend, Nucleophilic substitution reactions of dihalomethanes with hydrogen sulfide species. *Environ. Sci. Technol.* **1992**, *26*, 2263 - 2274.

Sanchez-Martin, M. J. and M. Sanchez-Camazano, Relationship between the structure of organophosphorus pesticides and adsorption by soil comnonents. *Soil Sci.* **1991**, *152*, 283-288.

Schwarzenbach, R. P., W. Giger, C. Schaffner and O. Wanner, Groundwater contamination by volatile halogenated alkanes: abiotic formation of volatile sulfur compounds under anaerobic conditions. *Environ. Sci. Technol.* **1985**, *19*, 322-327.

Schwarzenbach, R. P., P. M. Gschwend and D. M. Imboden *Environmental Organic Chemistry*; 2nd ed.; John Wiley: Hoboken, NJ, 2003.

Sharrna, B. K. and G. N., Photodegradation of the organophosphorus insecticide, Phorate. *Toxicol. Environ. Chem.* **1994**, *41*, 249-254.

Singh, R. P., I. D. Brindle, C. D. Hall and M. Chiba, Kinetic study of the decomposition of methyl [1-(butylcarbamoyl)-1*H*-benimidazol-2-yl] carbamate (benomyl) to methyl-1*H*-benzimidazol-2-yl carbamate (MBC). *J. Agric. Food Chem.* **1990**, *38*, 1758-1762.

Skoog, D. A., D. M. West, F. J. Holler and S. R. Crouch *Analytical Chemistry: An Introduction*; ed.; Saunders College Publishing: Fort Worth, TX, 1999.

Smolen, J. M. and A. T. Stone, Divalent metal ion-catalyzed hydrolysis of phosphorothionate ester pesticides and their corresponding oxonates. *Environ. Sci. Technol.* **1997**, *31*, 1664-1673.

Smolen, J. M. and A. T. Stone, Metal (hydr)oxide surface catalyzed hydrolysis of Chlorpyrifos-Methyl. Chlorpyrifos-Methyl Oxon, and Paraoxon. *Soil Science Society of America J* **1998**, *62*, 636-643.

Sogorb, M. A. and E. Vilanova, Enzymes involved in the detoxification of organophosphorus, carbamate and pyrethroid insecticides through hydrolysis. *Toxicology Letters* **2002**, *128*, 215-228.

Strathmann, T. J. and A. T. Stone, Reduction of the carbamate pesticides oxamyl and methomyl by dissolved Fe^{II} and Cu^{I}. *Environ. Sci. Technol.* **2001**, *35*, 2461-2469.

Strathmann, T. J. and A. T. Stone, Reduction of the pesticides oxamyl and methomyl by FeII: effect of pH and inorganic ligands. *Environ. Sci. Technol.* **2002**, *36*, 653-661.

Sujatha, C. H. and J. Chacko, Organophosphorus pesticide adsorption variability in diverse estuarine sediments. *Toxicol. Environ. Chem.* **1992**, *36*, 65-73.

Swain, C. G. and C. B. Scott, Quantitative correlation of relative rates. comparison of hydroxide ion with other nucleophilic reagents toward alkyl halides, esters, epoxides and acyl halides. *J. Am. Chem. Soc.* **1953**, *75*, 141-147.

Tomlin, C. *The Pesticide Manual: A World Compendium*; 10th ed.; Crop Protection Publications: Surrey, U.K., 1994.

Torrents, A. and A. T. Stone, Oxide surface-catalyzed hydrolysis of carboxylate esters and phosphorothioate esters. *Soil Sci. Society of America Journal* **1994**, *58*, 738-745.

Trudinger, P. A. and R. E. Loughlin Metabolism of simple sulfur compounds. In *Comprehensive Biochemistry*; ed.; A. Neuberger and L. v. Deenen; Elsevier, 1981; Vol. 165-256.

USEPA, Preliminary Cumulative Risk Assessment of the Organophosphorus Pesticides. *U.S. Environmental Protection Agency, Office of Pesticide Programs, Washington, DC.* **Dec. 3, 2001**.

Veith, G. D., D. L. Defoe and B. V. Bergstedt, Measuring and estimating the bioconcentration factor of chemicals on fish. *J. Fish. Res. Board Can.* **1979**, *36*, 1040-1048.

Wall, G. R., K. Riva-Murray and P. J. Phillips *Water quality in the Hudson River Basin: New York and adjacent states, 1992-95*; U.S. Geological Survey Circular 1165: http://ny.water.usgs.gov/projects/hdsn/report/Circular1165.pdf; (Accessed Dec.13, 2005)

Wan, H. B., M. K. Wong and C. Y. Mok, Comparative study on the quantum yields of direct photolysis of organophosphorus pesticides in aqueous solution. *J. Agric. Food Chem.* **1994**, *42*.

Wan, H. B., M. K. Wong and C. Y. Mok, Mercury(II) ion-promoted hydrolysis of some organophosphorus pesticides. *Pestic. Chem.* **1994**, *42*, 93-99.

Wanner, O., T. Egli, T. Fleischmann, K. Lanz, P. Reichert and R. P. Schwarzenbach, Behavior of the insecticides disulfoton and thiometon in the

Rhine River: a chemodynamic study. *Environ. Sci. Technol.* **1989**, *23*, 1232-1242.

Weber, K., Degradation of parathion in seawater. *Water Res.* **1976**, *10*, 237-241.

WHO *Organophosphorus Insecticides: a General Introduction*; ed.; WHO: Geneva, 1986.

WHO World Health Organization, Effects of organophosphorus insecticides on the nervous system. In *Organophosphorus Insecticides: a General Introduction*; ed.; WHO: Geneva, 1986; Vol. 58-69.

WHO World Health Organization, Metabolism and mode of action. In *Organophosphorus Insecticides: a General Introduction*; ed.; WHO: Geneva, 1986; Vol. 39-48.

Wolfe, N. L., Organophosphate and organophosphorothionate esters: application of linear free energy relationships to estimate hydrolysis rate constants for use in environmental fate assessment. *Chemosphere* **1980**, *9*, 571-579.

Wolfe, N. L., B. E. Kitchens, D. L. Macalady and T. J. Grundl, Physical and chemical factors that influence the anaerobic degradation of methyl parathion in sediment systems. *Environ. Toxicol. Chem.* **1986**, *5*, 1019-1026.

Wolfe, N. L., D. F. Paris, W. C. Steen and G. L. Baughman, Correlation of microbial degradation rates with chemical structure. *Environ. Sci. Technol.* **1980**, *14*, 1143-1144.

Wolfe, N. L., R. G. Zepp, J. A. Gordon, G. L. Baughman and D. M. Cline, Kinetics of chemical degradation of malathion in water. *Environ. Sci. Technol.* **1977**, *11*, 88-93.

Wolfe, N. L., R. G. Zepp and D. F. Paris, Use of structure-reactivity relationships to estimate hydrolytic persistence of carbamate pesticides. *Water Res.* **1978**, *12*, 561-563.

Wolfe, N. L., R. G. Zepp, D. F. Paris, G. L. Baughman and R. C. Hollis, Methoxychlor and DDT degradation in water: rates and products. *Environ. Sci. Technol.* **1977**, *11*, 1077 - 1081.

Yamashiro-Matsumura, S. and F. Matsumura, Purification and characterization of actin-bundling 55K protein from HeLa cells. *J. Biol. Chem.* **1985**, *260*, 5087-5097.

Zaki, M. H., D. Moran and D. Harris, Pesticides in groundwater: the aldicarb story in Suffolk County, NY. *Am. J. Public Health* **1982**, *72*, 1391-1395.

Zeinali, M. and A. Torrents, Mercury-promoted hydrolysis of parathion-methyl: effect of chloride and hydrated species. *Environ. Sci. Technol.* **1998**, *32*, 2338-2342.

Zepp, R. and D. Cline, Rates of direct photolysis in the aqueous environment. *Environ. Sci. Technol.* **1977**, *11*, 359-366.

Zepp, R. G., N. L. Wolfe, J. A. Gordon and G. L. Baughman, Dynamics of 2,4-D esters in surface waters. Hydrolysis, photolysis, and vaporization. *Environ. Sci. Technol.* **1975**, *9*, 1144-1150.

Zika, R. G., J. W. Moffett, R. G. Petasne, W. J. Cooper and E. S. Saltzman, Spatial and temporal variations of hydrogen peroxide in Gulf of Mexico waters. *Geochim. Cosmochim. Acta* **1985**, *49*, 1173-1184.

Zoldoske, D. F. and G. S. Jorgensen, Careful chemigation could help growers. *Western Fruit Grower* **1990**, *110*, 26-28.